

Final Report

Chemical and Biological Survey of Lakes and Streams Located
in the Emerald Lake Watershed, Sequoia National Park

by

J. M. Melack, S. D. Cooper, and R. W. Holmes;
J. O. Sickman, K. Kratz, P. Hopkins, H. Hardenbergh, M. Thieme, L. Meeker
Marine Science Institute and Department of Biological Sciences
University of California
Santa Barbara, CA 93106

February 18, 1987

California Air Resources Board Contract A3-096-32
Prepared for California Air Resources Board

ABSTRACT

Emerald Lake (36°35'N, 118°40'W) is located in Sequoia National Park at an elevation of 2780 m in the Sierra Nevada. The lake has one surface outflow and is fed by several inflowing streams that drain a ca. 113 ha catchment; it is 2.85 ha in area and has a maximum depth of 10.5 m. Emerald Lake contains calcium-bicarbonate water with very low acid neutralizing capacity as is typical of high-altitude lakes in the Sierra Nevada. Its current pH (5.6-6.6) is near the low end of the range observed in Sierran lakes. Low values (5.6-6.0) are associated with intense summer rains and snowmelt. During ice-cover and mid-summer the lake is thermally stratified and low dissolved oxygen and elevated concentrations of ammonium, base cations and acid neutralizing capacity (ANC) develop in the deeper water. The major contributors to alkalinity generation in Emerald Lake from the sediments are ammonium production from the breakdown of organic matter (44%) and the exchange of hydrogen ion for calcium in the sediments (34%).

During the initial stages of snowmelt in 1986, sulfate and nitrate concentrations increased while base cations and ANC declined in the subsurface water being influenced by runoff. Inflows varied in pH from 5.7 to 6.5 with minima during snowmelt; inflow ANC ranged from 4 to 45 $\mu\text{eq l}^{-1}$ with minima during intense summer rain and snowmelt. Aluminum was very low (0.6 to 2 μM) in the inflowing streams.

Phytoplankton productivity as measured using tracer techniques employing isotopes of nitrogen (^{15}N) and carbon (^{14}C) were low during the ice-free seasons of 1984 and 1985. Carbon uptake rates reached their highest levels in the spring and autumn. Chlorophyll vertical profiles measured throughout 1984, 1985 and 1986 had deep chlorophyll maximum at 7 to 9.5 meters during the summer; mid-winter chlorophyll levels are very low.

Ammonium uptake rate, particulate nitrogen and chlorophyll were used as indices of phytoplankton response to experimental additions of the acids and nutrients associated with acid precipitation to replicated 3000-4000 liter bags suspended in Emerald Lake. No significant differences were found among controls and acid treatments without phosphorus. Significant differences are observed among controls and both phosphorus and acid plus phosphorus treatments.

Equations which estimate pH and ANC in high-elevation Sierra Nevada lakes from the species composition of diatom assemblages found in surface sediments were applied to diatom assemblages observed in the upper 20 cm of Emerald Lake sediments. The results indicate that both pH and ANC have varied somewhat since about 1825, but that there is no overall trend in either of these variables.

The zooplankton assemblage in Emerald Lake is dominated by a copepod (Diaptomus signicauda), three cladocerans (Daphnia rosea, Bosmina longirostris, Holopedium gibberum), and three rotifers (Keratella cochlearis, Polyarthra vulgaris, and Conochilus unicornis). Abundances of all common taxa were highest during the summer and early autumn. Daphnia, Diaptomus, and Conochilus were very sensitive to experimental acidic inputs to large bags in the lake with Daphnia and Diaptomus densities declining abruptly as pH was reduced from 5.6 to 5.5. Densities of Keratella and Bosmina, and, in some experiments, Polyarthra, were greater in bags acidified to pH 5.1 - 5.5 than in non-acidified controls probably owing to release from competition with Daphnia. Densities of Keratella, Rosmina, and Holopedium were all reduced below pH 5.0.

The zoobenthic assemblages of the Emerald Lake inlet and outlet streams were dominated by chironomid larvae. Simuliid larvae, Baetis nymphs, and Rhyacophila larvae were commonly collected in both inflow and outflow streams, particularly on hard substrates, and ephemereid and leptophlebiid mayflies, nemourid stonefly nymphs, tipulid larvae, water mites, oligochaetes, and sphaeriid clams were also commonly collected in the outlet stream. Simuliids, Baetis, and Malenka displayed nocturnal increases in their drift rates, mites and chironomids showed different drift patterns, depending on the date or stream sampled, and trichopterans appeared to be aperiodic.

During experimental acid additions to replicate stream channels, Baetis spp. drift in acidified channels was ca. 7 times higher than in control channels, and the percentage of drifting baetids that was dead was significantly higher in acidified than control channels. Other taxa showed no significant drift responses. The dominant benthic invertebrates in Emerald Lake were chironomids and sphaeriid clams, and acidification of large bags had no effect on the densities of these taxa.

ACKNOWLEDGEMENTS

We thank the many personnel from the National Park Service and the California Air Resources Board for logistical and financial support. We are especially grateful to David Parsons, David Graber, and Tom Stohlgren for facilitating our research efforts and to Harold Werner for assistance in starting our zoological investigations. Special thanks goes to Kathy Tonnessen of the ARB for all of her help. We would like to thank the National Park Service for allowing us to conduct our studies in Sequoia National Park.

The limnological investigations were coordinated by John M. Melack and conducted by coauthors of this report, James O. Sickman and Helen Hardenbergh. Thomas R. Fisher provided valuable advice and help with the sediment flux and ^{15}N work. We sincerely thank Warren Myers, Paul Schwartz, Michael Williams, Patti Hagerty and Annie Esperanza for their enthusiastic and able field assistance. We appreciate the laboratory assistance provided by Frank Setaro and Delores Lucero-Sickman, and the statistical analyses done by Mark Williams.

The Emerald Lake sediment cores employed in this study were collected by J. Sickman and P. Schwartz using SCUBA. These individuals, together with P. Hopkins, also assisted in extruding the core. We wish to thank Dr. D. Hammond of the University of Southern California for counting the lead-210 samples and calculating the dates for Emerald Lake core Mid-2.

The botanical aspects of this project were supervised by Robert Holmes and John M. Melack and performed largely by Mary Thieme, Lisa Meeker with valuable assistance from Sheila Wiseman and Mark Whiting. Samples were collected by James Sickman, Kim Kratz, Roland Knapp and Michael Williams, and field assistance was provided by Pam Hopkins, Helen Hardenbergh and Dough Erwin.

The zoological investigations were directed by Scott Cooper. During the summer and fall of 1984 field and laboratory projects were carried out by Warren Myers, Nina Hemphill, and Paul Schwartz. In 1985 and 1986, field efforts were overseen by Kim Kratz with assistance from Pam Hopkins, Roland Knapp, Chris Dwyer, and Robert Durand. Pam Hopkins was primarily responsible for the analyses of data associated with the stream channel experiment and stream drift. Jim Sickman was primarily responsible for construction and

monitoring of the bag experiments, and for plankton monitoring, with assistance from Helen Hardenbergh, Mike Williams, and Lisa Meeker. Laboratory analyses were directed by Kim Kratz with assistance from Sheila Wiseman, Pam Hopkins, and Chris Dwyer. Mario Moreno counted most zooplankton samples. Chris Dwyer prepared many of the computer-generated figures. We also acknowledge the assistance of many work-study assistants in processing benthic samples.

All the authors thank Lance Lesack for his invaluable aid with the computer analyses and plotting, and Melanie Fujii for exceptional word processing.

Disclaimer

The statements and conclusions in this report are those of the contractor and not necessarily those of the California Air Resources Board. The mention of commercial products, their source or their use in connection with material reported herein is not to be construed as either actual or implied endorsement of such products.

TABLE OF CONTENTS

	Page
Abstract.....	i
Acknowledgements.....	iii
Table of Contents.....	v
List of Figures.....	vi
List of Tables.....	xii
Summary and Conclusions.....	1
Recommendations.....	7
I. Introduction.....	10
II. Limnological conditions	
1. Seasonal variability in solute chemistry.....	15
2. Primary productivity and regeneration of nitrogen.....	44
3. Sediment-water fluxes.....	76
4. Experimental acidification of large enclosures.....	102
III. The pH and alkalinity history of Emerald Lake since 1825 estimated from diatom assemblages.....	120
IV. Botanical aspects	
1. Phytoplankton.....	146
2. Phytobenthos.....	161
V. Zoological aspects	
1. Zooplankton.....	189
2. Zoobenthos.....	219
3. Fish.....	304
VI. Kaweah River (Marble Fork) drainage survey.....	309
References.....	320

List of Figures

Fig. I-1	Location of Emerald Lake in Sierra Nevada.....	12
Fig. I-2	Upper Marble Fork of Kaweah River drainage.....	13
Fig. I-3	Bathymetric map of Emerald Lake.....	14
Fig. II-1	Temperature time series, subsurface and 9.5 m.....	22
Fig. II-2	Dissolved oxygen time series, subsurface and 9.5 m.....	22
Fig. II-3	Electrical conductivity time series, subsurface and 9.5 m.....	23
Fig. II-4	pH time series, subsurface and 9.5 m.....	24
Fig. II-5	Acid neutralizing time series, subsurface and 9.5 m.....	24
Fig. II-6	Nitrate time series, subsurface and 9.5 m.....	25
Fig. II-7	Sulfate time series, subsurface and 9.5 m.....	25
Fig. II-8	Chloride time series, subsurface and 9.5 m.....	26
Fig. II-9	Silica time series, subsurface and 9.5 m.....	26
Fig. II-10	Sum of Ca+Mg+Na+K time series, subsurface and 9.5 m.....	27
Fig. II-11	Calcium time series, subsurface and 9.5 m.....	28
Fig. II-12	Magnesium time series, subsurface and 9.5 m.....	28
Fig. II-13	Sodium time series, subsurface and 9.5 m.....	29
Fig. II-14	Potassium time series, subsurface and 9.5 m.....	29
Fig. II-15	Ammonium time series, subsurface and 9.5 m.....	30
Fig. II-16A	Snowmelt time series for cations, ANC and SO_4+NO_3 , subsurface and 9.5 m.....	31
Fig. II-16B	Snowmelt time series for cations, ANC and SO_4+NO_3 , subsurface and 9.5 m.....	31
Fig. II-17	Electrical conductivity time series, Main inflow.....	32
Fig. II-18	pH time series, Main inflow.....	33
Fig. II-19	Acid neutralizing capacity time series, Main inflow.....	33
Fig. II-20	Nitrate time series, Main inflow.....	34
Fig. II-21	Sulfate time series, Main inflow.....	34
Fig. II-22	Chloride time series, Main inflow.....	35
Fig. II-23	Silica time series, Main inflow.....	35
Fig. II-24	Sum of $H+NH_4+Ca+Mg+Na+K$ time series, Main inflow.....	36
Fig. II-25	Calcium time series, Main inflow.....	37
Fig. II-26	Magnesium time series, Main inflow.....	37
Fig. II-27	Sodium time series, Main inflow.....	38
Fig. II-28	Potassium time series, Main inflow.....	38

Fig. II-29A	Unfiltered metal time series, Main inflow.....	39
Fig. II-29B	Unfiltered metal time series, West inflow.....	39
Fig. II-30	Calcium vs ANC, subsurface.....	40
Fig. II-31	Cations vs ANC, subsurface.....	40
Fig. II-32	All cations vs. ANC, subsurface.....	41
Fig. II-33	Base cations vs. ANC, 9.5 m.....	42
Fig. II-34	All cations vs. ANC, 9.5 m.....	42
Fig. II-35	Sum of NO ₃ +SO ₄ vs. ANC, subsurface.....	43
Fig. II-36	Typical photosynthesis vs. light curve.....	59
Fig. II-37AB	Atom %P- ¹⁵ N vs. Time; 15-July-85, 26-Sept-85.....	60
Fig. II-38AB	Atom %P- ¹⁵ N vs. Time; 11-Oct-85, 16-Oct-85.....	61
Fig. II-39	Atom %P- ¹⁵ N vs. Time; 17-Oct-85.....	62
Fig. II-40AB	Atom %P- ¹⁵ N vs. Time; 18-May-86, Epilimnion + Hypolimnion..	63
Fig. II-41AB	Atom % ¹⁵ N-NH ₄ vs. Time; 26-Sept-85, 11-Oct-85.....	64
Fig. II-42AB	Atom % ¹⁵ N-NH ₄ vs. Time; 16-Oct-85, 17-Oct-85.....	65
Fig. II-43AB	Atom % ¹⁵ N-NH ₄ vs. Time; 15-Feb-86, Epilimnion + Hypolimnion.....	66
Fig. II-44AB	Atom % ¹⁵ N-NH ₄ vs. Time; 18-May-86, Epilimnion + Hypolimnion.....	67
Fig. II-45AB	Chlorophyll specific carbon uptake vs. light; 23-Oct-84, 18-May-86.....	68
Fig. II-46	Chlorophyll specific carbon uptake vs. light; 13-July-85...	69
Fig. II-47	PmB during summer 1984 and 1985.....	70
Fig. II-48	Pm during summer 1984 and 1985.....	71
Fig. II-49	Alpha during summer 1984 and 1985.....	72
Fig. II-50	Chl _a during summer 1984 and 1985.....	73
Fig. II-51	Secchi disk transparency summer 1984 and 1985.....	74
Fig. II-52	Typical mid-summer vertical profiles of Chl _a	75
Fig. II-53	Fall 1984 vertical profiles of Chl _a	75
Fig. II-54	Typical mid-winter vertical profiles of Chl _a	75
Fig. II-55	Typical snowmelt vertical profiles of Chl _a	75
Fig. II-56	Diagram of benthic chamber.....	93
Fig. II-57ABC	Solute concentration changes in benthic chambers.....	94-96
Fig. II-58	Alkalinity changes in large enclosures.....	97
Fig. II-59	Alkalinity changes in microcosms with and without chironomids.....	98

Fig. II-60	Calcium vs. ANC, benthic chamber.....	99
Fig. II-61	Sum of base cations vs. ANC, benthic chamber.....	100
Fig. II-62	Sum of base cations and ammonium vs. ANC, benthic chamber.....	101
Fig. II-63	pH time series - all treatments; Experiment 3.....	112
Fig. II-64AB	Ammonium uptake and chlorophyll specific uptake; Day 0.....	113
Fig. II-65AB	Ammonium uptake and chlorophyll specific uptake; Day 11.....	114
Fig. II-66AB	Ammonium uptake and chlorophyll specific uptake; Day 23.....	115
Fig. II-67AB	Chlorophyll <u>a</u> and particulate nitrogen; Day 0.....	116
Fig. II-68AB	Chlorophyll <u>a</u> and particulate nitrogen; Day 9-11.....	117
Fig. II-69AB	Chlorophyll <u>a</u> and particulate nitrogen; Day 23.....	118
Fig. II-70	Nitrate time series - all treatments; Experiment 3.....	119
Fig. III-1	Sediment dry weight and ignition loss in three cores from Emerald Lake.....	140
Fig. III-2	²¹⁰ Pb profile in Emerald Lake core Mid-2.....	141
Fig. III-3	Observed and predicted air equilibrated pH and alkalinity in 27 high elevation Sierra Nevada lakes.....	142
Fig. III-4	Observed and predicted air equilibrated pH in 27 high elevation Sierra Nevada lakes using multiple linear regression equation 6A.....	143
Fig. III-5	pH reconstruction of Emerald Lake core Mid-2 using Log Index B and multiple linear regression equation 6A.....	144
Fig. III-6	Alkalinity reconstructions of Emerald Lake core Mid-2.....	145
Fig. IV-1	Seasonal abundance of Emerald Lake phytoplankton by size class.....	157
Fig. IV-2	Relative abundance of phytoplankton by size class.....	158
Fig. IV-3	Seasonal biomass of phytoplankton by size class.....	159
Fig. IV-4	Phytoplankton, bag experiment #3.....	160
Fig. IV-5	The average number of species (richness) per sample by substrate type, location, and month.....	181
Fig. IV-6A-L	Diatom relative abundances averaged over four to six samples by substrate type and location for July, September, and October (lake only) 1986 sampling dates. All species with an average abundance greater than or equal to 1.5% are represented.....	182-187
Fig. IV-7	Lorenz curves for four samples.....	188

Fig. V-1	Abundances of common zooplankton taxa in Emerald Lake; July 1984-March 1985.....	206-209
Fig. V-2	Abundances of common zooplankton taxa in Emerald Lake; June-September 1985.....	210-213
Fig. V-3	Densities of common zooplankton taxa in bags assigned to different treatments in Experiment 1.....	214
Fig. V-4	Densities of common zooplankton taxa in bags assigned to different treatments at the end of Experiment 2.....	215
Fig. V-5	Densities of common zooplankton taxa in bags assigned to different treatments in Experiment 3.....	216
Fig. V-6	Densities of common zooplankton taxa in bags assigned to different treatments in Experiment 4.....	217
Fig. V-7	Relationships between percentage response to acid addition and pH for common zooplankton taxa over all experiments.....	218
Fig. V-8	Map of Emerald Lake showing streams.....	251
Fig. V-9	Design of the replicate experimental stream channels set up along the Marble Fork of the Kaweah River in July 1985.	252
Fig. V-10	Densities of common benthic macroinvertebrates in Emerald Lake inlet channels A, B, C, and D in the summer and autumn of 1984.....	253-255
Fig. V-11	Densities of common benthic macroinvertebrates in Emerald Lake inlet channels A, B, C, and D in the summer and early autumn of 1985.....	256-258
Fig. V-12	Mean densities of common benthic macroinvertebrates on clean vs. moss hard substrates in the Emerald Lake outlet on two dates in 1984.....	259-262
Fig. V-13	Mean densities of common benthic macroinvertebrates on clean vs. moss hard substrates in the Emerald Lake outlet on three dates in 1985.....	263-266
Fig. V-14	Mean densities of common benthic macroinvertebrates on hard substrates in the Emerald Lake outlet in summer and autumn of 1984.....	267-270
Fig. V-15	Mean densities of common benthic macroinvertebrates on clean hard substrates in the Emerald Lake outlet in summer and autumn of 1985.....	271-274

Fig. V-16	Densities of common benthic macroinvertebrates on soft and cobble substrates in the Emerald Lake outlet in the summer and autumn of 1984.....	275-278
Fig. V-17	Densities of common benthic macroinvertebrates on soft and cobble substrates in the Emerald Lake outlet in the summer and autumn of 1985.....	279-282
Fig. V-18	Diel temperatures (°C) of Emerald Lake (A) inflow, 1985 and (B) outflow streams, 1985.....	283
Fig. V-19	Discharge (liters/second) through drift nets at Emerald Lake streams.....	284-286
Fig. V-20	Total number of benthic aquatic organisms captured in drift nets per hour in the Emerald Lake streams.....	287-288
Fig. V-21	The number of chironomid larvae captured in drift nets per hour in the Emerald Lake streams.....	289-290
Fig. V-22	The number of simuliid larvae captured in drift nets per hour in the Emerald Lake outflow.....	291-292
Fig. V-23	The number of <u>Baetis</u> spp. captured in drift nets per hour in the Emerald Lake streams.....	293-294
Fig. V-24	The number of <u>Malenka</u> captured in drift nets per hour in the Emerald Lake outflow.....	295
Fig. V-25	The number of aquatic mites captured in drift nets per hour in the Emerald Lake outflow.....	296-297
Fig. V-26	The number of terrestrial insects captured in drift nets per hour in the Emerald Lake streams.....	298
Fig. V-27	(A) Discharge (liter/minute) taken at drift sets throughout the experiment, (B) pH, (C) Alkalinity, (D) Nitrate concentrations, (E) Sulfate concentrations before, during, and after acid addition, (F) Dissolved aluminum, iron, and manganese concentrations before, during, and after acid additions in control and acidified channels.....	299
Fig. V-28	Stream invertebrate benthic densities for <u>Baetis</u> , <u>Simuliidae</u> , <u>Isoperla</u> , <u>Rhyacophila</u> , and Chironomidae before and after acid addition in control and acidified channels.....	300

Fig. V-29	(A) <u>Baetis</u> , (B) chironomid larvae, (C) aquatic mites, (D) <u>Isoperla</u> , (E) Simuliidae, and (F) trichopteran drift rates throughout the experiment.....	301
Fig. V-30	Percent of drifting <u>Baetis</u> that were dead throughout the experiment.....	302
Fig. V-31	Mean densities of chironomid larvae and sphaeriid clams in acidified and non-acidified bags in Experiment 4.....	303
Fig. V-32	The size structure of the brook trout population in the Emerald Lake outlet, July and October 1984.....	308

List of Tables

Table II-1	Chemical analyses scheme for dissolved constituents.....	21
Table II-2	Ammonium regeneration rates - ice-free season 1985 and underneath ice in the winter of 1985-86.....	54
Table II-3	Ammonium uptake rates - dark incubated. From the ice-free season of 1985 and underneath ice in the winter of 1985-86.....	55
Table II-4	Ammonium uptake rates - light incubated. From the ice-free seasons of 1984 and 1985.....	56
Table II-5	Nitrogen regeneration and uptake rates reported in some other lakes. Range of reported values.....	57
Table II-6	Carbon productivity in some other lakes. Maximum observed productivity.....	58
Table II-7	Fluxes of chemical constituents in benthic chambers.....	87
Table II-8	Chemical fluxes with high and low oxygen.....	88
Table II-9	Chemical fluxes in large enclosures.....	89
Table II-10	Alkalinity fluxes calculated for hypolimnion.....	90
Table II-11	Boundary layer thickness in chambers and lake.....	91
Table II-12	Comparison of fluxes measured by four methods.....	92
Table II-13	Design of bag experiments.....	109
Table II-14	Mean and standard deviation of H, NO ₃ , PO ₄ , SO ₄ ; Day 0, Day 1.....	110
Table II-15	Mean and standard deviation of H, NO ₃ , PO ₄ , SO ₄ ; Day 9, Day 23.....	111
Table III-1	Lead-210 data from Emerald Lake core Mid-2.....	135
Table III-2	Lead-210 data from Emerald Lake core Mid-2.....	136
Table III-3	pH estimates for Emerald Lake core Mid-2 using equations developed from the Sierra Nevada lake survey of 1985 and recent modifications of them. Equation numbers refer to the equations given in the text of this report...	137
Table III-4	Alkalinity estimates for Emerald Lake core Mid-2 using equations 4 and 7. The equation numbers refer to the equations given in the text of this report.....	138

Table III-5	pH estimates from four core depth intervals in three Emerald Lake cores using five equations developed in the present and previous study.....	139
Table IV-1	Living diatoms species collected from Emerald Lake and associated streams July and October 1985.....	176-178
Table IV-2	Summary of Emerald Lake pH inferences.....	179
Table IV-3	Summary of inlet stream pH inferences.....	180
Table V-1	Emerald Lake zooplankton and macroinvertebrate taxa collected in net tows, 1984-1985.....	204
Table V-2	Results of statistical analyses of Emerald Lake bag experiments, 1985.....	205
Table V-3	Emerald Lake outlet and inlet stream macroinvertebrate taxa, 1984-1985.....	245
Table V-4	Emerald Lake stream taxa found in stream drift, July-October 1984, and August-September 1985.....	246-248
Table V-5	Stream invertebrates found in benthic and drift samples collected from experimental stream channels, July 1985....	249
Table V-6	Densities of common benthic macroinvertebrates collected from Emerald Lake in 1984-1985.....	250
Table VI-1	Chemical composition of lakes in Tokopah drainage.....	314
Table VI-2	Zooplankton taxa and number of species collected in Tokopah drainage.....	315
Table VI-3	Taxa collected using sweep nets from lakes in Tokopah drainage.....	316-317
Table VI-4	Taxa collected using sweep nets in outlet streams of lakes in Tokopah drainage.....	318-319

SUMMARY AND CONCLUSIONS

Lakes in the Sierra Nevada are among the most dilute and weakly buffered in the United States. The very low concentrations of solutes is owed to the large volume of extremely dilute snow that provides most of the runoff, and to the granitic rocks in the watersheds that weather slowly.

Emerald Lake has calcium-bicarbonate water with very low acid neutralizing capacity (ANC) as is typical of high altitude lakes in the Sierra Nevada. The lake's watershed drains an area of ca. 113 ha, and the lake itself lies at 2780 m above sea level and has a surface area of 2.85 ha and a maximum depth of 10.5 m. Emerald Lake is drained by one major outflow stream and fed by several small inflow streams.

The purposes of our studies of major solute chemistry in Emerald Lake are to characterize the chemical composition and its episodic, seasonal and interannual variability. These measurements permit evaluation of potential chemical influences on the biota, and of how the lake responds to inflows from its watershed and from exchanges with its sediments.

Emerald lake is thermally stratified under ice, mixed from top to bottom at ice out, restratified in midsummer and mixed again in autumn. Associated with periods of thermal stratification are low concentrations of dissolved oxygen near the sediments which enhance release of nutrients and ANC. In subsurface waters pH ranged from 5.6 to 6.6 with low values associated with a rain storm in 1984 and snowmelt in 1986. Near bottom pH's declined to 5.7 to 5.8 during stratified periods and reached highs of 6.2 to 6.3. ANC or alkalinity fell to minima of zero after a mid-July 1984 rain storm and during snowmelt in 1986. A maximum occurred under ice in the water of 1984-85. During the initial stages of snowmelt, sulfate and nitrate concentrations increased while base cations and ANC declined in the subsurface water. This result implies dilution and some titration by nitric and sulfuric acids contribute to declines in acid neutralizing capacity.

To evaluate the relations among major solutes as an indication for the importance of weathering reactions in ANC generation and of nitric and sulfuric acids as acidifying species, a series of regression analyses were performed using chemical data for Emerald Lake. The implication of these analyses is that weathering reactions and organic matter decomposition in the lake sediments contribute most of the ANC.

Summer rain in the Sierra Nevada is usually acidic and intense storms occasionally occur. In mid-July 1984 Emerald Lake experienced 4.5 cm of pH 4.3 rain. The limnological consequences of this storm were conspicuous and persistent. Five days after the storm, the upper water had zero acid neutralizing capacity. Coincident with the runoff from the storm, turbidity increased, and the lake developed stronger thermal stratification than in other years. In the deep water, dissolved oxygen declined to almost zero, and ANC and dissolved inorganic phosphorus increased. An autumn peak in algae was likely caused by the availability of phosphorus as the lake mixed. In turn, the decay of organic matter derived from this autumnal algal peak contributed to the development of low oxygen under the ice. The near anoxic conditions of the sediment-water interface resulted in enhanced release of ANC and phosphorus which, in turn, stimulated a spring phytoplankton increase just after ice out in 1985. This scenario is reasonable and probable but speculative. However, the point to be made is that acidic rains are likely to have multifarious affects not solely tied to their acidity.

The interface between lake sediments and the overlying water plays an important role in the flux of solutes into lake water. These fluxes contribute ANC which may buffer inputs of acidity via atmospheric deposition or runoff.

Recent interest in the supply and recycling of nutrients has led to methodological improvements which permit in-situ measurement of sediment-water fluxes. Chambers have been designed that are placed over the sediment surface and sequential samples collected as a direct measure of exchange. The two main purposes of our work on sediment-water fluxes were to provide measurements of ANC flux from the sediments into the overlying water and to quantify the relative importance of biogeochemical processes that contribute to ANC generation in Emerald Lake.

Fluxes of ANC measured with benthic chambers deployed at a depth of 9 meters were similar in the summers of 1984 and 1985. Calcium, ammonium and magnesium concentrations increased inside the chamber for all experiments; nitrate and sulfate concentrations decreased in most experiments. The levels of dissolved oxygen in the chamber would be expected to affect the relative contribution of nitrate, sulfate and iron reduction to ANC generation, and ANC flux was greater in experiments with low levels of dissolved oxygen. ANC fluxes were also calculated from changes in the lake during stratified

periods. Low levels of oxygen for longer than two weeks coincide with higher ANC fluxes. The larger values are comparable to those obtained from the benthic chamber experiments.

ANC is produced by three primary mechanisms in watersheds and lakes: redox reactions (sulfate, nitrate, iron and manganese reduction), decomposition of organic oxidizable substrates and chemical weathering reactions which occur when water comes into contact with rock and soils. Our data indicate that ANC flux inside the benthic chambers is mainly the result of decomposition of organic matter and the hydrolysis of minerals in the sediments.

Measurements of primary production and heterotrophic nutrient regeneration indicate that Emerald Lake is a very infertile ecosystem. Therefore, seasonal changes in nutrients have a marked affect on the temporal and spatial distribution of the phytoplankton. Higher nutrient levels associated with spring snowmelt and the breakdown of the summer thermal stratification induce yearly increases of phytoplankton biomass and productivity. Higher ammonium regeneration rates are also associated with spring snowmelt and contribute to the inorganic nitrogen supply to the phytoplankton.

Year to year variation in primary production and phytoplankton biomass can be large. A single rain event in 1984 caused a large influx of silt which induced strong thermal stratification which dramatically effected the plankton. Nutrient stress in the phytoplankton in the summer was followed by a large autumn bloom as nutrients trapped in the deeper water were mixed into the upper waters. Phytoplankton abundances derived from cell counts were highest in autumn and lowest during winter; abundance peaks of smaller magnitude were found in spring and late summer. Microalgae (cells smaller than 5 microns) dominate total biomass at all times except during brief periods in winter and midsummer.

Ecologists have recently begun performing experiments in large enclosures in lakes or large, outdoor stream channels. Not only do such mesocosms allow replicated study systems under nearly natural conditions, they also allow similar conditions among replicates at the experiment's outset, circumventing problems associated with sampling variability.

Field experiments were conducted during the summer of 1985 in large bags suspended in the middle of Emerald Lake. In Experiments 1 and 2 sulfuric and nitric acid were added to experimental bags to create two levels of acid

treatment; control bags did not receive acid inputs. The proportions of sulfuric and nitric acid added to each bag represent the proportions of these acids found in summer rains in the Emerald Lake area.

In Experiment 3 we attempted to differentiate the effects of the ions associated with acid deposition (H^+ , NO_3^- , SO_4^{2-}), as well as the effects of nutrient inputs (PO_4^{3-}), on plankton assemblages. Because chloride ions have little effect on planktonic populations at the concentrations we used, additions of hydrochloric acid should indicate the effects of hydrogen ions on plankton populations. Similarly, because sodium and potassium ions are unlikely to impair plankton at the concentrations we used, addition of KNO_3 and Na_2SO_4 to bags should indicate the effects of nitrate and sulfate ions on plankton populations. By comparing the responses of plankton populations to additions of sulfuric and nitric acid with their responses to hydrochloric acid vs. potassium nitrate and sodium sulfate additions, we should be able to differentiate the effects of protons from the effects of nutrient additions (as NO_3^- and SO_4^{2-}) on plankton assemblages. We were also interested in the effects of orthophosphate additions on plankton assemblages because orthophosphate was demonstrated to be limiting to phytoplankton growth in Emerald Lake and because orthophosphate levels in Emerald Lake increased following an acid rain event in the summer of 1984.

In Experiment 4, we attempted to determine if the presence of bottom sediments had any effect on plankton responses to acidic inputs. Eight bags enclosed the whole water column and sediments, and another eight bags only enclosed the water column. Biological responses to these treatments are described for phytoplankton, zooplankton and zoobenthos.

In Experiment 3, there was a complex response in the plankton to nutrient and acid inputs. To fully understand the effects of these inputs, both phytoplankton and zooplankton responses had to be integrated. Phosphorus additions caused significant increase in ammonium uptake, and there appears to be a detrimental affect on ammonium uptake caused by high hydronium concentrations. Accumulations of chlorophyll and particulate nitrogen occurred when the phytoplankton had a sufficient supply of nitrogen to utilize the phosphorus input. This effect was enhanced in the phosphorus plus acid treatment because of lower zooplankton density and grazing pressure.

Acidification accompanied by phosphate addition resulted in a significant increase in phytoplankton cell abundance. Phosphate addition alone resulted in a cell abundance increase of smaller magnitude. No significant change in total abundance resulted from acidification alone. Additional biological effects of acidification include shifts in morphotype composition.

Our experimentals indicate that a variety of invertebrate taxa will show sensitive responses to acidic inputs. Among the zooplankton, Daphnia rosea and Diaptomus signicauda will decline abruptly as pH is reduced below 5.6. Other species, such as Bosmina longirostris and Keratella cochlearis will increase at intermediate levels of acidification but will decline as pH drops below 5.0. Among the stream benthos, the drift and mortality rates of Baetis will increase, and population levels will decline, with advancing acidification. These experiments, then will allow us to predict the effects of increased acidic inputs on Sierra Nevada lakes and streams.

Diatom assemblages in the sediments of Emerald Lake accurately confirm the current lake pH, corroborating the effectiveness of the predictive equations recently developed to predict pH in Emerald Lake. Hard substrates are not sufficiently represented within Emerald Lake to significantly impact the lake sediment pH inferences. Very few diatoms were found in the phytoplankton; the few encountered were primarily suspended benthic forms. Hence, the Emerald Lake sedimentary record is simplified by the absence of euplanktonic diatom taxa, and appears to provide a good record of the periphytic diatom communities in terms of floristic composition. A shift toward more acidobiontic taxa or an increase in their relative abundances would be indicative of decreasing lake pH.

Minor fluctuations of alkalinity are estimated to have occurred since about 1825 in Emerald Lake based on the diatom composition of dated sediment cores. Neither estimated pH nor alkalinity exhibit a consistent time-related trend. Thus, this analysis does not provide evidence of significant or permanent changes in pH and alkalinity in Emerald Lake caused by recent increases in acidic atmospheric deposition.

Our monitoring program has allowed us to characterize zooplankton and zoobenthos populations in the Emerald Lake system, and allowed us to obtain some data on fish populations. Surveys of other waters in the Kaweah drainage indicate that the zooplankton and zoobenthos populations in the

Emerald Lake system are representative of high elevation waters containing brook trout. Comparisons of our monitoring results with our experimental and literature data indicate that the Emerald Lake system possesses a wealth of indices for assessing current and potential biotic responses to acidification. Continued monitoring of sensitive taxa constitutes an early-warning system for detecting system responses to acid stress.

Because many sensitive taxa are currently abundant or common in the Emerald Lake system, acid deposition has not had any long-term effects on aquatic systems in the southern Sierra Nevada. Our experiments show, however, that a number of components of the Emerald Lake system will show sensitive responses to acidic inputs. Continued examination of the Emerald Lake system, then, will provide us with data for evaluating and predicting the effects of acid deposition on aquatic habitats in the Sierra Nevada.

RECOMMENDATIONS

To assess the influence and possible affects of acidic atmospheric deposition on aquatic ecosystems in California requires both a long-term measurement scheme and experimental investigations. A prime focus for such studies should continue to be high altitude lakes and streams in the Sierra Nevada because these waters are especially sensitive to acidic inputs. Emerald Lake and its associated streams has proven to be an exemplary site for examination of a representative high Sierra aquatic ecosystem and offers opportunities for further, pertinent study. Specific recommendations derived from our previous research follow:

1. Measurements of the major solutes in the streams and lake are required on a seasonal and episodic basis. Special emphasis should be placed on snowmelt and summer rain storms. To improve evaluation of the portion of the lake influenced by episodic inputs requires automatic recording of thermal structure in the lake.
2. Calculation of in-situ alkalinity production in Emerald Lake from a mass balance approach should be done as an independent verification of alkalinity flux as calculated from the benthic chamber experiments.
3. Dissolved oxygen levels in benthic chamber should be made to mimic ambient lake levels whenever possible. This could be accomplished by experiments of shorter duration and by more frequent monitoring of dissolved oxygen levels within the chamber.
4. Ammonium regeneration should be measured seasonally. More intensive work should be conducted during the winter and snowmelt when this activity could be significantly altering the inorganic nitrogen pool.
5. Heterotrophic regeneration of phosphorus using ^{33}P , a weakly radioactive short-lived (half-life = 25 days) isotope, should be initiated. Because of the small risks, these experiments could be conducted in the field. Not only is phosphorus the limiting nutrient in Emerald Lake, but the rate of its recycling in the summer probably determines phytoplankton productivity.
6. Acidification experiments conducted either in the laboratory using carbon-14 or in the field using phosphorus-33 should be done to increase our understanding of the detrimental effects of low pH on nutrient uptake.

7. Phytoplankton productivity and abundance should be an integral part of experiments designed to determine the affects of the chemicals associated with acid deposition on biological systems of Emerald Lake.
8. Monthly measurements of carbon-14 uptake measurements should be continued. Rates should be determined at discrete depths and photosynthetically available radiation measured to allow for more accurate estimates of areal carbon production.
9. Further information on seasonal variability in phytoplankton composition is needed to characterize the seasonal pattern. More frequent sampling and a larger number of sampling stations are necessary components of such an effort. Vertical differences in composition and abundance is relevant should an acid event affect surface waters and be neutralized at some mid-depth. The problem of phytoplankton identification needs to be addressed.
10. Periodic composite sampling of surfical lake sediments, preferably examining live assemblages, would be sufficient to monitor lake diatom species composition and relative abundances. Hard substrates should be monitored as well and samples weighted according to the actual area represented by each substrate type within the lake before pH estimates were calculated. By using live assemblages, the confounding influence of valves imported from the inlet streams, which tend to support more acidobiontic individuals, is avoided. More frequent sampling is desireable for a better evaluation of seasonal variability.
11. The only test of the accuracy and precision of the pH and alkalinity predictive equations developed for the Sierra Nevada has been in Emerald Lake. It is highly desirable to test the accuracy and precision of these equations in other acid sensitive Sierra Nevada lakes. This could be done by obtaining replicate core samples in an additional 8-10 lakes for which pH and alkalinity records have been obtained over the past 3-5 years. The collection of additional 20 - 25 cm. long cores from several high elevation, acid sensitive Sierra Lakes is highly desireable. The diatom pH reconstructions from these additional lakes would provide additional paleo-pH information which could be compared with that obtained in Emerald Lake. It would also be very useful to examine the concentrations and distribution of soot particles, polycyclic aromatic hydrocarbons, and some trace metals (e.g. As, Cr, Zn, Pb, and V) in these latter cores inasmuch as they may provide a useful record of the products of fossil fuel combustion in the region.

12. Zoobenthos and zooplankton should be monitored to obtain a long-term data base on the dynamics of these populations. Long-term records are necessary to characterize the extent of natural variation so that anthropogenic disturbances can be distinguished from natural variation, and to discern subtle, gradual changes resulting from chronic perturbations. Furthermore, much useful information can be generated by following the time course of biotic responses to acid deposition events such as summer rains.

13. Owing to their recreational importance and responses to acidification, we recommend a detailed study on the behavior, diets, growth, reproduction, size and age structure, and population dynamics of brook trout populations. From our study already underway it is evident that there is large inter-annual variation in recruitment to the Emerald Lake trout population, underlining the need for additional investigations to characterize the extent of natural variation in trout populations and determine the sources of this variation.

14. Because of the ease with which zooplankton can be sampled, because zooplankton are easy to experimentally manipulate, and because zooplankton show sensitive responses to acidic inputs, we recommend further field experiments involving zooplankton. Enclosure experiments should be performed in the lake to examine the direct and interactive effects of acid and aluminum on plankton assemblages. Furthermore, we recommend that large enclosure experiments be performed where the precise responses of plankton to a graded series of pH depressions be measured. As part of this experiment, we recommend that zoobenthos responses to different pH levels also be measured because little is known regarding the effects of acidic inputs on lake zoobenthos.

15. We strongly emphasize the need to integrate the results of investigations with results obtained from other projects. For example, data on zoobenthos, zooplankton, and drift could be compared to data on fish diets to examine fish selectivity and caloric intake. Similarly, relationships among fish behavior, invertebrate drift, and stream hydrology could be evaluated. Data on water chemistry could be compared to data on the biota to determine if changes in water chemistry, say after an acid deposition event, have any effects on the lake and stream fauna.

Chapter I

INTRODUCTION

Accumulating evidence indicates that acid precipitation is falling in many areas of California (Lawson and Wendt 1982, Liljestrang and Morgan 1981, McColl and Bush 1984, Sickman and Melack 1984, McColl 1980). Furthermore, dry deposition of acids and other contaminants (Kerr 1981) and acid fogs (Waldman et al. 1982) increase acidic inputs. In the Sierra Nevada, the Tahoe basin and eastern and western slopes of the central crest receive acid precipitation during portions of the year (Leonard et al. 1981, Melack et al. 1982, Stohlgren and Parsons 1987).

The lakes and streams of the Sierra Nevada are among the most weakly buffered in the world. At present, however, it is not known if acidic inputs are affecting the biota of these aquatic systems, or what the responses of these systems would be to increased acid deposition. To investigate the effects of acidification on Sierran aquatic habitats we are conducting research on Emerald Lake, and its inlet and outlet streams, in Sequoia National Park, California. Emerald Lake was chosen as the focus of our studies because it is representative of subalpine and alpine waters in the Sierra Nevada, and accessible at all times of the year. Our investigations consist of two approaches: (1) A monitoring program and sediment analyses to provide the time series needed to distinguish the effects of anthropogenic disturbance from natural variation. (2) Experimental investigations to examine the sensitivity of aquatic communities to acidic inputs, and to predict the responses of aquatic communities to increased acidification.

Emerald Lake (lat. 36°35'N, long. 118°40') is located in Sequoia National Park at an elevation of 2780 m in the Sierra Nevada (Figures I-1 and I-2). The lake's watershed drains an area of ca. 113 ha, and the lake itself has a surface area of 2.85 ha and a maximum depth of 10.5 m. The watershed is granitic with sparse vegetation and little soil. Soils in the basin are representative of much of the subalpine region of the Sierra Nevada and are known to be weakly buffered against acidic inputs (EPA 1975, McColl 1981). Most of the subalpine and alpine lakes in the Sierra Nevada contain weakly buffered, calcium bicarbonate waters (Melack et al. 1985). Emerald Lake's chemical composition is representative of high altitude Sierra Nevada waters, with a summer alkalinity of ca. 30 μeq^{-1} and summer pH ca. 6.3 (Melack et al. 1985).

Emerald Lake has a simple morphometry with two small islands near its inflows and near its outflow (Fig. I-3). Below 8 m the sediments are organic rich and flocculent. The steeper upper slopes are slabs of granite, with patches of gravel and sand conspicuous in the south east corner. Sample stations referenced in subsequent chapters are indicated on Figure I-3.

Emerald Lake is drained by one major outflow stream and fed by four small inflow streams. The outflow stream has a mean width of 1.5 meters, a mean depth of 20 cm, and is composed of small pools and riffles. Approximately 100 m below Emerald Lake the outlet stream flows into a large pool. The outflow stream is shaded by willows and lodgepole pine. Rock surfaces are often covered with moss and algae. The inflow streams are shallow (2 - 3 cm) and narrow (0.5 m) and flow over steeply-sloped granitic bedrock just above the lake. Two of the inflows usually cease flowing in late summer, whereas the other two flow year around. The permanent inflows receive little shading and dense growths of macroalgae often grow on bedrock surfaces. The lake tended to moderate the hydrology of the outflow stream, making it a stable habitat compared to the inflow streams, and inflow streams are often scoured in the winter by ice and snow.

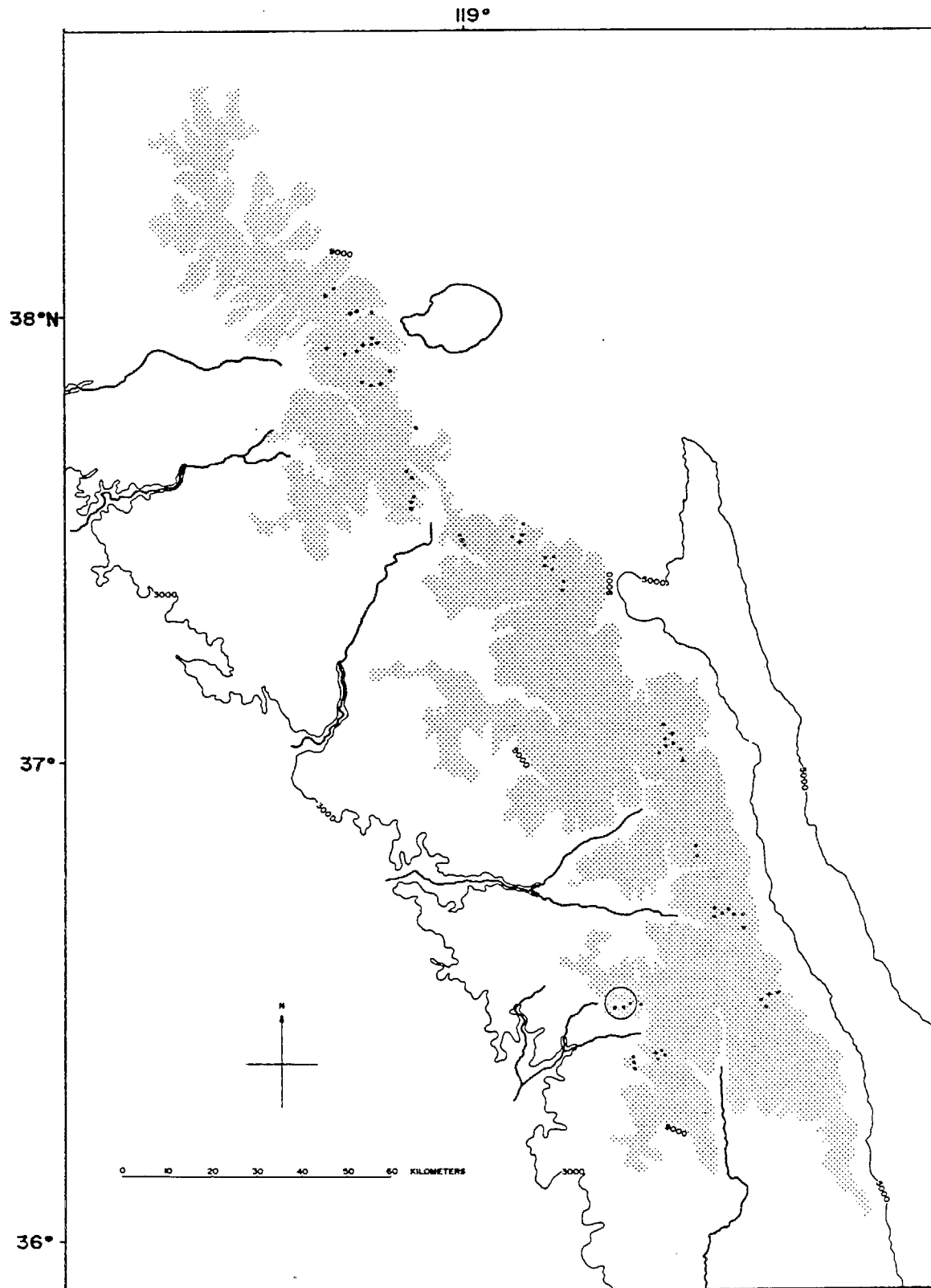


Figure I-1. Circle indicates location of Emerald Lake and upper Marble Fork, Kaweah River basin. Dots mark lakes sampled in summer of 1981 (Melack et al. 1982). Shaded area lies along Sierra Nevada crest and is over ca. 3000 m in elevation.

Upper Marble Fork of Kaweah River Drainage

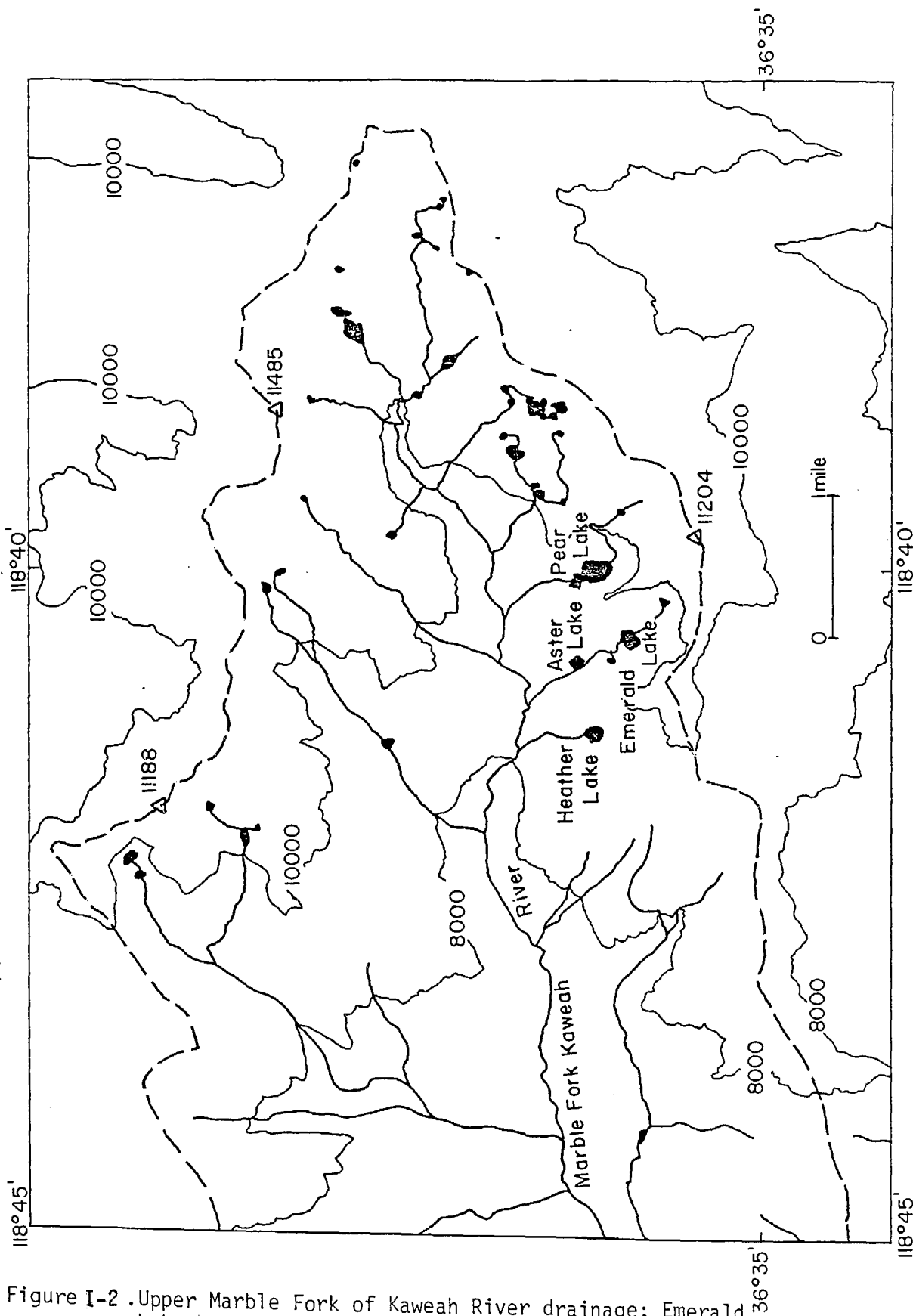
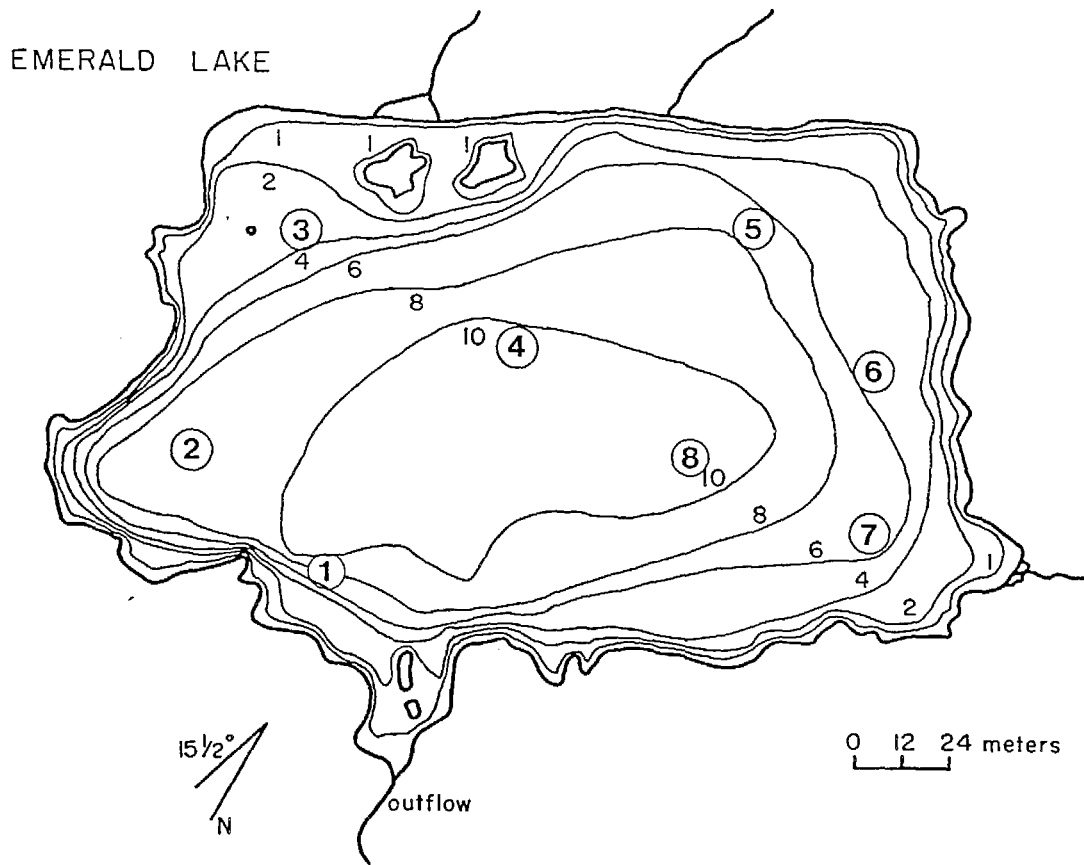


Figure I-2. Upper Marble Fork of Kaweah River drainage; Emerald Lake basin in center. Contours are in feet above sea level. Dashed line demarcates drainage of Upper Marble Fork.

Figure I-3. Bathymetric map of Emerald Lake. Contour intervals in meters. Circled numbers are stations used for chemical and biological sampling.



Chapter II.1

SEASONAL VARIABILITY IN SOLUTE CHEMISTRY

Introduction

Lakes in the Sierra Nevada are among the most dilute and weakly buffered in the United States (Melack et al. 1985, EPA 1986). The very low concentrations of solutes is owed to the large volume of extremely dilute snow (Laird et al. 1985), that provides most of the runoff, and to the granitic rocks in the watersheds that weather slowly (Garrels and MacKenzie 1967). Hence, the lakes of the Sierra Nevada are likely to closely resemble the chemical composition of the snow melt (Melack et al. 1982). The congruence will depend upon the residence time of the water and reaction kinetics in the soil of the watershed and in the lakes and their sediments.

Emerald Lake has calcium-bicarbonate water with very low acid neutralizing capacity (ANC) as is typical of high altitude lakes in the Sierra Nevada (Melack et al. 1985). Its current pH is near the low end of the range observed in Sierra lakes, but it has shown no declining pH trend over the last 160 years (Chapter III). Brief, episodic pH and ANC depressions have occurred during intense summer rains and snowmelt (see below).

The purposes of our studies of major solute chemistry in Emerald Lake are to characterize the chemical composition and its episodic, seasonal and interannual variability. These measurements permit evaluation of potential chemical influences on the biota, and of how the lake responds to inflows from its watershed and from exchanges with its sediments. The data described here span the period from 14 June 1984 to 29 July 1986. Thermal and dissolved oxygen stratification and changes in concentration of major anions, cations and trace metals are considered.

Methods

We collected samples from four depths in the lake and in the outflow biweekly during the ice-free and snowmelt seasons and monthly during the winter. Two inflows were sampled during the ice-free season every two weeks. Vertical profiles (one meter intervals) of temperature and dissolved oxygen was measured on each sampling data. Temperature was recorded with a thermistor and Wheatstone bridge circuit (Yellowsprings Instrument Model 58)

readable to 0.1°C. Treatment of chemical samples in the field and laboratory procedures were performed as outlined in Table II-1. Samples are collected via a Tygon hose attached to a peristaltic pump or with a plastic Kemmerer bottle. Samples for major solutes and nutrients were collected in linear polyethylene bottles that were cleaned with 10% HCl and rinsed at least six times with deionized, distilled water. Sample bottles for trace metals were cleaned as described in Tonnessen (1983). Filtration, if indicated, was done immediately after sample collection. Alkalinity and pH could be done on site, but our experience suggests that the short delay (2-4 hours) required to return to the laboratory did not adversely influence the data. Electrical conductance and dissolved inorganic nutrients are determined immediately upon return to the laboratory. Cations (Na, K, Mg, Ca), anions (Cl, SO₄, NO₃), silica and metals (Al, Fe, Mn) were stored at 4°C.

Results

Emerald lake is dimictic: it is thermally stratified under ice, mixed from top to bottom at ice out, restratified in midsummer and mixed again in autumn. Periods of complete mixing are evident in Fig. II-1 where the temperature traces for subsurface and 9.5 m water overlap or cross. Ice cover is indicated by the cross hatched bars across the top. Where the lines diverge, the lake is thermally stratified. During the autumn the lake remains isothermal for several weeks, while in the spring when the lake is warming, it is isothermal for less time. An anomaly is apparent in July 1984; the lake almost became isothermal. This feature was caused by an intense rain storm which will be discussed further below.

When the lake is ice covered the thermal gradient begins under or within the ice and reaches maximum density at between 3 and 6 m. The depth of gradient descends during snowmelt. In mid-summer, the epilimnion reaches to 5 to 7 m, and the thermocline continues to the bottom. These differences in stratification near the bottom have important implications for sediment-water exchanges (see section II.3).

Maximum summer temperatures in subsurface waters reached 16°C in 1984 and 18.5°C in 1986; the winter minimum was 0°C. The hypolimnion decreased to only 4°C, the maximum density of freshwater, and warmed to 11.5°C in 1984 and 15°C in 1985.

The annual cycle of dissolved oxygen stratification (Figure II-2) paralleled that of temperature. Under ice, dissolved oxygen is stratified with depletion near the sediments. During holomixis in spring and autumn, dissolved oxygen is near saturation throughout the water column. In midsummer, anoxia develops in the hypolimnion. The periods of low oxygen have important implications for sediment water exchange and ANC generation (see section II.3).

Times series plots of important chemical species at subsurface and 9.5 m depths are presented in Figures II-3 to II-16. Electrical conductivity of Emerald lake is low, ranging from 2 to 9 $\mu\text{S cm}^{-1}$. Minima are associated with snowmelt, and gradual increases occur during the ice free season. In subsurface waters pH (Fig. II-4) ranged from 5.6 to 6.6 with low values associated with a rain storm in 1984 and snowmelt in 1986. Near bottom pH's declined to 5.7 to 5.8 during stratified periods and reached highs of 6.2 to 6.3. ANC (Fig. II-5) reached minima of zero after a mid July 1984 rain storm and during snowmelt in 1986. A maximum of 60 $\mu\text{eq/l}$ occurred under ice in the water of 1984-85. In general, ANC is higher in the deeper water than in the near surface water when the lake is thermally stratified.

Nitrate concentrations (Fig. II-6) ranged from 0.5 to 14 μM but were generally between 1 and 5 μM . The highest values occurred during snowmelt in 1986. Depth differences were usually slight. Sulfate (Fig. II-7) ranged from 5.4 to 7.5 $\mu\text{eq/l}$ except during the spring of 1986 when it rose to 9 and then fell to 1.5 $\mu\text{eq/l}$. Chloride (Fig. II-8) ranged from 2 to 7.5 $\mu\text{eq/l}$ in subsurface waters and from 2 to 5 $\mu\text{eq/l}$ in near bottom waters. Silica (Fig. II-9) was high, ranging 15 to 58 μM .

Base cations (Ca, Mg, Na, K; Figures II-10 to II-14) are dominated by Ca and, in general, follow a seasonal pattern similar to the electrical conductivity. An anomalously high Na concentration in July 1984 is associated with a major rain storm; a peak in chloride occurred simultaneously (Fig. II-8). The sum of base cations (Fig. II-10) range in concentration from 8 $\mu\text{eq/l}$ to 60 $\mu\text{eq/l}$. Ammonium (Fig. II-15) remains low ($< 1.5 \mu\text{M}$) in the epilimnion but can reach 12.5 μM in the hypolimnion during periods of stratification.

Ten dates were sampled during snowmelt in 1986 (Figures II-16 A and B). During the initial stages (April and May), sulfate and nitrate concentrations increased while base cations and ANC declined in the subsurface water. A

minima in all constituents occurred on 9 June 1986. Samples from 9.5 m changed little until June, when a pronounced decline in base cations and ANC contrasted with the slight decline in sulfate and nitrate. Multiple stations in a transect across the lake were sampled on 6 May, 18 May, 25 May, 10 June and 2 July 1980. These vertical profiles indicated considerable variability just under the ice compared to the near bottom water. In May, nitrate and sulfate were higher nearer the ice than deeper, while ANC and base cations showed the opposite trend; pH varied little with depth. Not until early July were the concentrations of major solutes fairly homogeneous from top to bottom.

Time series plots of concentrations of chemical species in the main inflow are shown in Figures II-17 to II-28. Outflow values paralleled those in the subsurface lake. Inflow pH's ranged from 5.7 to 6.5 with minima during snowmelt. ANC varied from 4 to 45 $\mu\text{eq/l}$; minima occurred during snowmelt and during a rain storm in July 1984. Nitrate concentrations were modest during summer and reached high levels when the watershed was snow covered and during snowmelt. Sulfate was less variable than nitrate, but did peak during snowmelt. Silica and base cations had strong seasonal changes with minima during snowmelt and maxima in early autumn with high values continuing into the early winter.

Aluminum concentrations are very low in the inflows to Emerald lake (Figure II-29 A and B). Unfiltered samples varied in concentration from 0.6 to 2 μM . Iron (0.1 to 1 μM) and manganese (<0.01 to 0.2 μM) were also very low. In the main inflow slightly higher values of all the trace metals occurred during late summer in 1984 and 1985.

Discussion

Only three high altitude California lakes have been sampled year round. Stoddard (1986, 1987) investigated Gem Lake, an alpine lake on the eastern side of the Sierra crest, in 1982-1984. Southern California Edison initiated in 1983 an ongoing study of subalpine Eastern Brook Lake (Lund and Nodvin, personal communication). Emerald lake has been sampled since 1982. These three investigations have included vertical profiles of temperature, dissolved oxygen, pH, acid neutralizing capacity, nutrients and major solutes.

Several important features are evident in the seasonal variability of the three lakes. Under ice, the lakes are thermally stratified and dissolved oxygen decreases and ANC increases. However, much higher ANC occurred under the ice in Gem and Eastern Brook Lakes than in Emerald lake. During snowmelt the lakes are flushed with very dilute water. Reduced dissolved oxygen in mid-summer can be associated with increased ANC near the bottom.

The conditions in Gem Lake and its watershed responsible for its elevated ANC under ice cover and low ANC during snowmelt are discussed in detail by Stoddard (1987). His major conclusions are that dilution rather than acidification accounts for the snowmelt related decrease in ANC, and that ANC increases in autumn and winter can be attributed entirely to weathering reactions in the watershed. No evidence for reduction reactions contributing to ANC in the lake was found. By application of a mass balance, Stoddard deciphered the role of weathering products in surface runoff and in deep circulation to the lake's ANC dynamics.

To evaluate the relations among major solutes as an indication for the importance of weathering reactions in ANC generation and of nitric and sulfuric acids as acidifying aspects, a series of regression analyses were performed for Emerald Lake. Calcium, summation of Ca, Mg, Na and K and summation of Ca, Mg, Na, K, H and NH_4 explained 55 to 71% of the variance in ANC (Figures II-30 to II-34); the best prediction is provided by the summation of all cations. Slightly more variance was explained for samples from 9.5 m than from subsurface. The implication of these results is that weathering reactions and organic matter decomposition in the lake sediments contribute ANC. Regression analyses of sulfate and nitrate versus alkalinity indicated little or no relation ($r^2 < 0.001$ to 0.17). During snowmelt in 1986 r^2 rose to 0.82 (Fig. II-35) and imply some contribution of strong acids to the depression in pH and alkalinity. Further elaboration of these processes is provided in Chapter II.3.

Summer rain in the Sierra Nevada is usually acidic (Melack et al. 1982, Stohlgren and Parsons 1987), and intense storms occasionally occur. In mid-July 1984 Emerald lake experienced 4.5 cm of pH 4.3 rain. The limnological consequences of this storm were conspicuous and persistent. Five days after the storm, the first date sampled after the rain, the upper water had zero ANC, a decrease from ca. 10 $\mu\text{eq/l}$. Coincident with the runoff from the storm, the Secchi disk transparency declined from 7 m to 0.5 m. As a

consequence of the increased turbidity, the lake developed stronger thermal stratification than in other years. In the hypolimnion dissolved oxygen declined to almost zero, ANC reached 60 $\mu\text{eq/l}$ and dissolved inorganic phosphorus increased. The autumn peak in chlorophyll was likely caused by the availability of phosphorus as the lake mixed. In turn, the decay of organic matter derived from this autumn algal peak, contributed to the development of low oxygen in the hypolimnion under the ice. The near anoxic conditions of the sediment-water interface resulted in enhanced release of ANC and phosphorus which, in turn, stimulated a spring phytoplankton increase just after ice out in 1985. This scenario is reasonable and probable but speculative. Factors other than the mid-July storm surely contribute to the chain of events. However, the point to be made is that acidic rains are likely to have multifarious affects not solely tied to their acidity.

Table II-1. Chemical analysis scheme for dissolved constituents.

<u>Constituent</u>	<u>Sample Treatment in Field</u>	<u>Analysis Technique</u>
Electrical conductance	Unfiltered	Conductivity bridge
pH	Unfiltered	Low ionic strength, glass combination electrode; digital meter
Acid neutralizing capacity (ANC)	Unfiltered	Gran titration with micrometer buret, pH as above
Dissolved oxygen	In situ	Polarographic oxygen electrode
Ca, Mg, Na, K	Filtered (glass fiber filter)*	Atomic absorption spectrophotometry (Varian)
Cl	Filtered*	Ion chromatography
SO ₄	Filtered*	Ion chromatography
NO ₃	Filtered*	Ion chromatography
PO ₄	Filtered*	Molybdenum blue - ascorbic acid (Strickland and Parsons 1972)
NH ₄	Filtered*	Indophenol blue (Strickland and Parsons 1972)
Al, Fe, Mn	Unfiltered and filtered (0.1 Nucleopore filter) acidified with Ultrex HNO ₃	Atomic absorption spectrophotometry with graphite furnace
SiO ₂	Filtered*	Silico-molybdate (Strickland and Parsons 1972)

Fig. II-1

TEMPERATURE TIME SERIES

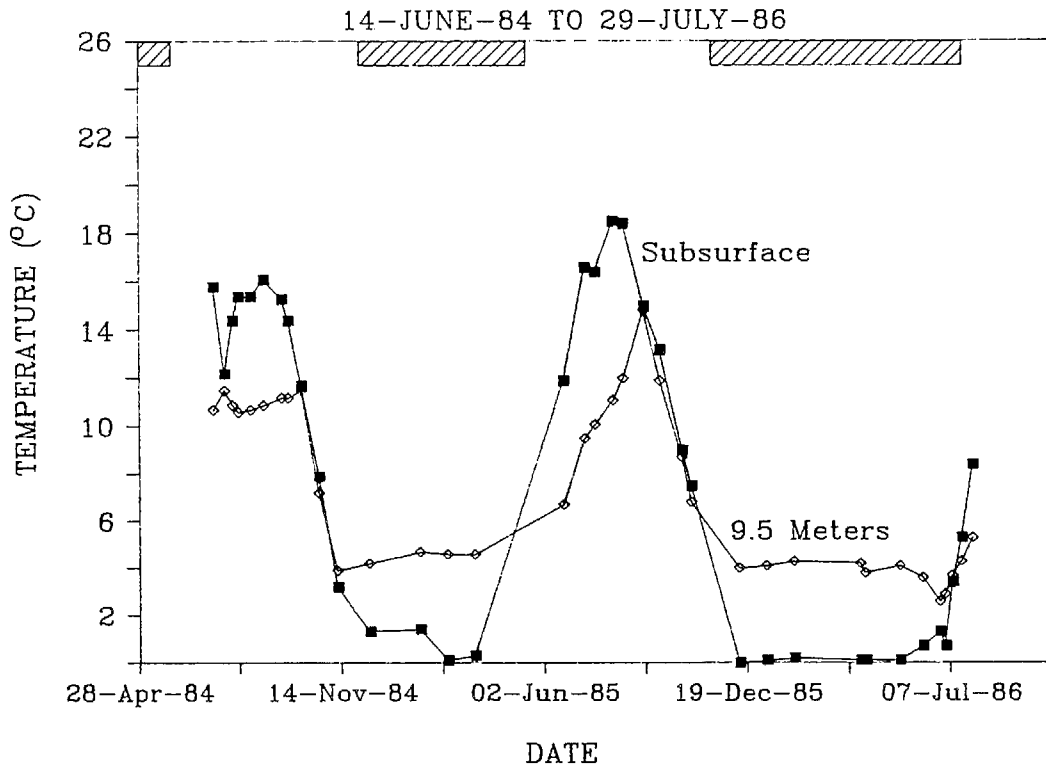


Fig. II-2

OXYGEN TIME SERIES

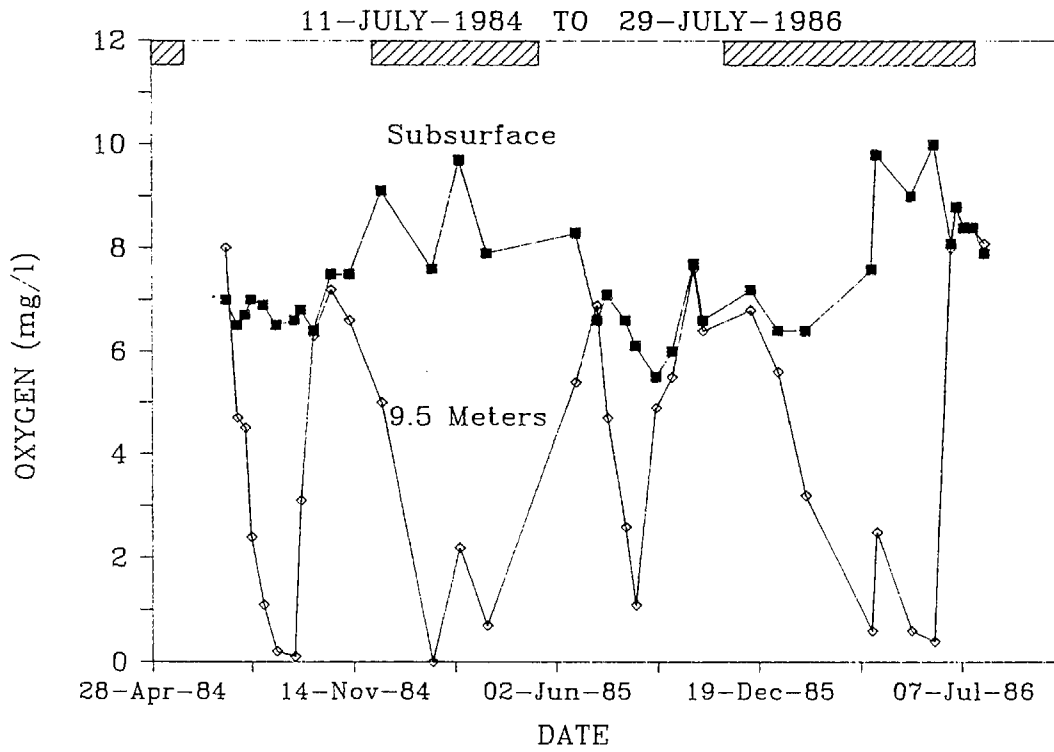


Fig. II-3

CONDUCTIVITY TIME SERIES

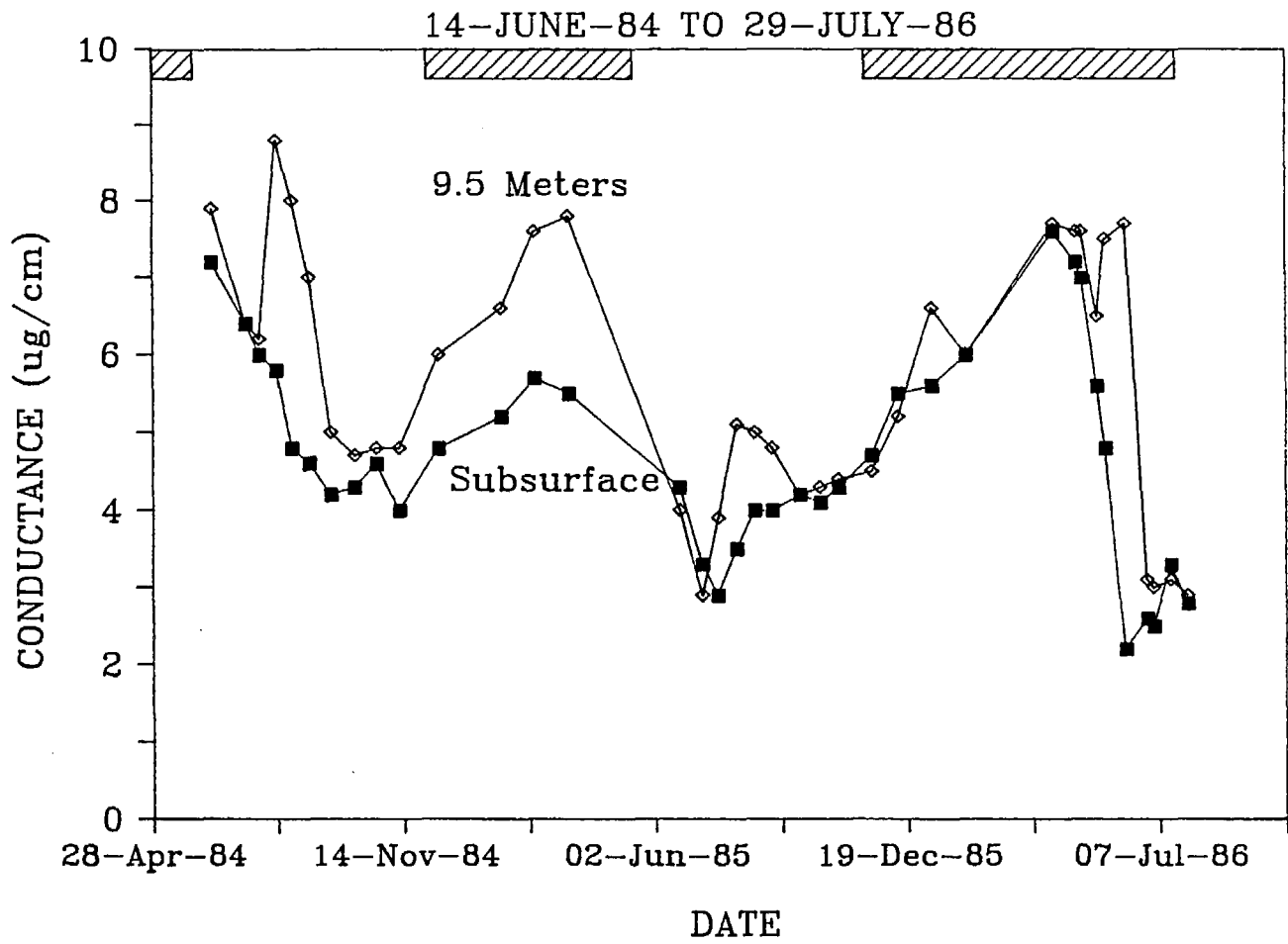


Fig. II-4

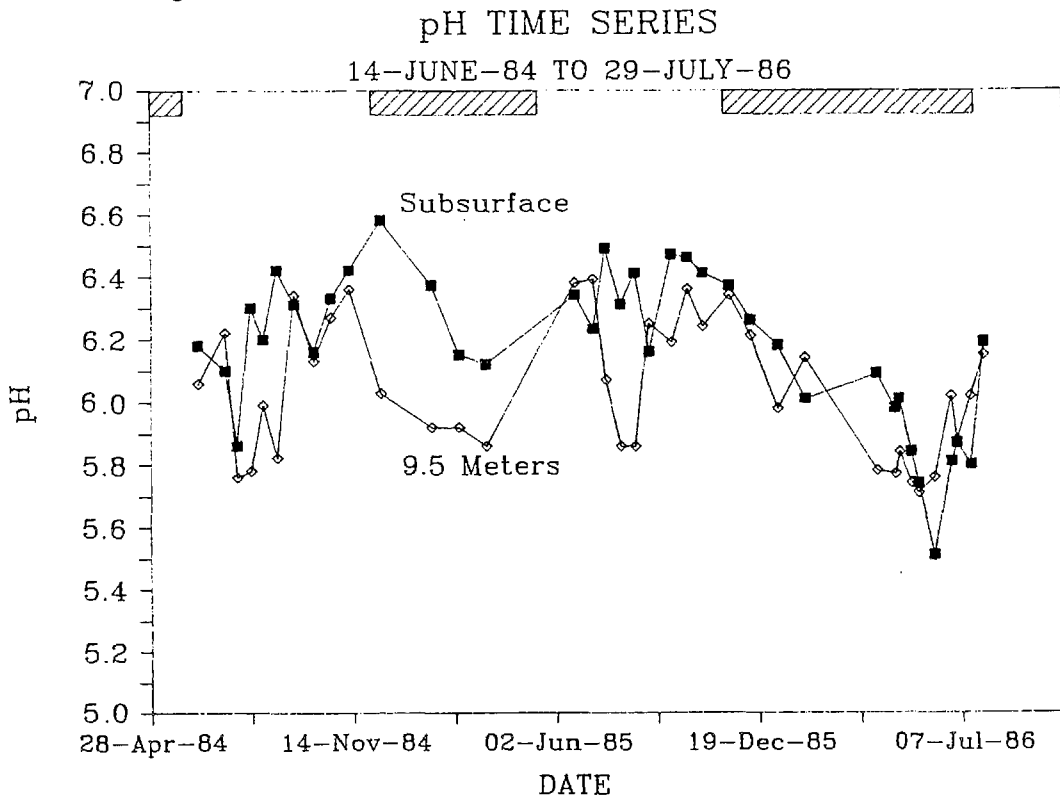


Fig. II-5

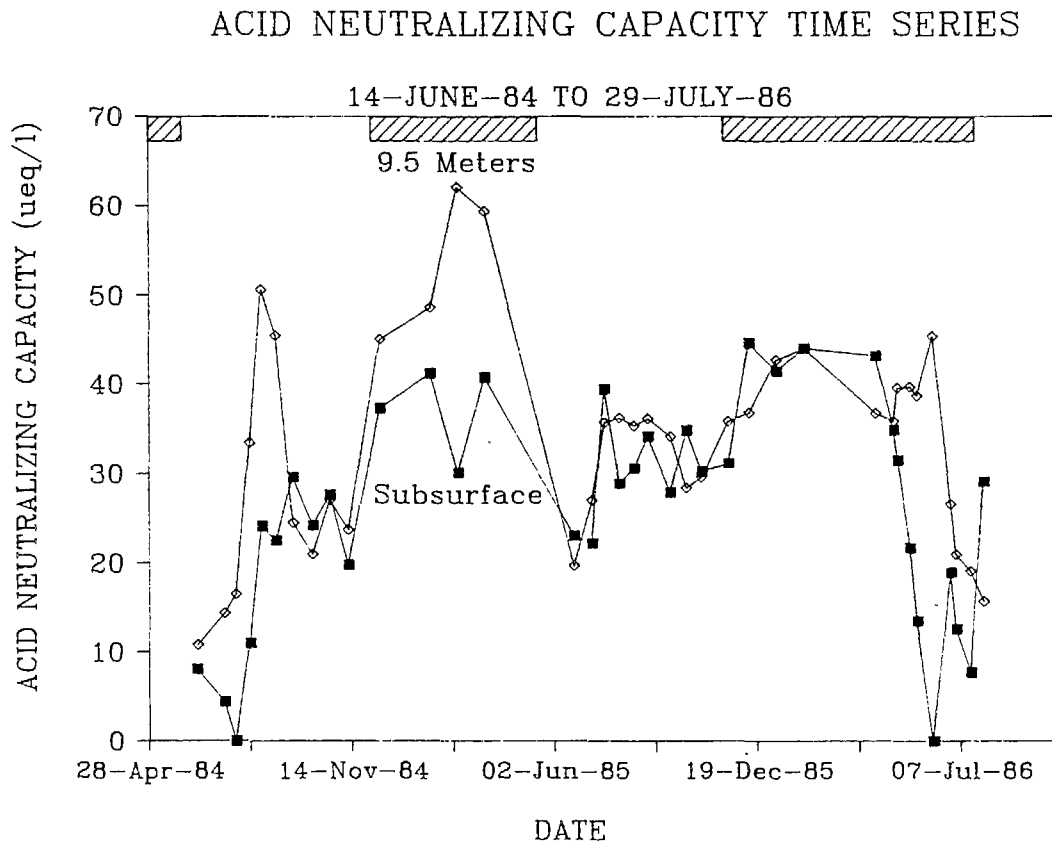


Fig. II-6

NITRATE TIME SERIES

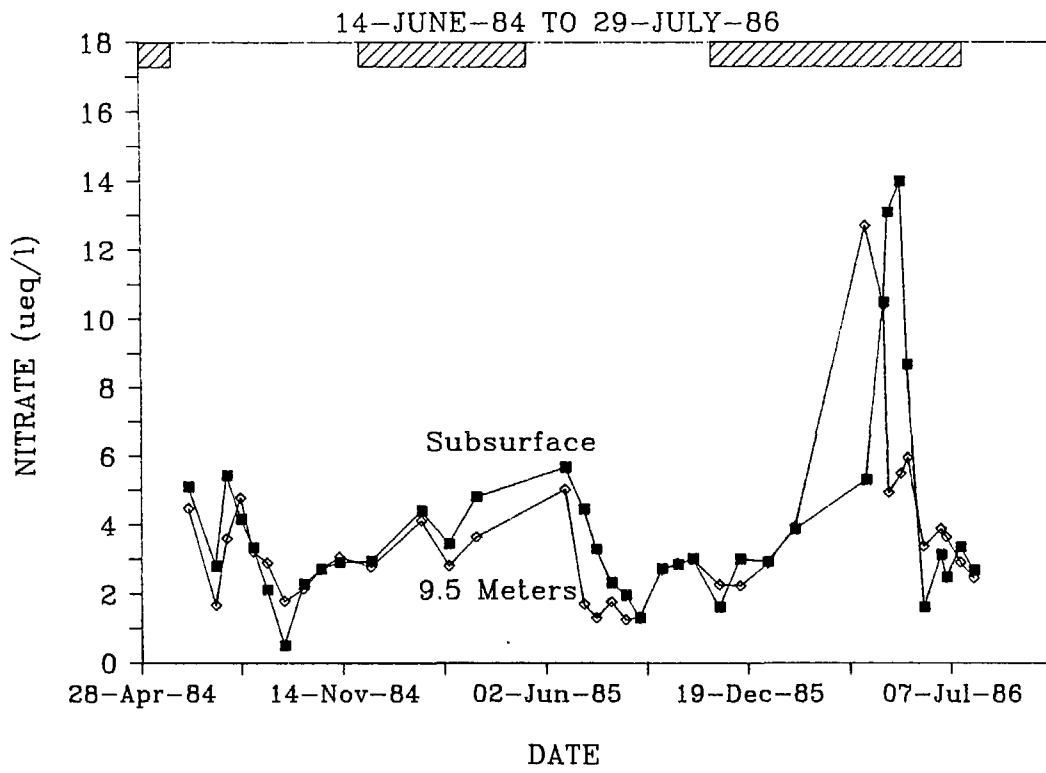


Fig. II-7

SULFATE TIME SERIES

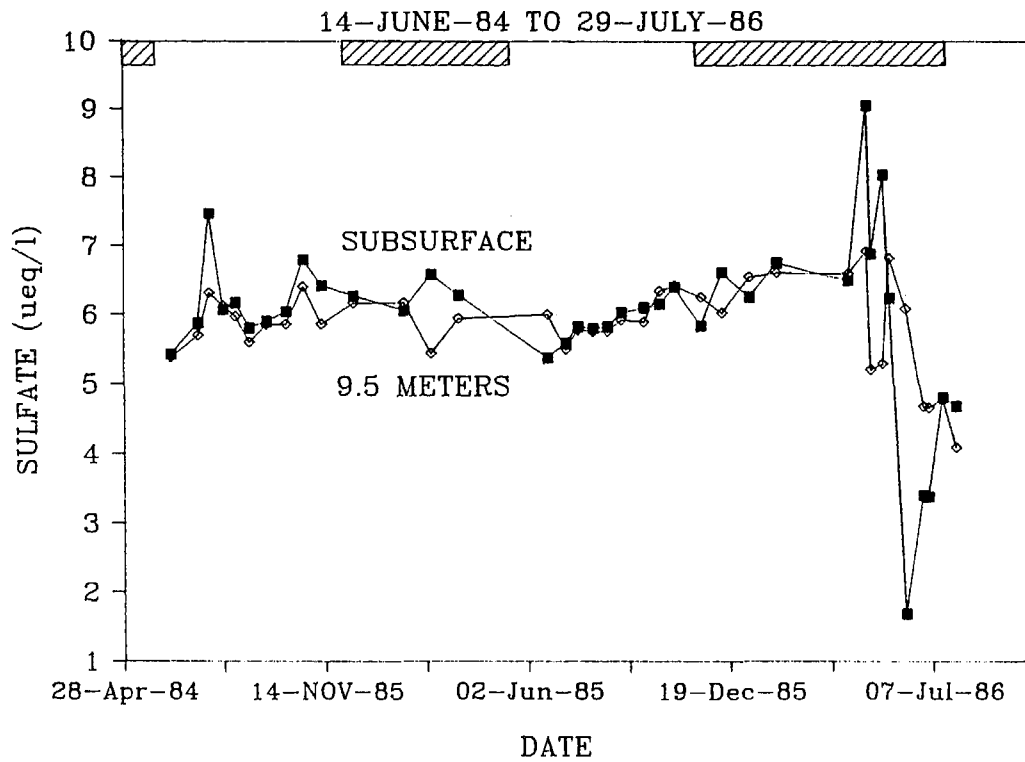


Fig. II-8

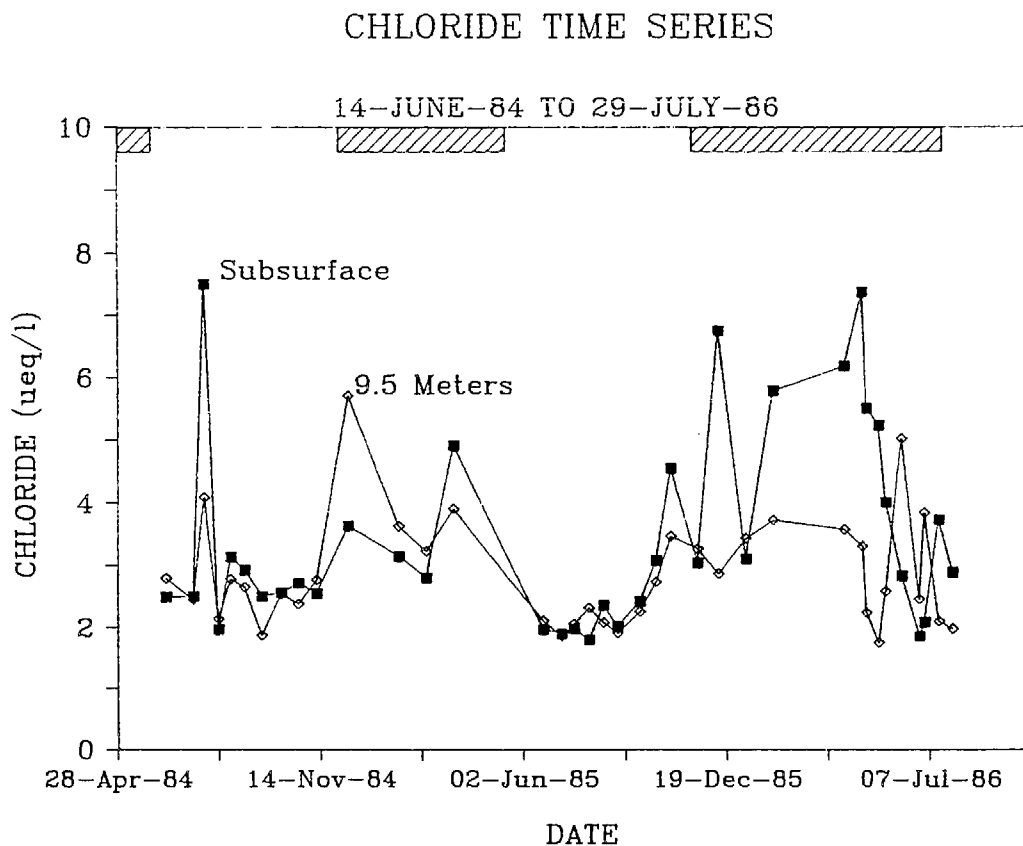


Fig. II-9

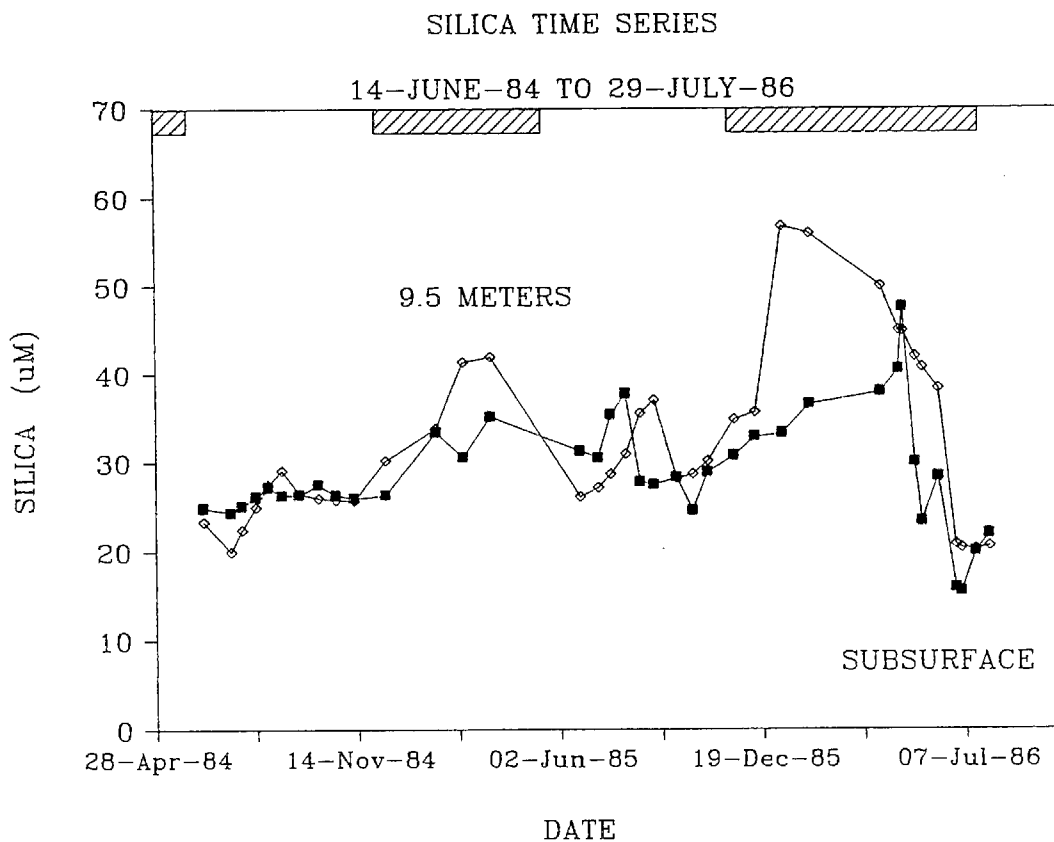


Fig. II-10

SUM OF Ca + Mg + Na + K TIME SERIES 14-JUNE-84 TO 29-JULY-86

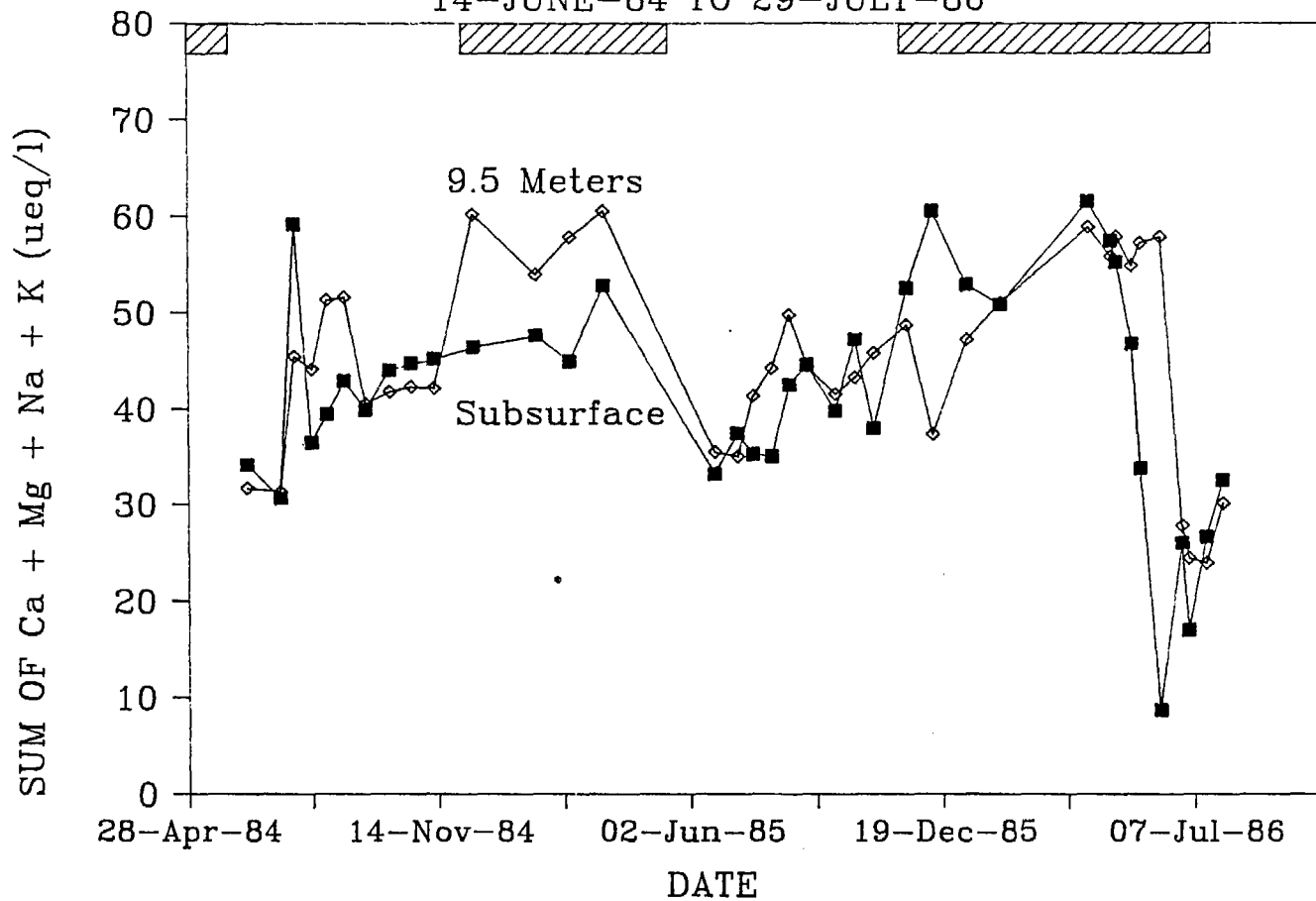


Fig. II-11

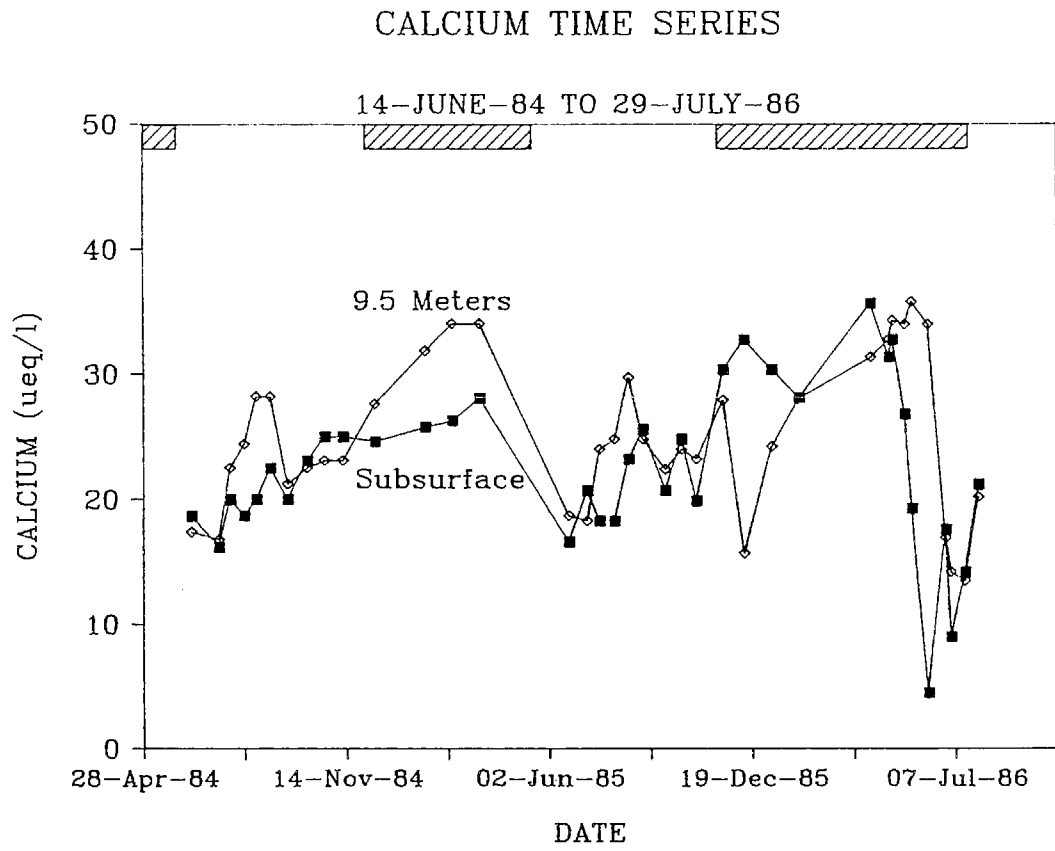


Fig. II-12

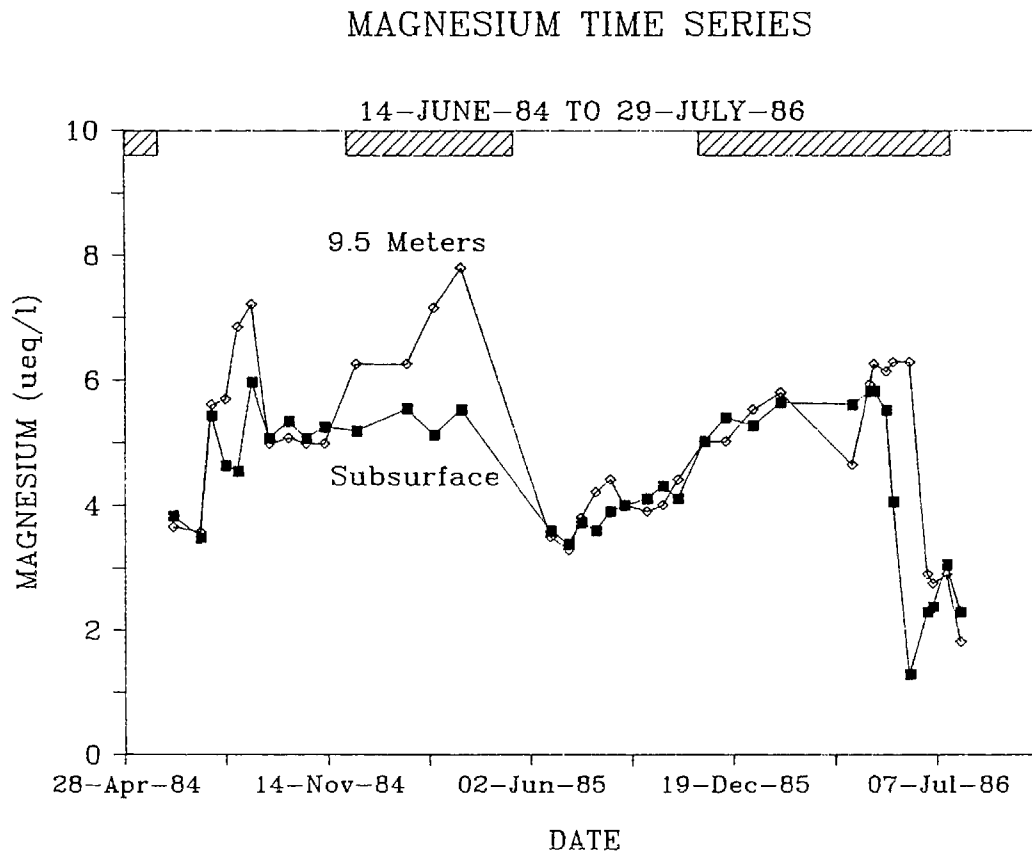


Fig. II-13

SODIUM TIME SERIES

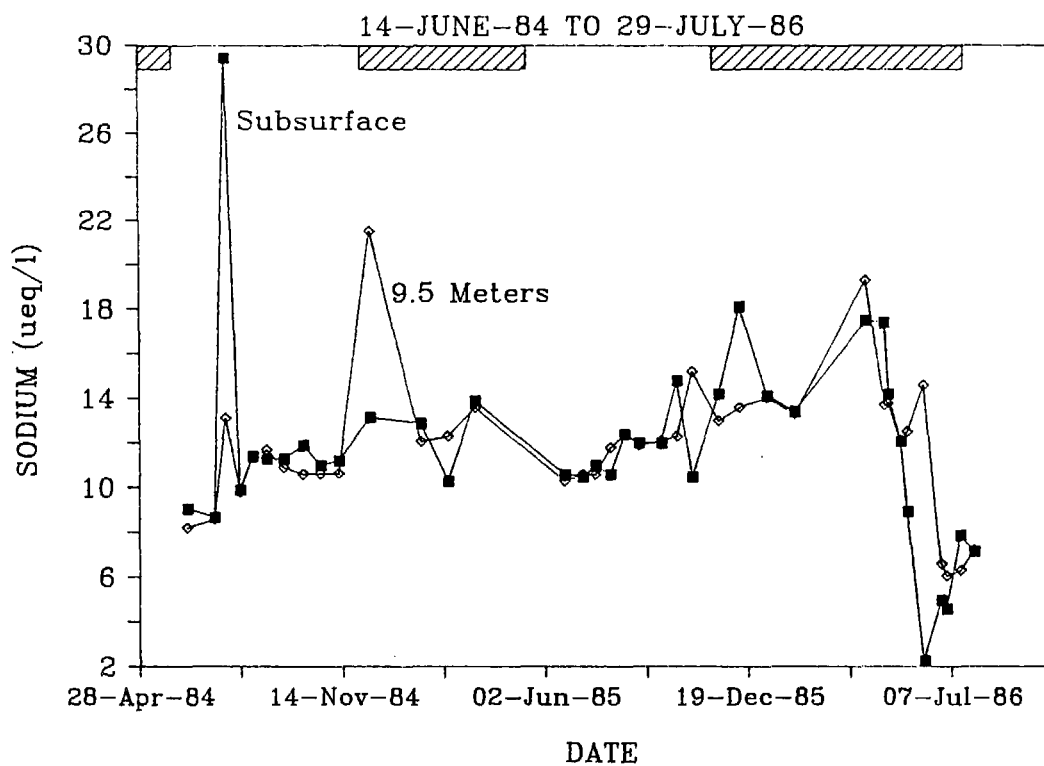


Fig. II-14

POTASSIUM TIME SERIES

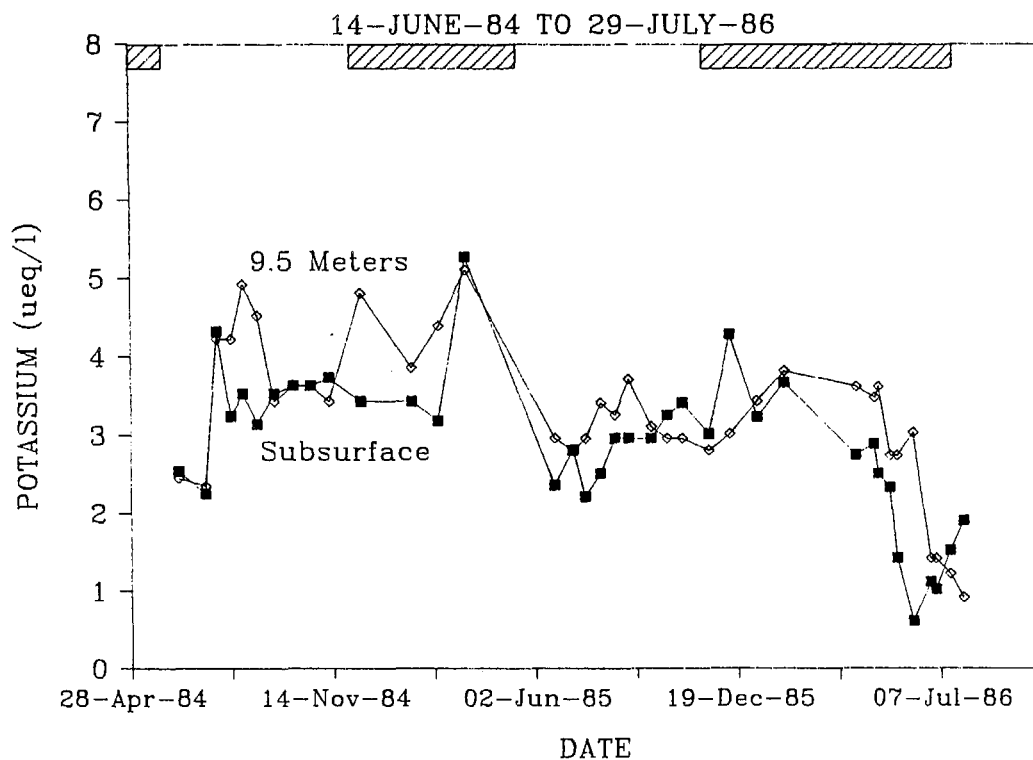


Fig. II-15

AMMONIUM TIME SERIES

14-JUNE-84 TO 29-JULY-86

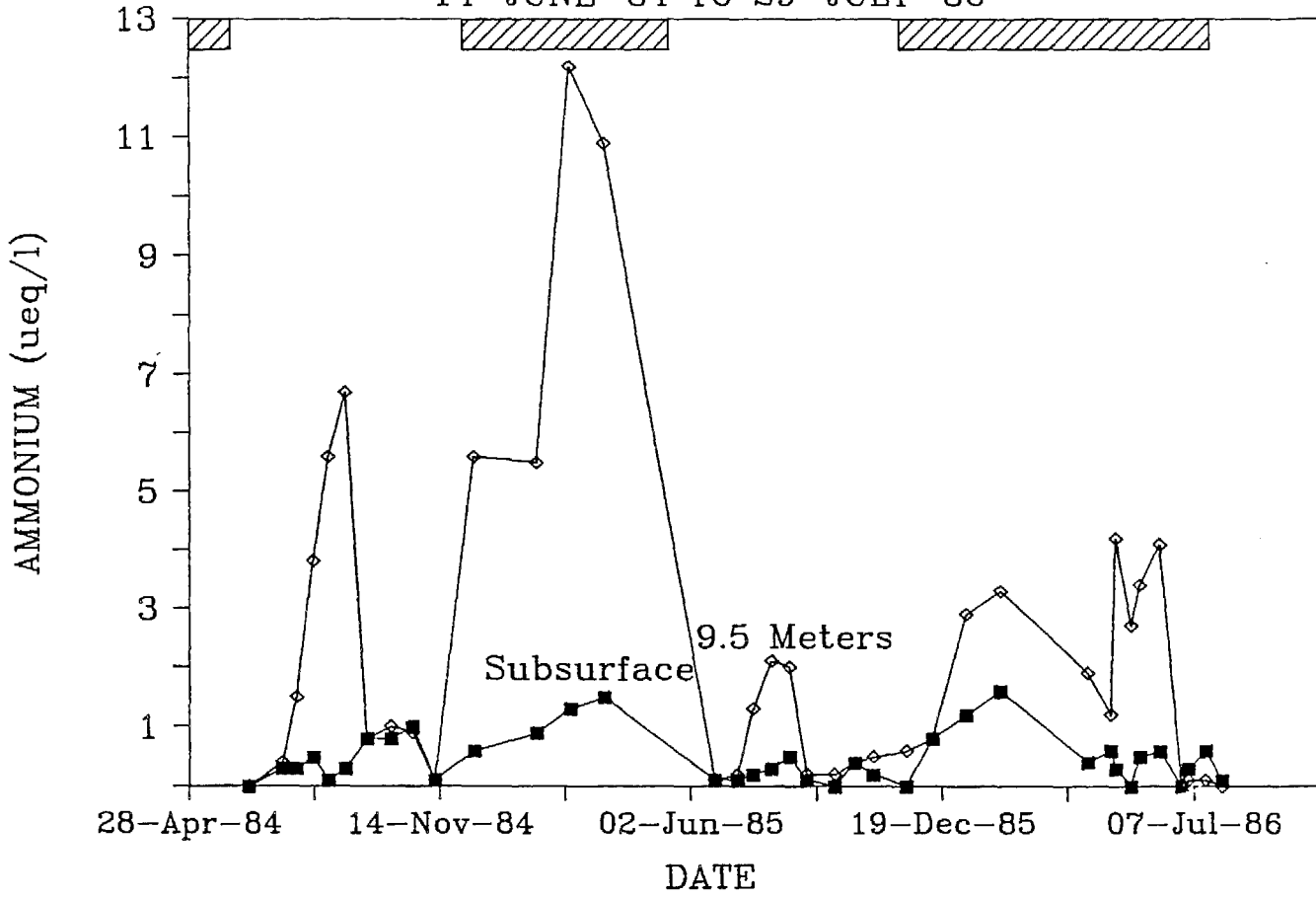


Fig. II-16A
 TIME SERIES THROUGH SNOWMELT-SUBSURFACE

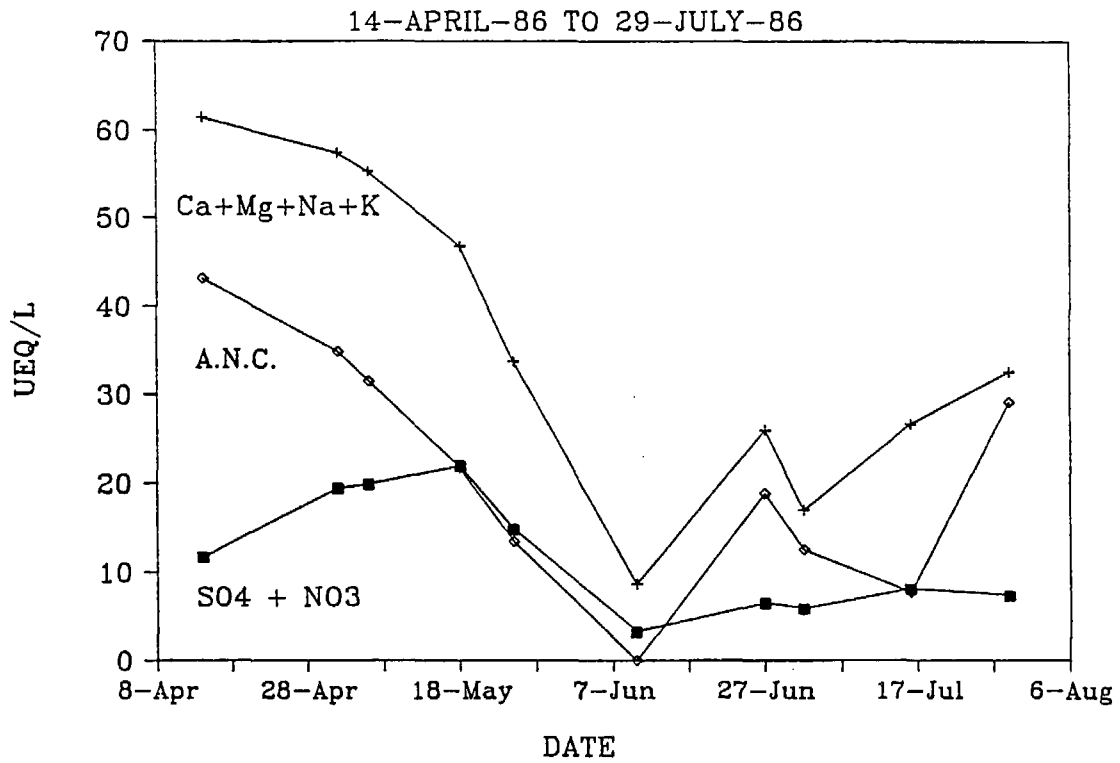


Fig. II-16B
 TIME SERIES THROUGH SNOWMELT-9.5 METERS

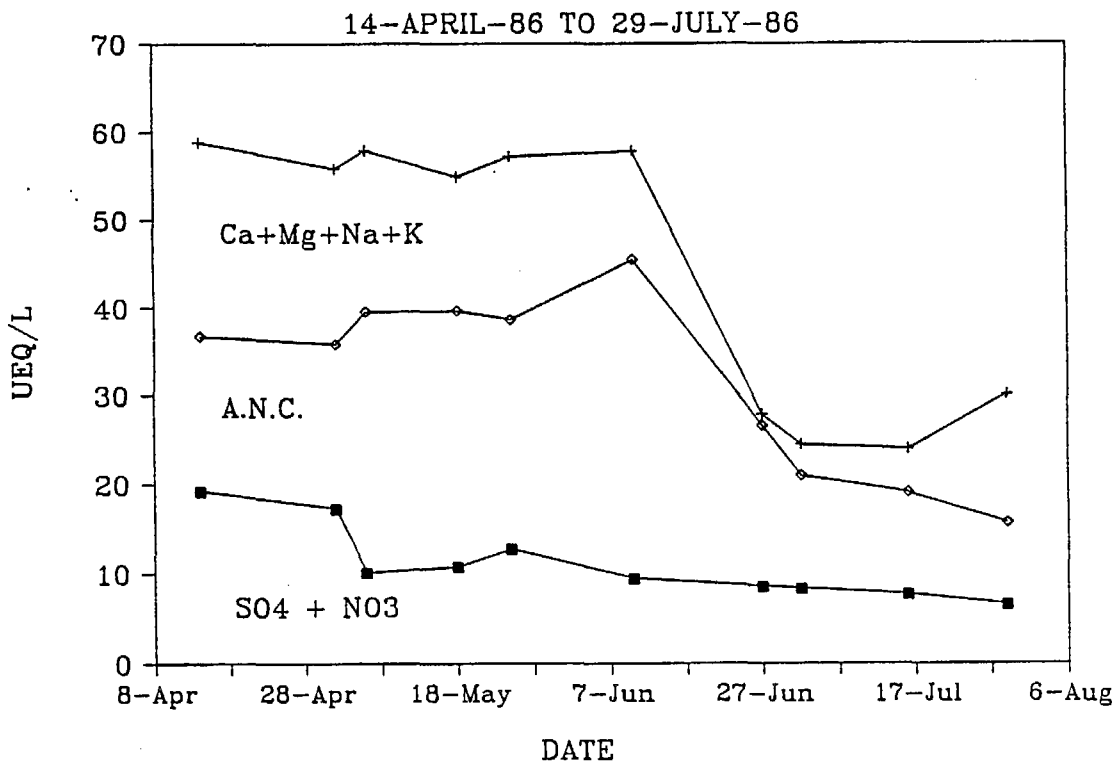


Fig. II-17
CONDUCTIVITY TIME SERIES - MAIN INFLOW

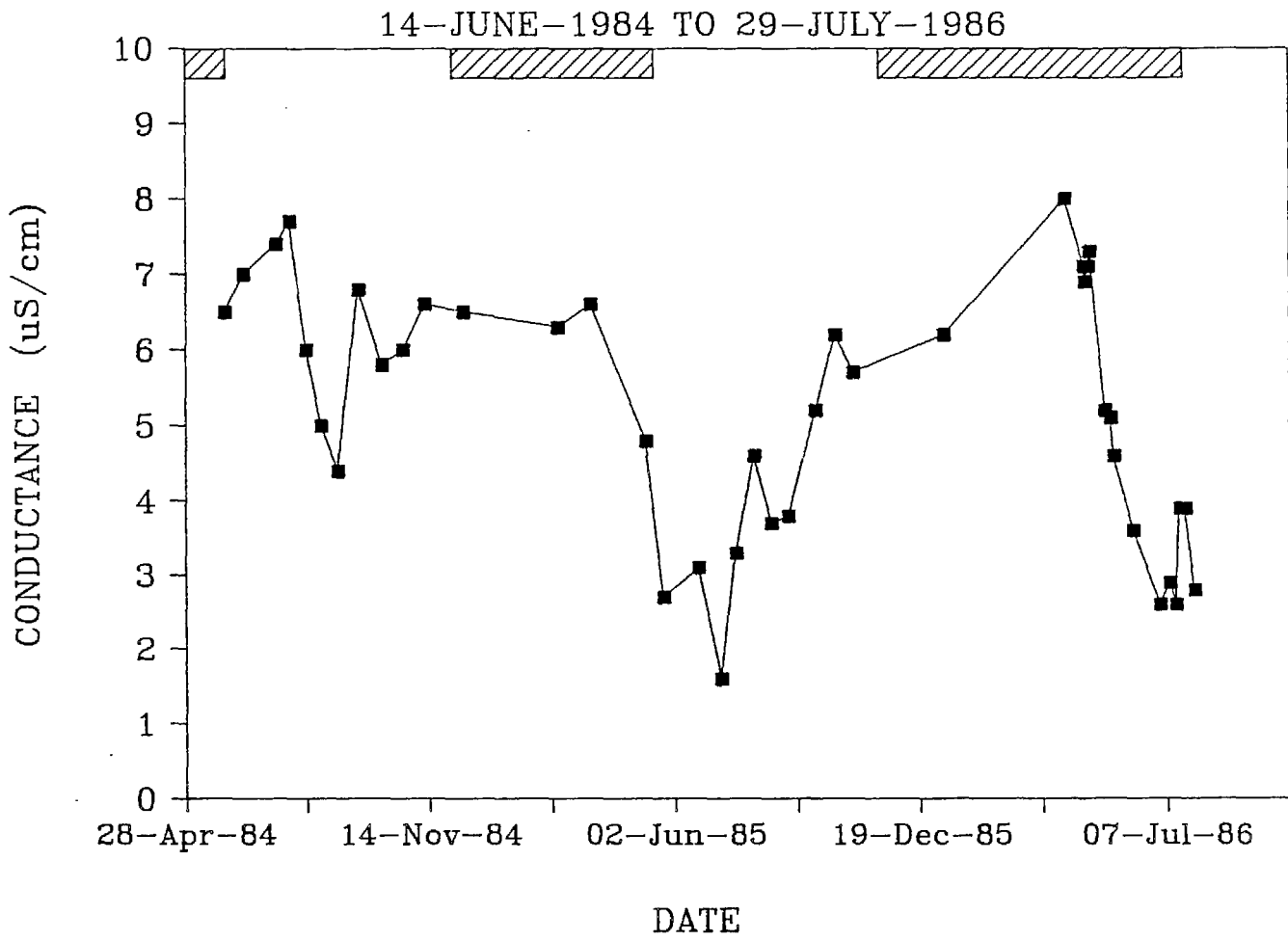


Fig. II-18

pH TIME SERIES - MAIN INFLOW

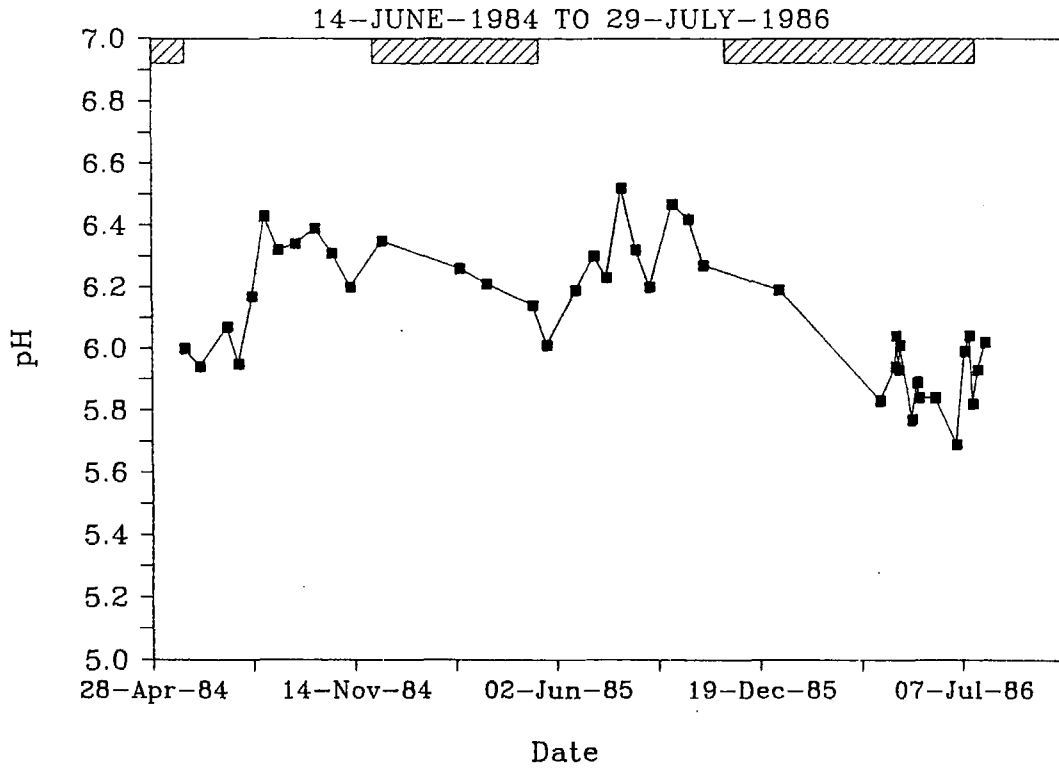


Fig. II-19

A.N.C. TIME SERIES - MAIN INFLOW

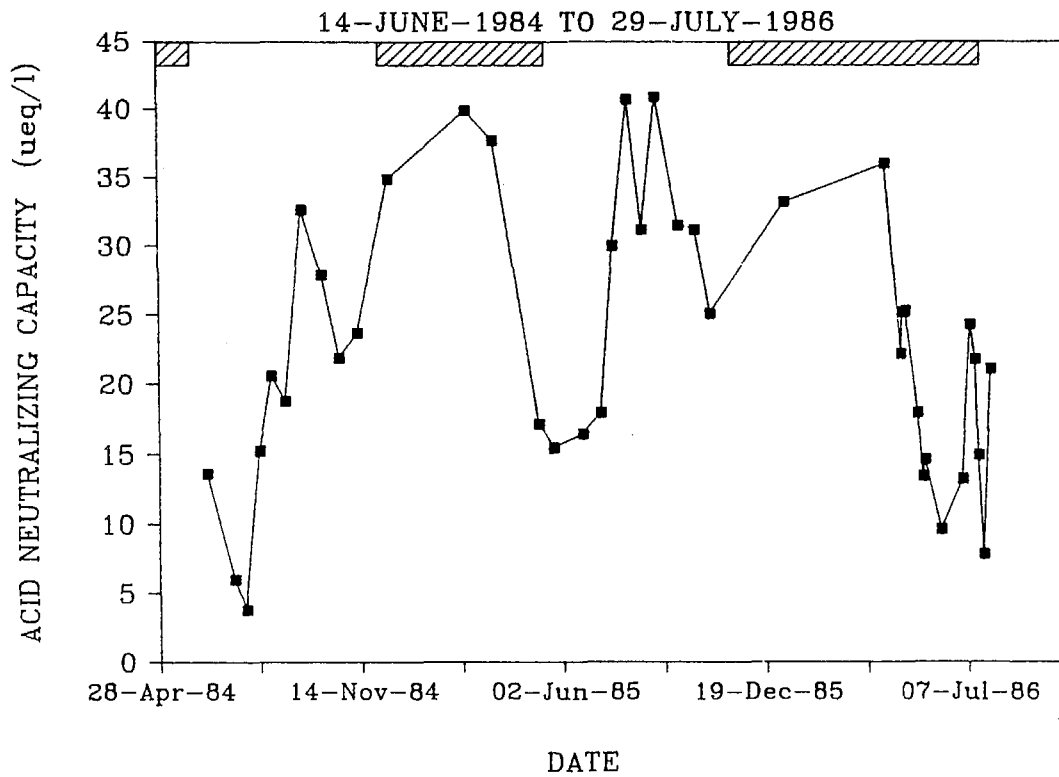


Fig. II-20

NITRATE TIME SERIES - MAIN INFLOW

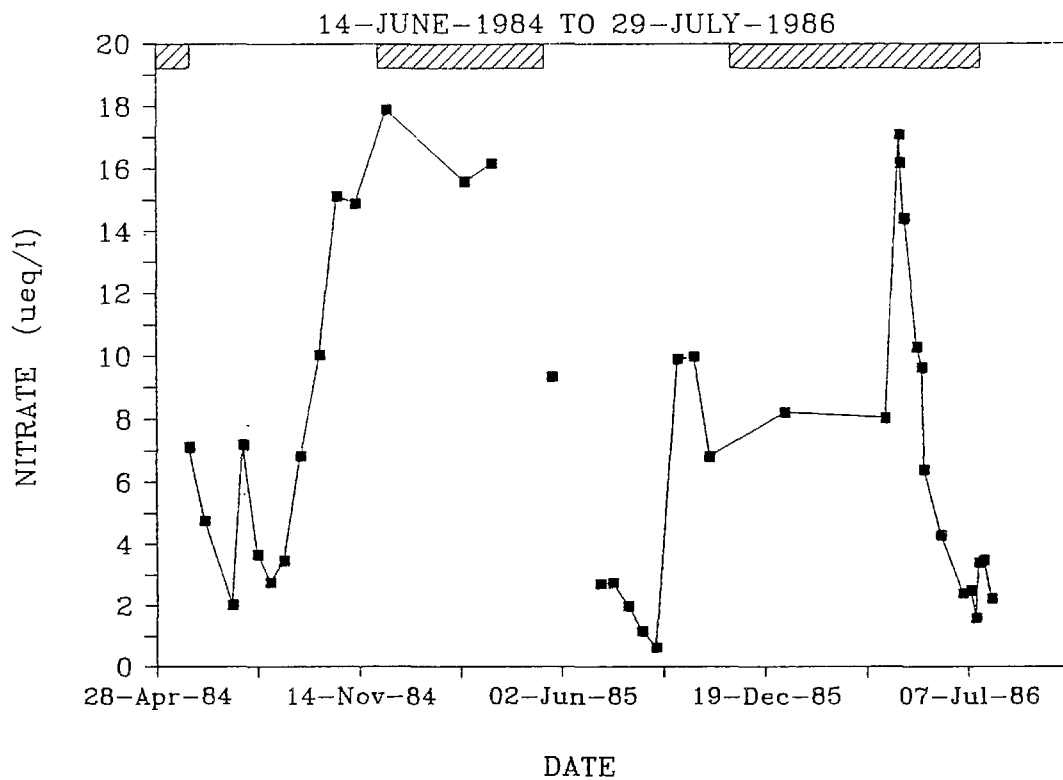


Fig. II-21

SULFATE TIME SERIES - MAIN INFLOW

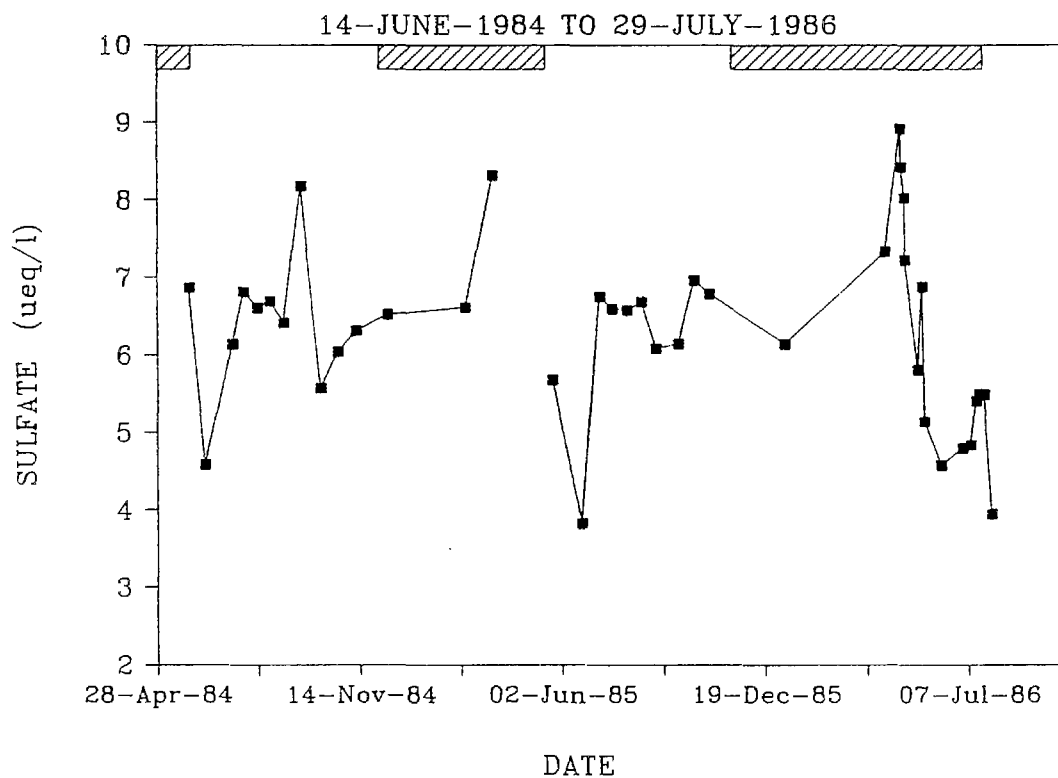


Fig. II-22

CHLORIDE TIME SERIES - MAIN INFLOW

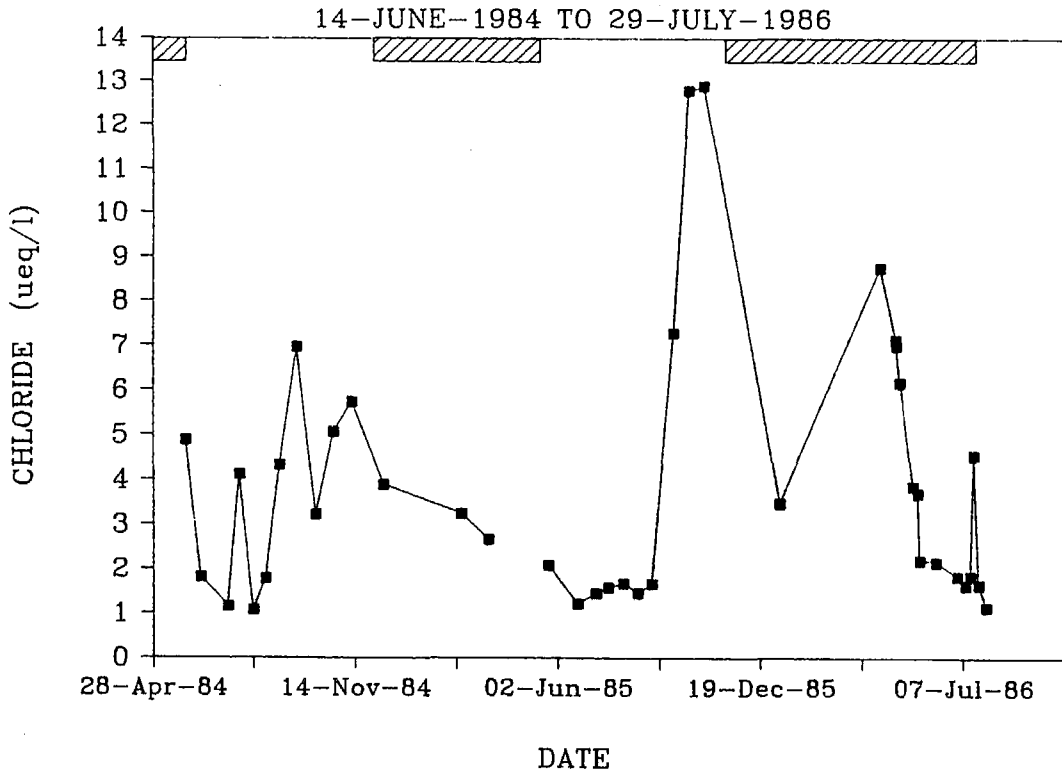


Fig. II-23 c

SILICA TIME SERIES - MAIN INFLOW

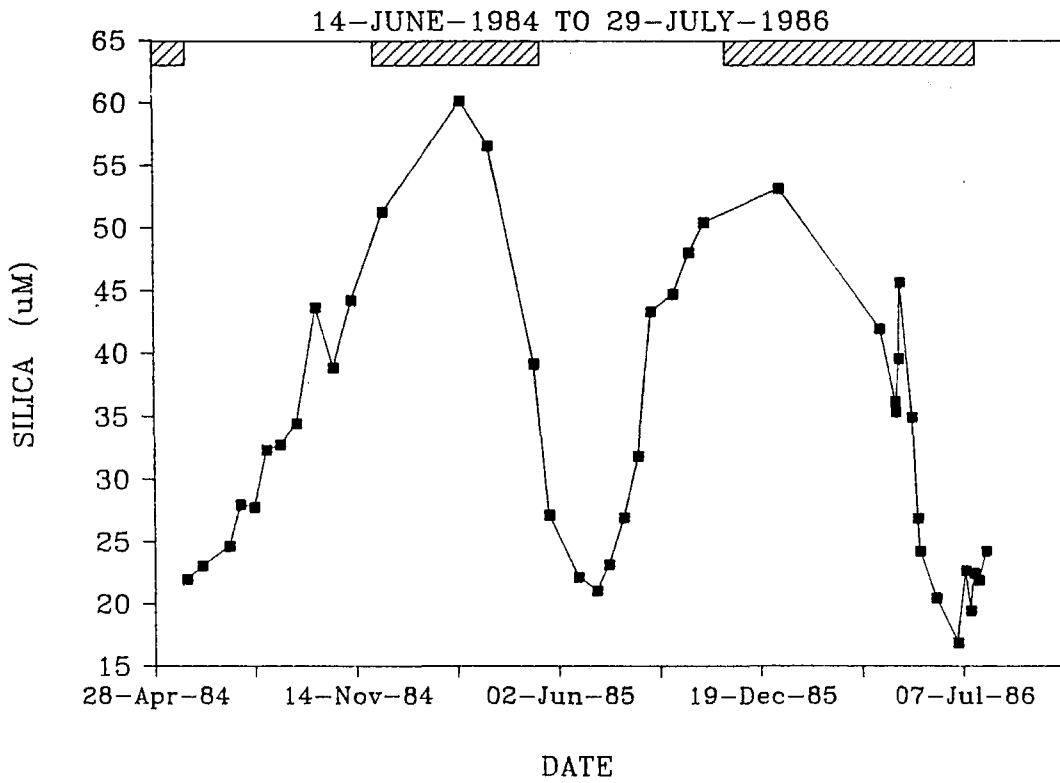


Fig. II-24
SUM OF CATIONS TIME SERIES—MAIN INFLOW

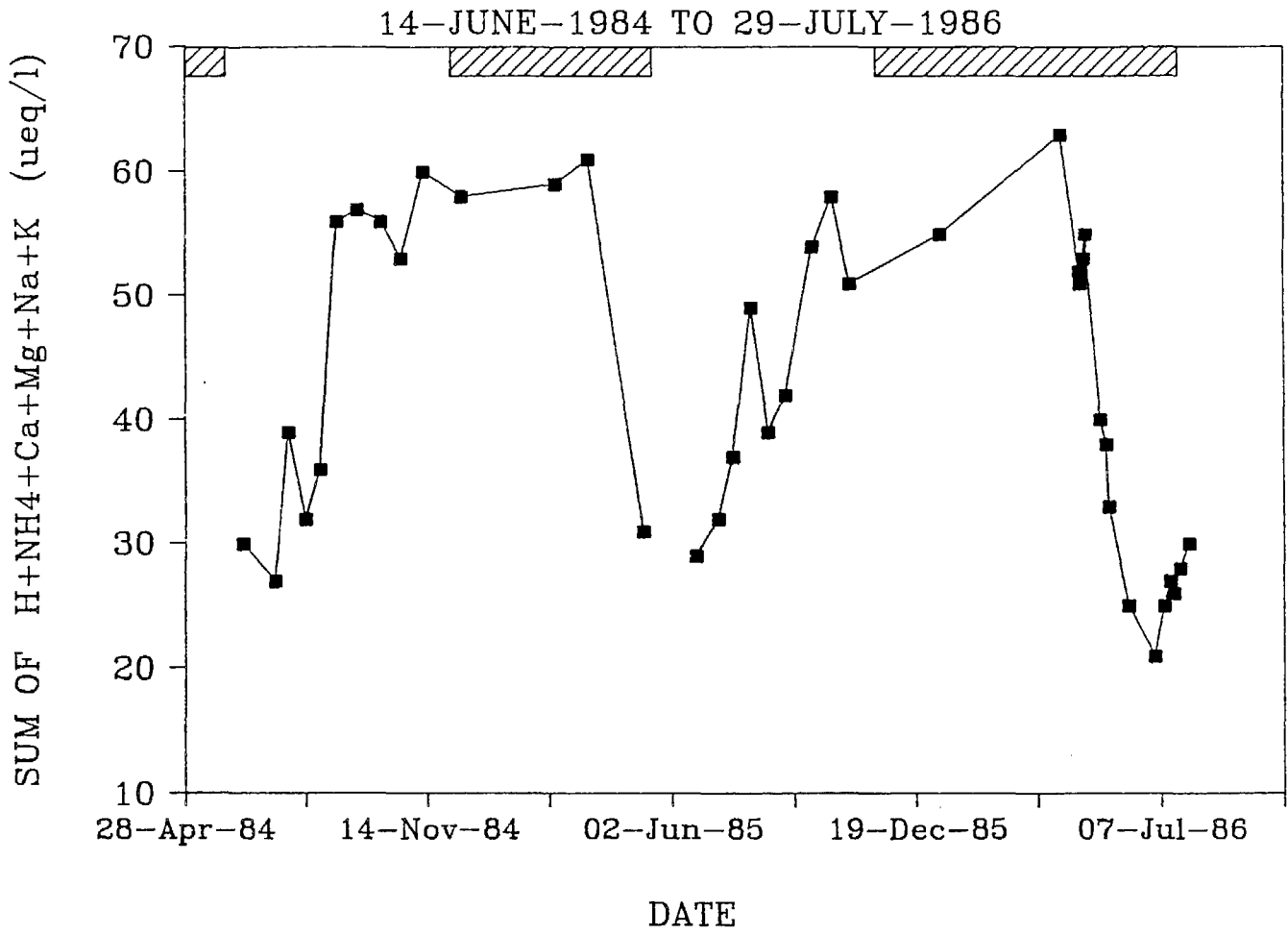


Fig. II-25

CALCIUM TIME SERIES - MAIN INFLOW

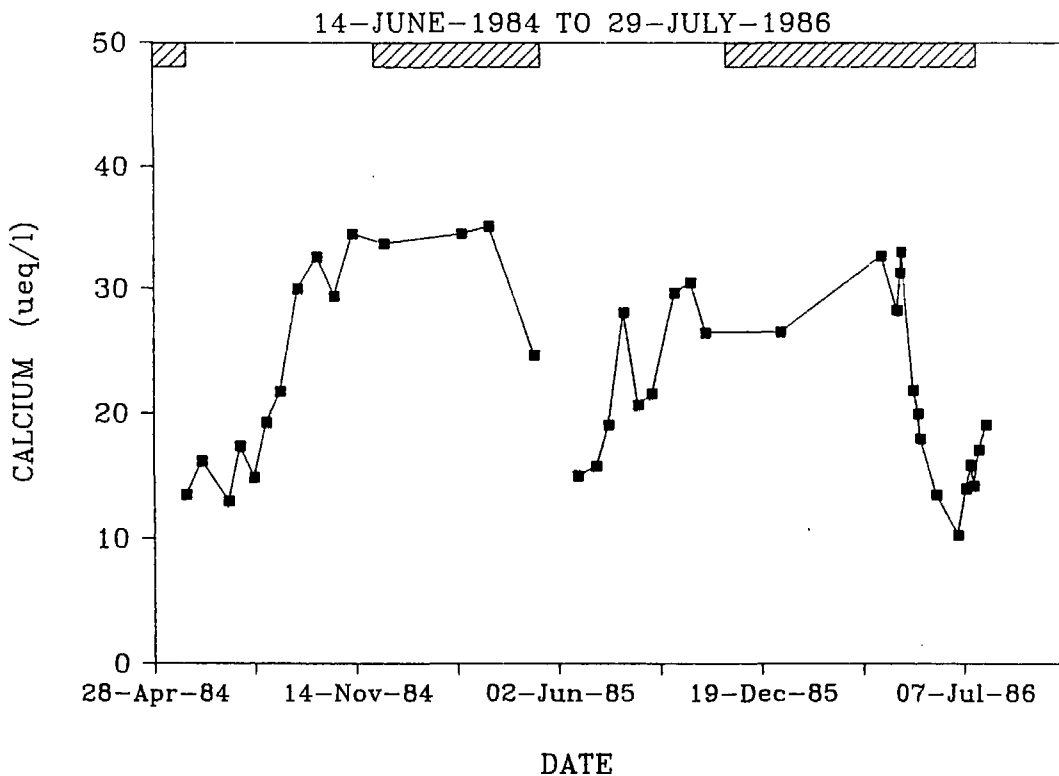


Fig. II-26

MAGNESIUM TIME SERIES - MAIN INFLOW

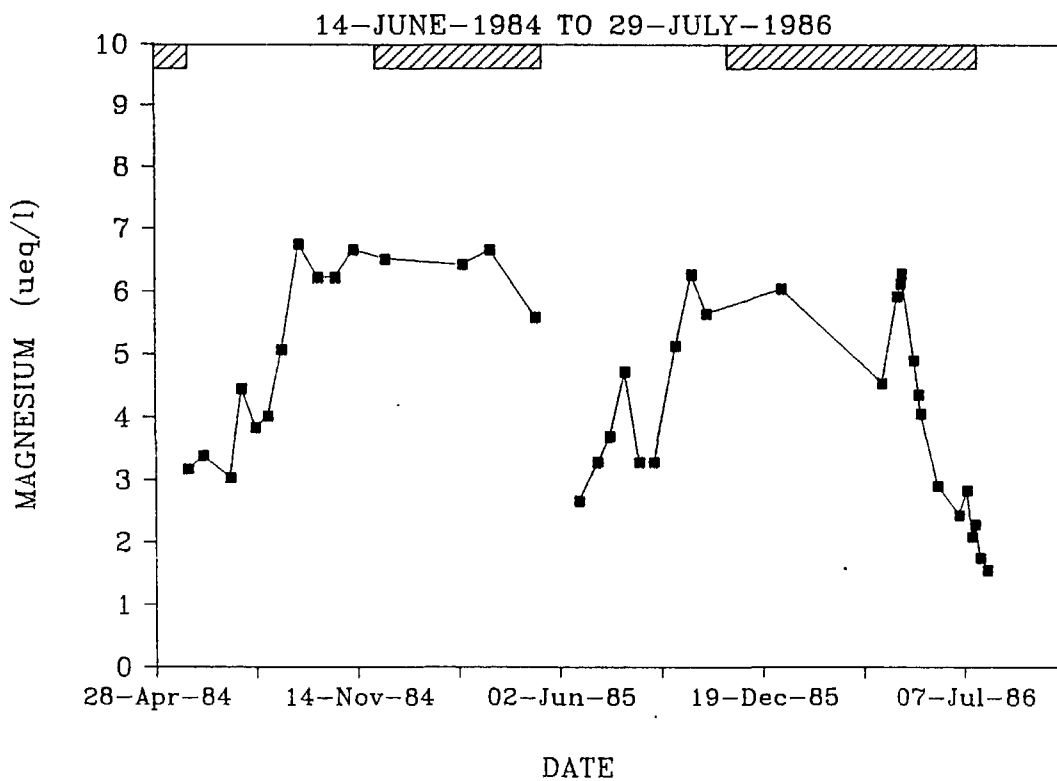


Fig. II-27

SODIUM TIME SERIES - MAIN INFLOW

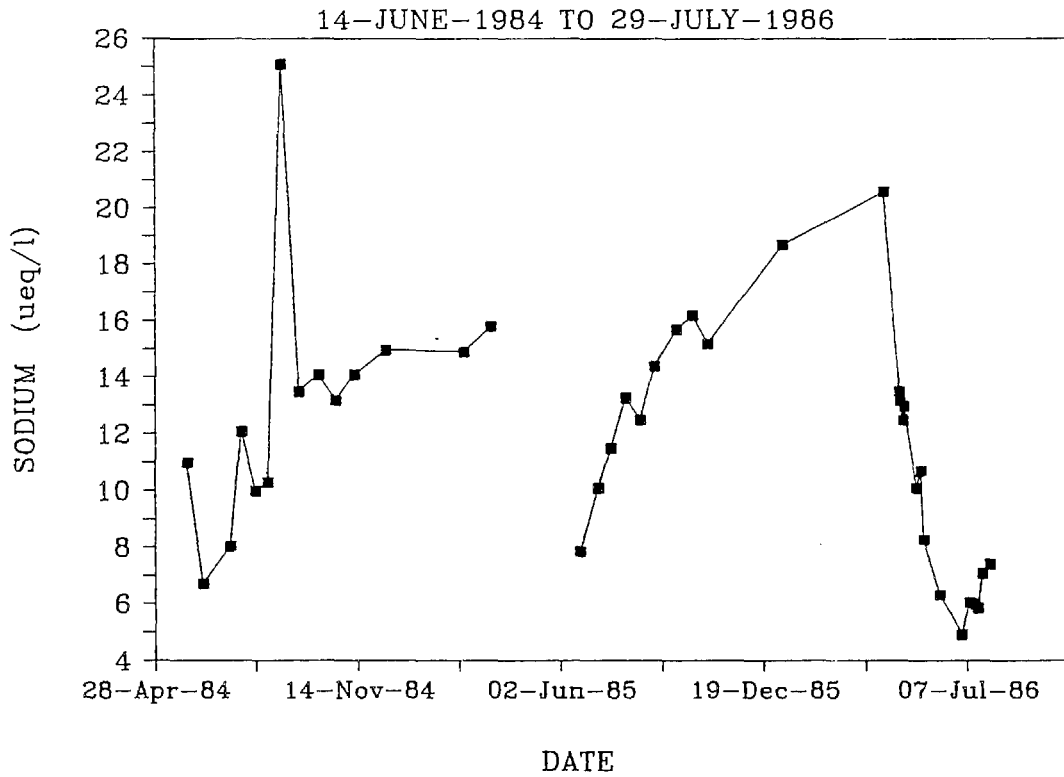


Fig. II-28

POTASSIUM TIME SERIES - MAIN INFLOW

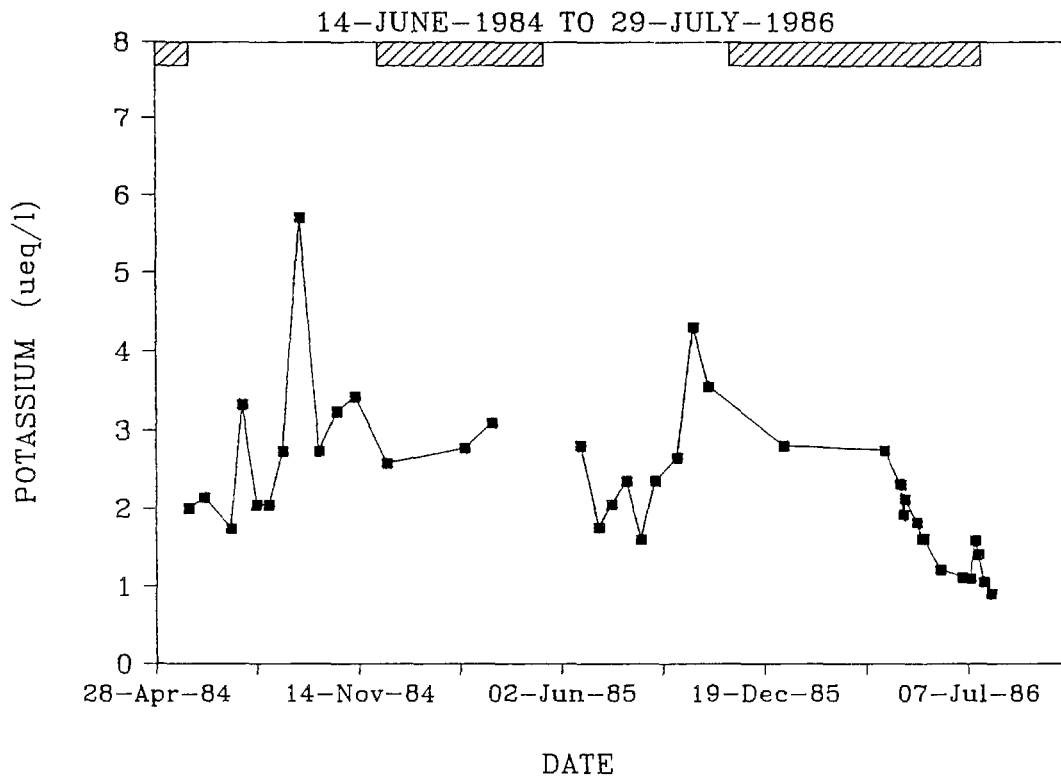


Fig. II-29A
UNFILTERED METAL TIME SERIES—MAIN INFLOW

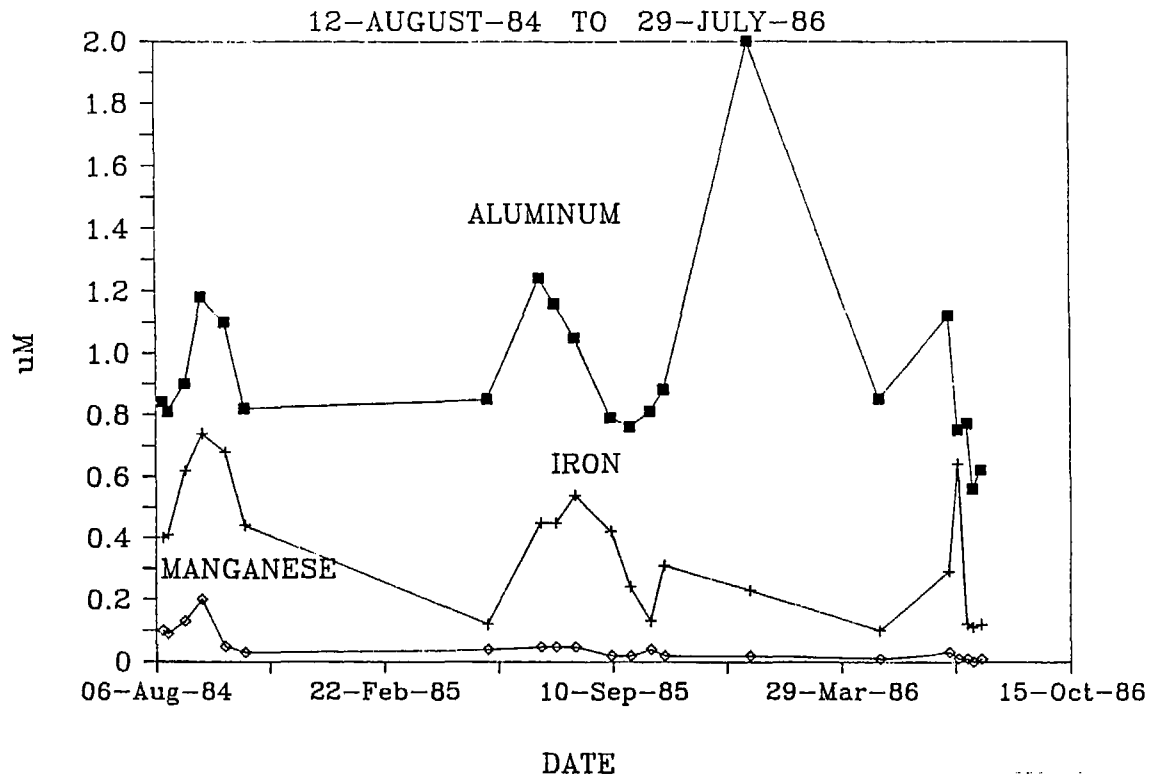


Fig. II-29B
UNFILTERED METAL TIME SERIES—WEST INFLOW

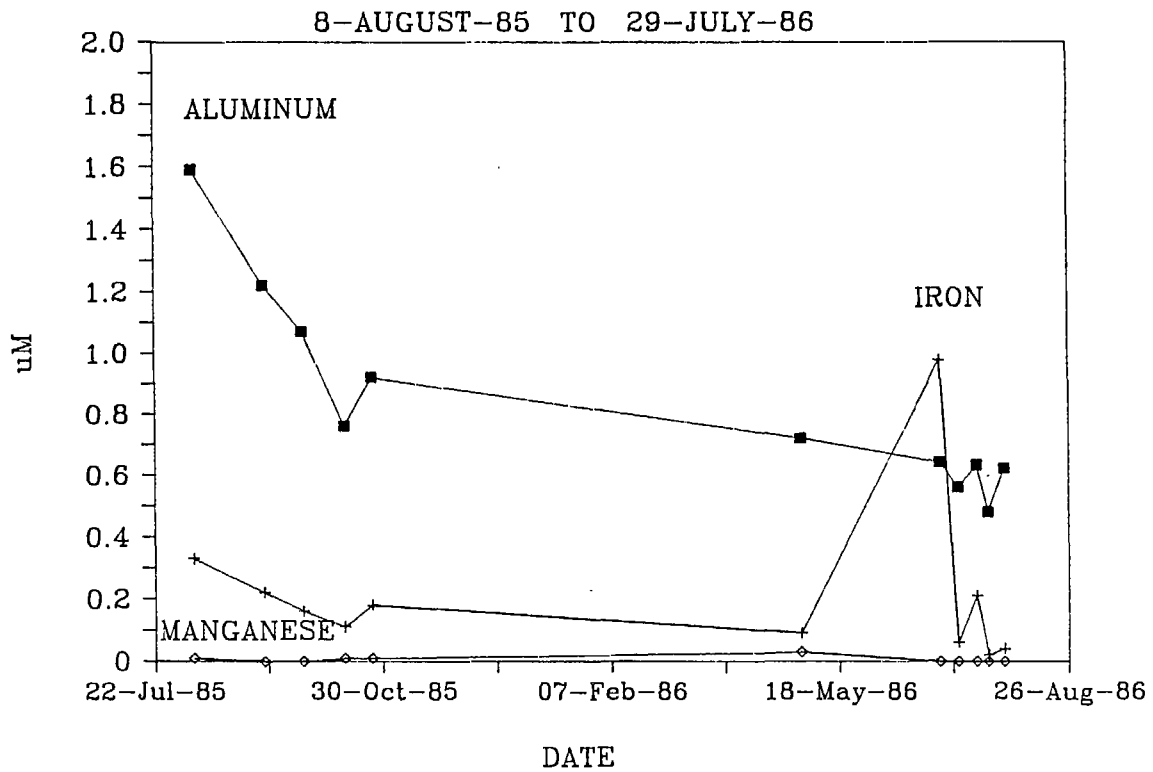


Fig. II-30
CALCIUM vs ACID NEUTRALIZING CAPACITY

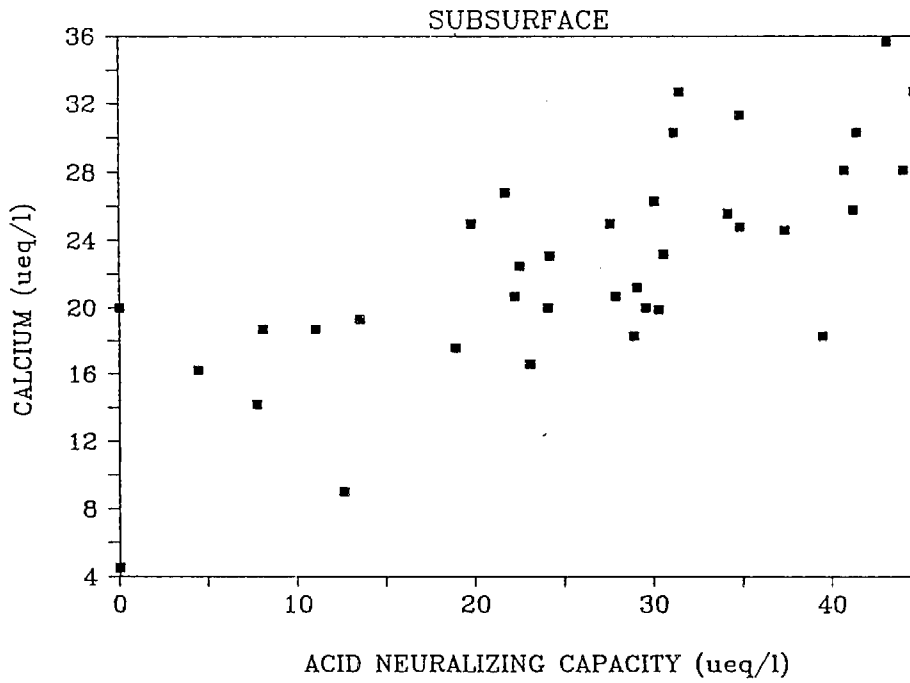


Fig. II-31
CATIONS vs ACID NEUTRALIZING CAPACITY

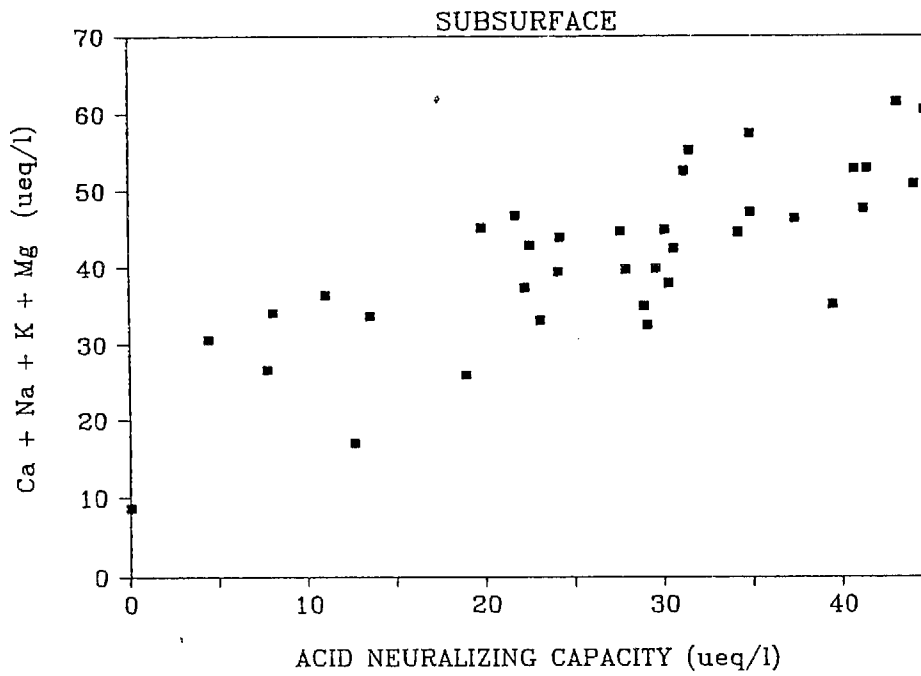


Fig. II-32
ALL CATIONS vs ACID NEUTRALIZING CAPACITY

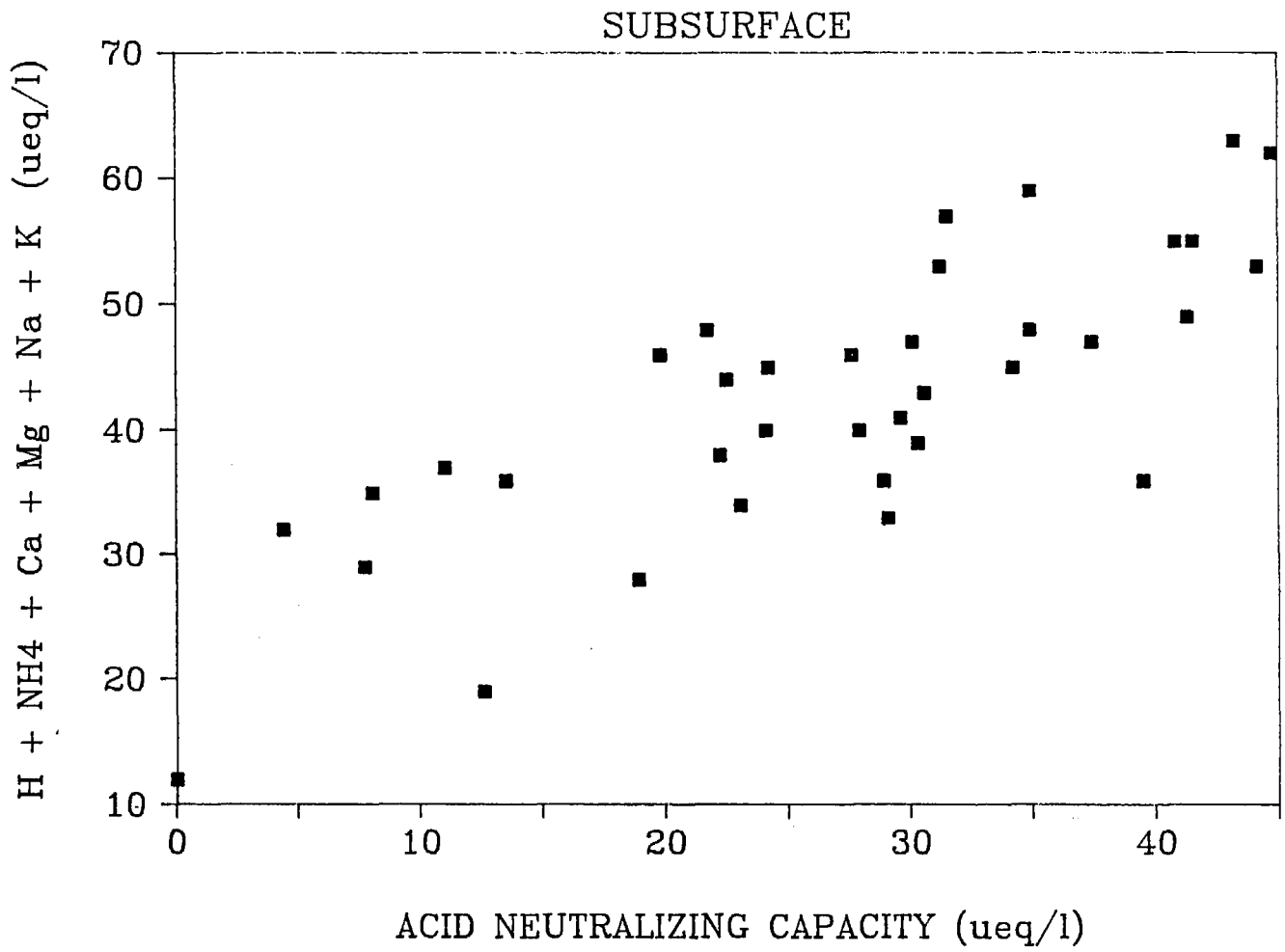


Fig. II-33

BASE CATIONS vs ACID NEUTRALIZING CAPACITY

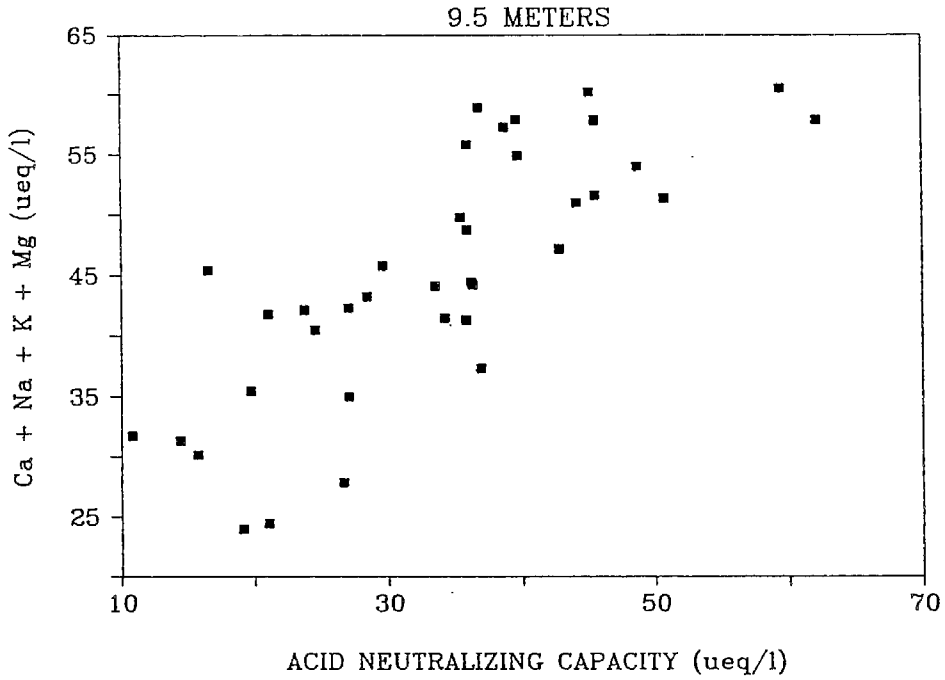


Fig. II-34

ALL CATIONS vs ACID NEUTRALIZING CAPACITY

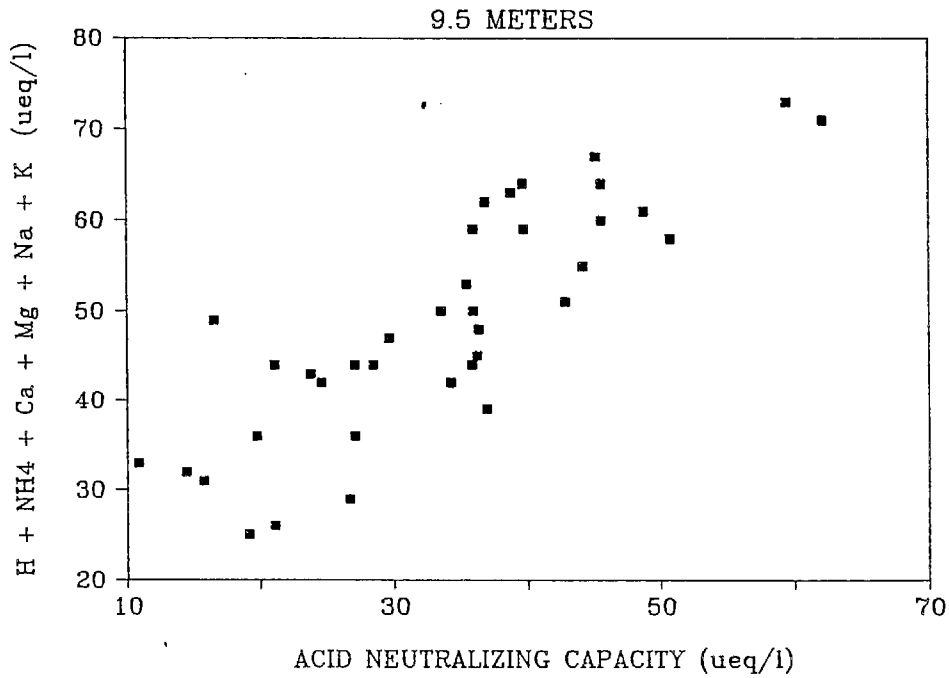
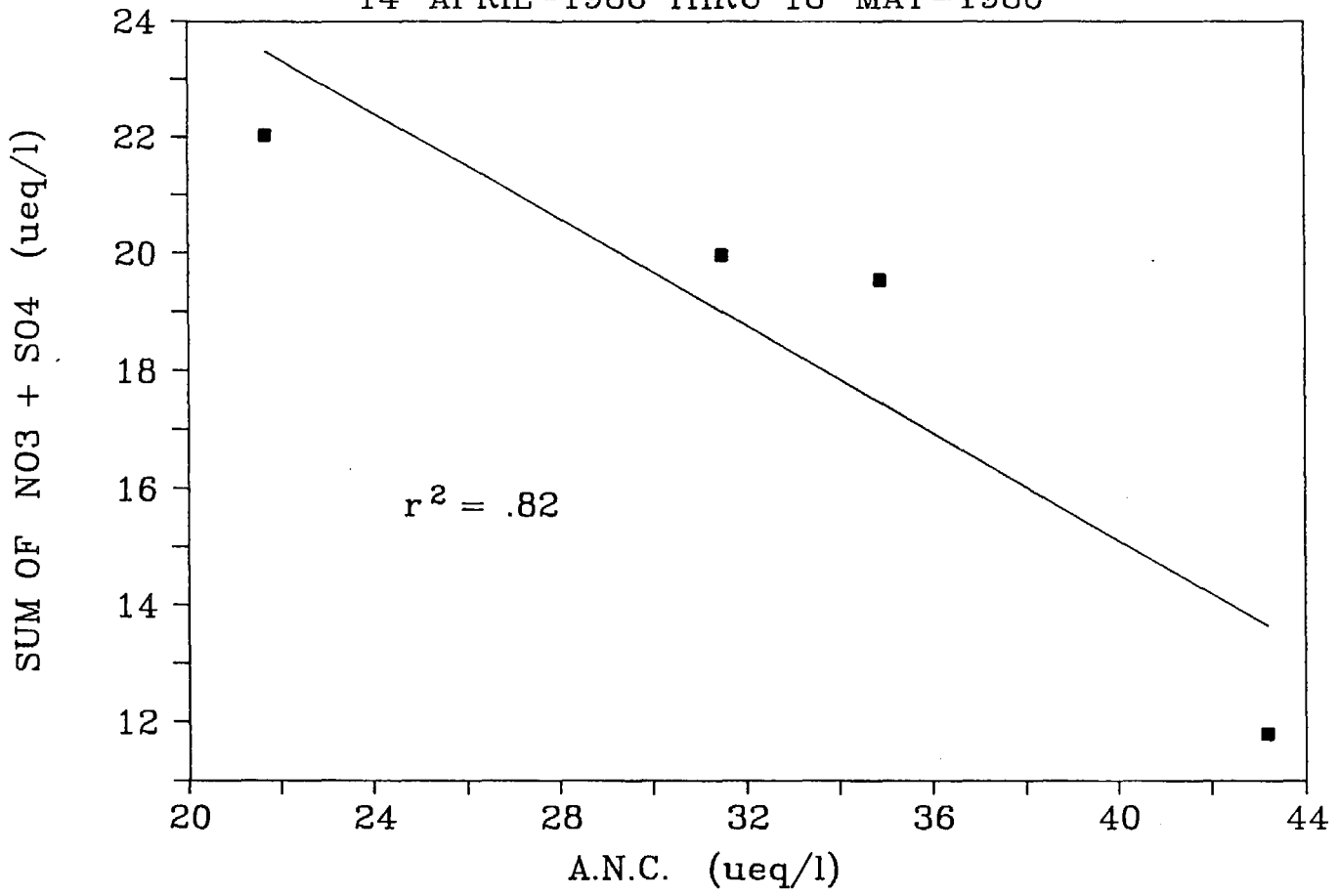


Fig. II-35
SUM OF NO3+S04 vs A.N.C. - SUBSUFACE

14-APRIL-1986 THRU 18-MAY-1986



Chapter II.2
PRIMARY PRODUCTIVITY AND REGENERATION
OF NITROGEN IN EMERALD LAKE

Introduction

Primary production by phytoplankton sustains most of the energetic needs of the food webs of montane lakes (e.g. Pechlaner et al. 1972). Given the low densities of macrophytes in Emerald Lake and the heterogenous distribution of periphyton, measurements of phytoplankton productivity are a valuable index for evaluating long term trends in photosynthetic activity in Emerald Lake. Moreover phytoplankton productivity responds to many chemical factors (e.g. Morris 1980, Harris 1978) and may be a sensitive indicator of lake acidification. In this study primary productivity was estimated using isotope uptake methods employing carbon and nitrogen.

Nutrient supply is a limiting factor for primary productivity in oligotrophic waters. Therefore, recycling of nitrogen and phosphorus by metabolic activity of the biota (especially bacteria) is an important ecological process. Decreases in nutrient decomposition and recycling in acidified waters can occur (Hendry et al. 1976) and may lead to significant changes in the trophic structure. Ammonium production is an index of the activity of these processes and was measured using the ^{15}N isotope dilution method in this study.

Methods

Water sampling

Experiments were conducted during the ice-free seasons of 1984 and 1985 and under the ice during the winter of 1986. Lake samples were collected mid-lake using either a 2 liter acrylic Kemmerer bottle (for epilimnion and hypolimnion sampling) or a 10 meter length of 2.5 cm diameter Tygon tubing used as an integrating sampler. The entire water sample was then placed in an opaque plastic container. Water used for laboratory experiments was backpacked 8 kilometers to a trail head, then driven by automobile 45 kilometers to the laboratory. Elapsed time between collection and start of an experiment was about 5 hours. Experiments at the lake were initiated immediately after water collection.

Isotope dilution technique

Heterotrophic regeneration of ammonia is commonly determined by direct measurement of increases in the dissolved ammonium of a sample during an incubation in darkness (Axler et al. 1981). This method is suitable if the ambient ammonium concentration is large or regeneration rates high, but is unacceptable in oligotrophic waters such as Emerald Lake. Instead, a more sensitive method employing measurements of changes in the isotopic composition of the ammonium pool was used. The isotope dilution method involves enriching a water sample with a stable isotope of ammonium, $^{15}\text{N-NH}_4$ and measuring the dilution of the isotope caused by heterotrophic excretion of $^{14}\text{N-NH}_4$ (Fiedler and Proksch 1975). The isotope ratios are expressed as a percentage of the total ammonium pool. For example, an atom% $^{15}\text{N-NH}_4$ of 25 means that the ammonium pool is composed of 25% $^{15}\text{N-NH}_4$ and 75% $^{14}\text{N-NH}_4$. The natural abundance of the ^{15}N isotope is approximately 0.37%.

The following procedures apply to regeneration experiments done in the field and in the laboratory.

Four liters of water were placed in each of two transparent polyethylene containers (i.e., cubitainers) and an amount of 99 atom% enriched $(\text{NH}_4)_2\text{SO}_4$ added to bring the final ammonium concentration to 2 μM . Ambient $^{14}\text{N-NH}_4$ concentration was low (less than 0.1 μM) and, as a result, the atom% $^{15}\text{N-NH}_4$ at the beginning of the experiments was usually greater than 50%. This enrichment was necessary because the sensitivity of the mass spectrometer was 2 μM .

After inoculation, liter subsamples were removed periodically from each cubitainer. The water was incubated for 12 to 24 hours in either an unlighted refrigerator (laboratory experiments) or inside a black plastic bag on a partially submerged raft (lake experiments). In both cases the incubations were conducted in the dark and at ambient temperatures of lake water. After the incubation period, liter subsamples were filtered with a vacuum not exceeding 125 mm Hg, through an ashed glass fiber filter (Gelman A/E) to remove the particulate fraction. This filter was then rinsed with approximately 30 ml of deionized water. The edge of the filter was also rinsed by removing the top portion of the filter holder and pipetting 10 ml of deionized water along the edges. The filtrate and rinse were collected in a flask and 100 milligrams of the Zeolite clay IONSIV was added. IONSIV is an ion-exchange clay which rapidly and effectively adsorbs dissolved

ammonium. Next, the IONSIV was removed by filtration through an ashed glass fiber filter. This second filter contained the entire dissolved ammonium pool. Blanks were carried through the entire procedure to detect and correct for contamination. These blanks typically contained less than 0.05 μ moles of nitrogen. A sample for colorimetric determination of ammonium by the indophenol blue method (Strickland and Parsons 1976) was collected concurrently with the 1 liter subsample. Both filters were then dried at 40°C and stored in a desiccator. Several months later the filters were analyzed on a mass spectrometer (Associated Electrical Industries Limited - type MS10) using the micro-Dumas technique (Fiedler and Proksch 1975). This technique requires that the filters be ground in a mortar and sealed under vacuum (<10 mtorr) in glass ampules containing Cu, CaO, CuO, and Cuprox. The ampules were combusted at 550°C for approximately 12 hours during which the particulate nitrogen on the filters was converted to nitrogen gas. Next the ampules were broken under vacuum (<1 μ torr) in the inlet system of the mass spectrometer. The N₂ gas was introduced into the magnetic field of the instrument through a variable leak calibrated to acetanilide standards to yield μ moles N in the sample.

The following equation was used to calculate regeneration rates between all sampling intervals:

$$R = \frac{[\ln(\text{atom\% excess } ^{15}\text{N-NH}_4)\text{initial} - \ln(\text{atom\% excess } ^{15}\text{N-NH}_4)\text{final}][\text{NH}_4]}{\text{Time}}$$

Where: R is regeneration rate in nanomoles liter⁻¹ hour⁻¹; [NH₄] is ammonium concentration (nM) at midpoint of experimental interval. This term corrects for changes in the size of the ammonium pool due to uptake; Atom% excess ¹⁵N-NH₄ is measured ¹⁵N-NH₄ atom% in the dissolved fraction (second filter) minus natural abundance (0.37%), and Time is time interval (hours).

Regeneration does not need to be corrected for phytoplankton discrimination between the two isotopes because, unlike carbon isotopes, they require the same amount of energy to assimilate (Fisher, T.R., personal communication).

Ammonium and carbon uptake techniques

Carbon uptake by phytoplankton is often measured using a radioisotope tracer technique. Small amounts of carbon (^{14}C) are added to a water sample which is incubated at natural light and temperature levels. The phytoplankton in the sample take up the carbon during photosynthesis and incorporate it into their tissues. After filtration, the radioactivity of the particulate fraction in the water sample is measured using scintillation or Geiger counting. The amount of carbon taken up is directly proportional to the radioactivity of the phytoplankton (Vollenweider 1969). Radiotracer techniques are sensitive, allow for rapid processing of samples and avoid the problem of gross changes of ambient nutrient levels. Their major drawbacks are safety concerns due to radioactivity. This problem made them unsuitable for in-situ work at Emerald Lake. For field work an alternative was to use a stable isotope such as ^{15}N and measure the atom% change in the phytoplankton as they incorporate $^{15}\text{N-NO}_3$ or $^{15}\text{N-NH}_4$. Both $^{14}\text{C-HCO}_3$ (in the laboratory) and $^{15}\text{N-NH}_4$ (in the field) were used to estimate primary productivity in Emerald Lake.

Lake water was measured into 125 ml borosilicate glass bottles and inoculated with 5 μCi of $^{14}\text{C-HCO}_3$ and thoroughly mixed. Initial activity were determined by immediately removing 0.5 ml of sample from a subset of bottles and adding each to a scintillation vial containing 0.1 N NaOH and 10 ml of PCS fluor (Amersham). Samples were illuminated at a series of light levels by cool-white power groove, fluorescent lamps (GE F48PG17CW). A range of light intensities was obtained by enclosing the bottles in layers of neutral density screen. The incubations took place in an insulated container which was kept at current lake temperature. After incubation, samples were filtered through glass fiber filters (Gelman A/E) at a pressure not exceeding 125 mm Hg and rinsed with 30 ml of filtered Emerald Lake water. The perimeter of the filters was also rinsed by removing the upper part of the filter holder and pipetting an additional 10 ml of filtered lake water around the edge. The filters were then placed in 10 ml of PCS fluor. The ^{14}C activity on the filters and the initial activity was determined with a Rackbeta model 1217 automatic scintillation counter. Total inorganic carbon content of the lake water was determined by Gran titration (Talling 1973). Chlorophyll a was determined by filtering 1 liter of the water used in the ^{14}C experiment through a glass fiber filter. The filter was macerated with a

teflon homogenizer and the pigment extracted in the dark for 45 minutes with 90% acetone. After extraction the slurry was centrifuged and the fluorescence of the extracted pigments measured on a fluorometer (Turner model 110) which was calibrated against a spectrophotometer using fresh spinach pigments. The concentrations were corrected for phaeopigments. The carbon uptake rate was then calculated by the following equation:

$$^{12}\text{C Uptake} = \frac{^{14}\text{C Assimilated}}{^{14}\text{C Available}} \times \frac{^{12}\text{C Available}}{\text{Time}}$$

(µg C l⁻¹hr⁻¹)

Where: ¹⁴C Assimilated is sample activity (disintegrations per minute (dpm) from scintillation counter) x 1.06. The factor 1.06 is used because ¹⁴C is assimilated 6% slower than ¹²C because of its greater mass; ¹⁴C Available is the initial activity (dpm) of the sample times a dilution factor. This dilution factor was based on the size of the initial activity aliquot and the original sample volume; ¹²C Available is Gran alkalinity in µg C liter⁻¹, and Time is elapsed time (hours) of the experiment.

Photosynthetically active radiation (PAR, 400 to 700 nm), was measured during sample collection at each meter of the water column with a Licor model LI-185B quantum sensor. PAR was also measured during incubations with the same sensor. Transparency was determined with a Secchi disk (diameter = 20 cm).

Maximum chlorophyll specific carbon uptake (PmB) rates were estimated by the following procedure. Carbon uptake rates (P) were normalized to chlorophyll a and plotted versus light intensity (I) (Figure II-36). The parameters of the P vs. I curves were then estimated by fitting the hyperbolic tangent equation:

$$PB(I) = PmB \times \tanh(\alpha/PmB) - R$$

Where: PB(I) is the specific carbon uptake rate (µg C l⁻¹hr⁻¹ per µg Chla) as a function of light intensity; PmB is the maximum specific uptake rate (same units as PB(I)); Alpha is the initial slope of the P vs. I curve and R is the Y intercept. The fitting routine minimizes the sum of the squared

residuals by searching the entire 3-dimensional parameters space defined by PmB, alpha, and R (see Gallegos and Platt, 1981).

Nitrogen uptake by phytoplankton was determined using the stable isotope, ^{15}N . Four liters of lake water were placed in each of several (2 to 6) clear plastic cubitainers and inoculated with $^{15}\text{N-NH}_4$ to raise the concentration of ammonium to approximately 2 μM . Immediately, a subsample was removed from each and a quantitative filtration performed using an ashed glass fiber filter. The filter was then rinsed with about 30 ml of deionized water. This filter contained the particulate matter of the sample including primary producers. Additional samples were collected and filtered in the same manner periodically. The samples were incubated on a partially submerged raft in the lake and were shaded with 2 layers of neutral density screen. Each layer of screening reduced the incidence light approximately 50%.

The filters were dried at 40°C and stored for several months in a desiccator until they were analyzed on the mass spectrometer. For light incubated samples a single ammonium uptake rate was calculated using initial and final atom% P- ^{15}N values. No intermediate samples were collected. The dark incubated experiments had 3 to 5 sampling intervals and an ammonium uptake rate was calculated for each interval. The following equation was applied between all sampling intervals:

$$U = \frac{[(\text{atom\% P-}^{15}\text{N})_{\text{final}} - (\text{atom\% P-}^{15}\text{N})_{\text{initial}}] \times [\text{P.N.}]}{\text{Time} \times (\text{atom\% }^{15}\text{N-NH}_4)}$$

Where: U is nanomoles NH_4 liter $^{-1}$ hour $^{-1}$; [P.N.] is average particulate nitrogen concentration over experimental interval; Atom% $^{15}\text{N-NH}_4$ is the isotopic composition of the dissolved ammonium pool at the midpoint of the experimental interval. This term corrects uptake for changes in the available ammonium pool caused by regeneration. For experiments incubated in the lake this term was estimated from the original $^{15}\text{N-NH}_4$ spike; Atom% P- ^{15}N is the isotopic composition of the particulate nitrogen fraction (phytoplankton); and Time is time interval (hours).

Results

Isotope dilution of an enriched water sample was measured on four days in the late summer of 1985 and two days during the winter of 1985-86. Figures II-41 and II-44 are time series of the isotopic composition of the dissolved ammonium pool during the dark incubations. The atom% $^{15}\text{N-NH}_4$ declined during the experiment. The rate of decrease in the $^{15}\text{N-NH}_4$ pool usually lessened over the course of an experiment with the greatest rate occurring between 0 and 4 hours. Some experiments showed a constant regeneration rate (11 October 85) or an increase in the rate during the experiment (18 May 86; epilimnion).

A summary of the regeneration rates for each experiment are in Table II-2. The lowest regeneration rate measured during the ice free season was $1.5 \text{ nmol N l}^{-1} \text{ hr}^{-1}$ and the highest $66 \text{ nmol N l}^{-1} \text{ hr}^{-1}$. Turnover times of particulate nitrogen in the summer ranged from 36 hours to 90 days. Winter regeneration rates were measured in the epilimnion and hypolimnion of Emerald lake on 15 February 1986 (midwinter) and 18 May 1986. The rates reported for the February date are based on a single 24 hour time interval and are probably an underestimate of regeneration. Regeneration was almost three times as large in the epilimnion ($85 \text{ nmol N l}^{-1} \text{ hr}^{-1}$) compared to the hypolimnion ($30 \text{ nmol N l}^{-1} \text{ hr}^{-1}$). The particulate nitrogen turnover times on 15 February were 18 hours in the epilimnion and 2.7 days in the hypolimnion. The 18 May experiment was done during the snowmelt season; rates were the highest measured, $453 \text{ nmol N l}^{-1} \text{ hr}^{-1}$ (epilimnion) and $415 \text{ nmol N l}^{-1} \text{ hr}^{-1}$ (hypolimnion). The turnover time of the particulate nitrogen pool in the epilimnion ranged from 15 hours to 7 days and from 2 to 5 days in the hypolimnion. Regeneration rates were larger in the winter and reached a peak during the snowmelt season. Turnover times remained relatively stable.

Ammonium uptake was also determined for these experiments and the results presented in Table II-3. These values are dark ammonium uptake rates. Frequently there was a very rapid uptake of ammonium during these experiments. Other investigators (McCarthy and Goldman 1979) have made similar observations, but its generality and veracity needs further examination. The largest dark uptake rate was $285 \text{ nmol N l}^{-1} \text{ hr}^{-1}$ which was measured in the hypolimnion of the lake on 11 October 1985. If the very high initial rates are excluded, the highest dark uptake rate measured was $12 \text{ nmole l}^{-1} \text{ hr}^{-1}$ in the hypolimnion on 18 May 1986.

Light incubated ammonium uptake rates are presented in Table II-4 and ranged from $6 \text{ nmol N l}^{-1} \text{ hr}^{-1}$ measured on 15 October 85 to $37 \text{ nmol N l}^{-1} \text{ hr}^{-1}$ in a hypolimnion sample collected on 9 August 85 during the fall of 1985. Because these samples were incubated in situ, the rates reflect the seasonal and daily fluctuations of incident light.

Carbon-14 uptake was measured 14 times during the ice-free seasons of 1984 and 1985 and once with samples collected from underneath the ice in 1986. The P vs. I curves from three of these experiments are shown in Figures II-45 and II-46. Carbon uptake rates usually reached an asymptote at approximately $150 \text{ } \mu\text{Einstein s}^{-1} \text{ m}^{-2} \text{ s}^{-1}$ (e.g. 23 October 1986 and 18 May 1986), but occasionally no light saturation was reached (e.g. 13 July 85). The curves for 23 October 85 and 18 May 86 are very similar in shape even though the uptake rates differ by an order of magnitude. PmB for the May experiment was $0.03 \text{ } \mu\text{g C l}^{-1} \text{ hr}^{-1} \text{ per } \mu\text{g Chl}_a \text{ l}^{-1}$.

Time series of PmB for the ice-free seasons of 1984 and 1985 are shown in Figure II-47. In 1984, PmB showed an increase after snowmelt with a peak of $1.6 \text{ } \mu\text{g C l}^{-1} \text{ hr}^{-1} \text{ per } \mu\text{g Chl}_a \text{ l}^{-1}$ on 31 August. Thereafter PmB declined during the summer (lowest; $0.5 \text{ } \mu\text{g C l}^{-1} \text{ hr}^{-1} \text{ per } \mu\text{g Chl}_a \text{ l}^{-1}$ on 23 October) and increased again just after the breakdown of the strong summer thermocline. Overall 1985 PmB's were higher than 1984. They showed an increase after snowmelt from $1.4 \text{ } \mu\text{g C l}^{-1} \text{ hr}^{-1} \text{ per } \mu\text{g Chl}_a \text{ l}^{-1}$ to a peak summer value of $3.6 \text{ } \mu\text{g C l}^{-1} \text{ hr}^{-1} \text{ per } \mu\text{g Chl}_a \text{ l}^{-1}$. This high specific rate was maintained throughout the summer and early fall. Figure II-48 is a time series of unnormalized carbon uptake rates for the same experiments. This data is useful in following the overall carbon productivity of the lake through the summers. Both years' data show a classic spring and fall plankton bloom separated by low mid-summer productivity. Maximum carbon assimilation rates (Pm) ranged from 0.3 to $1.8 \text{ } \mu\text{g C l}^{-1} \text{ hr}^{-1}$ for 1984 and from 0.6 to $1.9 \text{ } \mu\text{g C l}^{-1} \text{ hr}^{-1}$ for 1985. Figure II-49 is a time series of the initial slope of the P vs. I-curve. Alpha was very low throughout both years (less than 0.02) and showed a pattern similar to PmB.

Time series of chlorophyll a concentration in the subsurface (depth, 1m) waters of Emerald Lake during the summers of 1984 and 1985 are shown in Figure II-50. The seasonal variations in chlorophyll a closely followed the changes in maximum carbon uptake and alpha. Data from both seasons shows

phytoplankton blooms in the spring and fall with lower standing crops at mid-summer. Subsurface chlorophyll a concentrations were the highest recorded during autumn 1984. At this time a chlorophyll maximum occurred at 4 meters. This was a shallow chlorophyll maximum compared to the typical 7-9 meter maximum during the summer and snowmelt seasons. Figures II-52 through II-55 are typical vertical profiles of chlorophyll a for 1984-85-86. Following the autumn increase, the plankton decline as ice-cover thickens. During the winter, chlorophyll concentrations fall to their lowest levels (0.01 to 0.2 $\mu\text{g Chl}_a \text{ l}^{-1}$; Figure II-55). As winter progresses and snowmelt begins, chlorophyll concentrations increase, with a maximum of about 1 to 2 $\mu\text{g l}^{-1}$ situated just underneath the ice (Figure II-55).

Secchi disk transparency from both summers are shown in Figure II-51.

Discussion

Our measurements indicate that during the ice-free season both phytoplankton production and heterotrophic regeneration of nutrients are low. Measurements from the winter of 1985-86 show that carbon and nitrogen uptake rates are extremely low because of an absence of light. Regeneration rates at midwinter may be slightly higher than summer rates but during the snowmelt period they are almost ten times greater. Tables II-5 and II-6 contain data on carbon and nitrogen uptake and on nitrogen regeneration rates measured in other lakes. In terms of carbon productivity Emerald Lake is similar to other alpine lakes and to lakes in the Canadian and Alaskan arctic. The range of values reported in Table II-6 for Emerald lake are estimates of areal production and assume a photo-period of 10 hours. Data on nitrogen uptake and regeneration are sparse in montane lakes. Castle Lake provides a good comparison to Emerald lake although no winter rates are reported. Both lakes have similar nitrogen uptake and regeneration rates but areal carbon production is lower in Emerald lake and is more similar to Lake Tahoe.

Seasonal variation was most evident in chlorophyll a and carbon uptake rate and was driven by changes in nutrient and light levels. The spring bloom was caused, in part, by increased light levels. Higher nutrient concentrations caused by a breakdown in the winter thermocline and an influx from streams also helped explain the higher levels of chlorophyll a and carbon productivity. Increased levels of productivity in the fall are caused by the breakdown of the summer thermocline and the subsequent release of

nutrients to depths with higher light levels. Therefore, the strength and longevity of this stratification will determine the magnitude of the fall bloom. In 1984 Emerald Lake received a large quantity of silt during a severe thunderstorm which induced a strong and lasting thermocline. As a result, nutrient concentrations built up to high levels in the hypolimnion of the lake. Strong stratification and high turbidity in 1984 reduced flux of nutrients to the photic zone. The chlorophyll specific carbon uptake rate was lower in 1984 compared to 1985. This suggests that the phytoplankton in 1984 were more nutrient stressed than in 1985, although alpha was very similar between the two summers. The term alpha describes the ability of the phytoplankton to respond to increasing light levels and is influenced by the nutritional status of the population. In 1985 there was also a thermocline, but a large build up of nutrients did not occur because the photic zone in the lake extended to 9.5 meters and the phytoplankton were able to utilize these nutrients (see Figures II-51 and II-52). The fall bloom was later in 1984 because of the stronger thermocline and later lake overturn. In 1985 the spring bloom was earlier in the year compared to 1984 because the winter snowpack was smaller and the melt occurred earlier.

Table II-2. Ammonium regeneration rates from dark incubated samples. Ice-free season 1985; beneath-ice 1986. For each date the incubation interval and regeneration rate is given. F = field incubated experiments and L = lab incubated experiments. N = the number of replicates used. The units for regeneration are nanomoles liter⁻¹ hour⁻¹. Turnover times are expressed in days and were calculated by dividing the particulate nitrogen concentration by the regeneration rate. Sample types coded as: INT = integrated water column, EPIL = epilimnion, and HYPOL = hypolimnion.

Date	Sample Type	Site	N	Time Interval (hours)	Regeneration	Turnover Time (days)
26 September 1985	INT	F	1	0-19	43	1.7
11 October 1985	INT	L	1	0-6	31	1.5
				6-19	27	1.8
16 October 1985	4 M	F	2	0-4	43	1.5
				4-23	2.5	45
17 October 1985	4 M	L	2	0-4	66	2.0
				4-16	1.5	90
15 February 1986	EPIL	F	1	0-24	85	0.75
15 February 1986	HYPOL	F	1	1-24	30	2.7
18 May 1986	EPIL	F	1	0-3.2	41	7.0
				3.2-3.6	280	1.0
				3.6-14	453	0.63
18 May 1986	HYPOL	F	1	0-2.3	315	2.6
				2.3-3.6	415	2.0
				3.6-14	167	4.9

Table II-3. Ammonium uptake rates from dark incubated samples. Ice-free season 1985; beneath-ice 1986. For each date the incubation interval and uptake rate is given. F = field incubated experiments and L = lab incubated experiments. N = the number of replicates used. The units for uptake are nanomoles liter⁻¹ hour⁻¹. Sample types coded as: INT = integrated water column, EPIL = epilimnion, and HYPOL = hypolimnion.

Date	Sample Type	Site	N	Time Interval (hours)	Uptake
26 September 1985	INT	F	2	0-0.2	10
				0.2-18	0.3
11 October 1985	INT	L	2	0-0.3	285
				0.3-6.5	1.0
				6.5-18	0.0
16 October 1985	4 M	F	2	0-0.1	30
				0.1-4.1	1.3
				4.1-22	0.4
17 October 1985	4 M	L	2	0-0.2	12
				0.2-3.7	1.0
				3.7-16	0.4
15 February 1986	EPIL	F	1	0-0.1	0.6
				0.1-24	1.7
15 February 1986	HYPOL	F	1	0-0.5	43
				0.5-24	0.7
18 May 1986	EPIL	F	1	0-0.1	62
				0.1-3.2	1.1
				3.2-3.6	0.0
				3.2-14	0.7
18 May 1986	HYPOL	F	1	0-0.3	23
				0.3-2.3	3.6
				2.3-3.6	12
				3.6-14	0.0

Table II-4. Ammonium uptake rates from light incubated samples. Ice-free season 1985. F = field incubated experiments. N = the number of replicates used. Standard deviations (s.d.) for replicates is shown. The units for uptake are nanomoles liter⁻¹ hours⁻¹. Sample types coded as: INT = integrated water column, EPIL = epilimnion, and HYPOL = hypolimnion.

Date	Sample		N	Uptake	s.d.
	Type	Site			
1 September 1984	INT	F	2	9	0.4
29 July 1985	INT	F	3	24	3.6
9 August 1985	EPIL	F	2	13	0.7
9 August 1985	HYPOL	F	2	37	5.1
25 September 1985	INT	F	2	8	2.2
15 October 1985	INT	F	5	6	0.8

Table II-5. Examples of nitrogen uptake and regeneration rates. For Emerald Lake, range in parentheses is from dark incubated experiments.

Lake	Range of Reported Values nanomole l ⁻¹ hr ⁻¹	
	Nitrogen Uptake	Nitrogen Regeneration
Mono, Calif. (T.R. Fisher personal comm.)	1000-34000	100-800
Calado, Brazil (Morrisey and Fisher 1987)	860	1920
Castle, Calif. est. (Axler et al. 1981)	7-75	4-37
Emerald Lake	6-37 (0-285)	2-453

Table II-6. Examples of carbon productivity rates during summer.

LAKE	MAXIMUM (mg C m ⁻³ h ⁻¹)
Char, N.W.T. Canadian arctic (Kalff and Welch, 1974)	0.2
Castle, California (Goldman and Amezaga, 1984)	4
Finstertaler See, Austria (Tilzer, 1972)	2.5
Tahoe, California (Holm-Hansen et al. 1976)	0.5
Emerald Lake	1.8

CARBON UPTAKE vs LIGHT LEVEL

23-OCTOBER-1984

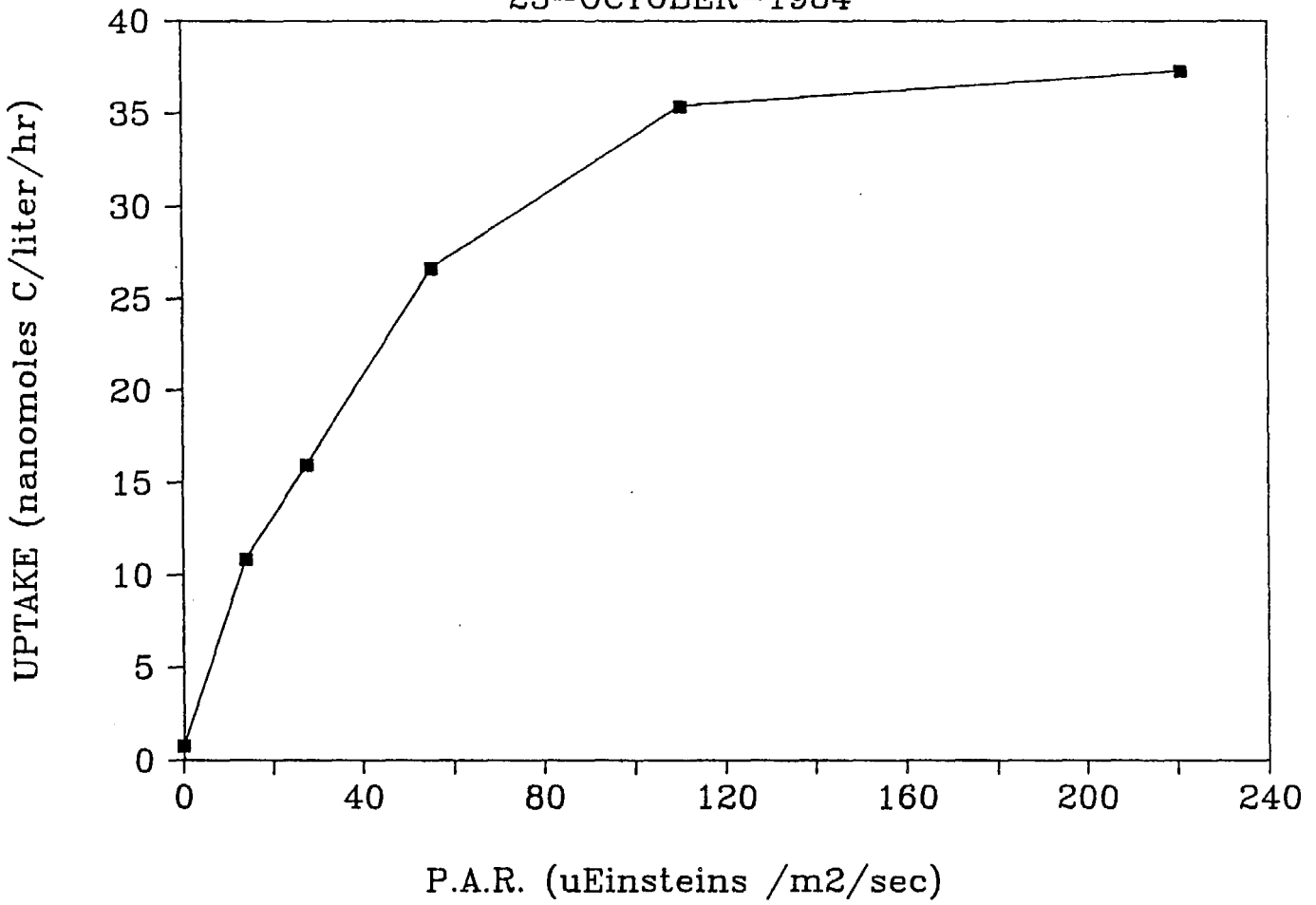
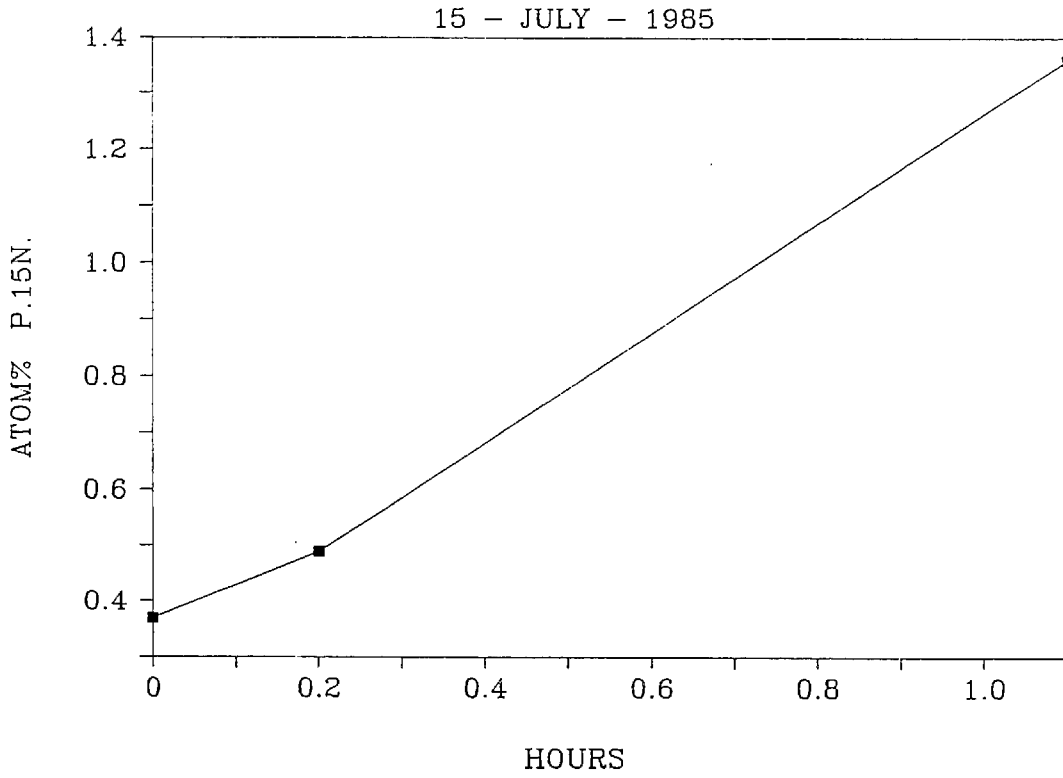


Figure II-36. Typical P/I curve.

ATOM%15N - PARTICULATE NITROGEN



ATOM%15N - PARTICULATE NITROGEN

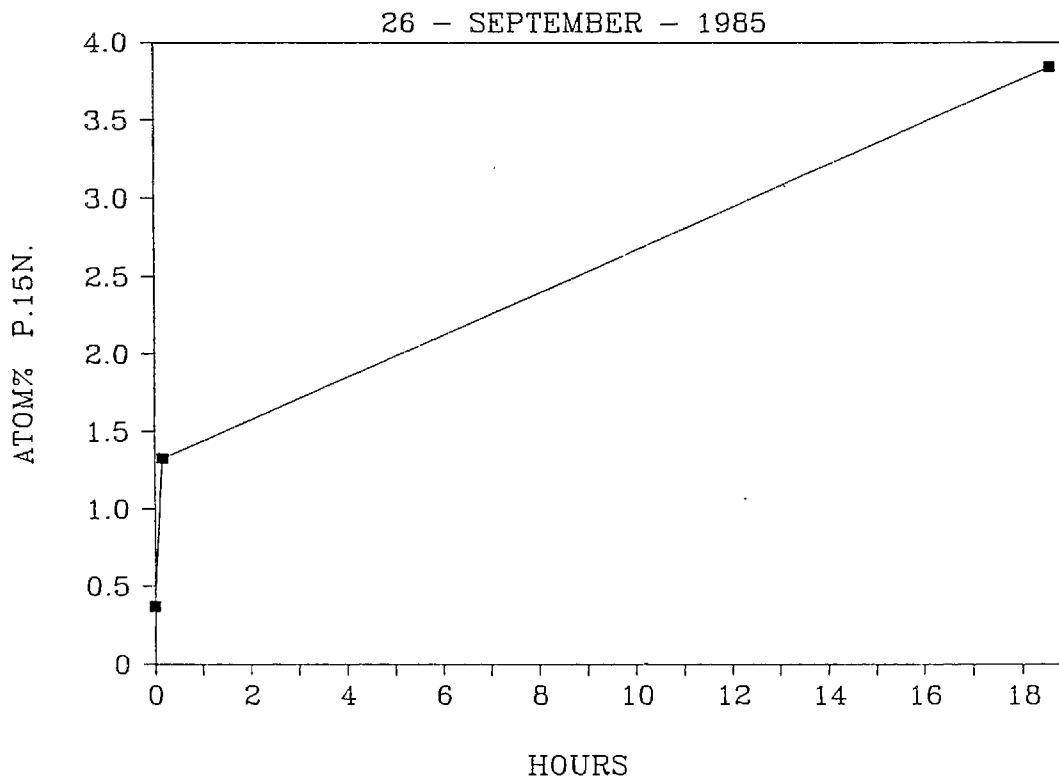
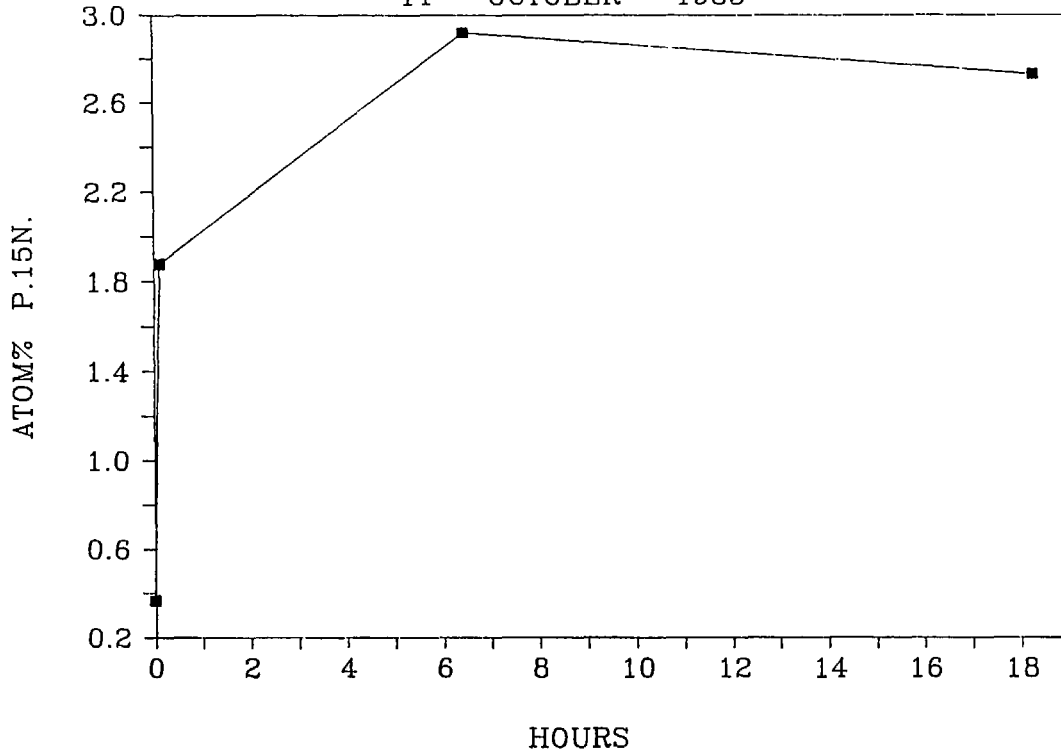


Figure II-37a+b. Atom% P-¹⁵N vs time; 15-July-85 and 26-September-85.

ATOM%15N - PARTICULATE NITROGEN

11 - OCTOBER - 1985



ATOM%15N - PARTICULATE NITROGEN

16 - OCTOBER - 1985

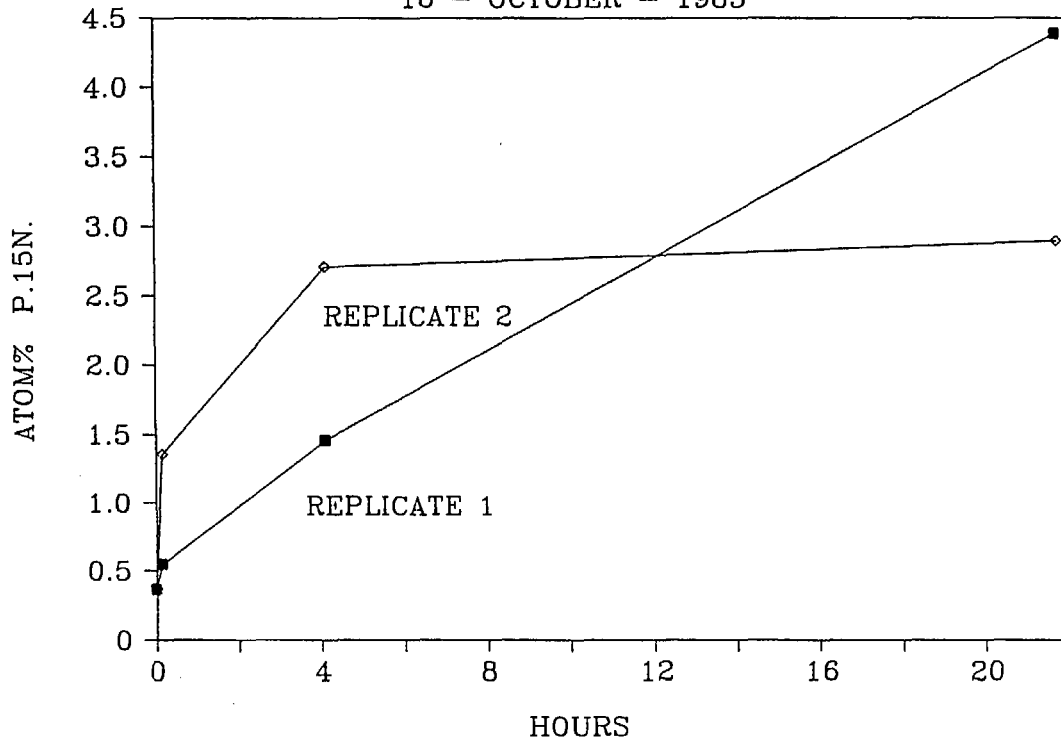


Figure II-38a+b. Atom% P-¹⁵N vs time; 11-October-85 and 16-October-85.

ATOM%15N - PARTICULATE NITROGEN

17 - OCTOBER - 1985

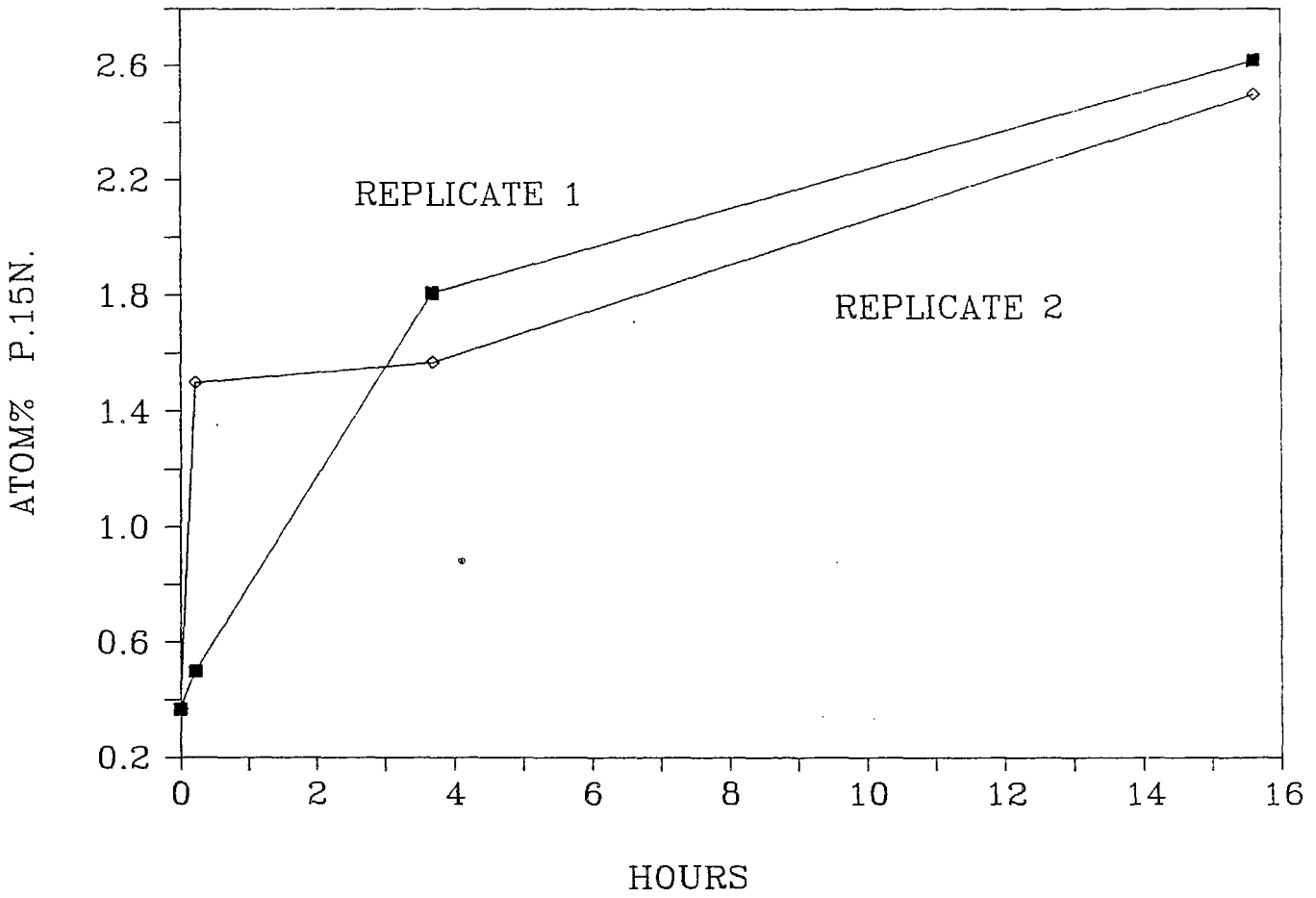
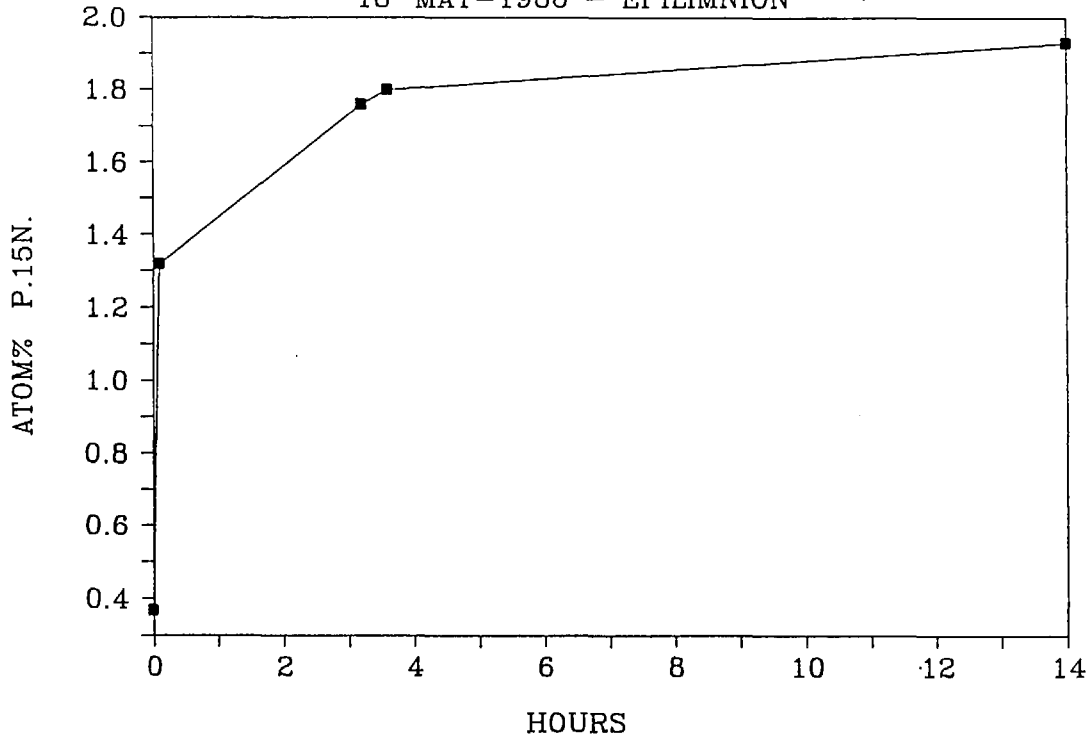


Figure II-39. Atom% P-¹⁵N vs time; 17-October-85.

ATOM%15N - PARTICULATE NITROGEN

18-MAY-1986 - EPILIMNION



ATOM%15N - PARTICULATE NITROGEN

18-MAY-1986 - HYPOLIMNION

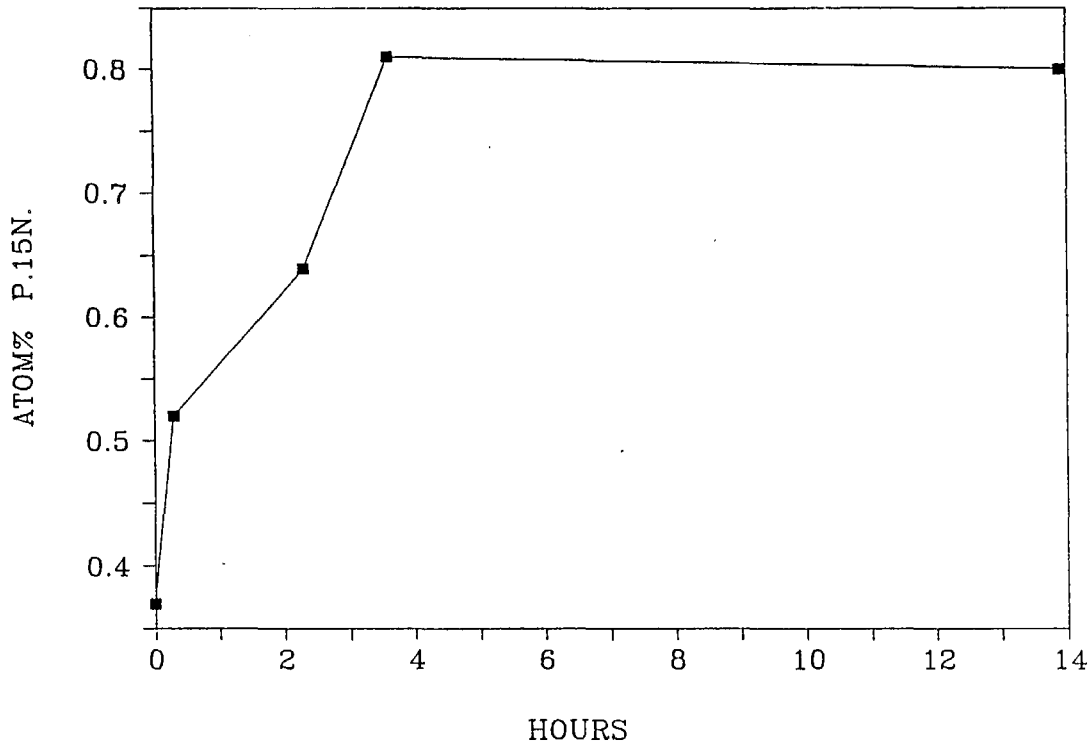
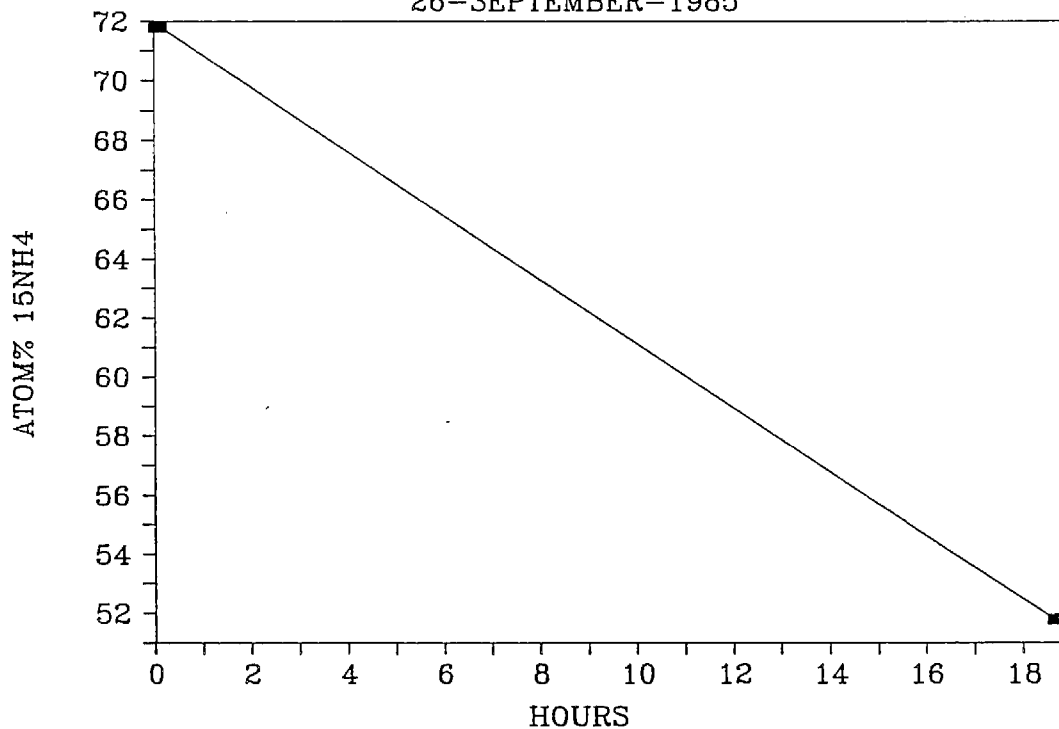


Figure II-40a+b. Atom% P-¹⁵N vs time; 18-May-86, epilimnion and hypolimnion.

ATOM% 15N DISSOLVED AMMONIUM POOL

26-SEPTEMBER-1985



ATOM%15N - DISSOLVED AMMONIUM POOL

11 - OCTOBER - 1985

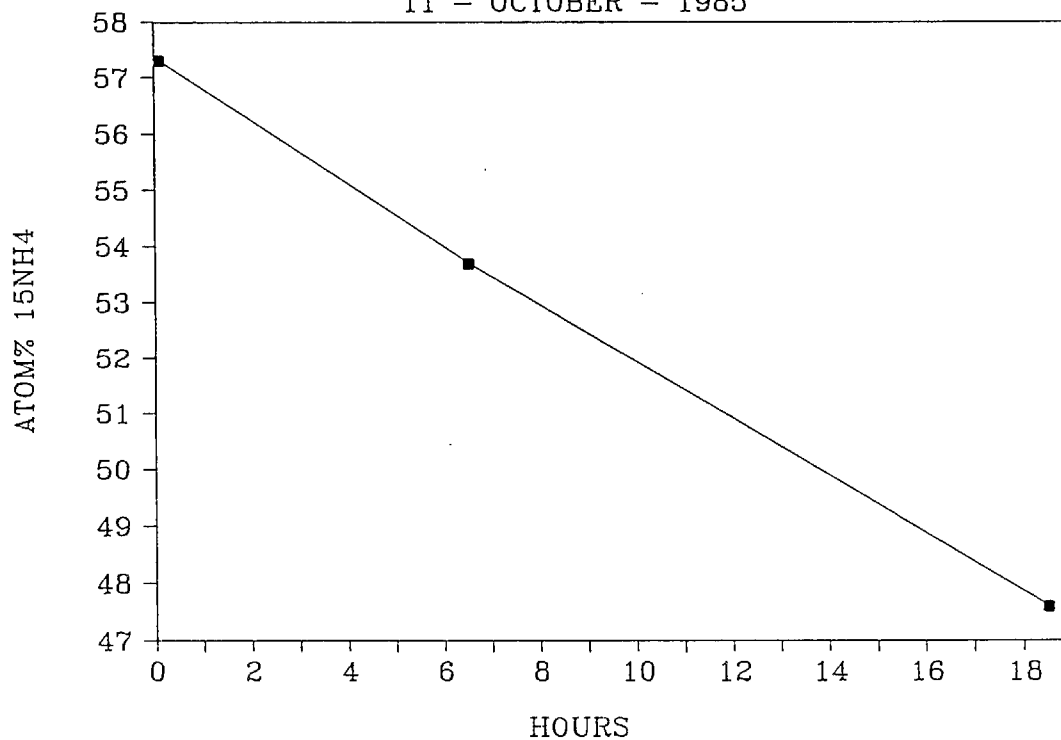
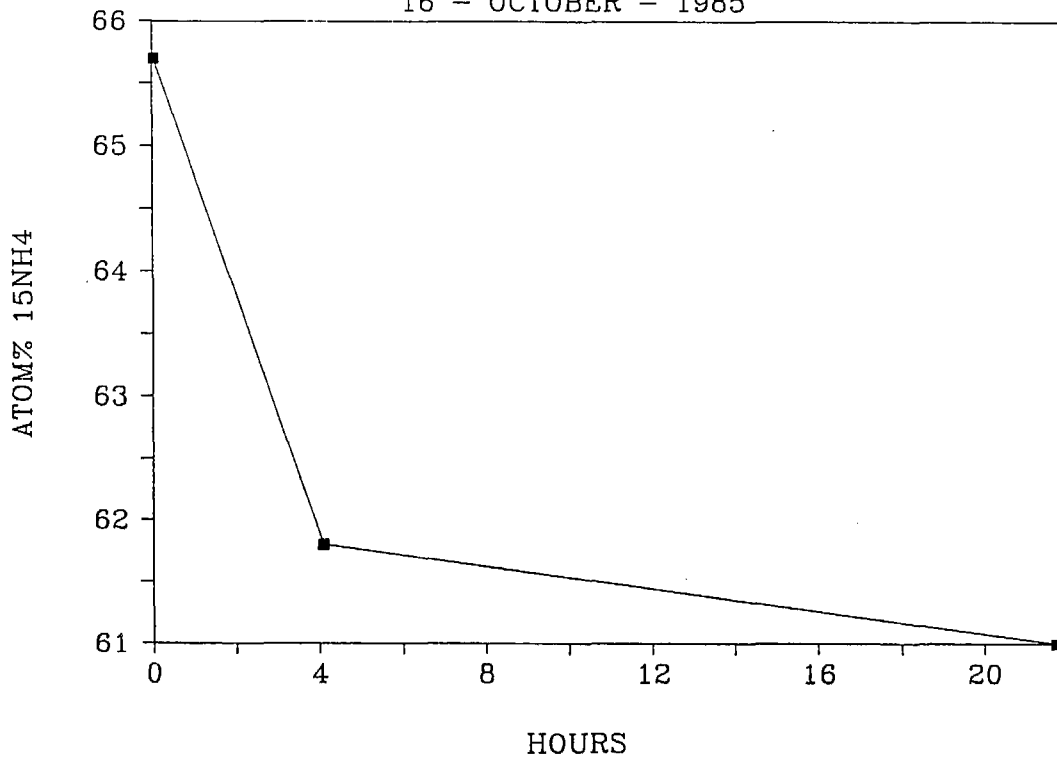


Figure II-41a+b. Atom% $^{15}\text{N-NH}_4$ vs time; 26-September-85 and 11-October-85.

ATOM%15N - DISSOLVED AMMONIUM POOL

16 - OCTOBER - 1985



ATOM%15N - DISSOLVED AMMONIUM POOL

17 - OCTOBER - 1985

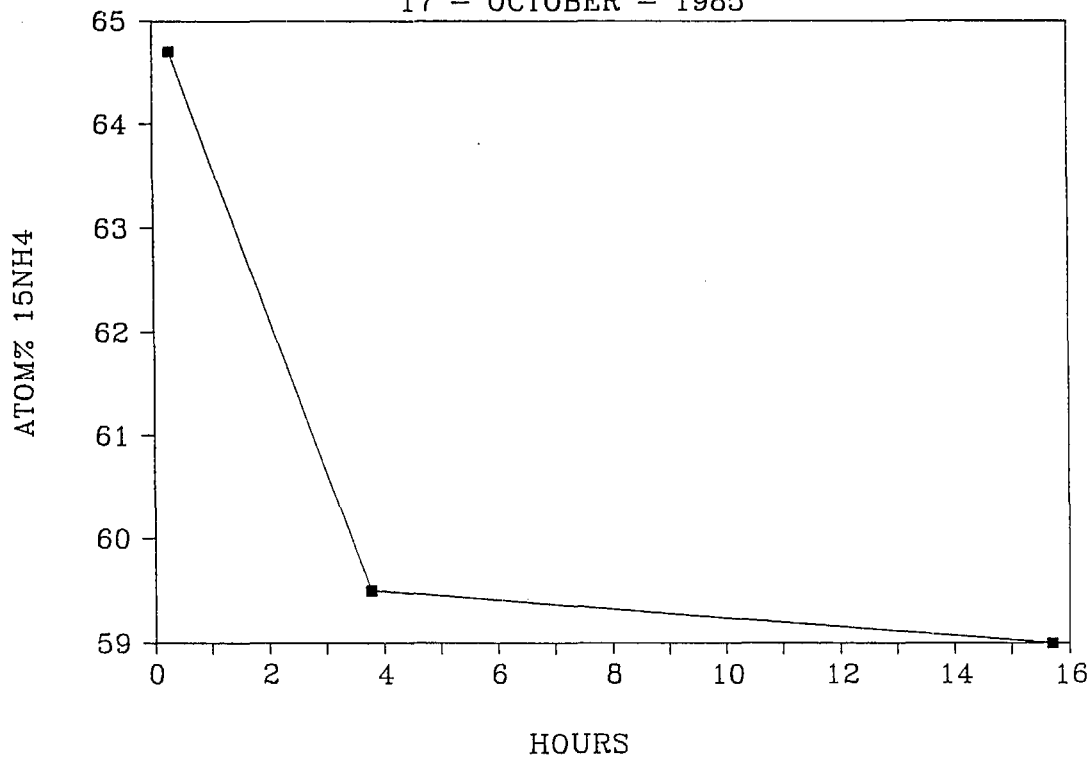


Figure II-42a+b. Atom% ¹⁵N-NH₄ vs time; 16-October-85 and 17-October-85.

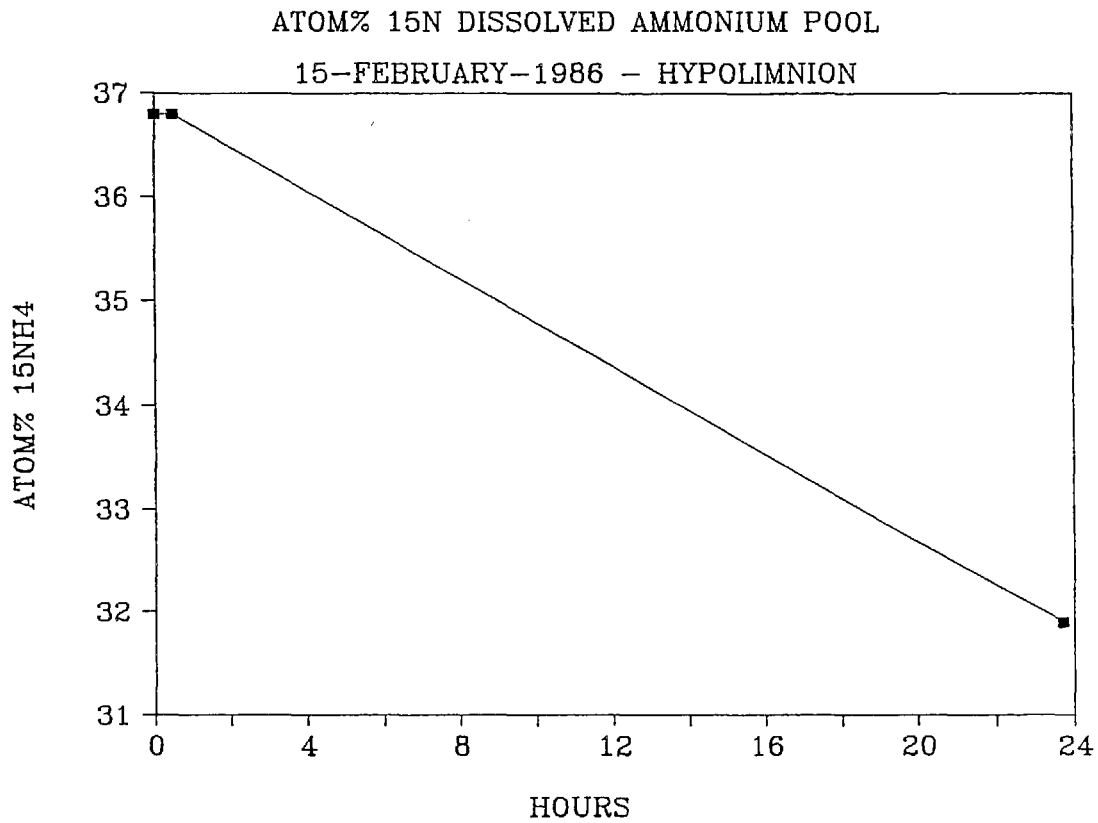
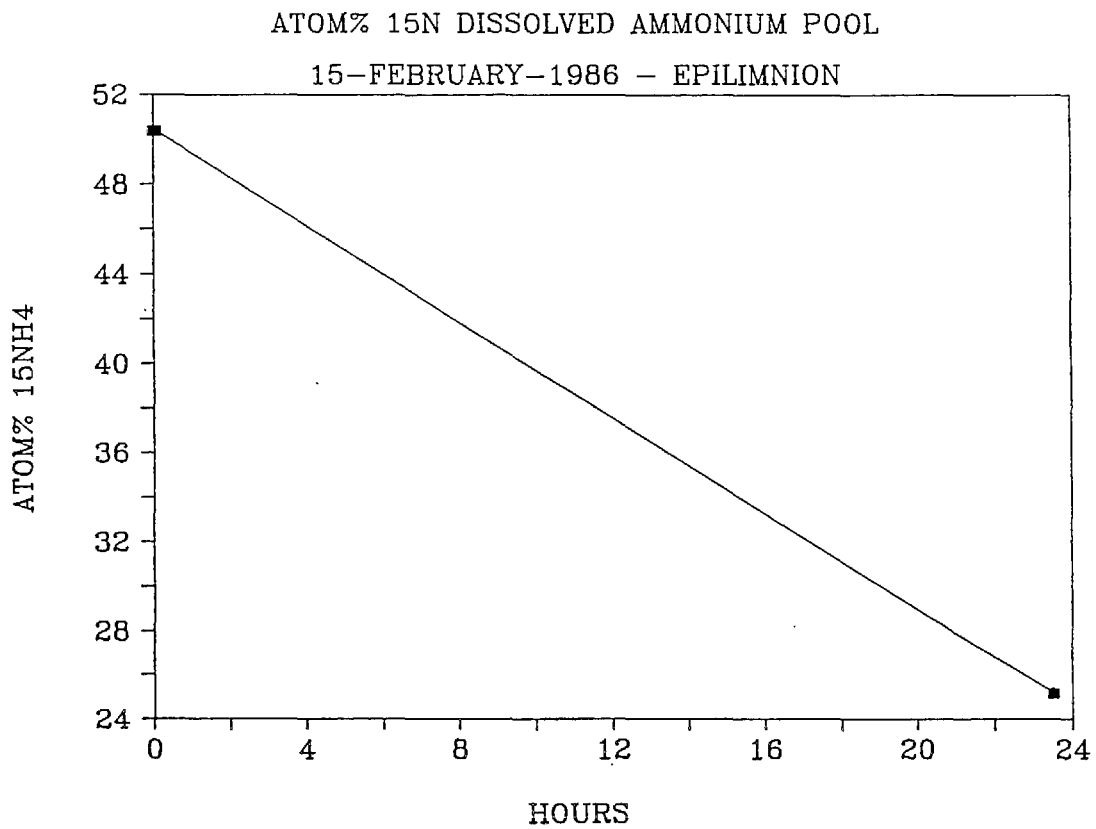
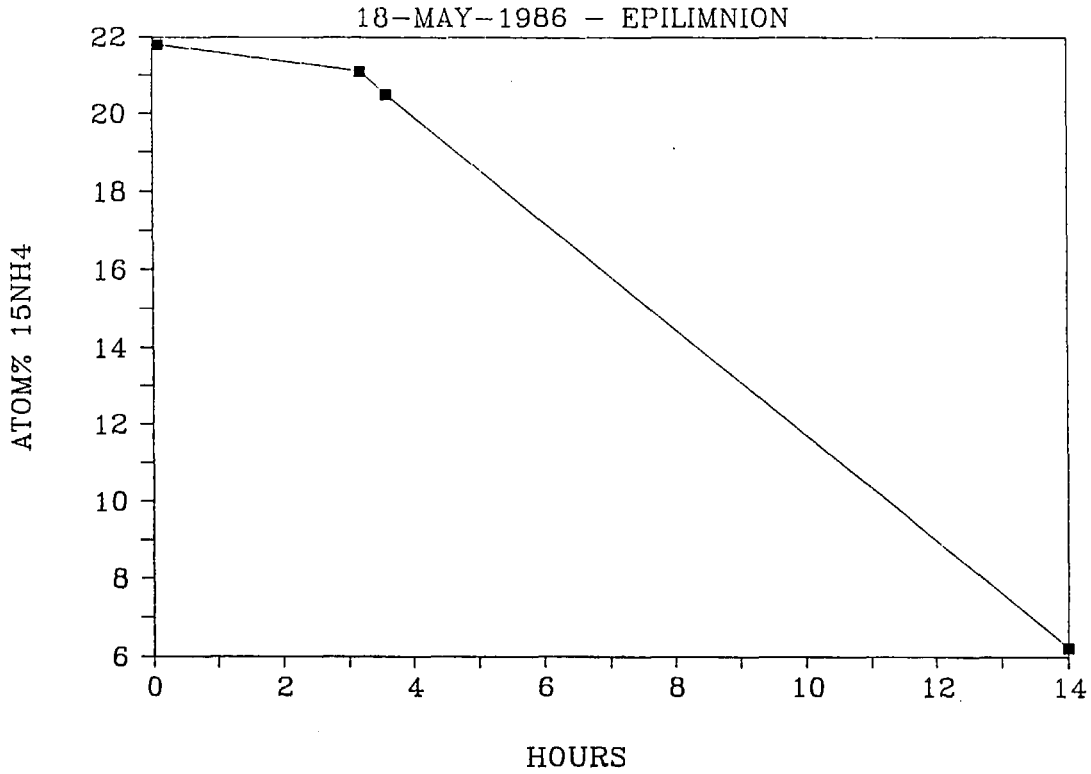


Figure II-43a+b. Atom% $^{15}\text{N-NH}_4$ vs time; 15-February-86, epilimnion & hypolimnion.

ATOM%15N - DISSOLVED AMMONIUM POOL



ATOM%15N - DISSOLVED AMMONIUM POOL

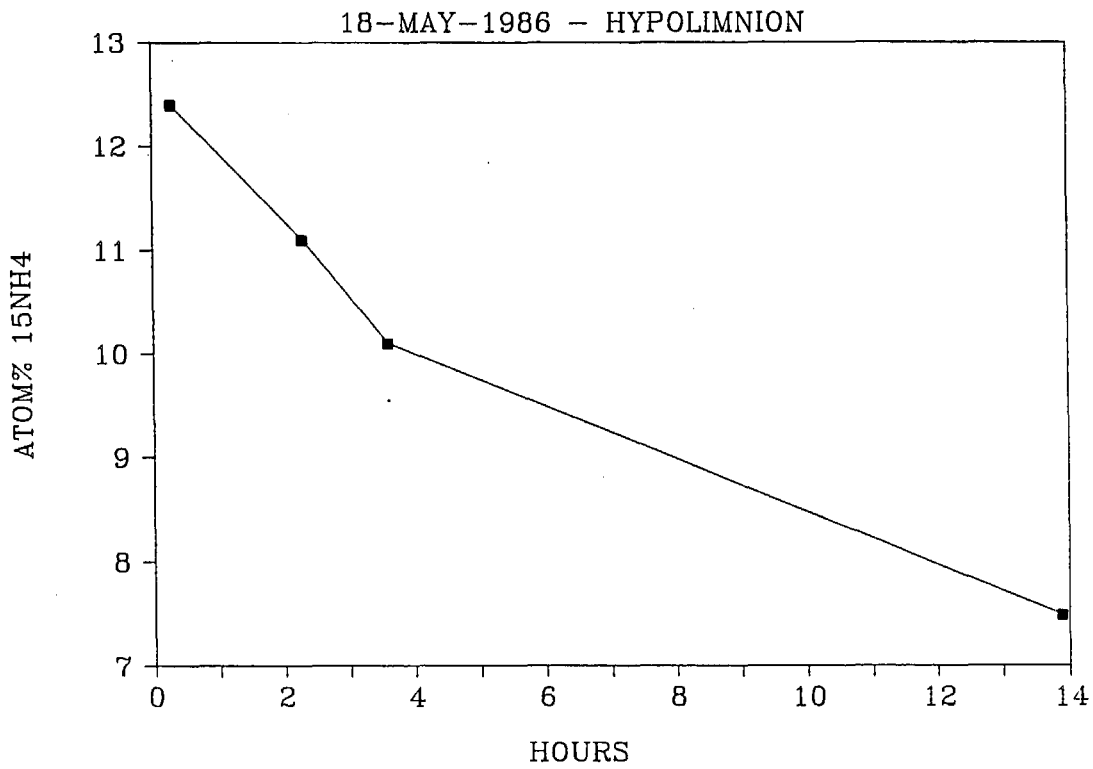
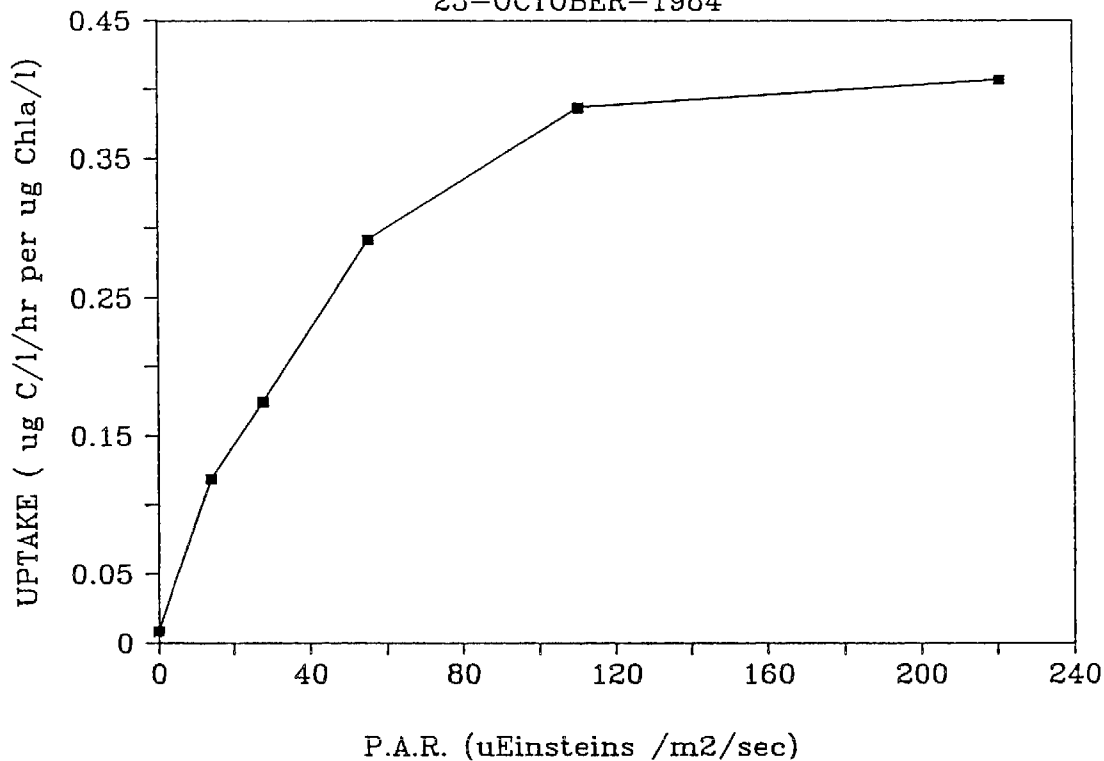


Figure II-44a+b. Atom% $^{15}\text{N-NH}_4$ vs time; 18-May-86, epilimnion & hypolimnion.

CHLOROPHYLL SPECIFIC UPTAKE

23-OCTOBER-1984



CHLOROPHYLL SPECIFIC UPTAKE

18-MAY-1986

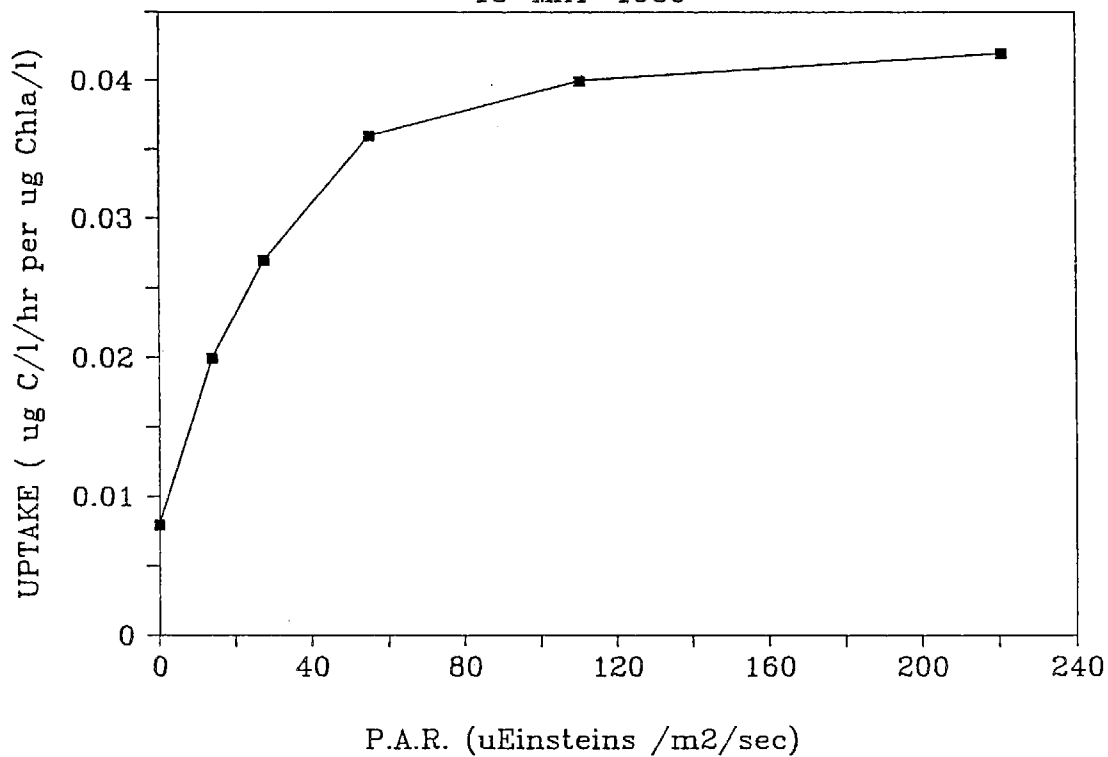


Figure II-45a+b. Chlorophyll specific carbon uptake vs light; 23-October-84 & 18-May-86.

CHLOROPHYLL SPECIFIC UPTAKE

13-JULY-1985

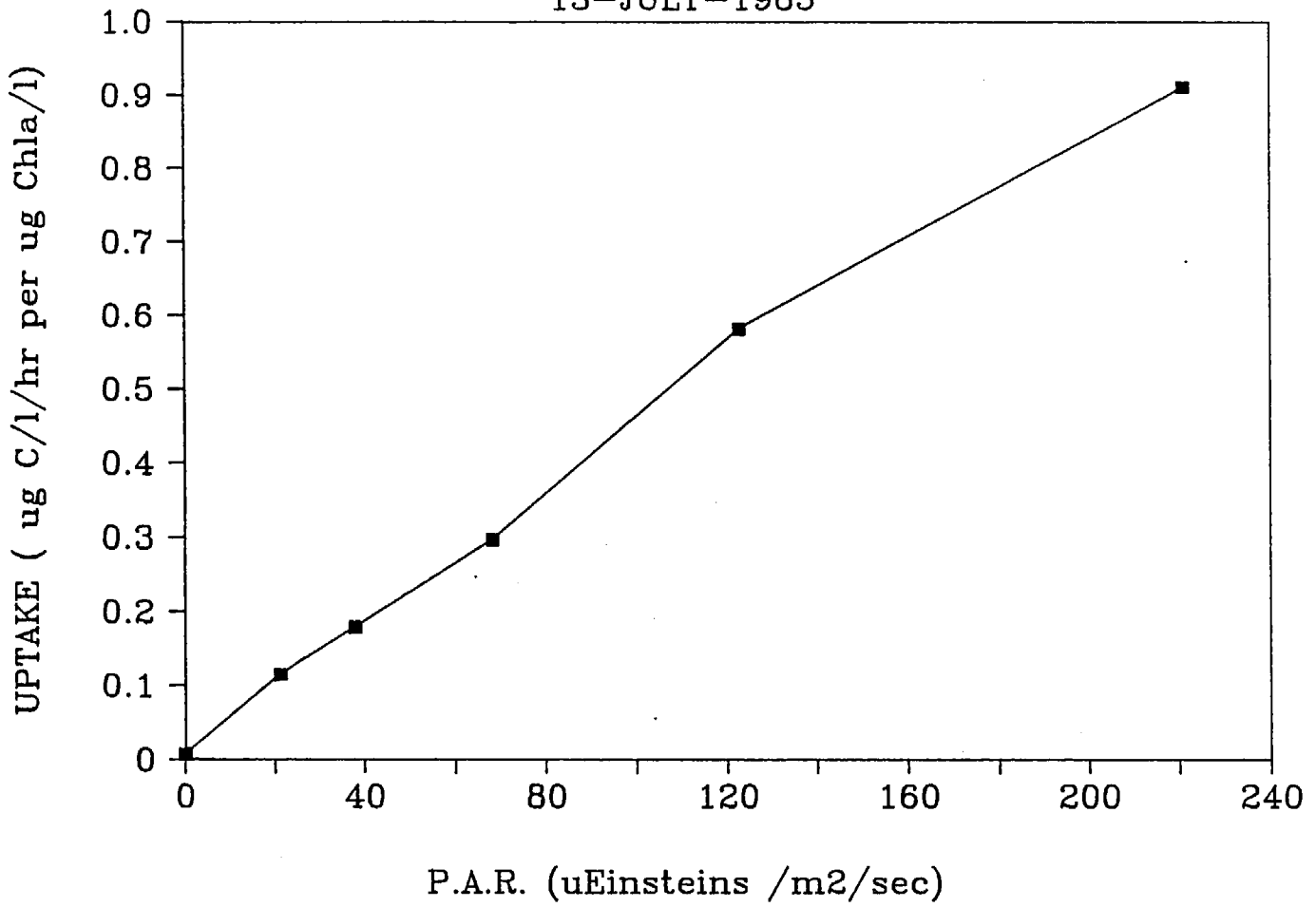


Figure II-46. Chlorophyll specific carbon uptake vs light; 13-July-85.

MAXIMUM CHLOROPHYLL SPECIFIC CARBON UPTAKE

SUMMER - 1984 AND 1985

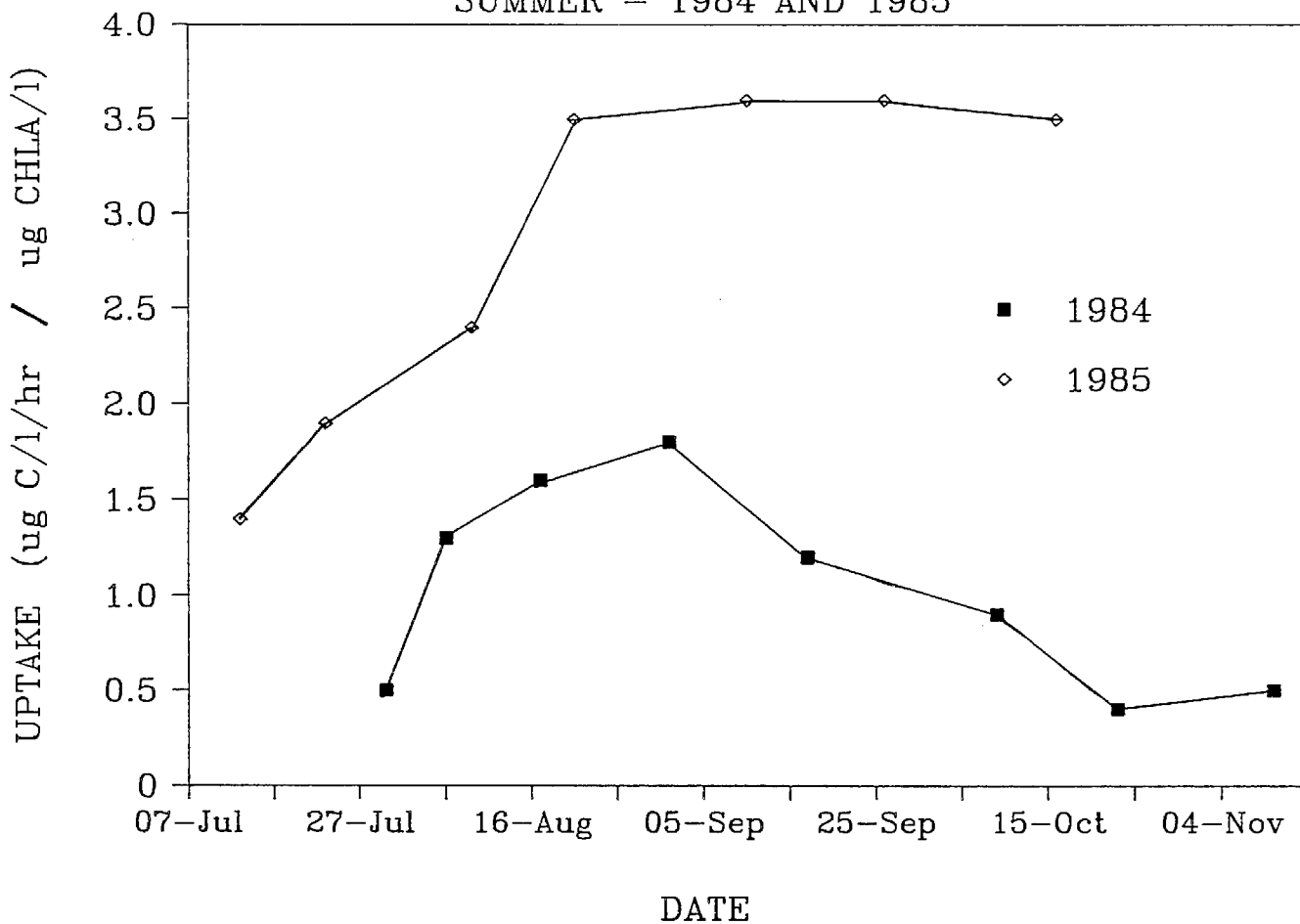


Figure II-47. PmB during the summers of 1984 and 1985.

MAXIMUM CARBON UPTAKE
SUMMER - 1984 AND 1985

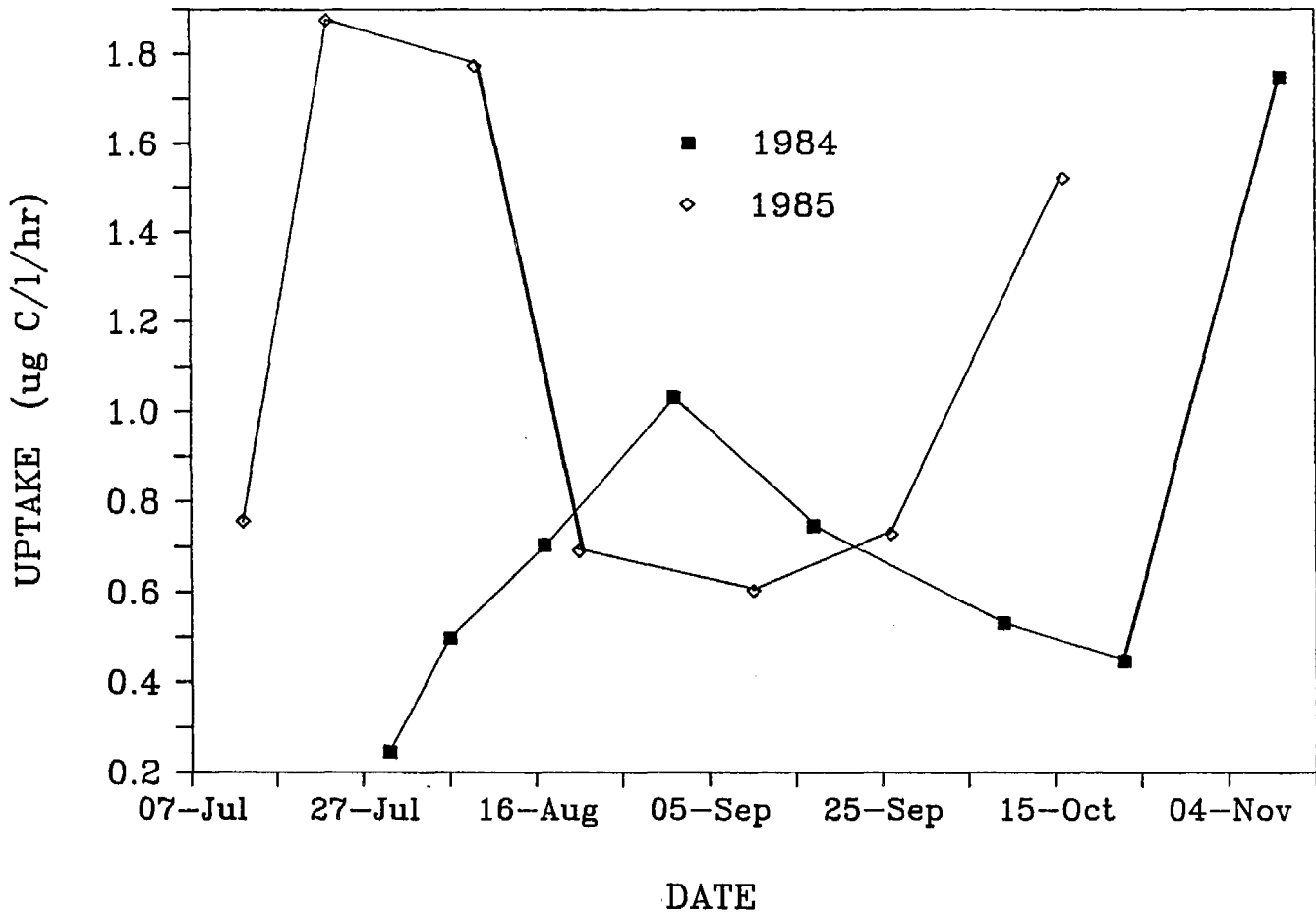


Figure II-48. Pm during the summers of 1984 and 1985.

ALPHA

SUMMER - 1984 AND 1985

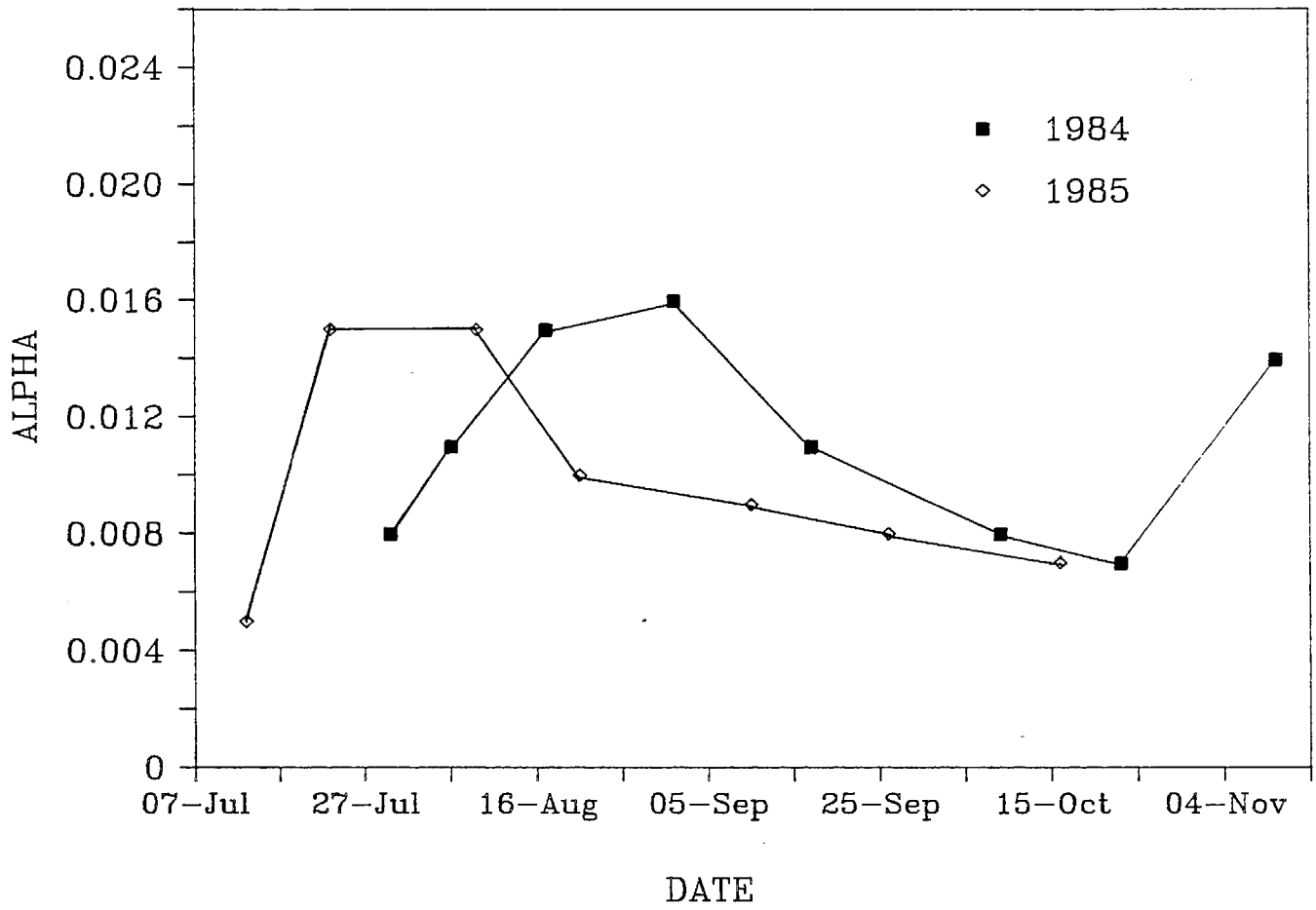


Figure II-49. Alpha during the summers of 1984 and 1985.

CHLOROPHYLL TIME SERIES - SUBSURFACE

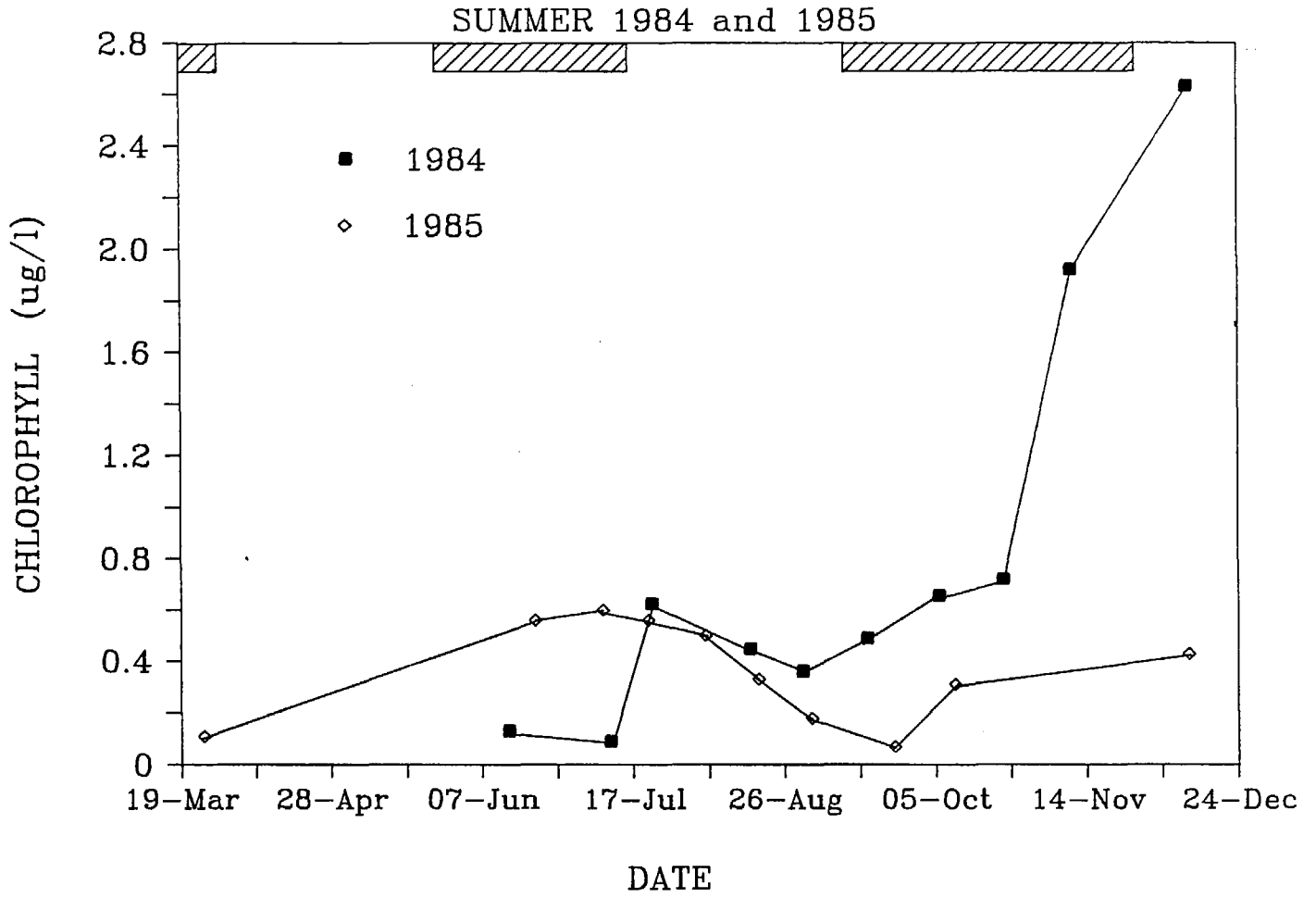


Figure II-50. Chlorophyll a levels during the summers of 1984 and 1985.

SECCHI DISK TRANSPARENCY

SUMMERS OF 1984 AND 1985

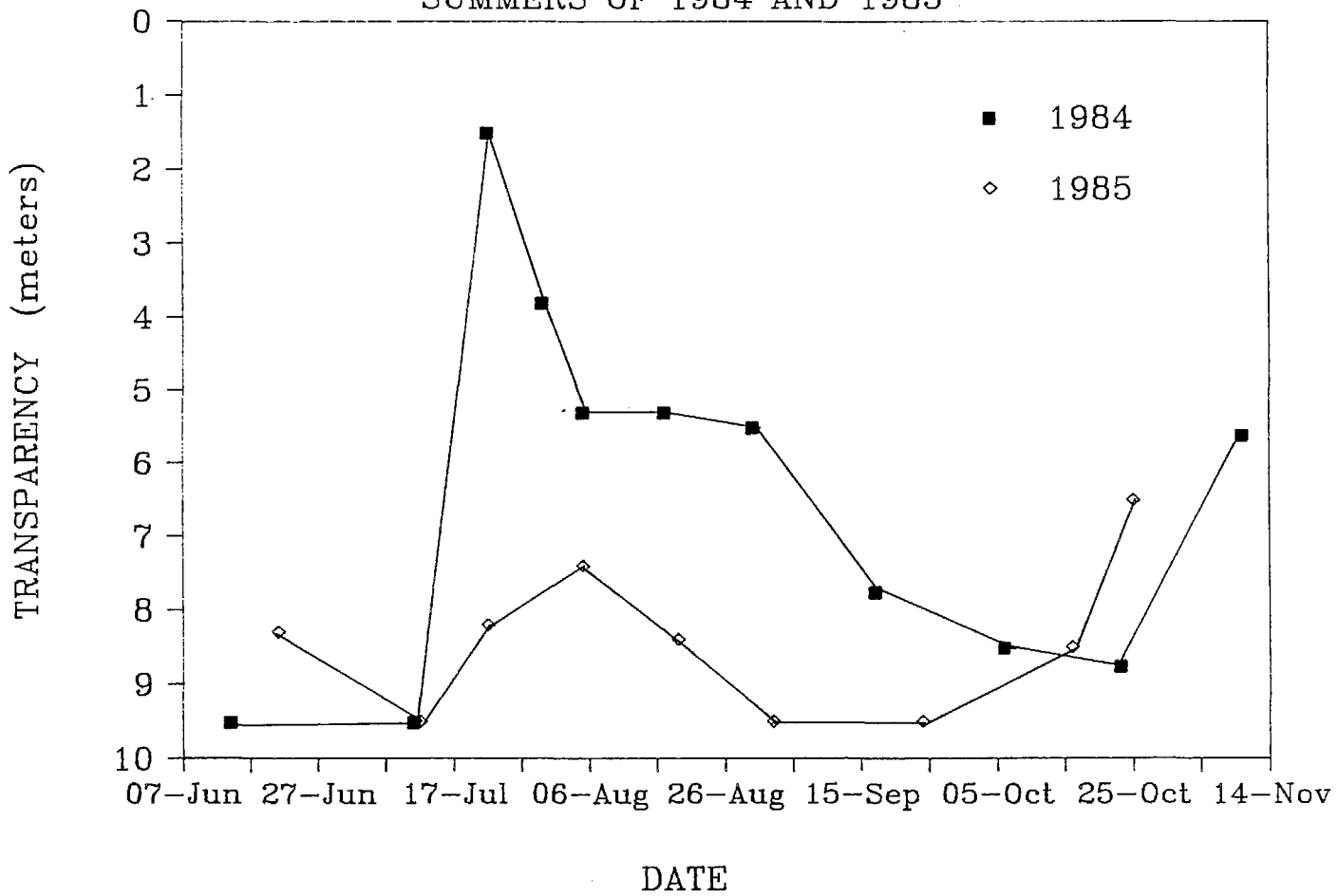


Figure II-51. Secchi disk transparency during the summers of 1984 and 1985.

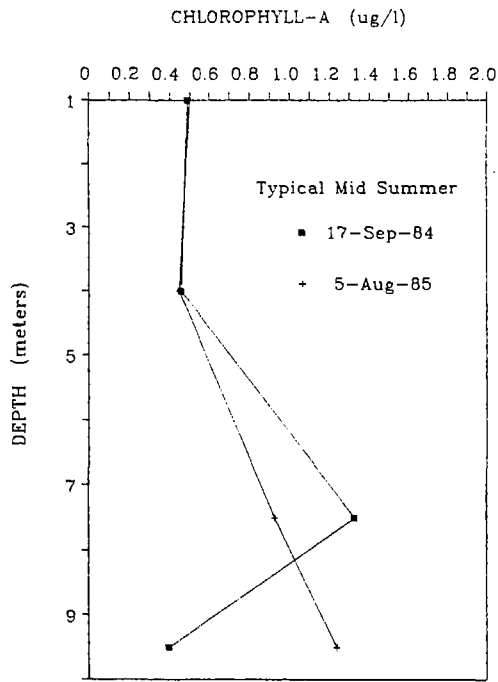


Fig. II-52

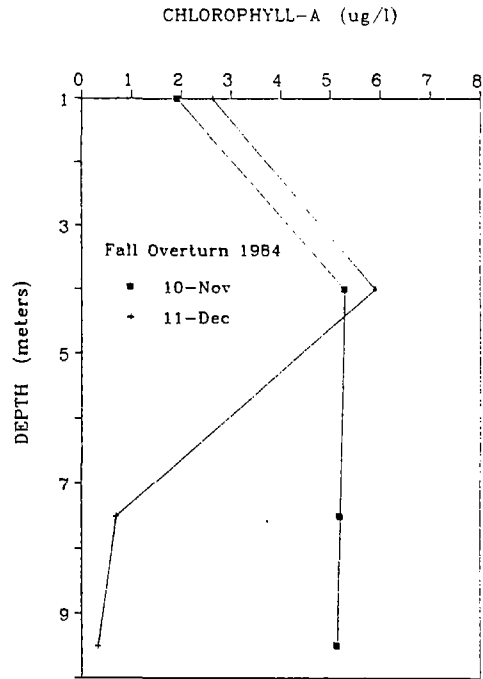


Fig. II-53

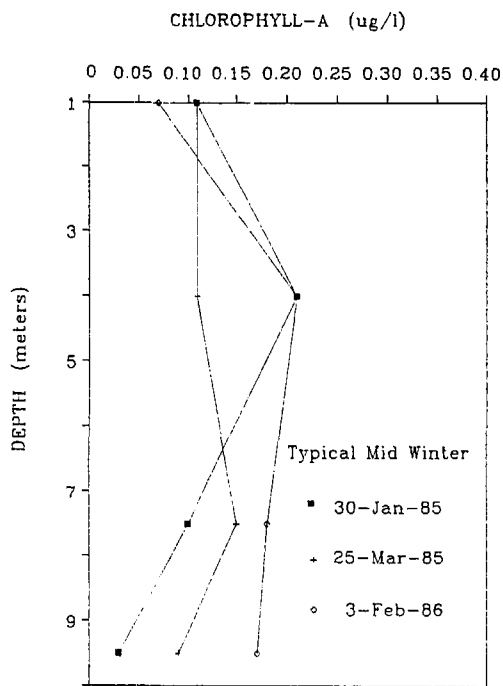


Fig. II-54

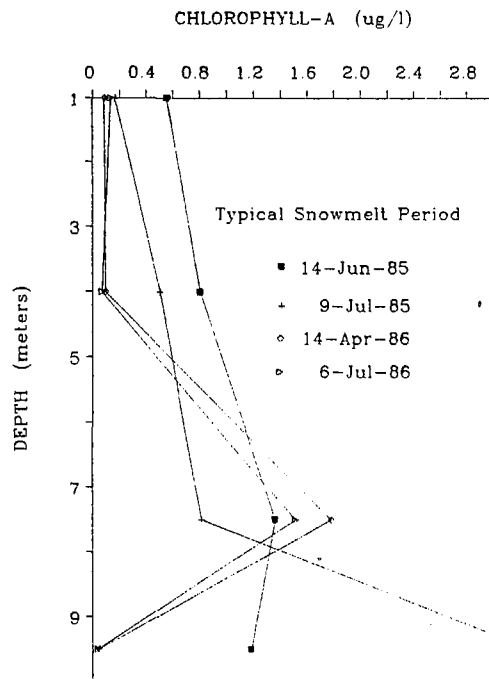


Fig. II-55

Chapter II.3 SEDIMENT-WATER FLUXES

Introduction

The interface between lake sediments and the overlying water plays an important role in the flux of solutes into lake water (e.g. Mortimer 1941, Lerman 1979, Hesslein 1980). These fluxes contribute alkalinity which may buffer inputs of acidity via atmospheric deposition or runoff. For example, Stoddard (in press) has measured considerable increases in alkalinity under ice in Gem Lake (Rock Creek Basin) and attributed those increases entirely to weathering reactions in the watershed. Corroborative evidence for the role of sediments in retarding acidification is provided by Oliver and Kelso (1983) for headwater lakes in Ontario. They reported the median value of sediment buffering capacity to be 1.3 times the median of the total buffering capacity of the lake water and attributed 80% of the production of bicarbonate to mineral weathering. Furthermore, an important role for reduction in sediments as sources of increased alkalinity has been proposed by Schindler et al. (1980), Kilham (1982), Kelly et al. (1982), Cook et al. (1986), and Rudd et al. (1986).

Recent interest in the supply and recycling of nutrients has led to methodological improvements which permit in-situ measurement of sediment-water fluxes. Chambers have been designed that are placed over the sediment surface and sequential samples collected as a direct measure of exchange (e.g. Fisher et al. 1982). The two main purposes of the work reported here were to provide measurements of alkalinity flux from the sediments into the overlying water and, secondly, to quantify the relative importance of biogeochemical processes that contribute to alkalinity generation in Emerald Lake.

Methods

In-situ measurements of sediment-water fluxes.

Benthic chambers - The transport of chemical constituents across the sediment-water interface was measured directly in Emerald Lake using benthic chambers placed over the sediment surface. The plexiglas chambers were 50 cm

in diameter and 18 cm high and were fitted with ports for sampling tubes, an oxygen electrode and a small bilge pump connected to a 12 volt battery which circulated water in the chamber (Fisher et al. 1982). The pump was seated on the top center of the chamber withdrawing water and recirculating it through plastic tubing to stoppered ports on the top periphery of the chamber (Fig. II-56). By disconnecting these stoppers, water was flushed through the chamber just prior to the onset of each experiment. A controller connected to the pump allowed for the setting of variable pump speeds. A small diameter (0.8 mm) plastic tube extended to the surface to permit collection of water samples for chemical analysis. A short tube on the top of the chamber allowed replacement of water withdrawn; this amounted to approximately 350 ml or less than 2% of the chamber volume for each experiment. Centimeter increments along the vertical wall of the chamber allowed determination of chamber height above the sediments and thus volume of water that was enclosed for each experiment.

The chambers were deployed by SCUBA divers who attempted to minimize sediment disturbance during placement. The oxygen meter, pump controller, power supply and sampling tube were placed in a boat securely anchored above the chamber. When possible, the chamber was inserted in the sediments with ports open at least one day prior to the onset of the experiment to allow for settling of any disturbed sediments. This procedure was employed for 2 experiments (July 17 and Aug. 8, 1985). The remaining experiments were begun the same day as deployment of the chamber; the enclosed water was flushed out prior to inserting the stoppers in the ports at the top of the chamber.

Dissolved oxygen and temperature were recorded after dissolved oxygen stabilized, usually within 15-30 minutes. For the 7 experiments conducted in August and October, 1985, water was kept circulating throughout the experiment. The pump speed ranged from 80% to 90% of its maximum output of 0.8 liter s^{-1} . In all other experiments the pump was on only for sampling periods to thoroughly mix the water in the chamber and until a stable reading for dissolved oxygen could be obtained.

The duration of most experiments was 24 hours or less during which the chamber was sampled 3 to 4 times. The intervals between sampling varied from 1.25 to 20 hours. For several experiments done in 1985 (July 17, August 8 and 20, October 15), a water sample was taken outside the benthic chamber and as close to the sediment surface as possible by divers using a 140 ml

syringe. This sample was compared chemically with the initial sample as an indicator of sediment disturbance during placement of the chamber.

The benthic chamber was deployed in 3 meters of water near the northeast inflow for 3 experiments and in 9.5 to 10 meters of water in the center of the lake for the other 10 experiments.

Chemical measurements included pH, alkalinity, conductance, major cations (calcium, magnesium, sodium, potassium), major anions (nitrate, sulfate, chloride), silica, and nutrients (ammonium and phosphate). Procedures and methods followed for collection and analysis of chemical samples are described in Section II-1.

The fluxes of chemical constituents were calculated from the time series measurements according to the equation:

$F = (C_2 - C_1) * V / (A * t)$ where F = flux ($\mu\text{eq m}^{-2} \text{hr}^{-1}$), $C_2 - C_1$ is change in concentration from beginning (1) to end (2) of each time interval ($\mu\text{eq/l}$), V is volume of the chamber (l), A is surface area of the sediments covered by the chamber (m^2), and t is elapsed time (hours).

Large enclosures - The fluxes of chemical constituents across the sediment-water interface were measured also using cylindrical (1 meter in diameter) clear polyethylene plastic enclosures (bags) that extended from the lake surface into the sediments. Each of the eight bags enclosed 5000-7000 liters of water and 0.5 m^2 of sediment surface. To allow possible contaminants from the plastic to diffuse into the surrounding water, the enclosures were placed in the lake one day prior to deployment. The bottom frame of each bag, which consisted of a rectangle made from PVC plastic pipe, was inserted into the sediments using SCUBA. The addition of a 1:1 solution (by equivalents) of nitric and sulfuric acids lowered the pH to between 5.3 and 5.5 in four of the eight bags.

The bags were sampled immediately before acidification and 1, 12, and 27 days after acidification. Samples for all chemical measurements except trace metals were taken using a 2-liter all plastic Kemmerer bottle at depths of 2 and 9 meters in each bag. Samples for trace metal analysis were obtained using a peristaltic pump. The lake was isothermal for the duration of the 4 week experiment conducted from September 7 to October 7, 1985.

Chemical measurements included pH, alkalinity, electrical conductance, ammonium, major cations (calcium, magnesium, sodium, potassium), major anions (nitrate, sulfate, chloride), trace metals (aluminum, iron, manganese),

silica, chlorophyll a and total particulate carbon and nitrogen. Procedures and methods followed for collection and analysis of chemical samples are described in Section II-1. The fluxes of chemical constituents were calculated from the same equation used for in-situ benthic chamber flux calculations.

Whole lake - The net flux of alkalinity into the hypolimnion was calculated during four periods of stratification in Emerald Lake (summer 1984, 1985 and winter 1984, 1985). From the vertical profiles of temperature and dissolved oxygen, the depths of the thermocline and oxycline for each sampling period were determined. Lake volume and sediment area below the thermocline and oxycline were derived from the bathymetric relationship between lake volume and sediment area and depth. Each depth interval was assigned an alkalinity value (eq/m³) based on chemical samples taken at 3-4 depths in the lake and vertical temperature profiles. The change in mass of alkalinity (eq) in the water column was computed between sampling dates (biweekly during the summer; monthly during the winter). The alkalinity flux to the hypolimnion was calculated according to the equation:

$F = m_2 - m_1 / (A * t)$ where $F = \text{flux (eq m}^{-2} \text{ d}^{-1})$, $m_2 - m_1$ is the change in alkalinity in a volume of water between sampling dates (eq), A is total sediment area below the hypolimnion or low oxygen layer above the sediments (m²), t is time between sampling dates (days).

Calibration of shear velocity inside the benthic chamber.

The shear velocity and the thickness of the boundary layer between liquid and solid, created by the artificial circulation inside the benthic chamber, were measured in the laboratory.

Alabaster plates (calcium sulfate dihydrate) embedded in a plastic matrix were exposed to distilled water according to the method developed by M. Buchholtz, P. Santschi and P. Bower (personal communication) and sequential samples were taken for calcium analysis.

A square plexiglas sheet 60 cm wide was fitted with a 50 cm diameter groove on which the benthic chamber was seated. Within this 50 cm circle were carefully cut and sanded pieces of alabaster embedded in plastic. The sides and backs of the alabaster pieces were coated with polyurethane paint to prevent dissolution on these edges in the event that water came in contact

with them and, secondly, to prevent the embedding substance from sticking to the alabaster. The total surface area of the alabaster was recorded. To minimize differential dissolution, the surfaces of the alabaster were level with those of the embedding material.

The chamber and the groove along the plexiglas sheet were sealed together with silicon sealant to prevent leakage. The chamber as well as the hoses used to circulate water were filled with distilled water so that no air spaces remained.

Dissolved oxygen, temperature, and time of day were recorded and a 5 milliliter sample for calcium analysis withdrawn. A constant temperature of 25°C was desired although it varied from 23° to 27°C. The experiments lasted for 24 to 48 hours during which samples were taken every 7 to 10 hours. A total of 3 calibrations were conducted; two at the controller setting of 80% and one at 90% maximum power. The pump remained switched on throughout each experiment.

Calcium analysis was performed using an air-acetylene flame on a Varian atomic absorption spectrophotometer. Standards were prepared using calcium sulfate dihydrate (gypsum) ranging in concentration from 0.25 mg/l to 4 mg/l. Samples were diluted correspondingly to minimize interference from the sulfate ion. To suppress ionization of calcium, potassium chloride was added to standards, samples, and blanks to give a final concentration of 2000 µg/ml potassium in all solutions.

The boundary layer thickness at the solid-liquid interface was calculated according to the equation: $z = D * A / k * V$ where D is the molecular diffusion coefficient at the appropriate temperature A is area of all alabaster exposed, V is volume of the enclosed water and k is the transfer coefficient. From the rate of calcium dissolution, the transfer coefficient can be computed from the following equation:

$[Ca^{2+}]_t = [Ca^{2+}]_{sat} - ([Ca^{2+}]_{sat} - [Ca^{2+}]_o) \exp(-kt)$ where $[Ca^{2+}]_o$ is initial calcium concentration, $[Ca^{2+}]_t$ is calcium concentration at any time t, $[Ca^{2+}]_{sat}$ is calcium concentration at saturation for the appropriate temperature and pressure. For a small kt this equation reduces to:

$$[Ca^{2+}]_t = [Ca^{2+}]_o + [Ca^{2+}]_{sat} * (1 - \exp(-kt)).$$

When dissolution is in the initial linear range of the curve for calcium sulfate dissolution, $1 - \exp(-kt)$ is equal approximately to kt and the equation reduces to:

$$[Ca^{2+}]_t = [Ca^{2+}]_o + [Ca^{2+}]_{sat} * kt \text{ or}$$

$$k = ([Ca^{2+}]_t - [Ca^{2+}]_o) / ([Ca^{2+}]_{sat} * t).$$

The equation for film thickness then becomes:

$$z = D * A * [Ca^{2+}]_{sat} * t / V * ([Ca^{2+}]_t - [Ca^{2+}]_o)$$

The value for $[Ca^{2+}]_{sat}$ at 25°C was used for all calculations. The values for diffusivity coefficients used in the computations varied depending on temperature (G. Gust, B. Opdyke and J. Ledwell, personal communication). The first time interval in each experiment was used for the computation of the transfer coefficient as the rate of calcium dissolution was more likely to be linear.

The shear velocity u , was then calculated according to the equation developed by G. Gust, B. Opdyke, and J. Ledwell (personal communication):

$z = 4 * v / u * (Sc^{1/7})$ where z is the boundary layer thickness, v is viscosity for the appropriate temperature, and Sc is the Schmidt number, a dimensionless ratio of v , kinematic viscosity and D , the molecular diffusion coefficient.

In-situ measurements of shear velocity on the bottom of Emerald Lake.

The shear velocity u , and boundary layer thickness z , at the sediment-water interface were measured in Emerald Lake in October 1985 when the lake was isothermal.

Two 100 cm square alabaster plates fitted with plexiglas pedestals were placed in the sediments at a depth of 10 meters using SCUBA. The sides and backs were coated with polyurethane paint to confine dissolution only to the top surface. The plates were carefully weighed on an analytical balance prior to deployment. The pedestals were inserted into the sediments with the plates level with the sediment surface. In a closed system, such as the laboratory calibration of pump settings, water samples were taken for calcium analysis throughout the exposure. For open systems, such as the lake deployment, weight loss of the alabaster was used to determine film thickness. Factors that contribute to weight loss are mean velocity at the interface, turbulence and temperature.

The plates remained in Emerald Lake for two weeks and were then recovered using SCUBA, dried at room temperature and weighed on an analytical

balance. The flux of calcium was calculated from weight loss according to the following equation:

Ca^{2+} ($\text{g cm}^{-2} \text{ s}^{-1}$) = (weight loss(g) of alabaster) * (.2328 g Ca^{2+} /g alabaster) / (surface area of alabaster) * (time exposed to dissolution). Assuming that dissolution was occurring in the initial linear range of the curve for calcium sulfate dissolution, the boundary layer thickness, z was calculated from the following equation:

$$z = D * [\text{Ca}^{2+}]_{\text{sat}} / \text{Flux}$$

where D is the molecular diffusion coefficient at 8°C which was the average temperature of the lake during the experiment. The value obtained for the diffusion coefficient of calcium at 8°C was extrapolated from values at 0°C and 18°C for tracer diffusion coefficients of ions at infinite dilution in water (Li and Gregory, 1974). Calcium saturation at 25°C was assumed to approximate calcium saturation at 8°C.

The shear velocity u, was computed according to the equation:

$$z = 4 * v / u * (\text{Sc}^{1/7})$$

where z is diffusive boundary layer thickness, v is kinematic viscosity at 8°C and Sc is the Schmidt number, a dimensionless ratio of kinematic viscosity and the molecular diffusion coefficient.

Effects of bioturbation on sediment-water fluxes.

The effect of bioturbation on the transport of chemical constituents across the sediment-water interface was tested in the laboratory using small (8 liter) microcosms. Chironomidae larvae are found in the upper 5 cm of sediment and occur at densities of ca. 5000 m^{-2} in Emerald Lake during the ice free season.

Using an Ekman dredge, sediment from Emerald Lake was collected in 10 meters of water in November 1985. The sediment was returned to the laboratory cold room (5°C) and filtered through a series of progressively finer wire mesh sieves to remove the chironomids. The live animals were counted and placed temporarily in petri dishes with sediment and water. The bottom (8 cm in diameter) of each microcosm was filled with 1.5 liters of sediment slurry. Chironomids were added to 3 of the 7 microcosms. Resulting densities of these invertebrates in the microcosms were similar to those found in the lake. Each microcosm was filled with 5 liters of filtered water

from Emerald Lake. All work was done in the laboratory cold room at 5°C to avoid temperature shock to the animals.

The microcosms were sampled 1 day after addition of the chironomids to the sediments and every 1-2 days for 14 days. Measurements included temperature, dissolved oxygen, pH, alkalinity, and ammonium.

Results

In-situ measurements of sediment-water fluxes.

Fluxes measured with the benthic chamber - The fluxes of chemical constituents between the sediments and the overlying water column calculated from the benthic chamber experiments are summarized in Table II-7. Alkalinity consistently increased inside the chamber for all experiments. Alkalinity fluxes ranged from 2.5 to 15.4 meq m⁻² d⁻¹ for experiments conducted in the deep portion of the lake (9 m). Mean fluxes of alkalinity at a depth of 9 meters were not significantly different (P, 0.05) between the summers of 1984 and 1985. For both years, mean fluxes of alkalinity measured at depths of 9 and 3 meters were not significantly different (P, 0.05). Experimental methods in 1984 followed a different protocol (i.e., the water within the chamber was mixed only during sampling periods) than methods followed in 1985 (i.e., water was mixed continuously). Both methods yielded a similar range of fluxes.

Calcium, ammonium and magnesium concentrations increased inside the chamber for all experiments. Sodium and potassium concentrations increased in 11 of the 12 experiments. Nitrate concentrations decreased in all experiments except for two conducted in shallow water (3 meters). Sulfate concentrations decreased in 11 of the 12 experiments (Figure II-57a,b,c). The fluxes of chemical constituents were variable; standard deviations of measurements as grouped in Table II-7 were greater than 50% of the mean for alkalinity, ammonium, nitrate, calcium and magnesium and 100% of the mean for sulfate, sodium and potassium.

The levels of dissolved oxygen in the chamber would be expected to affect the relative contribution of redox reactions (e.g. nitrate, sulfate and iron reduction) to alkalinity generation (Kelly et al. 1982; Kilham 1982). Experiments in which the dissolved oxygen concentrations inside the

benthic chamber dropped below 10% of saturation (near-anoxia) were compared to those in which dissolved oxygen concentrations were maintained at levels greater than 25% saturation (Table II-8). In four experiments in 1985, dissolved oxygen concentrations inside the chamber dropped to less than 10% of saturation while ambient lake concentrations remained greater than 25% of saturation. In two experiments (Aug. 20, 1985 and Sept. 4, 1984) both the inside of the chamber and the lake bottom were anoxic. Mean alkalinity flux was greater in experiments with low levels of dissolved oxygen. The mean flux of ammonium was 4 times higher for chamber experiments that went anoxic than for those that remained oxygenated. The rate of loss of nitrate from the water column was approximately 3 times greater in the anoxic chamber experiments. The remaining fluxes of chemical constituents (e.g. sulfate) were similar for aerobic and anaerobic chamber conditions.

Large enclosures - Fluxes of alkalinity and other chemical constituents were not computed for the non-acidified enclosures because changes in alkalinity from day 1 to day 27 of the experiment were unmeasurable (Fig. II-58). There were no differences in alkalinity between the samples taken at depths of 2 and 9 meters as the lake was isothermal. The mean fluxes of chemical constituents, as calculated from the acidified four enclosures that included sediment, are summarized in Table II-9. Mean sulfate and nitrate fluxes were approximately 5 times greater than fluxes calculated from the benthic chamber experiments. Mean ammonium flux was approximately 20 times lower than fluxes computed from benthic chamber data. Calcium and alkalinity fluxes were comparable to those calculated from the benthic chamber experiments.

The bags exhibited variability within treatments; two of the four acidified bags showed no net change in alkalinity while the other two showed a distinct rise in alkalinity and decrease in nitrate and sulfate concentrations from day 1 to day 27 of the experiment.

Whole lake - Alkalinity fluxes calculated for the hypolimnion and low oxygen layer on the lake bottom during summer 1984 and 1985 are summarized in Table II-10. Fluxes were not corrected for exchange with the epilimnion. Alkalinity produced in the hypolimnion during summer 1984 was greater than alkalinity produced during the summer of 1985. Alkalinity generated in the hypolimnion during the winter 1985 was greater than that generated during winter 1984. Low levels of oxygen for longer than two weeks coincide with

higher alkalinity fluxes (Aug. 31-Sept. 17, 1984 and Feb. 26-Mar. 25, 1985). The larger values of hypolimnetic flux (e.g. 4.8 for Aug. 31-Sept. 17) are comparable to those obtained from the benthic chamber experiments.

Calibration of shear velocity inside the benthic chamber and measurement of shear velocity on the bottom of Emerald Lake.

Boundary layer thickness and shear velocity measured inside the benthic chamber for two pump speeds and in-situ on the bottom of Emerald Lake are shown in Table II-11. The shear velocity is approximately 6 and 14 times smaller in the lake than for pump settings of 80% and 90% of maximum power, respectively. The boundary layer is 5 and 19 times thicker for the lake than for pump settings of 80% and 90%, respectively.

The rates of alkalinity generation can be scaled down to approximate rates under the natural flow conditions on the lake bottom. Since flux is proportional to shear velocity and inversely proportional to boundary layer thickness, flux values from the benthic chamber can be corrected for artificial circulation by dividing by the appropriate factor for a pump setting (for example: 6 for 80% or 14 for 90%). Fluxes that have been corrected for artificial circulation are shown in Table II-12.

The effects of bioturbation on sediment-water fluxes.

There was no significant difference ($P, 0.05$) in alkalinity concentrations between microcosms that contained chironomids and microcosms in which chironomids were absent (Figure II-59).

Discussion

Hydrogen ions are consumed by two primary mechanisms in watersheds and lakes: redox reactions (sulfate, nitrate, iron and manganese reduction) which require anoxic conditions and an organic oxidizable substrate (Kelly et al., 1982) and chemical weathering reactions which occur when water comes into contact with rock and soils (e.g. Drever 1982). Nitrate can be reduced to nitrogen gas and ammonium by bacteria or to organic material by assimilatory metabolism; both processes result in alkalinity production. Bicarbonate and base cations are produced as the minerals of granodiorite

(plagioclase, biotite and potassium feldspar) weather to form kaolinite. Differential weathering of plagioclase results in higher concentrations of calcium and sodium than magnesium and potassium in lake water (Garrels and MacKenzie, 1967). The bedrock in the Emerald Lake basin consists primarily of granodiorite.

By assuming electroneutrality and ignoring organic anions, the relative contributions of various ions to alkalinity can be calculated from the benthic chamber data according to the following equation:

$$\text{alkalinity} = (\text{Ca}^{2+} + \text{Mg}^{2+} + \text{Na}^+ + \text{K}^+ + \text{NH}_4^+) - (\text{SO}_4^{2-} + \text{NO}_3^- + \text{Cl}^-)$$

Calcium and ammonium furnished 70-80% of the alkalinity in the benthic chamber. For mean fluxes at a depth of 9 meters, 44% and 34% of the alkalinity produced could be accounted for by increased ammonium and calcium concentrations, respectively. The linear regression between calcium and acid neutralizing capacity yielded an r^2 value of .47 (Fig. II-60). For experiments in which dissolved oxygen concentrations were near zero, ammonium accounted for 47% of the alkalinity produced compared to 17% for higher levels of dissolved oxygen. Magnesium and potassium each contributed 5-8% of the alkalinity generated in all experiments. Sodium furnished a larger proportion of alkalinity in the experiments conducted in the shallow sediments (29%) than in the deep sediments (19%). The linear regression between sum of the base cations and acid neutralizing capacity yielded an r^2 value of .62 (Fig. II-61). Sulfate reduction accounted for nearly 14% of the alkalinity produced in experiments conducted in shallow water (3 meters) and 4% of the alkalinity produced in deep water (9 meters). Nitrate reduction produced approximately 8% of the alkalinity generated in deep water.

The linear regression between sum of the base cations plus ammonium and acid neutralizing capacity for all benthic chamber experiments is highly significant ($r^2 = .93$; Fig. II-62). Steep concentration gradients (greater than 200 $\mu\text{eq/l}$ in sediment pore water for the top 10 centimeters of sediment) would favor the transport of ammonium and the products of mineral weathering from the sediment pore water into the overlying water column (Harvey Michaels, personal communication). Results indicate that alkalinity flux inside the benthic chamber is the result of decomposition of organic matter and the hydrolysis of minerals in the sediments.

Table II-7. Fluxes of chemical constituents calculated from benthic chamber experiments at two depths in the lake (9 m and 3 m). Units are in meq m⁻² d⁻¹ except dissolved oxygen (mM m⁻² d⁻¹). Values are means with standard errors in parentheses.

	<u>HCO₃⁻</u>	<u>NH₄⁺</u>	<u>NO₃⁻</u>	<u>SO₄²⁻</u>	<u>Ca²⁺</u>	<u>Mg²⁺</u>	<u>Na⁺</u>	<u>K⁺</u>	<u>O₂</u>
Summer 1984 (9m) n=3	7.9 (2.8)	2.5	-0.24	-0.18	3.8	0.4	1.9	1.5	-38
Summer 1985 (9m) n=5	8.8 (2.5)	4.2	-0.4	-0.5	2.3	0.4	1.4	0.3	-17
All Experiments (9m) n=8	8.5 (1.7)	3.7 (1.0)	-0.3 (0.1)	-0.3 (0.2)	1.9 (0.7)	0.4 (0.1)	1.6 (0.8)	0.8 (0.5)	-25 (8.1)
All Experiments (3m) n=3	3.4 (1.0)	1.1 (0.6)	.02 (0.2)	-0.5 (0.2)	1.6 (0.5)	0.2 (0.09)	1.0 (0.5)	0.2 (0.1)	-19.7 (6.3)

Table II-8. Comparison of mean flux values calculated from benthic chamber experiments in which dissolved oxygen concentrations were > 25% of saturation vs. experiments in which concentrations were < 10% of saturation. Units are in meq m⁻² d⁻¹ except dissolved oxygen consumption mM⁻² d⁻¹.

Experiment							
Description	<u>HCO₃⁻</u>	<u>NH₄⁺</u>	<u>NO₃⁻</u>	<u>SO₄²⁻</u>	<u>Ca²⁺</u>	<u>Mg²⁺</u>	<u>O₂</u>
Sept. 1984 (9m) oxygen > 2mg/l n=2	7.1	1.2	-0.14	-0.5	2.33	0.5	-46
Sept. 1984, Summer 1985 (9m) oxygen < 0.7mg/l n=6	10.2	4.8	-0.4	-0.5	3.4	0.4	-18

Table II-9. Fluxes of chemical constituents calculated from large in-situ enclosures that were acidified to pH 5.2-5.5 and included 0.5m² of sediment surface. Values are means with standard errors in parentheses (n=4). Fluxes were calculated between 1 day and 27 days after acidification. n.d. means no detectable change.

<u>HCO₃⁻</u>	<u>NH₄⁺</u>	<u>NO₃⁻</u>	<u>SO₄²⁻</u>	<u>Ca²⁺</u>
3.0	n.d.	-2.3	-1.9	1.4
(1.8)		(0.8)	(0.9)	(.06)

Table II-10. Alkalinity fluxes calculated for the hypolimnion and low oxygen layer on the lake bottom during summer 1984 and 1985 (biweekly) and winter 1984 and 1985 (monthly). The depth of the top of the hypolimnion and oxycline, respectively, are in parentheses. Units are meq m⁻² d⁻¹ except for dissolved oxygen (mg l⁻¹).

<u>Summer 1984</u>	<u>O₂</u>	<u>Summer 1985</u>	<u>O₂</u>
Aug. 5 - Aug. 17		July 12 - July 22	
3.6 (6m)		1.0 (6m)	
2.2 (9.0-9.5m)	2.9-1.1	0.46 (9.5m)	7.3-4.7
Aug. 17 - Aug. 31		July 22 - Aug. 5	
-0.82 (7m)		-1.5 (6m)	
-0.34 (9m)	2.4-0.2	.02 (9.5m)	6.0-2.6
Aug. 31 - Sept. 17		Aug. 5 - Aug. 20	
3.0 (7m)		0.43 (7m)	
4.8 (8m)	0.5-0.1	0.90 (9.5m)	3.7-0.5
<u>Winter 1984</u>	<u>O₂</u>	<u>Winter 1985</u>	<u>O₂</u>
Jan. 29 - Feb. 29		Dec. 11 - Jan. 30	
-0.9 (5m)		1.6 (5m)	
0.03 (9m)	3.1-2.8	0.06 (9m)	5.3-1.0
Feb. 29 - Mar. 28		Jan. 30 - Feb. 26	
no net flux	2.8-2.2	0.5 (5m)	
		0.4 (9m)	3.5-1.6
Mar. 28 - April 29		Feb. 26 - March 25	
0.23		-0.3 (5m)	
0.024	3.5	2.7 (9m)	1.3-0.7

Table II-11. Thickness of the boundary layer, Z (μm), and the shear velocity, μ (cm/s), measured inside the benthic chamber for 2 pump speeds compared to values measured on the bottom of Emerald Lake.

	<u>Pump</u>	<u>Speed</u>	<u>Emerald Lake</u>
	80%	90%	Oct. 2-16, 1985
Boundary layer thickness (μm)	225 149	60	1170
Shear Velocity (cm/s)	0.6 1.0	2.2	0.2

Table II-12. Comparison of alkalinity fluxes obtained from the 4 methods used: benthic chamber data, benthic chamber fluxes corrected for artificial circulation, hypolimnetic (whole-lake) fluxes calculated from vertical profiles and in-situ acidified enclosures. Units are in meq m⁻² d⁻¹. Depths and standard errors are in parentheses.

<u>Benthic Chamber</u> (9m)	<u>Corrected Benthic Chamber</u> (9m) corrected for shear velocity similar to lake bottom. Pump speed in parentheses	<u>Hypolimnion</u>	<u>Acidified Sediment Bags</u>
July 17, 1985 4.6	0.77 (80%)	July 12 - July 22, 1985 1.0 (6m)	Sept. 1985 3.0 (1.8)
Aug. 8, 1985 2.9	0.48 (80%)	July 22 - Aug. 5, 1985 -1.5 (6m)	
Aug. 20, 1985 7.8	0.56 (90%)	Aug. 5 - Aug. 20, 1985 0.43 (7m)	
Sept. 4, 1984 9.7	1.6 (80%)	Aug. 31 - Sept. 17, 1984 3.0 (7m)	

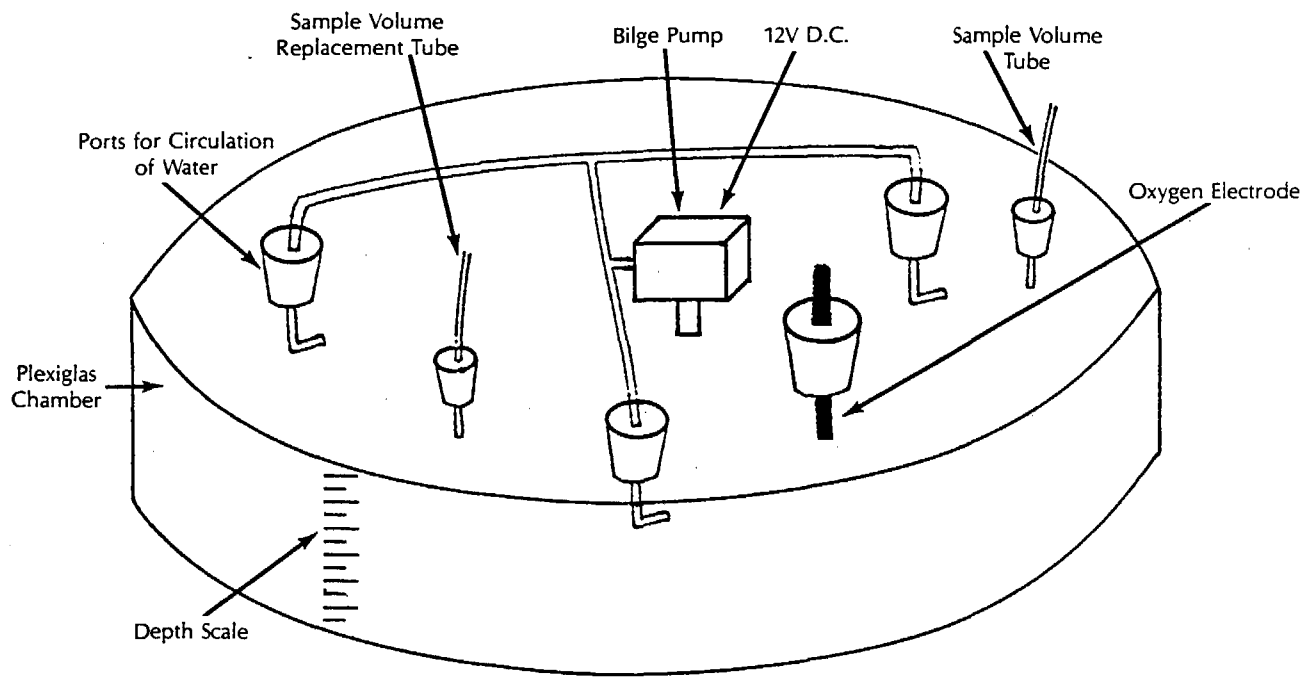


Figure II-56. The benthic chamber used to measure sediment-water column exchange of chemical constituents.

Benthic Chamber

August 20, 1985 (9m)

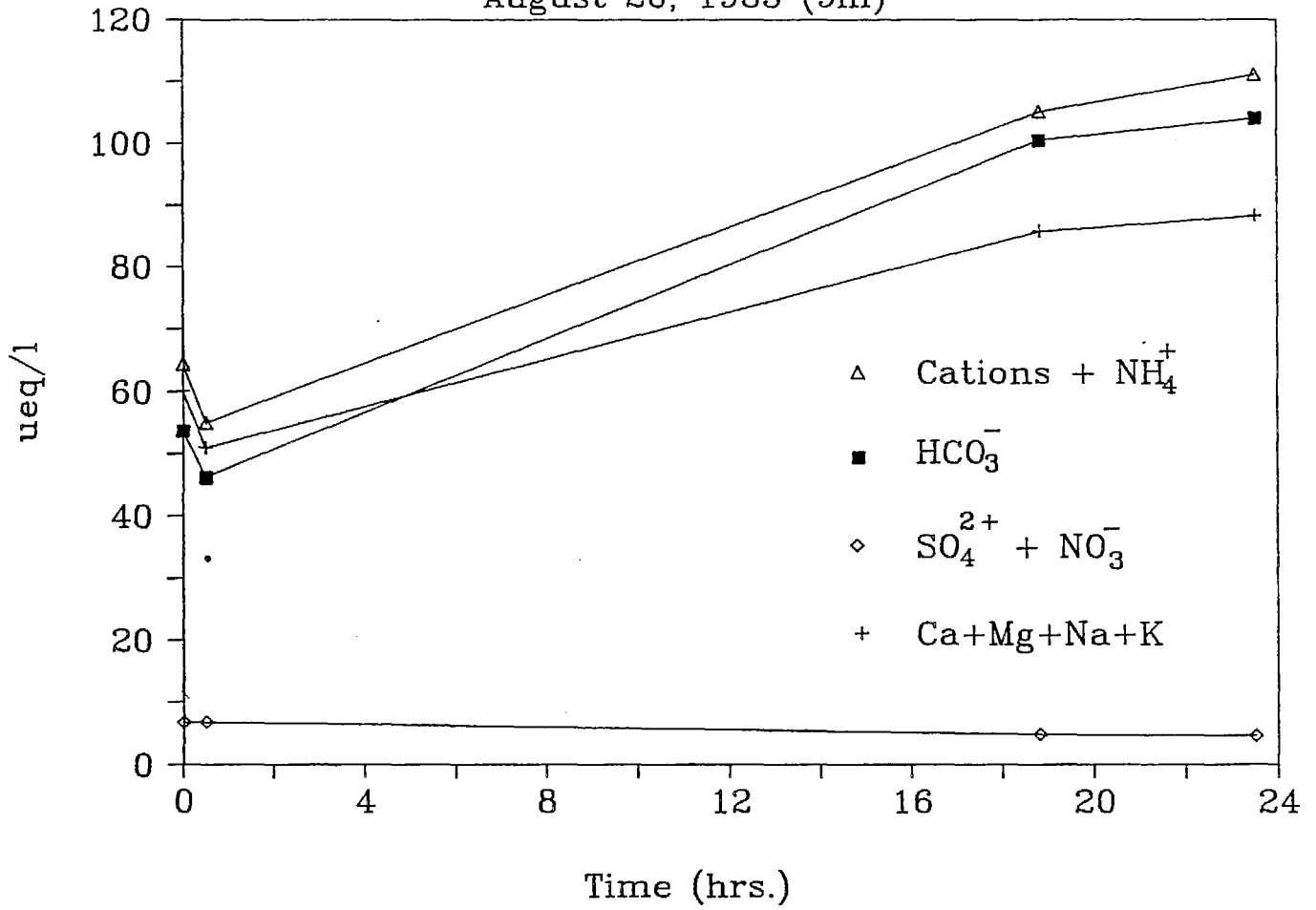


Figure II-57a. Solute concentration changes in benthic chamber.

Benthic Chamber

October 3, 1985 (9m)

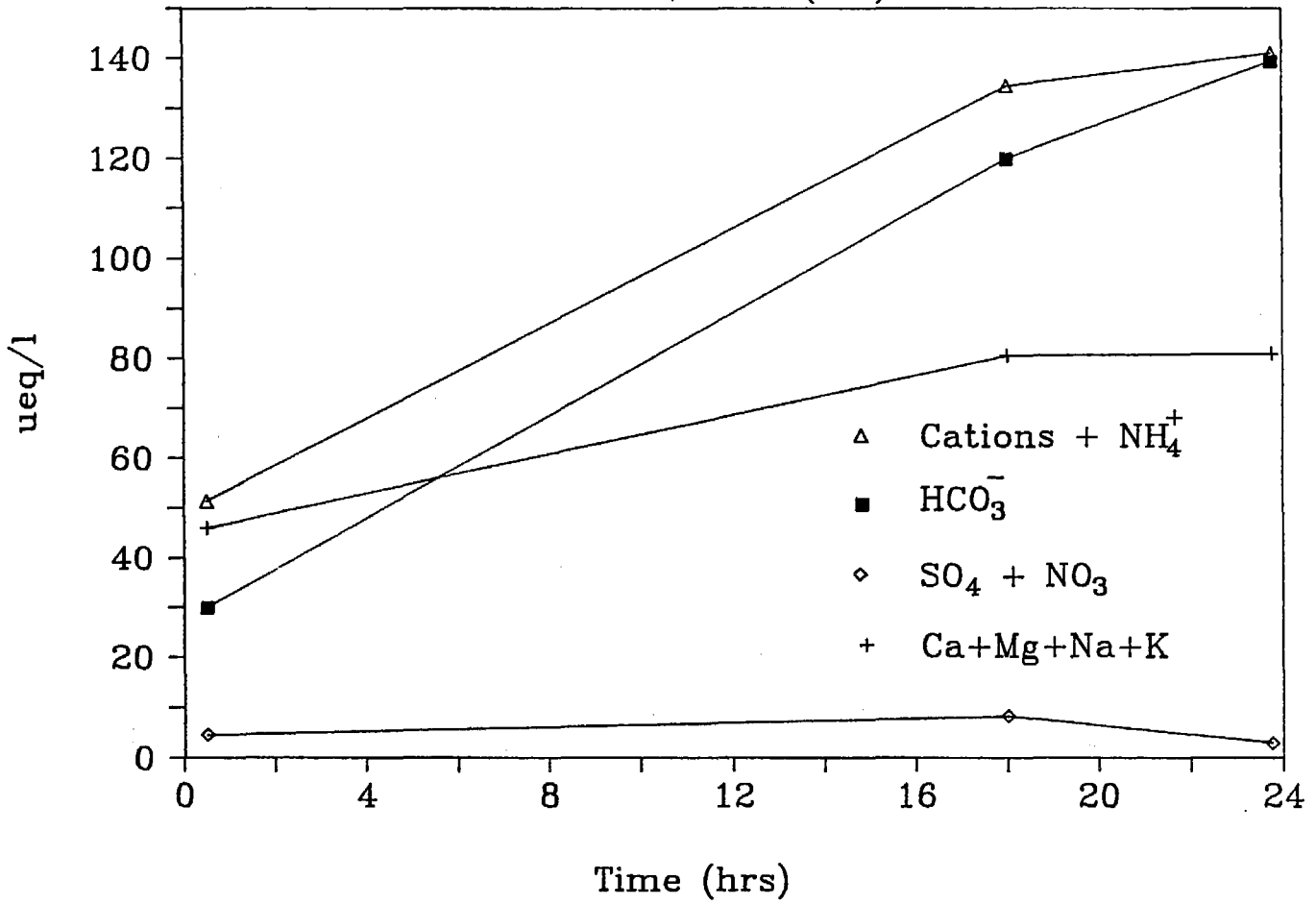


Figure II-57b. Solute concentration changes in benthic chamber.

Benthic Chamber

October 15, 1985 (3m)

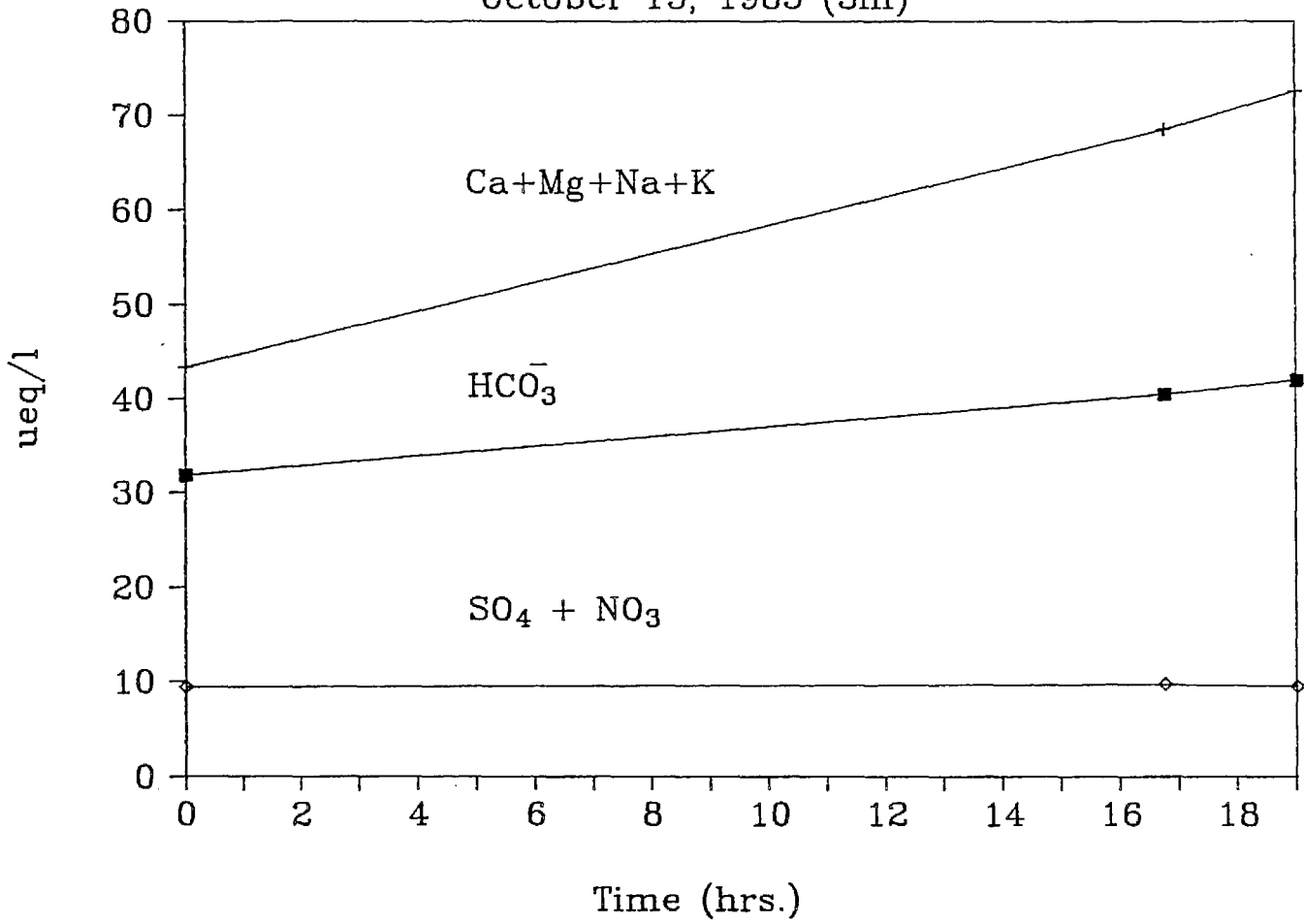


Figure II-57c. Solute concentration changes in benthic chamber.

Bag Experiment #4

Sediment Bags: Acid vs. Non-acid

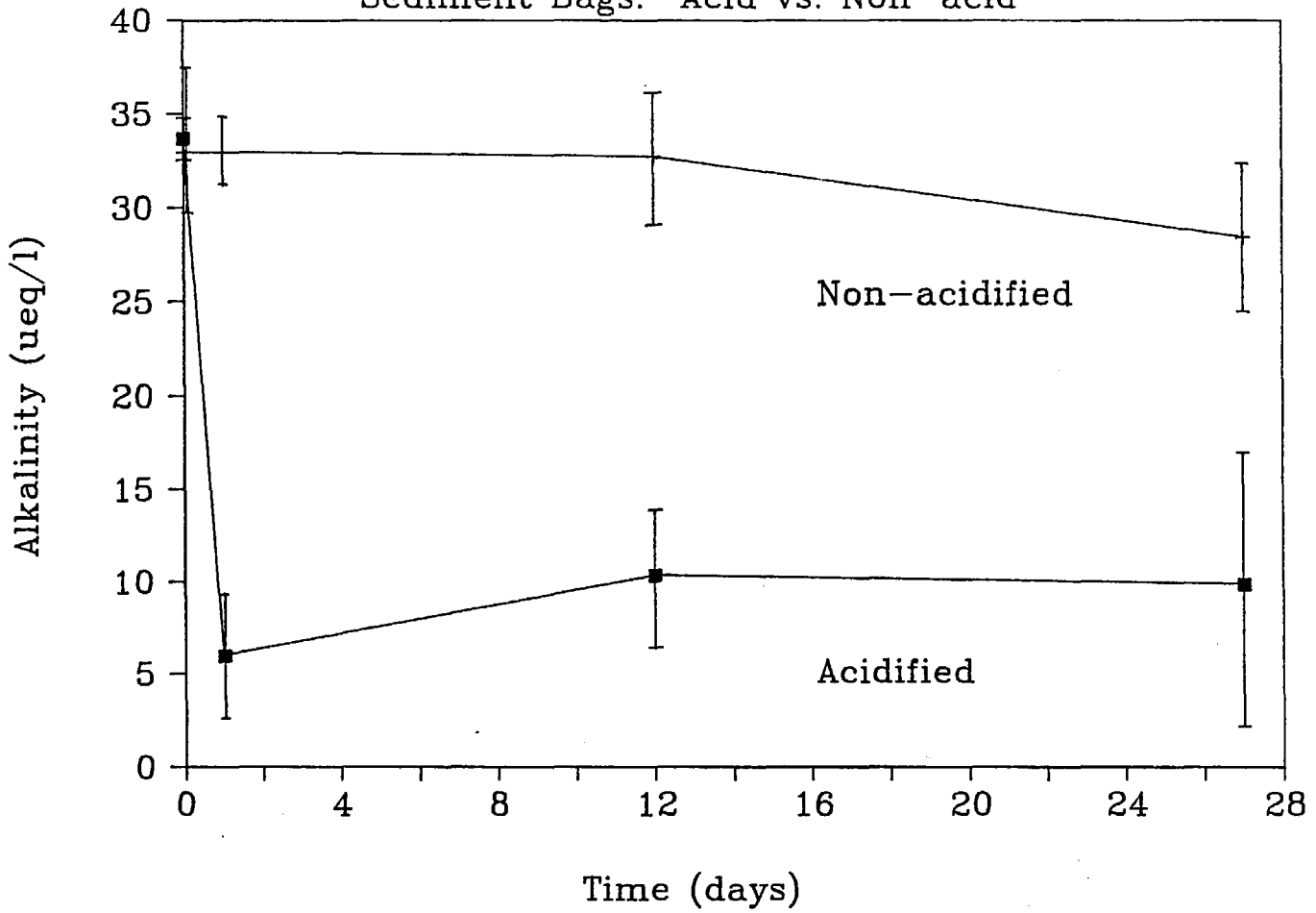


Figure II-58: Comparison of the change in alkalinity of acidified vs. non-acidified large plastic enclosures. Vertical bars are standard deviations.

Bioturbation Experiment

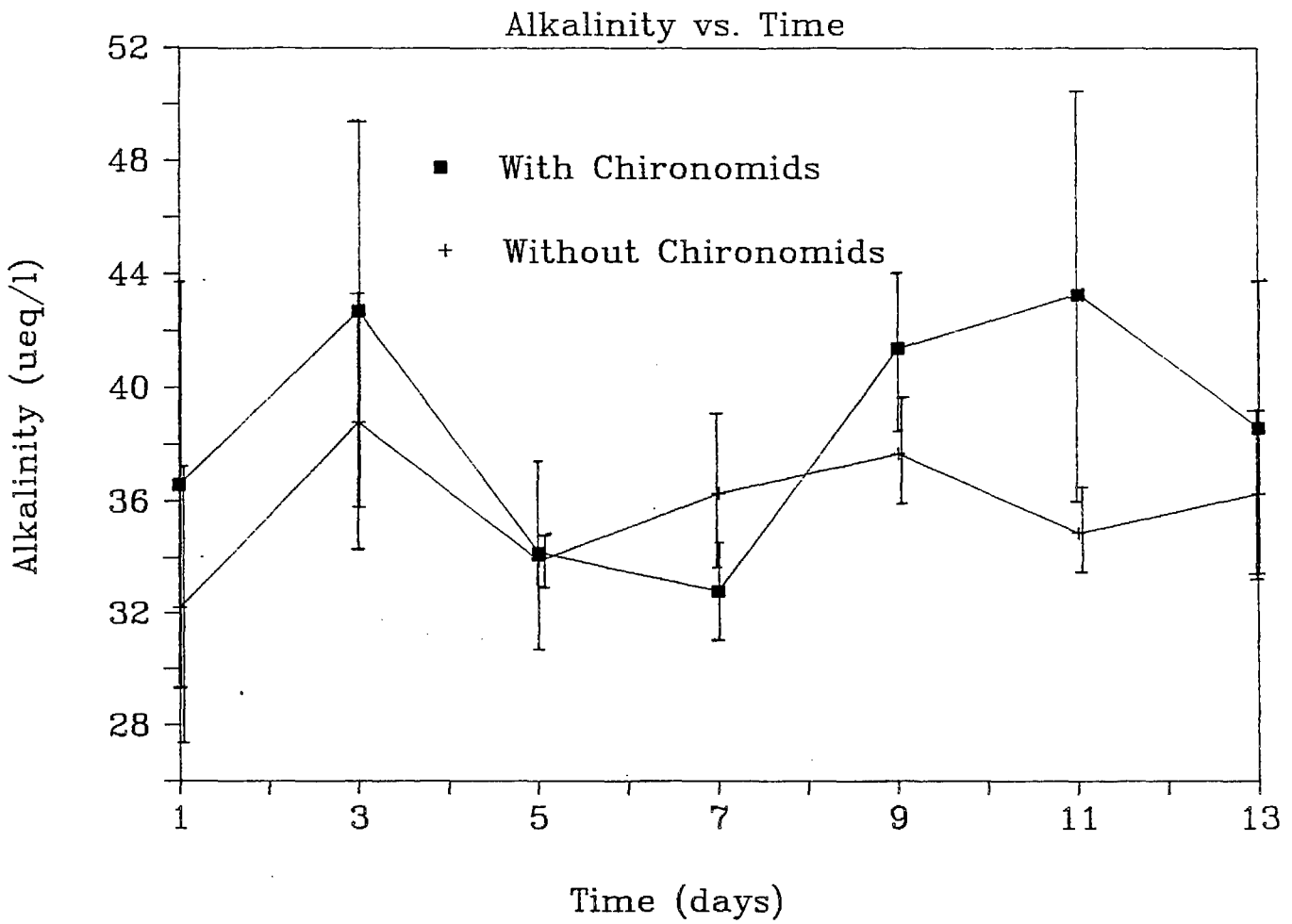


Figure II-59. Alkalinity generation in microcosms with chironomids compared to those without chironomids. Vertical bars are standard deviations.

CALCIUM vs. A.N.C.

BENTHIC CHAMBER EXPERIMENTS

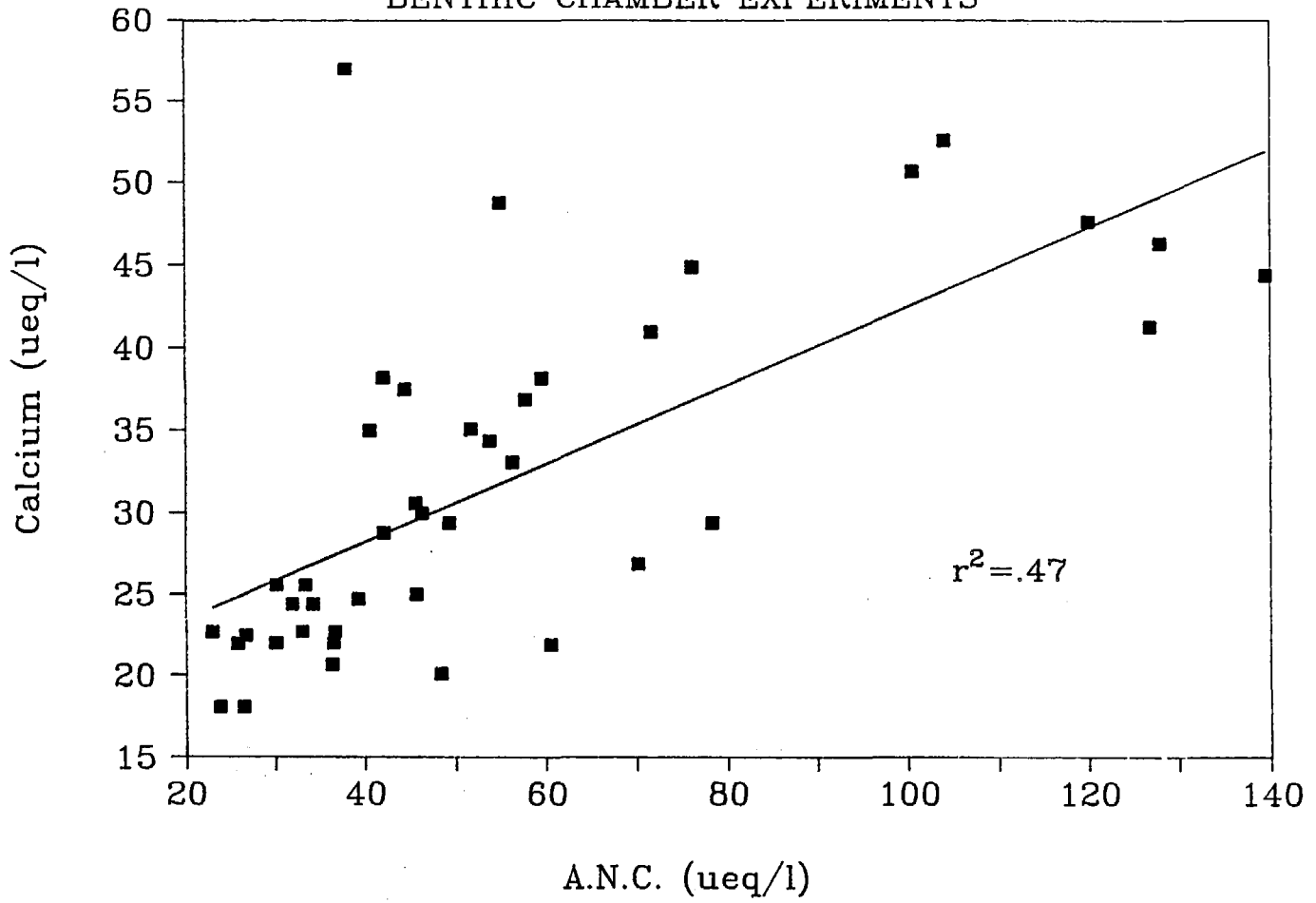


Figure II-60. Linear regression: Calcium vs. Acid Neutralizing Capacity.

BASE CATIONS vs A.N.C.

BENTHIC CHAMBER EXPERIMENTS

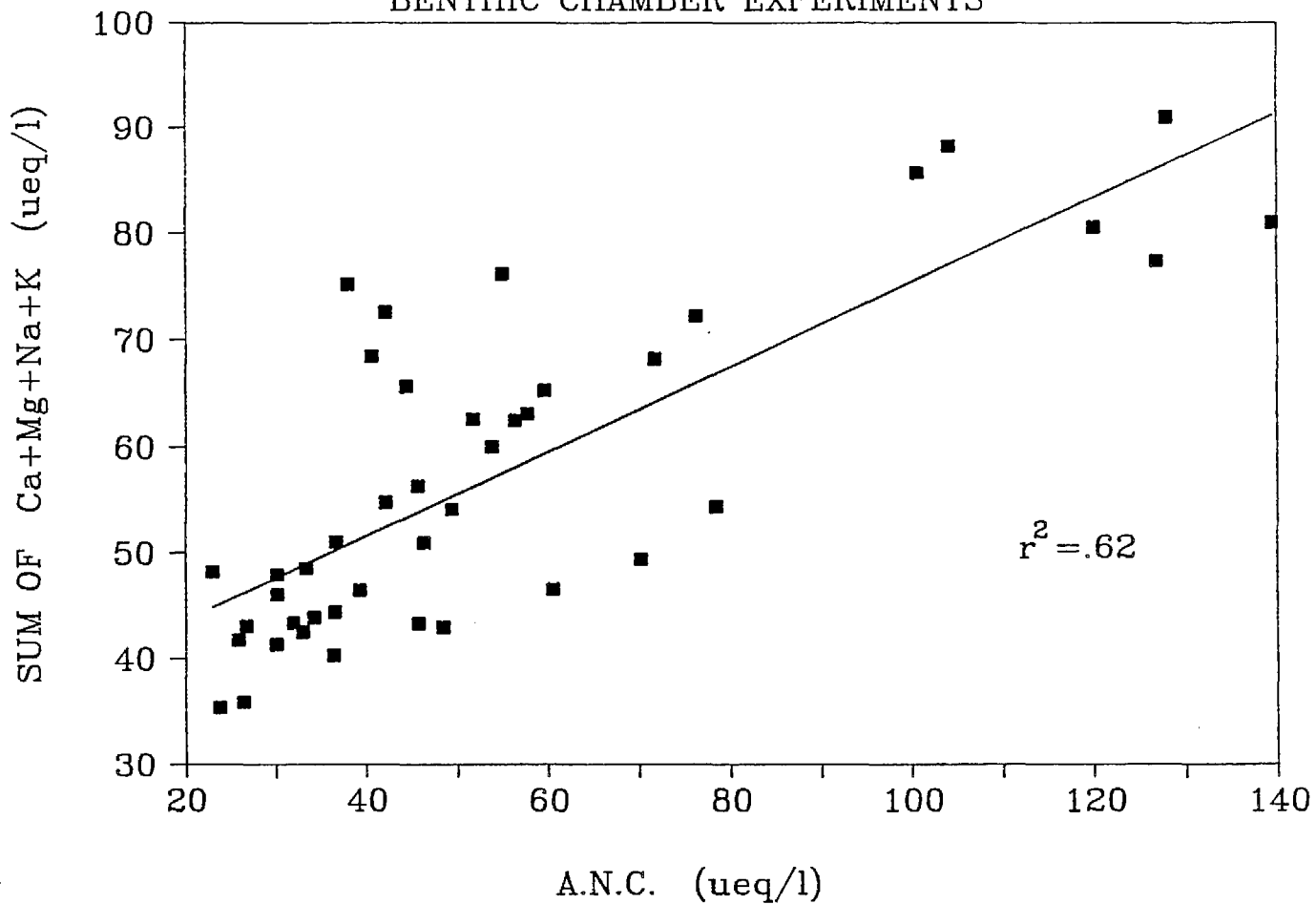


Figure II-61. Linear regression: Sum of Base Cations (Calcium, Magnesium, Sodium, Potassium) vs. Acid Neutralizing Capacity.

SUM OF MAJOR CATIONS vs A.N.C.

BENTHIC CHAMBER EXPERIMENTS

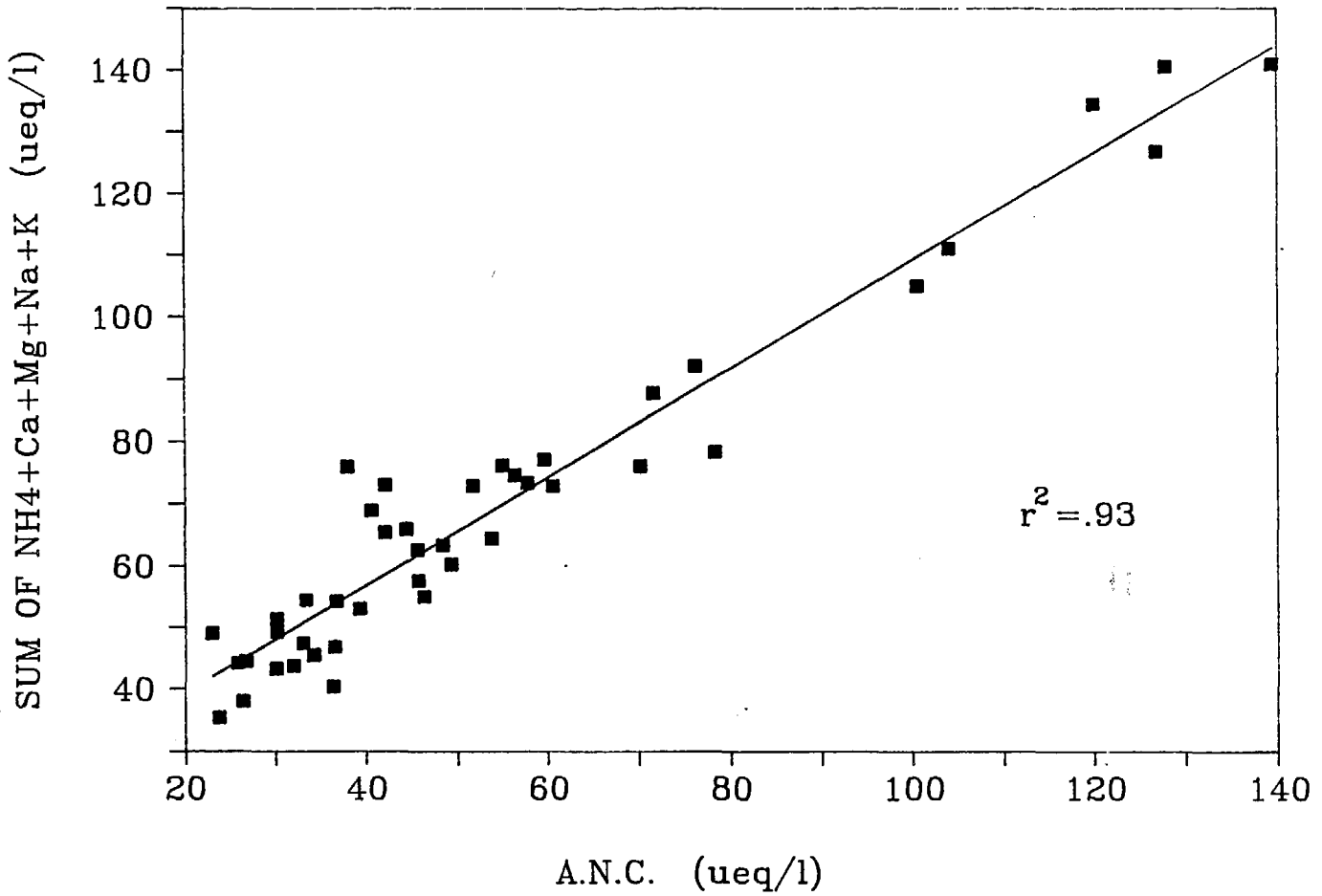


Figure II-62. Linear regression: Sum of Base Cations (Calcium, Magnesium, Sodium, Potassium) and Ammonium vs. Acid Neutralizing Capacity.

Chapter II.4

EXPERIMENTAL ACIDIFICATION OF LARGE ENCLOSURES IN EMERALD LAKE

Introduction

An approach for circumventing the problems inherent in surveys or laboratory assays is to perform controlled experiments which try to mimic the natural situation. One approach is to use laboratory microcosms to examine the responses of natural assemblages to environmental perturbations (Tonnessen 1983, Tonnessen and Harte 1980, Harte et al. 1981). These experiments differ from laboratory assays in that they try to mimic the natural situation by introducing natural assemblages into containers with natural sediment and water. Although certainly an improvement, in some cases microcosms diverge from larger natural systems and some processes are hindered or modified by the small size of the container. Also, other conditions, such as weather changes, are difficult to simulate.

As an alternative, controlled experiments can be conducted in situ. At one extreme, whole lakes and streams are manipulated (Schindler et al. 1985; Schindler and Turner 1982; Hall and Likens 1980; Hall et al. 1980). At the other extreme, manipulations are carried out in small bottles suspended in lakes or streams. Whole lake or stream experiments are logistically difficult, requiring large amounts of manpower, money and time. Also, because of their size, it is often difficult, if not impossible, to have replicate systems both for examining inter-system variability and for establishing concurrent controls. There is also the problem of altering whole systems, perhaps irreversibly. Finally, it is often difficult to determine densities of the biota of whole lakes and streams (Allan 1983, Hurlbert 1984, Morin 1985). A number of studies have indicated that large numbers of samples are needed to calculate density estimates for many freshwater, particularly benthic, organisms (Resh 1979, Allan 1984, Needham and Usinger 1956).

Ecologists have recently begun performing experiments in large bags in lakes or large, outdoor stream channels (Yan and Stokes 1978, Marmorek 1982, Wilzbach et al. 1983, Burton et al. 1985). Not only do such mesocosms allow replicated study of systems under nearly natural conditions, they also allow similar conditions among replicates at the outset, circumventing problems associated with sampling variability. We feel that large in situ enclosures

provide the best compromise in terms of replicability, ease of manipulation, size and similarity to natural conditions.

Methods

Field experiments were conducted during the summer of 1985 in large bags suspended in the middle of Emerald Lake. Cylindrical bags were constructed of 4 mil clear polyethylene, and were suspended from wooden platforms buoyed by floats. The tops of bags extended 30 cm above the water line and plastic hoops, placed at each vertical meter, provided internal stability to the enclosures. Each bag had an internal diameter of 1 m, and the depth and volume of each bag ranged from 5 m and 3.5 m³ in Experiments 1, 2, and 3 to 9 1/2 m and 6.5-9 m³ in Experiment 4. Bags were deployed and bottoms were tied shut by SCUBA divers in Experiments 1 to 3. In Experiment 4 the bottoms of half of the bags enclosed open cubes composed of PVC pipe. Upon deployment SCUBA divers pushed these cubes 0.5 m into soft bottom sediments so that bags enclosed the entire water column including sediments. The other half of the bags in Experiment 4 did not contain bottom cubes and were tied off just above the bottom. The number of replicate enclosures for each experiment was 12 in Experiments 1 and 2, 24 in Experiment 3, and 16 in Experiment 4.

In Experiments 1 and 2 sulfuric and nitric acid, in equal proportions (by equivalents) were added to experimental bags to create two levels of acid treatment (Table II-13). Control bags (pH = 6.3) did not receive acid inputs. In Experiment 1, which ran 17 days (June 30 - July 17), sufficient acid was added to decrease pH in one set of enclosures to 4.2 (range = 4.0-4.5) and to 4.8 (range = 4.7-5.0) in another set. In Experiment 2, which ran for eight days (July 18-26), experimental bags were acidified to pH 5.2 (range = 5.0-5.4) or 4.2 (range = 4.1-5.1). In Experiment 1 the average and range of pH values represent the average and range for mean pH measured in each bag at ca. one and two weeks after experiment initiation, whereas pH values for Experiment 2 represent pH measured in each bag eight days after experiments started. The proportions of sulfuric and nitric acid added to each bag represent the proportions of these acids found in summer rains in the Emerald Lake area. In Experiment 1 acid was added to the surface of each experimental bag and then mixed into the water column by repeatedly towing a bucket from the bottom to the surface of each bag. In Experiment 2 and

subsequent experiments, acid was added to bags through a 0.6 cm diameter weighted Tygon tube (5 m long in Experiments 2 and 3, 10 m in Experiment 4) which was continually moved up and down through the water column. Four replicate bags were randomly assigned to each treatment in Experiments 1 and 2.

In Experiment 3 we attempted to differentiate the effects of the ions associated with acid deposition (H^+ , NO_3^- , SO_4^{2-}), as well as the effects of nutrient inputs (PO_4^{3-}), on plankton assemblages (Table II-12). Because chloride ions have little effect on planktonic populations at the concentrations we used, additions of hydrochloric acid should indicate the effects of hydrogen ions on plankton populations. Similarly, because sodium and potassium ions are unlikely to impair plankton at the concentrations we used, addition of KNO_3 and Na_2SO_4 to bags should indicate the effects of nitrate and sulfate ions on plankton populations. By comparing the responses of plankton populations to additions of sulfuric and nitric acid with their responses to hydrochloric acid vs. potassium nitrate and sodium sulfate additions, we should be able to differentiate the effects of protons from the effects of nutrient additions (as NO_3^- and SO_4^{2-}) on plankton assemblages. We were also interested in the effects of orthophosphate additions on plankton assemblages because orthophosphate was demonstrated to be limiting to phytoplankton growth in Emerald Lake and because orthophosphate levels in Emerald Lake increased following an acid rain event in the summer of 1984.

Seven treatments were used in Experiment 3, which lasted for 35 days (July 28 - September 2). One set of bags was acidified to pH 5.3 (range = 5.2 - 5.5) by adding equal proportions of sulfuric and nitric acid, a second set was acidified to pH 5.2 (range = 5.2 - 5.3) by adding hydrochloric acid, and a third set was acidified to pH 5.8 (range = 5.8 - 6.0) by adding hydrochloric acid. The mean and range of pH values cited here and subsequently were based on mean pH values calculated for each bag for measurements taken 9 and 23 days after experiment initiation. Potassium phosphate was added to a fourth set of bags, potassium nitrate and sodium sulfate were added to a fifth set, sulfuric and nitric acid and potassium phosphate were added to a sixth set (mean pH = 5.6, range = 5.3 - 5.9), and a seventh set of bags acted as controls, receiving no chemical inputs. Concentrations of sulfate and nitrate ions were initially the same in the sulfuric and nitric acid treatment vs. the potassium nitrate and sodium

sulfate treatment, and initial concentrations of phosphate ions were the same in the potassium phosphate vs. the potassium phosphate + sulfuric and nitric acid treatments. Four replicate bags were assigned to all treatments with the exception of the hydrochloric acid treatments. In the latter case each hydrochloric acid treatment (pH 5.2 vs. 5.8) was replicated twice.

In Experiment 4, which ran for 24 days (September 9 - October 3), we attempted to determine if the presence of bottom sediments had any effect on plankton responses to acidic inputs. Eight bags enclosed the whole water column and sediments, and another eight bags only enclosed the water column (see above). Within each sediment treatment four bags were acidified by addition of equal proportions of sulfuric and nitric acid, and the other four bags acted as controls (no acid inputs). Based on mean pH values calculated for each bag from measurements taken 12 and 24 days after experiment initiation, mean (and range) pH values for each treatment were: acid, no sediment = 5.6 (5.6 - 5.7); control, no sediment = 6.3 (6.3 - 6.4); acid, sediment = 5.7 (5.6 - 6.0); control, sediment = 6.3 (6.2 - 6.3). Thermal stratification had no effect on the bags in any of our experiments as the bags in Experiments 1 - 3 were above the thermocline, and Experiment 4 was conducted after fall overturn.

Chemical and biological responses to these treatments and statistical analyses are described here for nitrogen uptake, in Chapter IV.1 for phytoplankton, Chapter V.1 for zooplankton and Chapter V.2 for zoobenthos.

Water was collected from the enclosures in experiment 3 with a 5 m piece of Tygon tubing 2.5 cm in diameter which provided an integrated sample of the bag. Measurements of chlorophyll a, particulate nitrogen and nitrogen uptake were made prior to treatment, on day 0, and on days 11 and 23 of the experiment. The method for these techniques are described in section II.2 of this report. Protocols for nitrate, sulfate, phosphate, and pH determinations are contained in section II.1 of this report.

Results

Figure II-63 is a time series of pH in each treatment during the experiment. Acid treatments started off with a pH of about 5.1 to 5.2 and increased to 5.2 to 5.6 by day 23 of the experiment. In all other treatments, pH was initially about 6.3 and remained unchanged during the rest

of the experiment. Tables II-14 and II-15 contain a summary of concentrations of H, nitrate, sulfate and phosphate in each treatment on day 0, 1, 9, and 23.

Plankton responses as indicated by ammonium uptake are shown in Figures II-64a to II-66a. These data indicate the size and activity of the entire phytoplankton population in a treatment. Prior to manipulation (day 0) the ammonium uptake rates showed no statistical difference among bags. By day 11 of the experiment, uptake was significantly different (Student t-test, $P < .005$) in the phosphorus treatments compared to controls (see Fig. II-65a). In addition, uptake rates in the acid plus phosphorus treatment were statistically lower ($P < .005$) than in the phosphorus alone treatment. Uptake rates showed much the same differences on day 23 of the experiment with statistically higher rates ($P < .005$) in the P treatments. Rates were, however, significantly higher ($P < .005$) in the acid plus P treatment compared to the P alone treatment.

Chlorophyll specific ammonium uptake rates standardize phytoplankton responses against standing crop and are presented in Figures II-64b to II-66b. All bags had similar uptake rates on day 0. Measurements done on day 11 of the experiment showed significantly higher ($P < .01$) uptake rates in the P alone treatment compared to both the controls and the acid plus P treatment. Data from day 23 of the experiment show no statistical differences among treatments.

Particulate nitrogen and chlorophyll a data are indicators of biomass responses and are presented in Figures II-67 to II-69. Differences in chlorophyll a occurred by day 9 of the experiment with the acid plus P treatment being significantly higher ($P < .005$) than controls. By day 23 chlorophyll a concentrations in both P treatments were statistically higher ($P < .005$) than controls with the acid plus P treatment being significantly higher ($P < .005$) than the P alone treatment. Particulate nitrogen showed no differences among treatments until day 23. By this day both P treatments were significantly higher than controls ($P < .005$ for the acid plus P treatment and $P < .01$ for the P alone treatment) and the acid plus P treatment was higher ($P < .005$) than the P alone treatment.

Figure II-70 shows data on nitrate levels in each treatment during the time course of the experiment. Nitrate was initially the same (day 0) and was increased to ca. 20-25 μM in the N treatments. Nitrate concentrations

in all treatments declined over the course of the experiment. The P treatments showed the greatest changes. Nitrate concentrations were below detection by day 11 in the P alone treatment and had dropped almost 20 μM in the acid plus P treatment.

Discussion

There were no significant differences in chlorophyll a and particulate nitrogen levels or ammonium uptake rates among control and acid without phosphorus treatments.

The phytoplankton responded with higher ammonium uptake rates and greater accumulation of chlorophyll a and particulate nitrogen most strongly to additions of phosphorus. However, after phytoplankton were released from P limitation they quickly reduced nitrate to below 0.1 μM and probably became nitrogen limited in the P alone treatment. During ammonium uptake experiments the phytoplankton in the P alone treatment had a supply of nitrogen ($^{15}\text{N-NH}_4$); therefore these measurements represent the potential uptake of N not ambient rates of assimilation. In contrast, accumulations of both chlorophyll a and particulate nitrogen continued in the acid plus P treatment because the phytoplankton had sufficient supply of phosphorus and nitrogen and because grazing by zooplankton was reduced (see Section V-1).

During the ammonium uptake experiment on day 11, uptake was higher in the P alone treatment than in the acid plus P treatment but chlorophyll concentrations were the same or smaller than in the acid plus P treatment. Therefore, the phytoplankton in the acid plus P treatment had to be assimilating nitrogen more slowly than those in the P alone treatment. This lower rate could have been caused by the lower pH in this treatment or the higher concentrations of nitrate or sulfate. The latter was not likely because the nitrate and sulfate levels were not of sufficiently high concentrations to cause toxicity. It is more likely that the lower chlorophyll specific uptake rate in the acid plus P treatment was induced by a lower pH. It may be that acid effects do not manifest themselves until the phytoplankton are photosynthesizing at elevated rates, hence the responses observed after P addition but not in the acid alone treatments.

On day 23 the ammonium uptake rate, chlorophyll and particulate N were higher in the acid plus P treatment than in the P alone treatment. By this date zooplankton densities were much lower in bags with acid, and the grazing

pressure on the phytoplankton was reduced accordingly. Lower zooplankton grazing coupled with high nutrient concentrations allowed the phytoplankton population in these bags to grow well.

The complexity of the plankton response to the chemicals associated with acid deposition demonstrates the need for multifactorial experiments. In order to fully gauge the affects of acid deposition one must study the interaction of nutrients, phytoplankton productivity and zooplankton population dynamics.

Table II-13. Design of bag experiments. Numbers in parentheses in the body of the table indicate the experimental pHs of sulfuric + nitric acid treatments. The asterisks in Experiment 4 indicate inclusion or exclusion of bottom sediments in control and acid addition bags in a cross-classified design.

Treatment	Expt. 1	Expt. 2	Expt. 3	Expt. 4
Control (pH=6.3)	X	X	X	X*
H ₂ SO ₄ +HNO ₃	X (4.8)	X (5.2)	X (5.2)	X* (5.6)
H ₂ SO ₄ +HNO ₃	X (4.2)	X (4.2)		
HCl (pH=5.7)			X	
HCl (pH=5.2)			X	
KNO ₃ +Na ₂ SO ₄			X	
PO ₄			X	
H ₂ SO ₄ +HNO ₃ +PO ₄ (pH=5.2)			X	

Table II-14. Concentrations ($\mu\text{eq/l}$) of H, NO_3 , PO_4 and SO_4 in Experiment 3 on days 0 and 1.

<u>DAY 0</u>									
TREATMENT	H		NO_3		PO_4		SO_4		
	mean	s.d.	mean	s.d.	mean	s.d.	mean	s.d.	
N+S	0.39	0.13	2.4	1.1	0.01	0.01	5.4	0.2	
H	0.34	0.11	3.0	0.5	0.01	0.00	5.4	0.6	
P	0.37	0.09	2.6	0.3	0.00	0.00	5.8	0.2	
N+S+H	0.33	0.04	3.2	0.4	0.01	0.00	5.7	0.3	
CONT	0.32	0.07	3.1	0.5	0.01	0.01	5.7	0.2	
N+S+P+H	0.34	0.03	3.2	0.6	0.00	0.00	5.7	0.3	

<u>DAY 1</u>									
TREATMENT	H		NO_3		PO_4		SO_4		
	mean	s.d.	mean	s.d.	mean	s.d.	mean	s.d.	
N+S	0.57	0.06	24.9	1.4	0.01	0.01	27.3	2.3	
H	7.82	3.38	2.9	0.5	0.00	0.00	5.6	0.2	
P	0.54	0.10	1.5	1.0	1.00	0.16	5.8	0.3	
N+S+H	8.28	2.67	22.0	2.0	0.00	0.00	19.8	1.9	
CONT	0.50	0.04	2.5	0.8	0.02	0.01	6.4	0.6	
N+S+P+H	8.83	4.51	20.4	3.7	1.23	0.26	19.6	2.9	

Table II-15. Concentrations ($\mu\text{eq/l}$) of H, NO_3 , PO_4 and SO_4 in Experiment 3 on days 9 and 23.

TREATMENT	<u>DAY 9</u>							
	H		NO_3		PO_4		SO_4	
	mean	s.d.	mean	s.d.	mean	s.d.	mean	s.d.
N+S	0.48	0.12	21.7	5.7	0.02	0.01	24.9	5.5
H	4.16	2.35	2.2	0.1	0.01	0.02	5.9	0.1
P	0.33	0.02	0.0	0.0	0.54	0.33	5.7	0.1
N+S+H	4.96	1.12	20.0	1.3	0.01	0.01	19.5	1.4
CONT	0.41	0.08	2.4	0.2	0.01	0.01	5.8	0.1
N+S+P+H	3.27	2.92	6.4	6.6	0.44	0.25	18.5	2.5

TREATMENT	<u>DAY 23</u>							
	H		NO_3		PO_4		SO_4	
	mean	s.d.	mean	s.d.	mean	s.d.	mean	s.d.
N+S	0.50	0.12	20.0	7.3	0.03	0.01	22.9	7.9
H	3.02	2.25	2.1	0.1	0.03	0.01	6.1	0.1
P	0.39	0.10	0.0	0.0	0.52	0.43	5.8	0.0
N+S+H	4.58	1.27	18.9	1.2	0.11	0.14	18.9	1.3
CONT	0.45	0.11	2.0	0.1	0.09	0.10	6.0	0.1
N+S+P+H	1.69	0.57	3.6	3.8	0.14	0.11	17.6	3.2

pH TIME SERIES - BAG EXPERIMENT 3

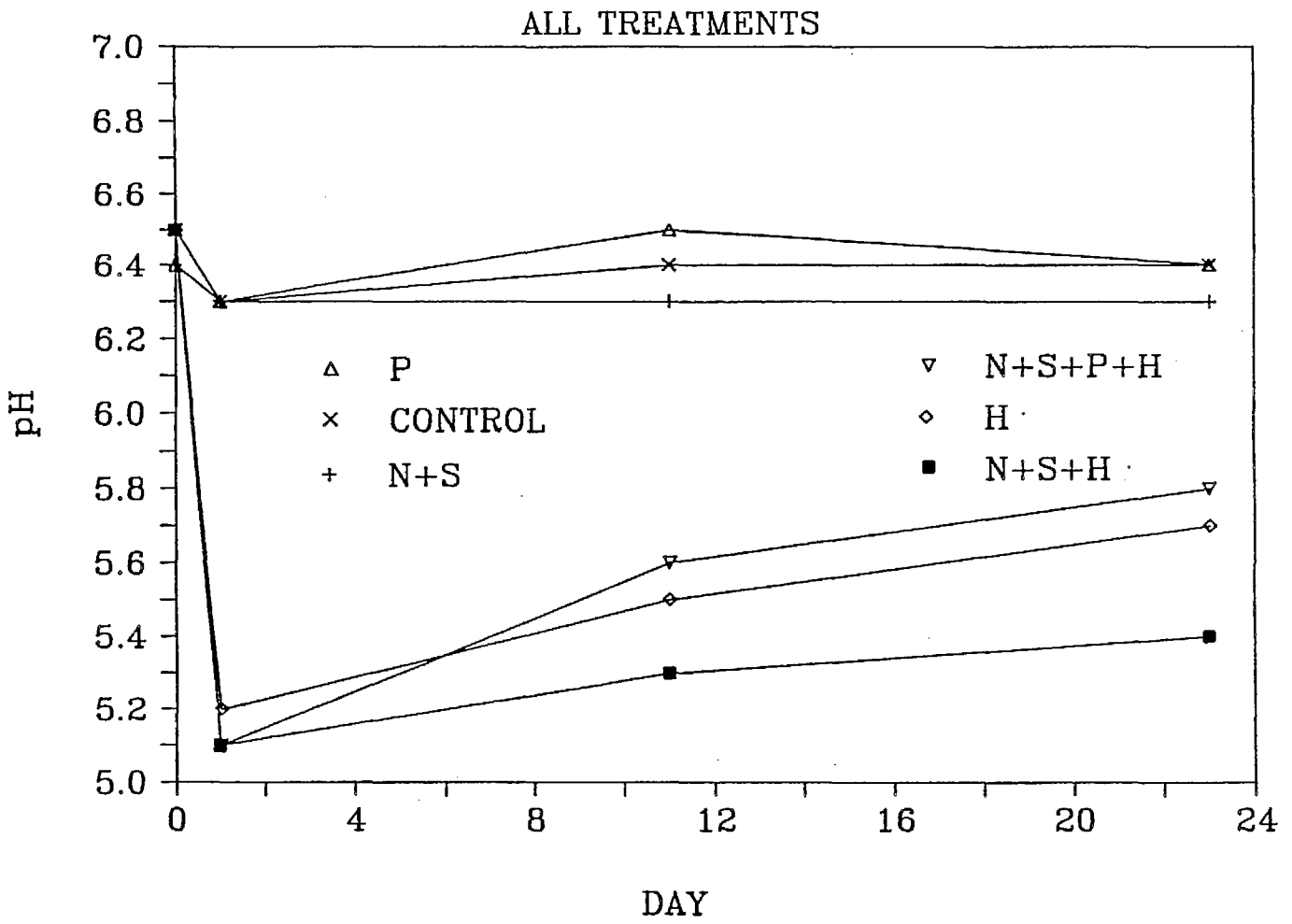


Figure II-63. pH time series - all treatments; Experiment 3.

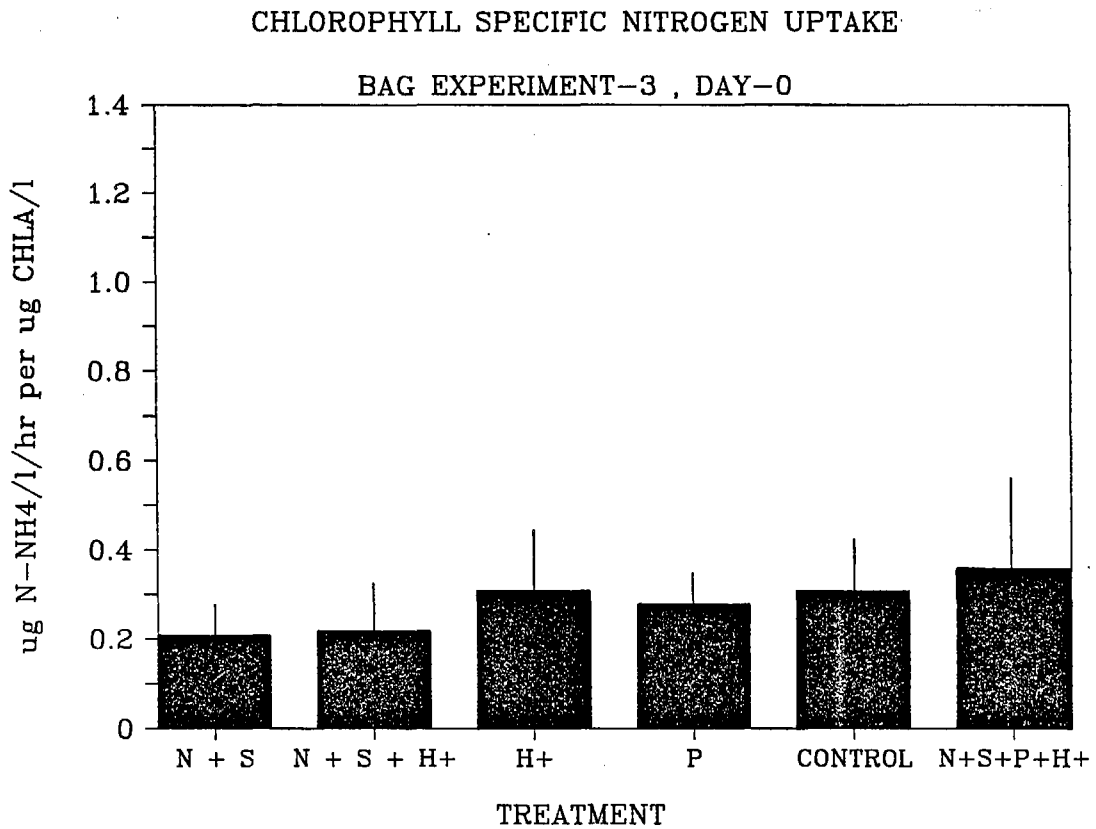
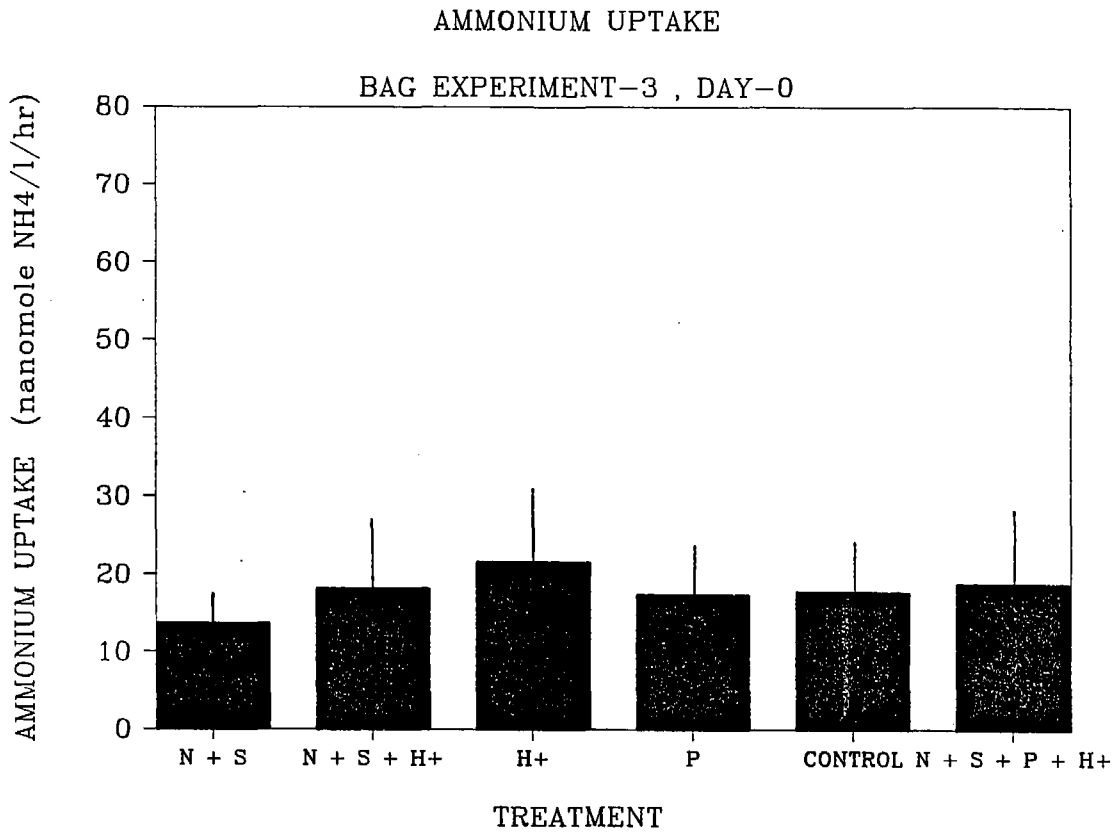


Figure II-64a+b. Ammonium uptake and chlorophyll specific uptake; Day 0.

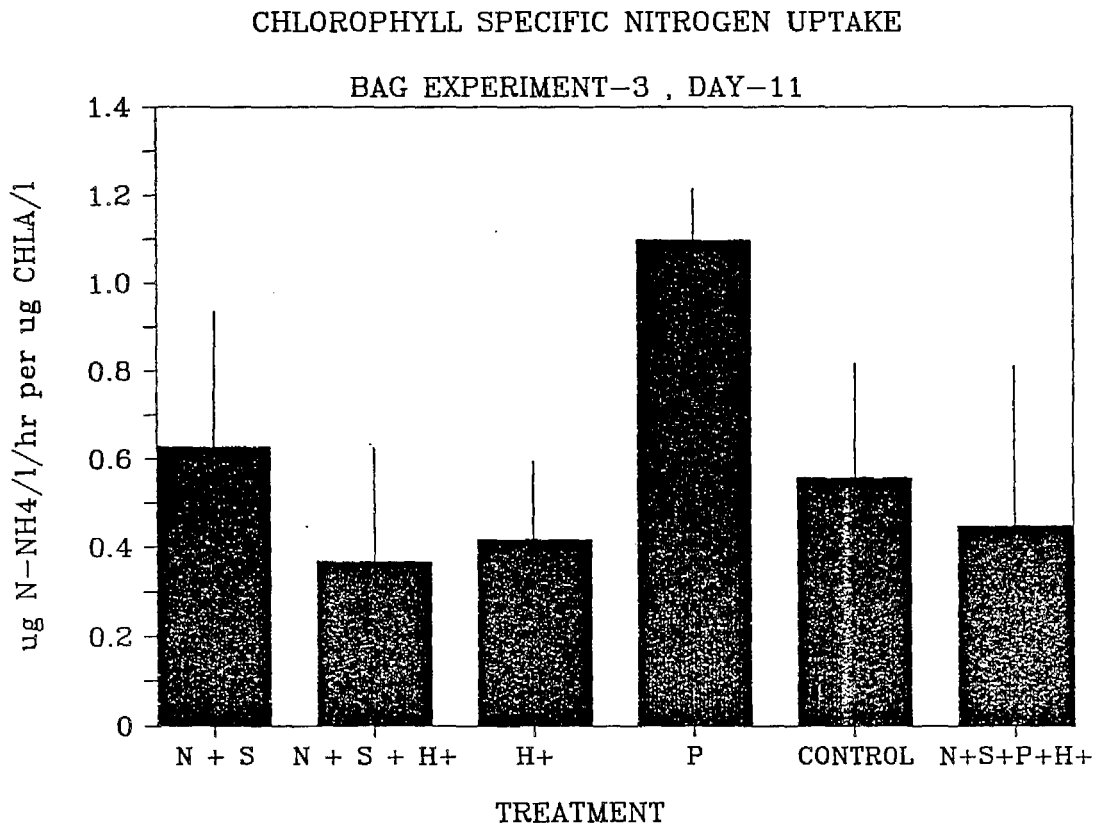
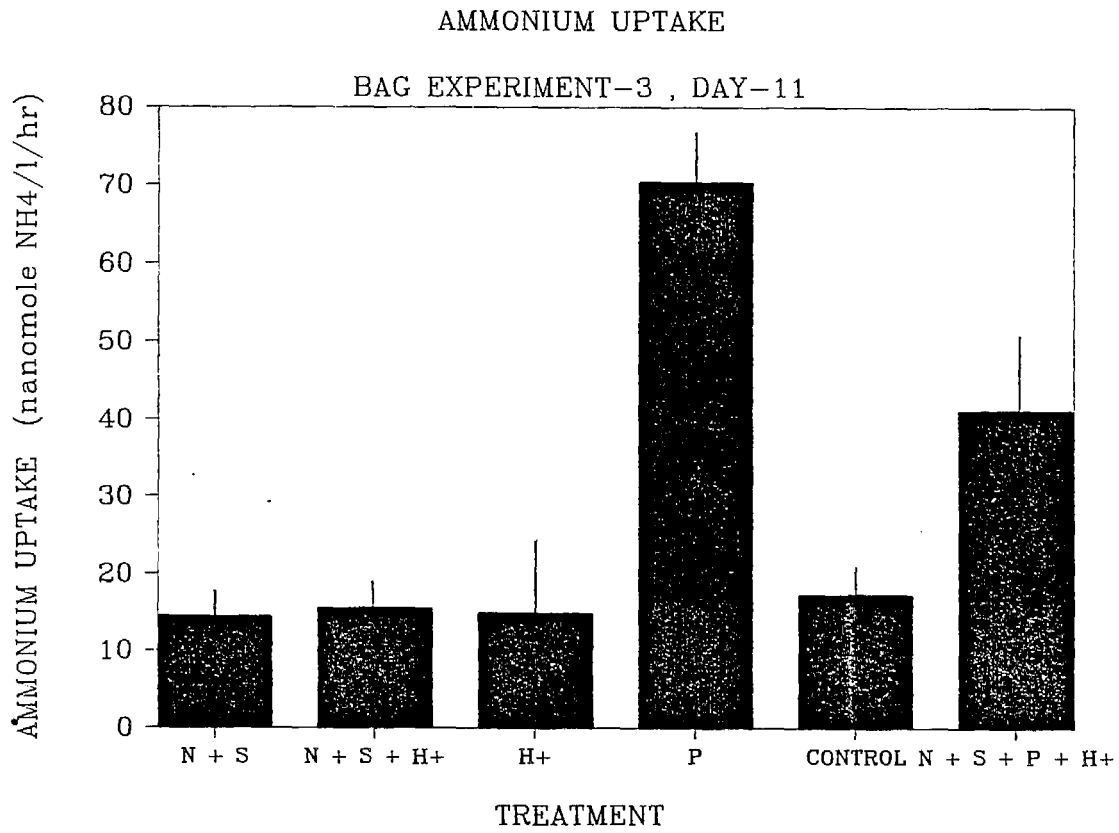


Figure II-65a+b. Ammonium uptake and chlorophyll specific uptake; Day 11.

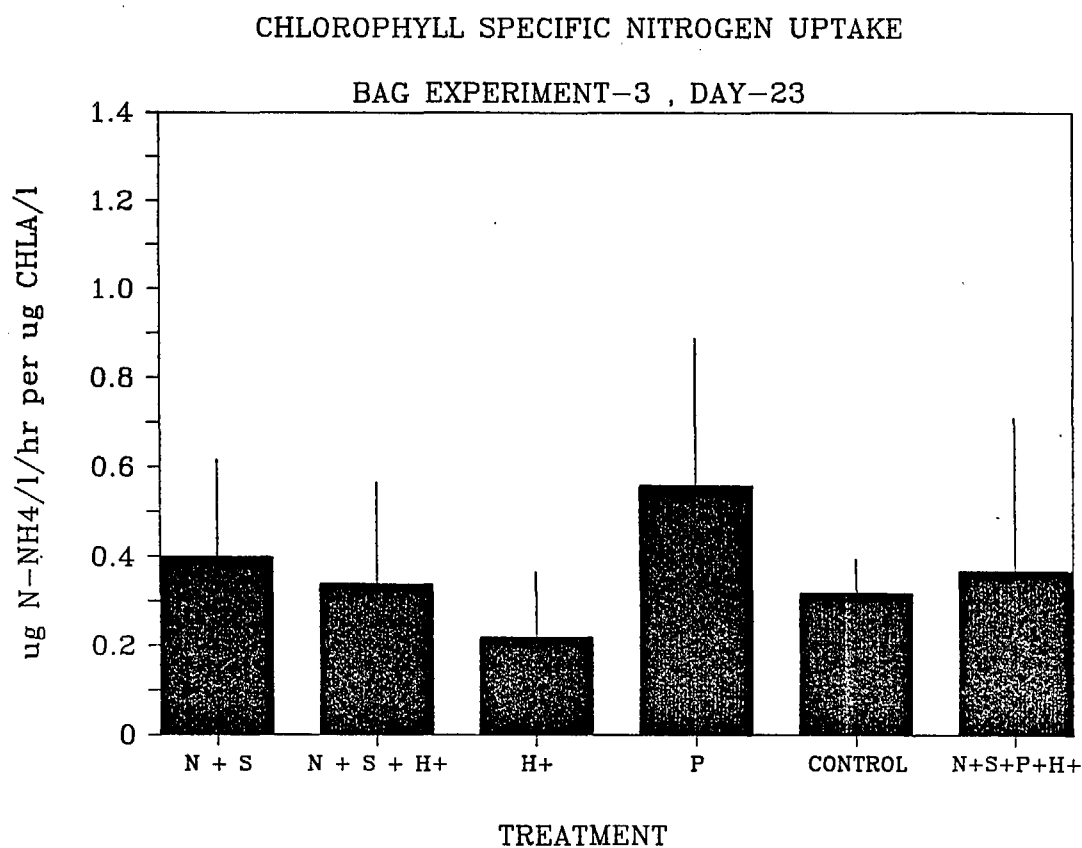
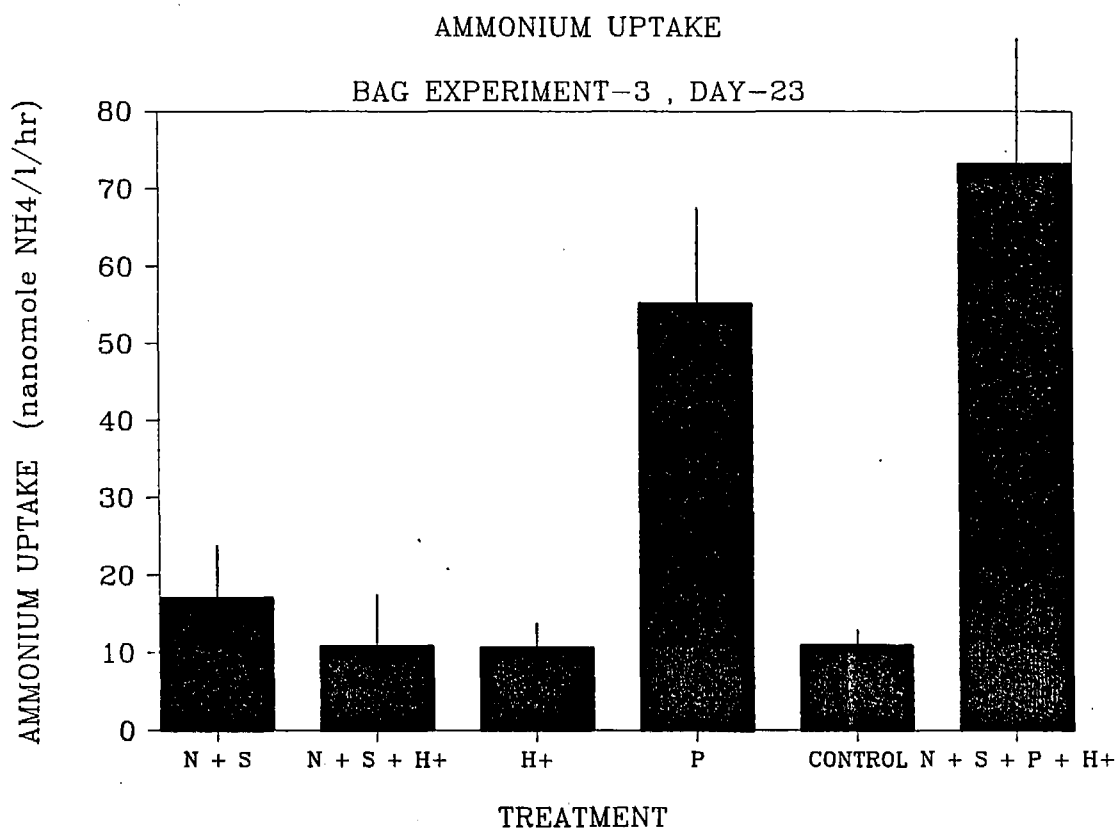


Figure II-66a+b. Ammonium uptake and chlorophyll specific uptake; Day 23.

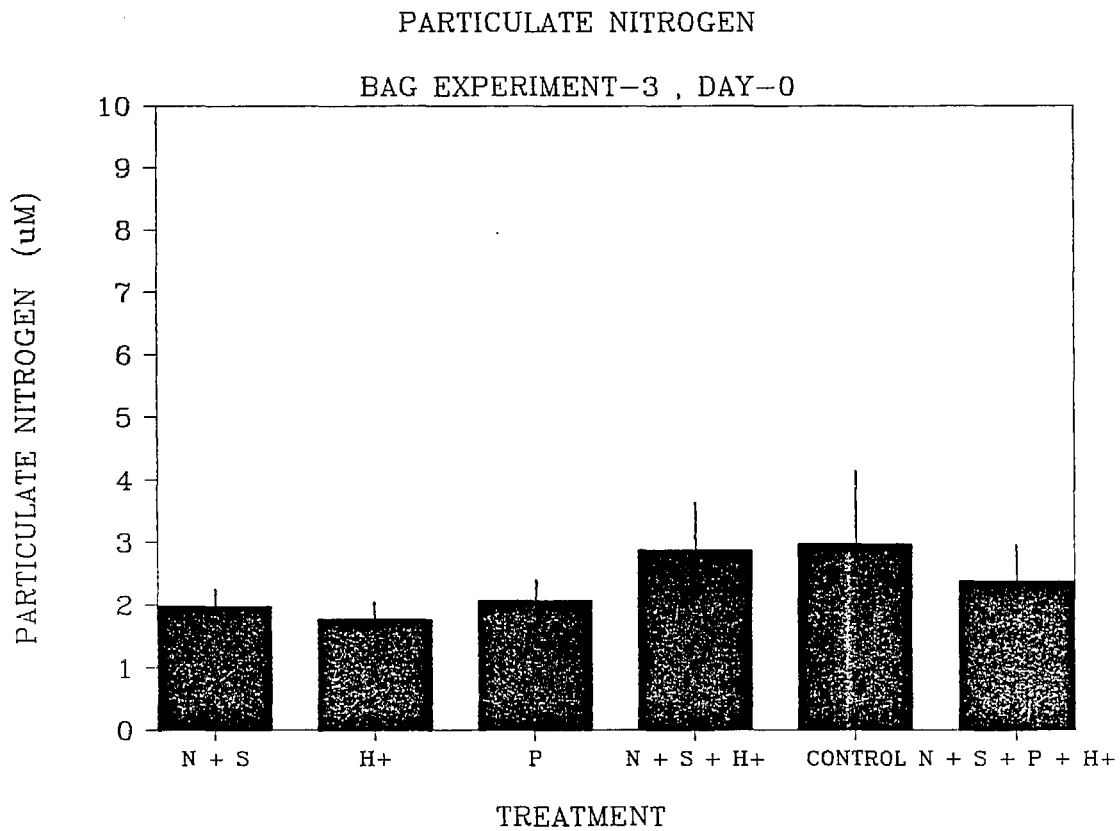
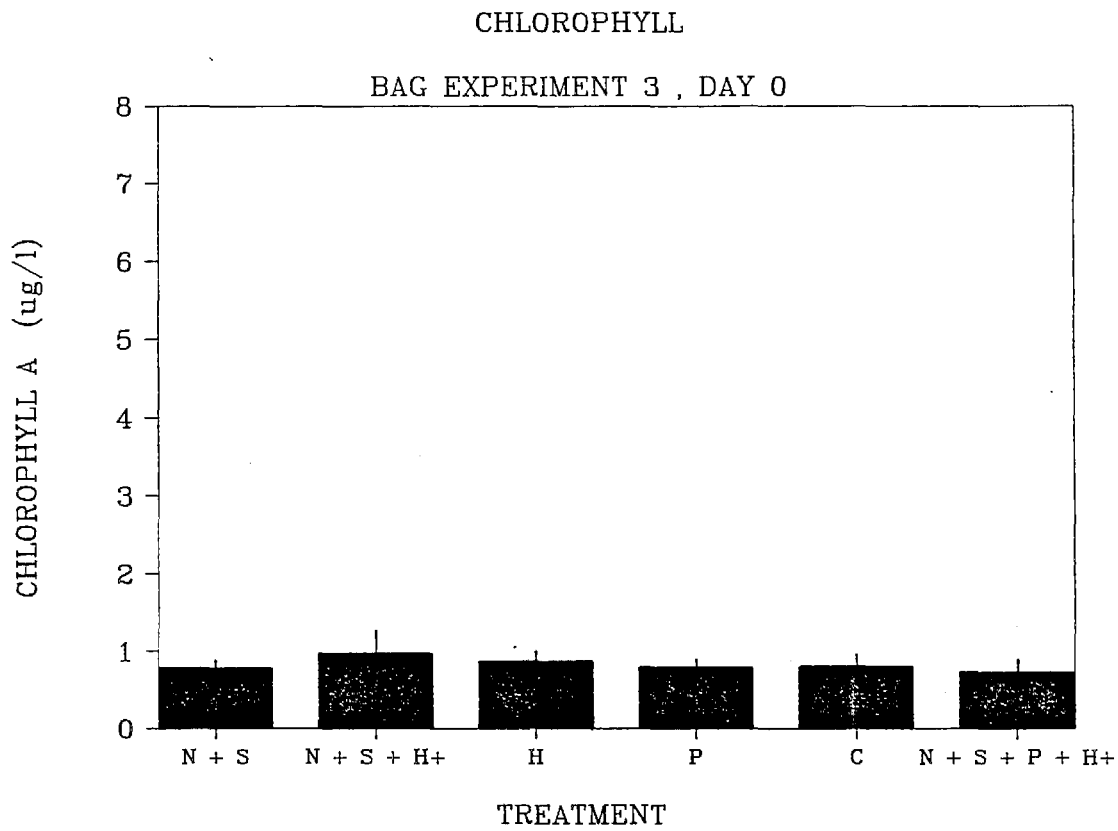
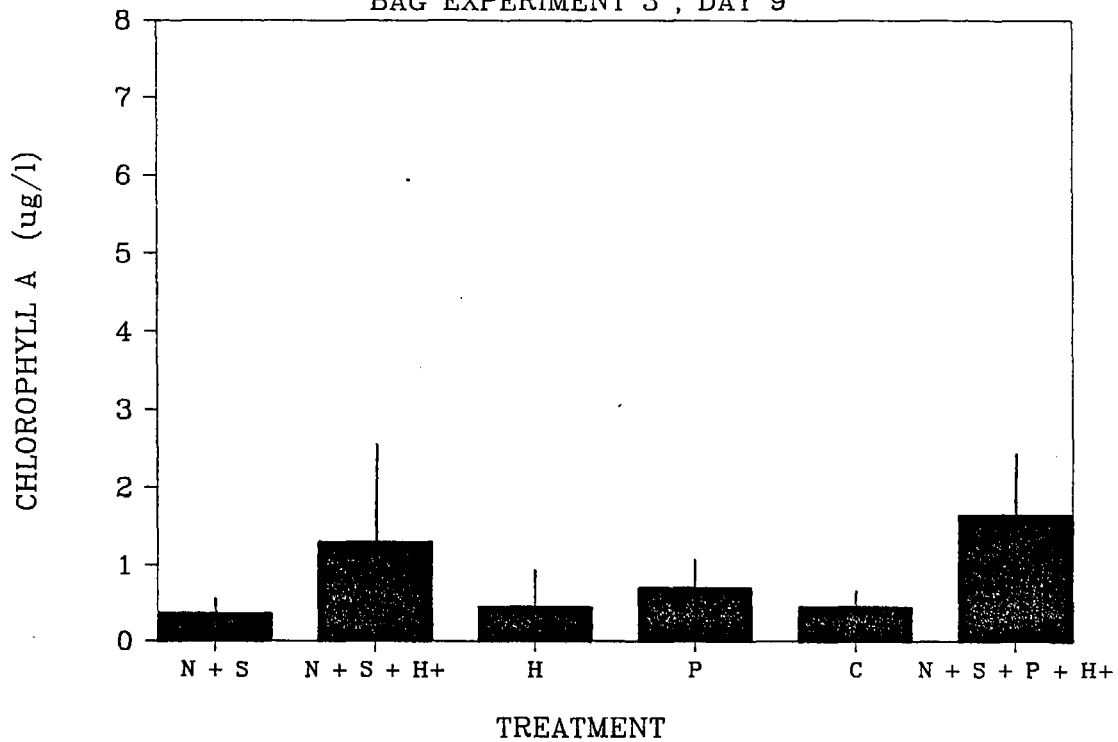


Figure II-67a+b. Chlorophyll a and particulate nitrogen; Day 0.

CHLOROPHYLL

BAG EXPERIMENT 3 , DAY 9



PARTICULATE NITROGEN

BAG EXPERIMENT-3 , DAY-11

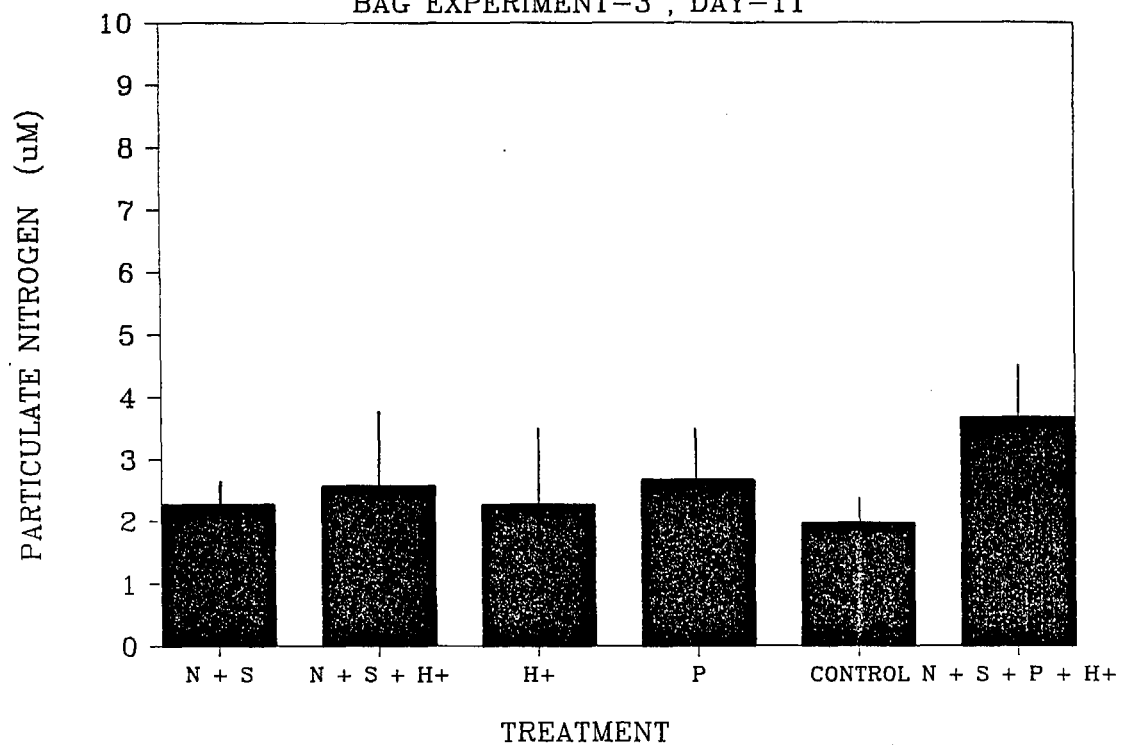
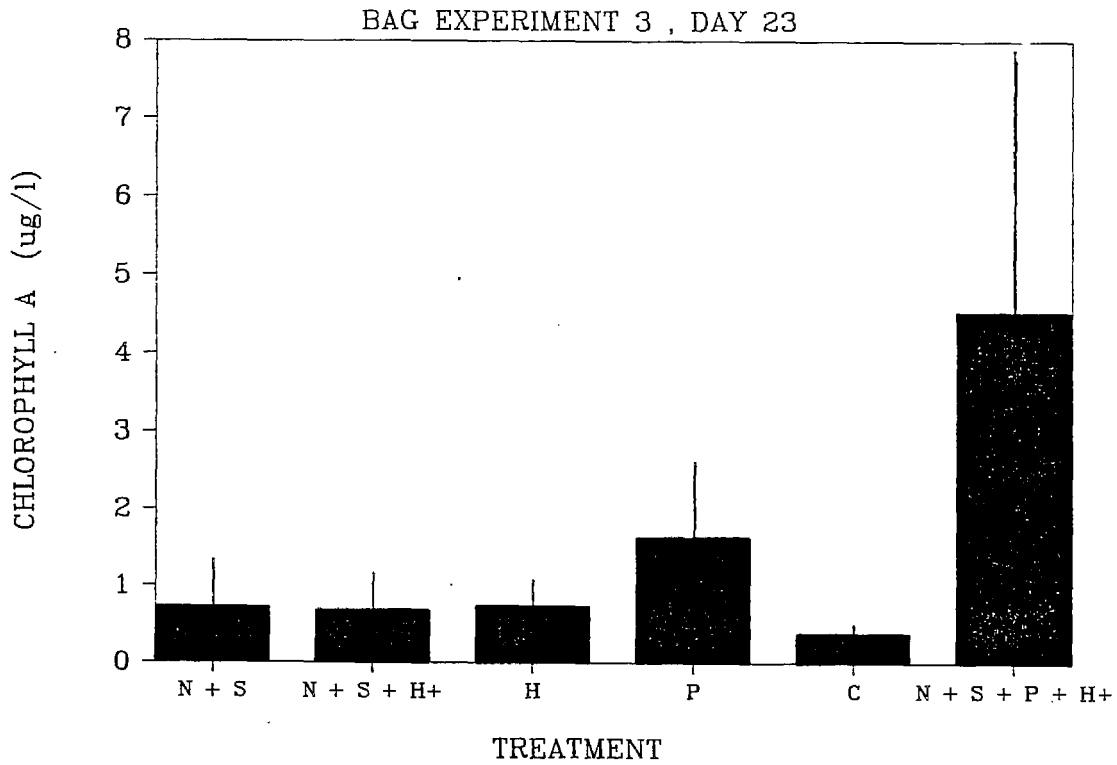


Figure II-68a+b. Chlorophyll a and particulate nitrogen; Day 9,11.

CHLOROPHYLL



PARTICULATE NITROGEN

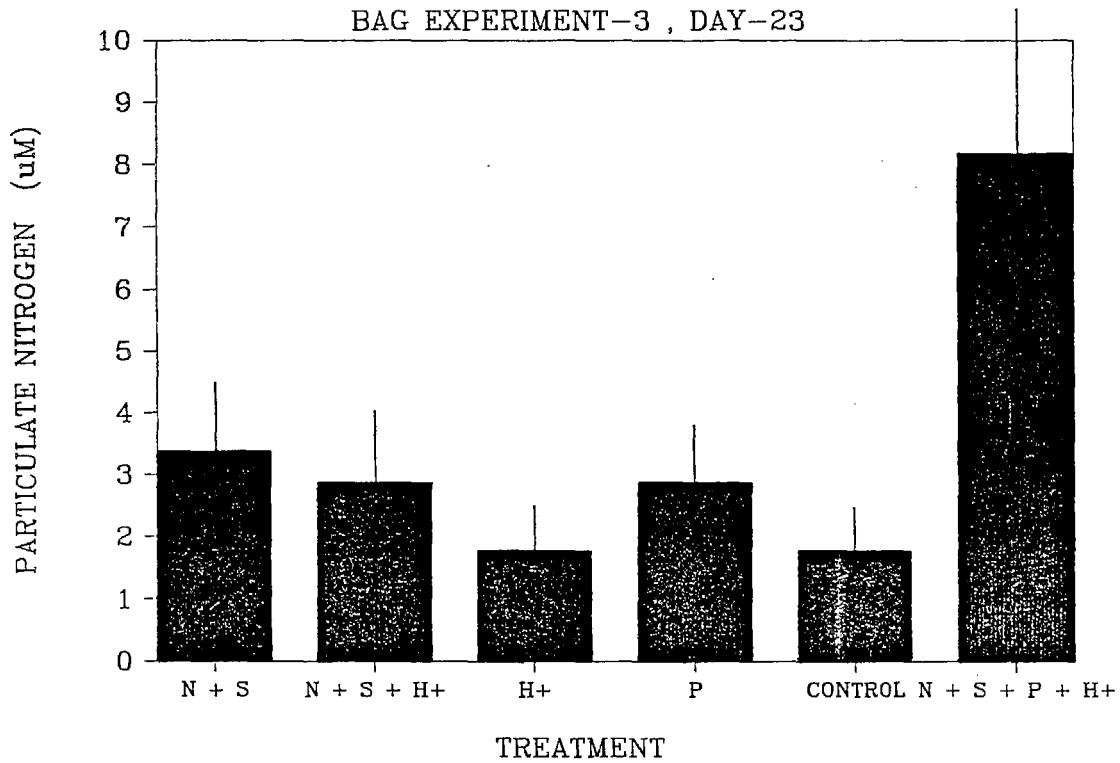


Figure II-69a+b. Chlorophyll a and particulate nitrogen; Day 23.

NITRATE - BAG EXPERIMENT 3

DAY 0 , 1 , 11 , 23

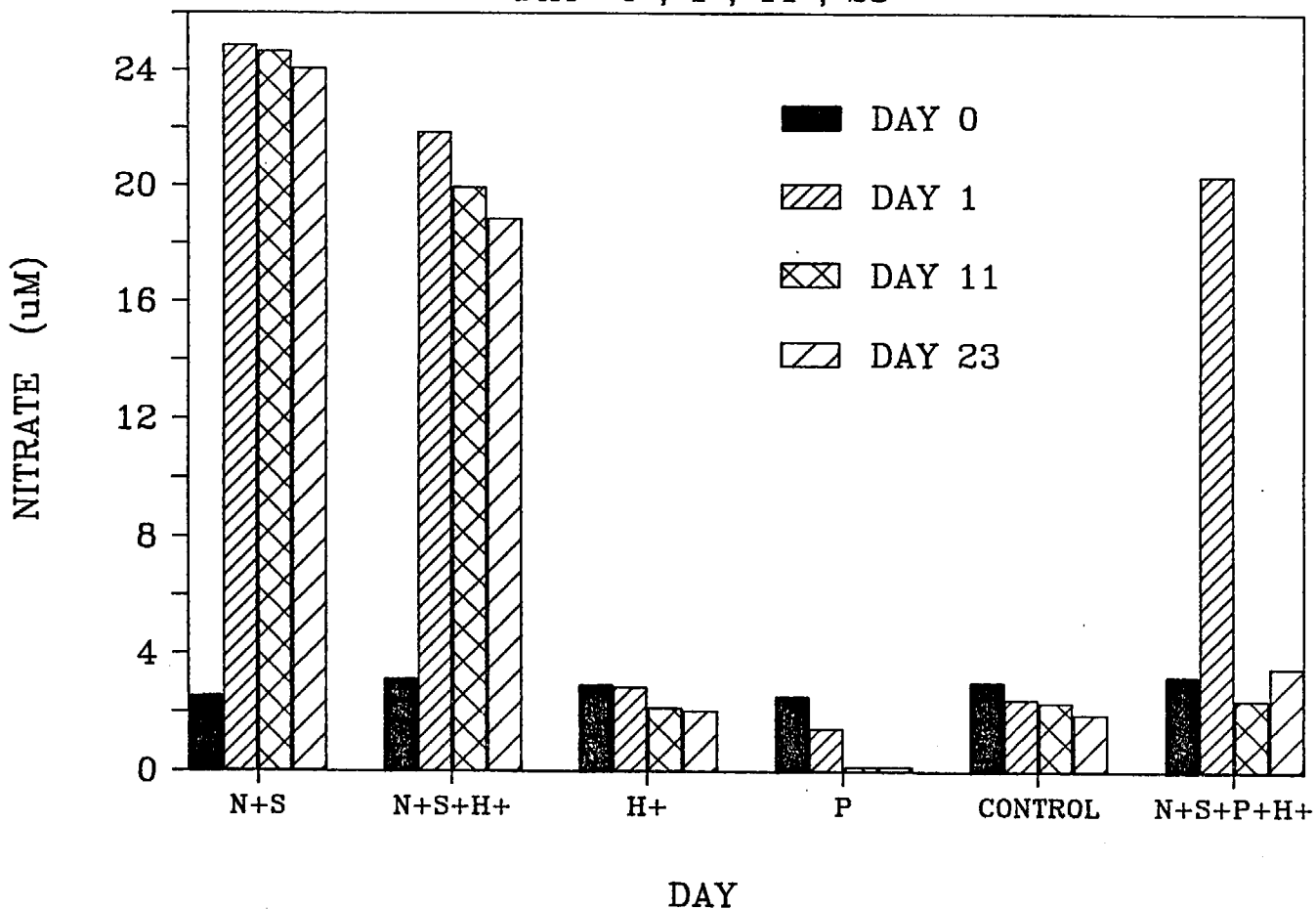


Figure 11-70 . Nitrate time series-all treatments; Experiment 3.

Chapter III
THE pH AND ALKALINITY HISTORY OF EMERALD LAKE SINCE 1825
ESTIMATED FROM DIATOM ASSEMBLAGES

Introduction

The examination of long-term pH records from lakes of different chemical composition may provide important information about the relationships between atmospheric deposition and acidification of lakes (Gibson 1986). When long-term pH observations are not available one method frequently employed to study past pH changes in lakes uses the composition of diatom assemblages preserved in lake sediments. The method relies on the observation that the occurrence of diatom species in aquatic environments can reflect the pH of their environment. Hustedt (1939) was probably the first investigator to formalize such relationships. He presented a pH classification scheme which recognized 5 diatom-pH categories:

- Acidobiontic (ACB): occurring below pH 7.0 with optimum distribution below pH 5.5
- Acidophilous (ACP): species occurring at about pH 7.0 with widest distribution at pH less than 7.0
- Indifferent (IND): equal occurrences on both sides of pH 7.0
- Alkaliphilous (ALP): occurring at pH about 7 with widest distribution at pH greater than 7
- Alkalibiontic (ALB): occurring at pH values greater than 7.0

It remained for Nygaard (1956) and Merilainen (1967) to develop semi-quantitative indices relating the composition of diatom assemblages observed growing attached to aquatic plants, rocks, or on the sediment, to lake pH. The indices developed by these investigators employed the diatom pH categories developed by Hustedt (1939) and the relative abundance of taxa in two or more of these pH categories. In 1982 Renberg and Hellberg developed an additional index (index B) and in 1984 Charles (1984, 1985) used multiple linear regression (MLR) methods to relate the occurrence of diatoms placed in Hustedt's pH categories to air-equilibrated lake pH. These indices and MLR have been employed in Scandinavia (Berge 1982, Davis and Anderson 1985, Davis and Berge 1980, Davis et al. 1983, Renberg and Hellberg 1982, Tolonen and

Jaakkola 1983, Tolonen et al. 1986), in Germany (Arzet et al. 1986), in the United Kingdom (Flower and Battarbee 1983), in Canada (Dickman et al. 1983, Dickman and Fortescue 1983, Dickman, Dixit and Evans 1986, Hudon et al. 1986), and the United States (Brugam and Lusk 1986, Charles 1984, 1986, Davis et al. 1983, Del Prete and Schofield 1981, Ford 1986, Whitehead et al. 1986) to reconstruct the past pH histories of lakes.

The absence of pH measurements in Emerald Lake over the past 40 - 50 years makes it impossible to ascertain directly whether this weakly buffered lake has changed in pH or acid neutralizing capacity (ANC) in recent years. Hence, we have of necessity used diatoms which have been preserved in the lake sediments to estimate past pH and alkalinity (or ANC).

Reconstruction of pH histories from diatoms as commonly practiced today is a three-step procedure. First, diatom pH ranges are determined in a study area by identifying diatoms from surface sediment in a suite of lakes, usually 20 - 50, of widely varying pH. Those diatom taxa which are sufficiently abundant and which occur over limited pH ranges are generally placed in one of five pH categories listed above.

The second step is to calculate the percentage of the diatoms in each pH category in each lake. The percentages of the diatoms in these pH categories are then employed to calculate an index, such as Index B, for each lake. A multiple linear regression equation is next obtained which relates the indices, such as Index B, and observed pH in each of the lakes in the calibration data set. Alternatively, a pH predicting equation may be obtained directly by using the frequency of occurrence of diatom taxa in each pH category in each lake in the lake survey data set using multiple regression analysis with observed lake pH as independent variable. The goodness of fit of both of these equations is evaluated by the multiple correlation coefficient and the standard error of the regression equation.

In common usage are indices developed by Scandinavian scientists, such as log Index B. Since the slope and intercept values of the equations employing these indices vary from one lake calibration set to another (e.g. Dickman et al. 1984) it is important to calibrate each study area in which diatom-pH relationships and predictions are sought. Such calibration sets from Scandinavia, Canada, Europe, the United Kingdom, and the northeastern United States have provided area-specific and statistically significant equations between such indices and lake pH. Since the coefficients obtained

in each pH category are also area-specific, indices generated in other areas are unlikely to work well in the Sierra Nevada.

In step three these equations are applied to the diatom occurrence data obtained from discrete samples from a number of depths in a lake sediment core. The estimated pH values, together with sediment age (or depth), are then used to reconstruct the pH history of the lake over the time interval encompassed by the core. The equations predict pH with a standard error of plus or minus 0.25 to about plus or minus 0.5 pH units.

Methods

Collection and fractionation of sediment cores--On October 3, 1984 sediment cores were collected in triplicate at three locations in Emerald Lake by SCUBA. One collection site was located in the deepest portion of the lake (10.5 meters). The remaining two core sites were located approximately 60 meters from the northeast and southwest shores of the lake. The water depth at these two locations was approximately 10 meters.

The cores were obtained by pushing a 7.3 cm diameter (inside diameter) transparent plastic tube into the sediment to a depth of 25-30 cm. The upper end of the core tube was capped immediately and was brought to the surface in a vertical position. A rubber stopper was inserted into the bottom of the tube before it was lifted from the water. The tubes were then transported to the shore in a vertical position and kept in this position until they were sectioned later the same day or on the following morning.

The sediment in the core tube was extruded by a rubber piston inserted into the bottom of the core tube. The piston was slowly moved upward by means of a mechanical jack while the core tube was maintained in a vertical position. A four cm length of core tubing was centered on the top of the core tube containing the sediment and held firmly in place while 0.5 or 1.0 cm of sediment was extruded into this piece of accessory tubing by the piston. An open whirl-pak plastic bag was held firmly against the core tube to catch the sediment as the accessory tube was slid off the core tube. All cores were sectioned at 0.5 cm intervals to a core depth of 5.0 cm. Between 5.0 and 20 cm one cm. thick sections were collected. The sample bags were carefully sealed, groups of 4-5 sample bags were then placed in zip-lock bags and transported to the laboratory where they were maintained at 5°C.

Preparation and enumeration of diatoms--1.2 cm³ of sediment from each interval was used for the diatom analysis. The sample from each depth interval was mixed thoroughly by kneading the plastic bag containing the sediment. A plastic spoon (volume 1.2 cm³) was dipped into the homogenized sample, withdrawn, and excess sediment removed from the lip of the spoon by drawing a metal spatula along the lip of the spoon. Any sediment clinging to the sides or bottom of the spoon was carefully removed with paper tissue. The sediment was then transferred with a jet of deionized water to a clean 1 liter glass beaker, approximately 30 ml of 30% hydrogen peroxide was added, and the beaker covered with parafilm. The beaker was then placed in an oven maintained at 50°C for 24-48 hours. The oxidation of the remaining organic matter in the sample was completed by adding approximately 1 cm³ of potassium dichromate after placing the beaker in a fume hood. Following the completion of the oxidation reaction the beaker was filled with deionized water, covered with parafilm, and set aside for 48 hours (or more) to allow the sediment to settle. Next, the supernatant in the beaker was carefully decanted and the remaining liquid and sediment transferred to a clean 250 ml beaker which was then filled with deionized water. After 48 hours the supernatant was clear and siphoned off. The sediment was then transferred to a 6 dram screw-cap vial and filled with deionized water. With the reduced dichromate concentration in the vial, the settling time of the sediment increased greatly and repeated centrifugation and resuspension of the sediment with deionized water was carried out until the supernatant was colorless.

The preparation of the permanent mounts for diatom counting and identification were made following the method of Battarbee (1973). The cleaned material in the vial was mixed thoroughly by shaking the vial for one minute. The vial was then placed in a vertical position for 30 seconds to allow the heavy material and sand to settle. An aliquot (usually 250 µl) was then removed and placed in a 25 ml volumetric flask. One drop of ammonium hydroxide was added to reduce clumping and the flask filled with deionized water. Following vigorous shaking of the flask, its contents were placed in a Battarbee (1973) chamber containing clean no. 1-1/2 cover glasses. The slide warmer on which the Battarbee chambers had been placed was maintained at 36-37°C until the water in the chamber evaporated. The chambers were shielded from dust during the evaporation process. The coverslips containing the sediment were removed and placed on a hot plate set at about 80°C to

drive off residual water. Naphrax, a high refractive index (ca. 1.75) mountant was then placed on each of the cover glasses. After the mountant solvent evaporated, the cover glasses were placed on a glass microscope slide. The microscope slide was gently heated with a micro Bunsen burner until the mountant flowed out to the edges of the cover glasses. If the cover glasses exhibited a badly clumped distribution of particulates, these were not used in the subsequent diatom enumeration.

The diatoms were identified and counted in transects across the cover glass until approximately 500 diatom valves were identified. Diatoms were counted and identified in 24 of the 25 intervals from the core taken in the deepest part of the lake (core mid-2), and at 3 intervals (0.0-0.5, 5.0-6.0 and 15.0-16.0 cm) in the cores taken at each of the other two locations.

Identification and quality assurance--Diatom identifications were made using standard reference works (Cleve-Euler 1951-1955, Germain 1981, Hustedt 1927-1966, 1930, Krammer and Lange-Bertalot 1985, 1986, Patrick and Reimer 1966, 1975) supplemented by numerous more specialized publications. The unpublished but widely distributed PIRLA Diatom Iconograph (Paleoecological Investigations of Recent Lake Acidification), compiled and prepared by Keith Camburn with contributions from other PIRLA diatomists, proved very useful. This series of photographic plates of diatom valves was prepared under an Electric Power Research Institute contract to D. Whitehead and D. Charles, Biology Department, Indiana University.

Verification of the diatom identifications (i.e., quality assurance) was achieved in several ways. Two PIRLA diatom identification workshops were attended. Photographs and prepared material of the Emerald Lake diatoms were examined by several PIRLA diatomists who helped verify our identifications. R. Holmes also spent a week with PIRLA diatomist K. Camburn who examined additional material and photographs and offered further comments on our naming of Sierra taxa. Thus our assignment of names to diatoms is consistent with PIRLA identifications. Lastly, a two-week visit to the Diatom Herbarium of the Academy of Natural Sciences, Philadelphia, helped resolve some of the remaining identification problems.

Dry weight, ignition loss and lead-210 dating--Material from each of the three cores was also analyzed for dry weight and ignition loss. Replicate 1.2 cm³ samples were taken at each core interval in the manner described above for core diatom subsampling. A sample of sediment (1.2 cm³) was placed

in an aluminum pan, dried to a constant weight at 80°C, and then combusted at 485°C in a muffle furnace. Percent organic matter (i.e. % ignition loss) was then calculated (Figs. III-1).

Lead-210 analyses were obtained for core mid-2. About 0.2 -1.0 g of dried sediment and a spike of 5 - 20 dpm of ^{208}Po was placed in a teflon beaker. Solid phases are totally dissolved by sequential leaching with concentrated hydrochloric acid, nitric plus perchloric acids, and hydrofluoric acid. After the sample had dissolved, it was taken to dryness, and the residue dissolved in 1 N hydrochloric acid. Ascorbic acid was added to complex iron, and polonium isotopes are spontaneously electroplated onto a silver disk. Activity on the disk was counted in an alpha spectrometer to measure the ratio of $^{210}\text{Po}/^{208}\text{Po}$. The solutions remaining after the plating were stored, and selected ones were combined for analysis of ^{226}Ra , measured by ingrowth of ^{222}Rn using alpha scintillation procedures. The ^{210}Po activity concentration was assumed to be identical to its parent ^{210}Pb concentration. Excess ^{210}Pb was calculated as the difference between measured ^{210}Pb and ^{226}Ra .

Results

Accumulation rates were derived by fitting excess ^{210}Pb (Table III-1, Fig. III-2) versus cumulative density in the core, assuming the density of the solid equalled 2.0 g/cm³. Cumulative density was calculated as the integral of dry density versus depth. Assumptions in this procedure are (1) that ^{226}Ra is constant with depth, (2) that incoming ^{210}Pb in incoming material is constant with time, (3) that accumulation rates are constant with time, and (4) that no bioturbation occurred in the sedimentary column. The data were fit to the following equation:

$$C = C_0 e^{-k d/s}$$

where C_0 = excess ^{210}Pb concentration at the sediment-water interface (dpm/g), d = cumulative density (g/cm), k = ^{210}Pb decay constant (per yr), and s = sedimentation rate (g/cm² yr). This equation was fit to the data to derive s and C_0 using a least squares technique that weighs each point equally, as described by Wolberg (1967). Uncertainties represent one standard deviation of the derived accumulation rates.

Sediment age (Table III-2) was determined as follows: the density of solids was assumed to equal 2.0 g/cm³, the density of dried sediment is equal to the fraction of the sediment which is solid times the density of the solid material. Sediment age is then calculated as follows:

$$\text{Age} = \frac{\int_0^z p \text{ dry } dz}{\text{sedimentation rate}} \quad \text{where}$$

p dry equals the fraction of material that is solid multiplied by the density of the solid phase.

The ²¹⁰Pb dates assigned to a number of core Mid-2 samples not only provide a time scale for the down-core pH inference, but also permit the calculation of sedimentation rates. A sedimentation rate of about 1.2 mm/yr is observed in core Mid-2. This rate is about twice that reported by Shirahata *et al.* (1980) for a small shallow, oligotrophic, high elevation, Sierra Nevada pond. This pond has a rather small drainage area (1.5 x 10⁶ m²) which is responsible in part for this low sedimentation rate. Whiting (personal communication) reports sediment accumulation rates of 0.7, 1.5, and 1.6 mm./yr. in Lake 45, Harriet, and Eastern Brook Lake, respectively, high elevation lakes also located in the Sierra Nevada.

The following four equations developed by Holmes (1986) or more recent modifications of them (Equations 5-7) were used to estimate the air-equilibrated pH and alkalinity values from the species composition of the diatom assemblages at each of the 24 depth intervals in Emerald Lake core Mid-2:

$$\begin{aligned} \text{pH} &= 7.11 - 0.40 \log \text{Index B} & (1) \\ F &= 117 \text{ Probability } > F = 0.0001 \\ r^2 &= 0.82, n = 27 \end{aligned}$$

where index B =

$$\frac{\% \text{ IND} + (5.0 \times \% \text{ ACP}) + (40 \times \% \text{ ACB})}{\% \text{ IND} + (3.5 \times \% \text{ ALP}) + (108 \times \% \text{ ALB})}$$

$$\begin{aligned} \text{pH} &= 7.08 - (0.0086 \times \% \text{ ACP}) + (0.0012 \times \% \text{ IND}) + \\ &\quad (0.0081 \times \% \text{ ALP}) + (0.021 \times \% \text{ ALB}) & (2) \\ F &= 37.5 \text{ Probability } > F = 0.001 \\ r^2 &= 0.87, n = 27 \end{aligned}$$

$$\text{pH} = 7.18 - (0.0097 \times \% \text{ ACP}) + (0.0070 \times \% \text{ ALP}) + (0.020 \times \% \text{ ALB}) \quad (3)$$

F = 52.0 Probability > F = 0.001
 $r^2 = 0.87, n = 27$

$$\text{Log alkalinity} = 2.089 - (0.0083 \times \% \text{ ACP}) + (0.0075 \times \% \text{ ALP}) + (0.0086 \times \% \text{ ALB}) \quad (4)$$

F = 35.0 Probability > F = 0.001
 $r^2 = 0.82, n = 27$

The method involves placing diatom species observed in each core sediment sample interval into their appropriate pH categories (see Appendices III-A and B). The relative abundances of all species in each sample for which pH categories have been assigned are summed for each category. These sums were then entered into equations 1, 2, and 3 to obtain pH estimates and into equation 4 to obtain an alkalinity estimate for each sediment interval.

The pH of Emerald Lake subsurface waters presently ranges between about 5.6 and 6.6; alkalinity ranges between about 0 and 45 $\mu\text{equiv./l}$. pH values most commonly fall between 6.2 and 6.4, and alkalinity between 20 and 40 $\mu\text{equiv./l}$. When applied to the upper one half centimeter of sediment, equations 1, 2, 3, and 4 overestimate the present pH and alkalinity in Emerald Lake (Table III-3 and Figs. III-3-A, III-4). This overestimation is the result, in part, of the pH range in the lakes used in developing these equations. The paucity of lakes in the Sierra Nevada with pH's below 6.4 and the apparent absence of lakes with pH's below about 5.8 introduces a bias in these equations. This leads to higher pH estimates in Emerald Lake than would be the case had additional lakes with a pH below 6.4 been available for inclusion in the data set used to develop the equations. This is because reconstructions work best for average lakes in a calibration data set rather than for end point lakes. No taxa could be placed with certainty in the acidobiontic category even though the data of other investigators suggest some Sierra taxa may fall into this category in other areas. Additionally, of the 88 acidophilic diatom taxa used in these equations, only 19, or 22%, had an abundance weighted mean pH of 6.4 or below. Since there are very few high elevation lakes in the Sierra Nevada with average pH's equal to or less than 6.4 it is unlikely that this bias can be reduced appreciably.

As can be seen in Table III-3 Log Index B (equation 1) consistently estimates lower pH values than the multiple linear regression equations 2 and 3. This is the result of the weighting given to acidophils and the manner in

which the indifferent taxa are handled and problems in classifying indifferent taxa. Even so, Log Index B also overestimates pH in the core for the reasons given above.

If some of the taxa encountered in the Sierra lake pH calibration data which are classified in this study as acidophils are in fact acidobionts and/or if some of the taxa which could not be classified fall into either the acidobiontic or acidophilic then the estimated pH of Emerald Lake will decrease. To test this hypothesis we transferred 7 taxa which Charles (1985) considers to be acidobionts (Cymbella hebridica, Eunotia exigua, E. incisa, E. tenella, Navicula subtilissima, Pinnularia cf. pseudomicrostauron, and Surirella delicatissima) from the acidophilic category to the acidobiontic category and an additional 6 taxa (Frustulia rhomboides v. capitata, Navicula radiosa v. parva, Neidium iridis v. amphigomphus, Pinnularia abaujensis, P. biceps, and Stauroneis anceps) which could not be placed in any pH category into the acidophilic category, again using information from Charles (1985). Three new pH predictive equations were then obtained: one using Index B (equation 5), and two using multiple linear regression techniques, one of which (equation 6) omitted the Indifferent taxa (making this equation analogous to equation 3), and one (equation 6) with the Indifferent taxa included (equation 6A). This is analogous to equation 2 in our earlier report. The new equations are as follows:

$$\begin{aligned} \text{pH} &= 7.12 - 0.39 \log \text{Index B} & (5) \\ F &= 106.4 \text{ Probability} > F = 0.0001 \\ r^2 &= 0.81, n = 27 \end{aligned}$$

$$\begin{aligned} \text{pH} &= 6.69 - (0.0185 \times \% \text{ACB}) - (0.00352 \times \% \text{ACP}) + (0.024 \times \% \text{ALP}) + \\ &\quad (0.0240 \times \% \text{ALB}) & (6) \\ F &= 17.73 \text{ Probability} > F = 0.0001 \\ r^2 &= 0.76, n = 27 \end{aligned}$$

$$\begin{aligned} \text{pH} &= 6.41 - (0.031 \times \% \text{ACB}) + (0.0014 \times \% \text{ACP}) + (0.010 \times \% \text{IND}) + \\ &\quad (0.021 \times \% \text{ALP}) + (0.13 \times \% \text{ALB}) & (6A) \\ F &= 21.06 \text{ Probability} > F = 0.0001 \\ r^2 &= 0.83, n = 27 \end{aligned}$$

The relationship between observed and estimated pH obtained with equations 5 and 6A are presented in Fig. III-3-A and Fig. III-4 together with the 95% confidence interval for an individual prediction of pH from diatom data.

Although equation 5 differed little from equation 1, it yielded, as expected, lower pH estimates (ca. 0.1 pH unit) than equation 1 at 15 out of 24 core depths (Table III-3). Equations 2 and 3 possessed satisfactory P and r^2 values. However, for the reasons mentioned above, they provided high pH estimates for the Emerald Lake surface sediment sample. The revised multiple linear regression equations 6 and 6A provided lower pH estimates than equations 2 and 3, as hypothesized. Equation 6A, which employs indifferent taxa has higher P and r^2 values than equation 6, and yielded 17 lower pH estimates (by 0.1 - 0.2 pH units) in core Mid-2 (Table III-3). Equation 5 produces, on average, somewhat lower estimates than equation 6A (Fig. III-4, Table III-3).

Fig. III-5 illustrates the estimated pH obtained with Log Index B (equation 5) and multiple linear regression equation 6A (also see Table III-3) in core Mid-2. The estimated pH obtained with equations 1, 2, 3, and 6 are also shown in Table III-3. As can be seen the hypothesized reduction in diatom inferred pH occurred. Log Index B pH estimates obtained with equation 5 average about 0.1 pH units lower than those estimates obtained with equation 1. A reduction of about 0.3 - 0.4 pH units occurs with equation 6A compared to equation 3. Equation 6A (which includes the indifferent pH category) also provides lower pH estimates than equation 6.

Regression analyses using estimated pH values obtained from each of these 7 equations in which pH regressed against depth (or date) in core Mid-2 reveal the slopes are not significantly different from zero. Correlation coefficients between core interval depth (or date) and estimated pH are not statistically significant. These results indicate that there has been no significant trend in pH in Emerald Lake during the last 160 years. The pH of Emerald Lake appears to have fluctuated slightly in a non-systematic manner since about 1825 AD and does not appear to have been affected by recent increases in acidic deposition.

Equation 4 was developed by Holmes (1986) to estimate alkalinity. The equation employed the same four pH categories as independent variables in the regression analysis. After applying this equation to the surface sediment diatom data it became apparent that the reconstructed alkalinity overestimated the present alkalinity in Emerald Lake. A new regression was then calculated which employed the revised pH categories used in equations 5, 6, and 6A. This revised regression also overestimated alkalinity and yielded an

r^2 value of 0.74, a lower r^2 value than that obtained with Equation 4. This is the result of the failure of the pH categories to adequately represent the alkalinity ranges of the diatom taxa used in the equations.

A new regression equation was then calculated (equation 7) with the diatoms assigned to 4 alkalinity categories rather than the Hustedt pH categories employed above. Category A contained taxa with alkalinity abundance weighted means (AWM) falling between 0 and 55 $\mu\text{equiv./l.}$, category B contained taxa with AWM's lying between 56 and 125 $\mu\text{equiv./l.}$, category C spanned the range 126 to 275 $\mu\text{equiv./l.}$ and category D included taxa with AWM's greater than 276 $\mu\text{equiv./l.}$ Only taxa which occurred with an AWM greater than about 1% in one or more lakes, or which occurred in three or more lakes regardless of their AWM, were employed in the analysis. Any taxa which met these criteria but which had distributions which exceeded these alkalinity optima by 25 - 30 or more $\mu\text{equiv./l.}$ were rejected since they are poor alkalinity indicators. These latter taxa were essentially the same ones which fell into the indifferent or circum-neutral pH categories in our previous study. The new equation (Equation 7) yields a higher r^2 and lower standard error than Equation 4. The new equation is as follows:

$$\begin{aligned} \text{Log Alkalinity} &= 2.09 - 0.0102 \times \% \text{ A} - 0.00129 \times \% \text{ B} + \\ &\quad 0.00306 \times \% \text{ C} + 0.00810 \times \% \text{ D} \end{aligned} \quad (7)$$

$F = 43.32$ Probability $> F = 0.0001$
 $r^2 = 0.89, n = 27$

The relationship between observed and estimated log alkalinity given by equation 7 together with the 95% confidence interval for an individual prediction of log alkalinity from diatom data is presented in Fig. III-3-B.

The alkalinity estimates in the core Mid-2 using equations 4 and 7 are listed in Table III-4 and presented graphically in Fig. III-6. Equation 7 yields a higher r^2 value than equation 4 (0.87 and 0.82, respectively) but leads to somewhat higher alkalinity estimates than equation 4. The alkalinity estimated for the upper 0.5 cm of sediment core Mid-2 by these two equations exceeds the present-day alkalinity of Emerald Lake. The reason that alkalinity is overestimated is probably the same as that which produces pH overestimates (see above).

Regression equations using the alkalinity estimates generated by equations 4 and 7 against core depth (or date) reveal, as was the case with

estimated pH, slopes which are not significantly different from zero. Estimated alkalinity is not correlated with core sample depth. Even though the alkalinity estimates are higher than those observed in Emerald Lake, these estimates, like the pH estimates, do not indicate any effects of recent increases in acidic deposition.

The two additional cores from Emerald Lake were used to provide a rough estimate of the spatial variability of the pH estimates obtained with equations 1, 2, 3, 5, and 6 in different parts of the lake. pH estimates were obtained from diatom data at several depth intervals from the replicate cores for comparison with similar estimates from core Mid-2, the core employed in the pH reconstruction. These estimates are presented in Table III-5.

The range of pH estimates from the core data (Table III-5) for any given depth interval obtained with the same equation is, with two exceptions, 0.3 pH units or less. Some of the variability in these estimates in the subsurface sediment samples may be due to slightly different sediment ages of the same depth intervals in the three cores. This close agreement affirms that the diatom identifications used to develop the pH predictive equations must of necessity be in close agreement with the the sediment core diatom identifications.

Discussion

Down-core pH and acid neutralizing capacity inferences were obtained with Emerald Lake core Mid-2 using equations developed in a previous study (Holmes 1986) and modifications of them developed in the present study. Fluctuations in diatom inferred pH and alkalinity have occurred since 1825. The pH and alkalinity values are not correlated with sediment age nor does regression analysis yield a data fit with a slope significantly different from zero. This analysis suggests that pH and alkalinity have varied randomly over about the past 160 years in Emerald Lake.

The references cited in the Introduction using diatom pH reconstruction methodology suggest that some lakes which are currently acidic (ca. pH 4.3-5.5) have become so since the 1930's to the 1970's as a result of increasing acidic atmospheric deposition derived from fossil fuel combustion. Some lakes, on the other hand, have apparently been acidic for hundreds to perhaps a thousand or so years, and their acidity is clearly not related to acidic

deposition. Some lakes with current pH's ranging from about 6.0 to 6.9 have maintained their current pH levels over the past 100 or so years. Emerald Lake is an example of this latter type.

While a considerable number of diatom pH reconstructions using lake sediments have already appeared in the scientific literature, only a small portion of these are from North American lakes (Brugam and Lusk 1986, Charles 1984, Del Prete and Schofield 1981, Dickman et al. 1984, Dickman, Dixit and Evans 1986, Ford 1986, Hudon et al. 1986, and Whitehead et al. 1986) and only one is for the western U.S. Baron et al. (1986). In eastern Canada Dickman et al. (1984) observed decreases in diatom inferred pH from pH 7.1 to 5.2 over the last 20 years in one lake and from pH 6.2 to 5.2 over the past 30 years in another. Hudon et al. (1986) developed pH reconstructions in two Quebec lakes. In the summer of 1983 Key Lake had an average pH of 5.5, Lake C-22 a pH of 5.75. The diatom inferred pH's of these two lakes were 5.2 and 5.4, respectively. No trends in pH were evident in Key Lake in the upper 10 cm of the core which represents a 43 year interval. A comparison of pH measurements made in Key Lake in 1970 (pH 5.7) and 1983 (pH 5.50) likewise suggests that its pH changed little if at all during this time interval. No evidence for trends in pH were apparent over the past 22 years in the Lake C-22 core.

In the Adirondacks diatom pH reconstructions from seven lakes have been published. In Big Moose Lake (Charles 1984) a rapid change in pH was inferred to have begun in about 1950 and has continued to at least 1982. According to Charles (1984) the most probable cause in this change (pH from 5.7 to 4.6) is acid deposition resulting from the combustion of fossil fuels. Whitehead et al. (1986) described long-term changes in diatom inferred pH in Upper Wallface Pond, Lake Arnold, and Heart Lake. They show that all three lakes gradually became acidic but at different rates and times between about 12,500 and 6,000 - 10,000 yr. B.P. Then followed a period of relative stasis, except in Heart Lake which exhibits small but probably significant changes in inferred pH. In the very uppermost sediments of Upper Wallface and Arnold inferred pH decreased rapidly. This decrease is most probably the result of acid deposition according to the authors. On the other hand, the pH in Heart Lake has gradually increased since 1500 yr. B.P. This increase is attributed to a steady decrease in hemlock and an increased frequency of fires in the watershed. Diatom pH reconstructions are available in an

additional three Adirondack lakes (Del Prete and Schofield 1982). In Honnedaga Lake the authors suggest a significant decrease in pH began in 1971, or earlier. Woodhull Lake showed no pH trends. Seventh Lake showed a rise in inferred pH at about the 4 cm level.

Cone Pond, N.H. (Ford 1986) is currently an acidic body of water with pH ranging from 4.48 to 4.80. Diatom inferred pH was calculated in the upper 40 - 50 cm of lake sediment using several different methods none of which revealed significant trends since 1829. Ford believes the pH in Cone Pond dropped below pH 5.0 more than 1000 years ago. Since buffering at this pH involves aluminum and/or organic complexes, the lake would not be expected to respond to recent increased acid inputs with a marked lowering of pH.

These reports suggest that some lakes which are currently acidic have only become so in the past 2 to 5 decades. At least one lake which is currently acidic has remained acidic for more than 1000 years. Another group of lakes which are only mildly acidic (i.e., pH 6.2-6.9, see Charles 1986) have remained at that pH over the past 2 - 4 decades. Since the current pH of a lake provides no certain indication of recent acidification, the need for and utility of pH reconstruction techniques is evident if impacts of recent increases in acidic deposition are to be evaluated.

As yet there are no diatom pH reconstructions published for lakes from states bordering on the Pacific Ocean. In Rocky Mountain National Park Baron et al. (1986) suggest that no demonstrable changes in pH have occurred in four lakes since the 1800's. However, the lake calibration data set used to infer core pH values encompassed a narrow pH range in which no convincing relationship between lake pH and the diatom flora was demonstrated.

The approach employed to estimate pH and alkalinity using diatoms preserved in lake sediments is purely correlative. Even when a good statistical fit is obtained between the relative abundance of certain diatom taxa and pH, there is no guarantee that pH is the only factor controlling distribution and abundance. In the present study alkalinity is strongly correlated with air-equilibrated pH. This covariance enables estimates of alkalinity as well as pH to be estimated with the equations developed in the present study. It is not known at present whether these diatoms are responding to pH, or alkalinity, or both, or with some other unknown covariant. Davis and Smol (1986) discuss these and related problems of inferential techniques as they apply to the interpretation of siliceous

microfossils preserved in the sedimentary record of lakes. These authors also point out the great utility of measuring independent parameters in the same core (e.g. trace metals, organic pollutants, carbon particles resulting from the combustion of fossil fuels, pollen, etc.) as they are potentially capable of strengthening the interpretation of the sedimentary record.

Table III-1. Lead-210 data from Emerald Lake core Mid-2.

Core Depth Interval (cm)	Lead-210 (dpm/gm)	Cumulative (at mid point) density (gm/cm ²)	Excess Pb-210 Units	Corrected (to calculate date)
0.0 - 0.5	105.6+/-3.9	0.07	93.3	97.7
1.0 - 1.5	66.7+/-3.0	0.44	54.4	57.0
2.0 - 2.5	69.6+/-2.2	0.89	57.3	60.0
3.0 - 3.5	56.9+/-2.2	1.41	44.6	46.7
4.0 - 4.5	48.8+/-1.7	1.95	36.5	38.2
5.0 - 6.0	44.5+/-1.8	2.66	32.2	33.7
7.0 - 8.0	19.5+/-1.8	3.66	7.2	7.5
9.0 - 10	19.7+/-0.7	4.54	7.4	7.7
12 - 13	19.3+/-0.9	6.35	7.0	7.3
15 - 16	16.4+/-0.5	8.07	4.1	4.3
19 - 20	14.7+/-0.5	10.41	2.4	2.5

Table III-2. Lead-210 dates for Emerald Lake core Mid-2.

Core Depth Interval (cm)	Density (dry) (gm/cm ³)	Cumulative Density (gm/cm ²)	Age
0.0 - 0.5	0.28		1982
0.5 - 1.0	0.38	00.33	1979
1.0 - 1.5	0.44		1976
1.5 - 2.0	0.44	00.77	1973
2.0 - 2.5	0.50		1969
2.5 - 3.0	0.52	01.28	1965
3.0 - 3.5	0.54		1961
3.5 - 4.0	0.52	01.81	1957
4.0 - 4.5	0.56		1953
4.5 - 5.0	0.58	02.38	1948
5.0 - 6.0	0.56	02.94	1940
6.0 - 7.0	0.52	03.46	1932
7.0 - 8.0	0.40	03.86	1926
8.0 - 9.0	0.44	04.30	1920
9.0 - 10	0.48	04.78	1913
10 - 11	0.70	05.48	1903
11 - 12	0.60	06.08	1893
12 - 13	0.54	06.62	1885
13 - 14	0.60	07.22	1876
14 - 15	0.58	07.80	1868
15 - 16	0.54	08.34	1860
16 - 17	0.58	08.92	1852
17 - 18	0.66	09.58	1841
18 - 19	0.58	10.16	1832
19 - 20	0.50	10.66	1825

Table III-3. pH estimates for Emerald Lake core Mid-2 using equations developed from the Sierra Nevada lake survey of 1985 and more recent modifications of them. Equation numbers refer to the equations given in the text of this report.

Core Depth Interval (cm)	Lead 210 Date	pH Estimates					
		Log Index B Eq. 1	Eq. 5	Eq. 2	Multiple Eq. 6	Reg. Eq. 6A	Eq. 3
0.0 - 0.5	1982	6.4	6.3	7.0	6.6	6.4	6.9
0.5 - 1.0	1979	6.5	6.5	6.9	6.6	6.4	6.8
1.0 - 1.5	1976	6.4	6.4	6.8	6.5	6.5	6.8
1.5 - 2.0	1973	6.6	6.5	6.8	6.5	6.5	6.8
2.0 - 2.5	1969	6.4	6.3	6.8	6.5	6.3	6.7
2.5 - 3.0	1965	6.3	6.2	6.7	6.5	6.4	6.6
3.0 - 3.5	1961	6.6	6.5	6.8	6.5	6.4	6.8
3.5 - 4.0	1957	6.4	6.3	6.8	6.4	6.3	6.7
4.0 - 4.5	1953	6.4	6.4	6.8	6.5	6.4	6.7
4.5 - 5.0	1948	6.2	6.2	6.8	6.5	6.4	6.7
5.0 - 6.0	1940	6.6	6.5	6.8	6.5	6.5	6.7
6.0 - 7.0	1932	6.4	6.3	6.8	6.5	6.4	6.7
7.0 - 8.0	1926	6.5	6.5	6.8	6.5	6.4	6.7
8.0 - 9.0	1920	6.4	6.3	6.7	6.5	6.4	6.7
9.0 - 10	1913	6.4	6.4	6.6	6.4	6.4	6.6
10 - 11	1903	6.3	6.2	6.7	6.5	6.4	6.7
11 - 12	1893	6.4	6.3	6.7	6.5	6.4	6.6
12 - 13	1885	6.3	6.2	6.7	6.5	6.3	6.6
13 - 14	1876	6.5	6.5	6.6	6.4	6.5	6.6
14 - 15	1868	6.6	6.5	6.7	6.5	6.5	6.7
15 - 16	1860	6.2	6.1	6.7	6.4	6.4	6.6
16 - 17	1852	6.7	6.6	6.9	6.5	6.4	6.8
18 - 19	(1832)	6.6	6.6	6.7	6.5	6.4	6.7
19 - 20	(1825)	6.4	6.4	6.8	6.5	6.4	6.8

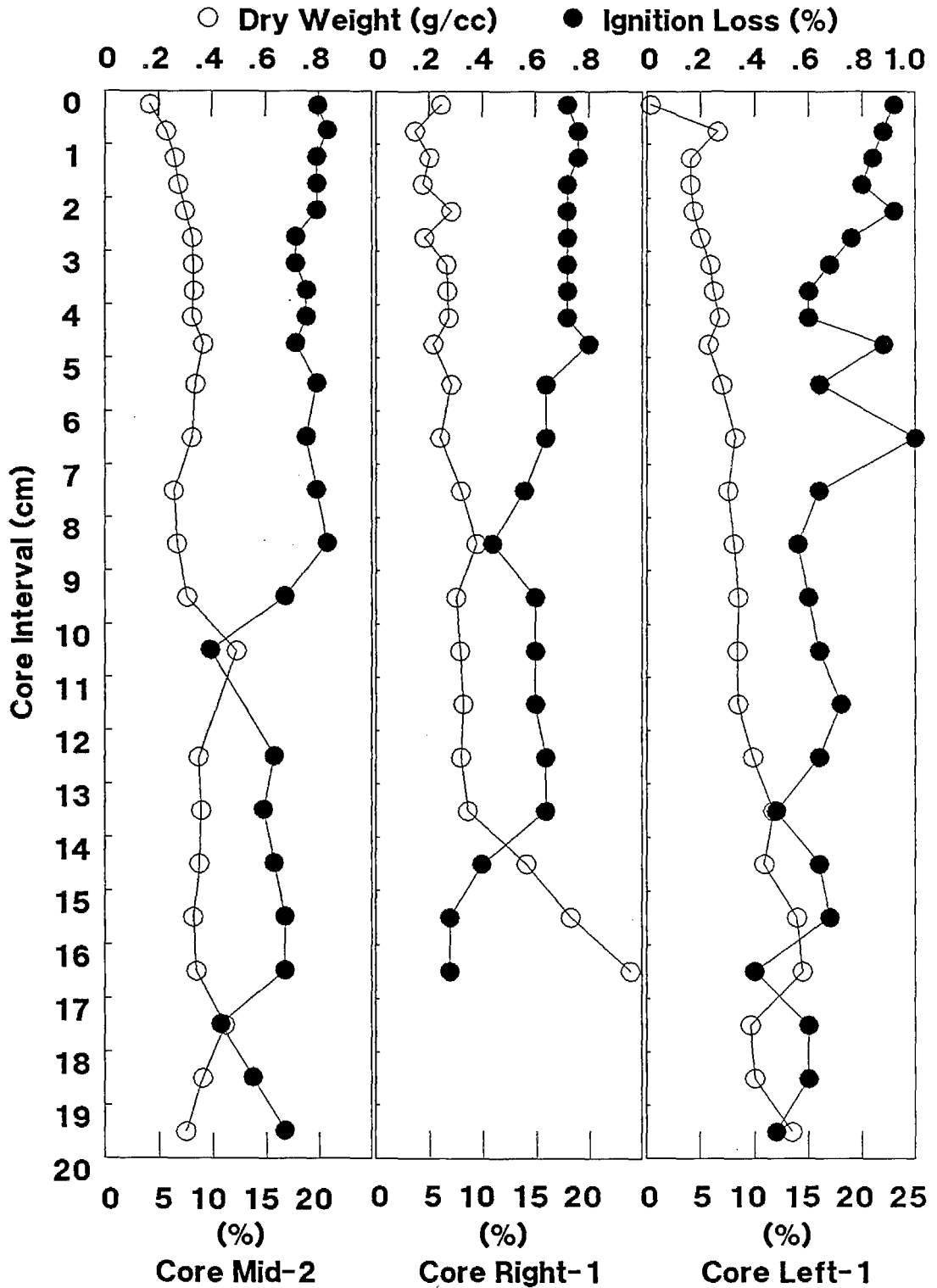
Table III-4. Alkalinity estimates for Emerald Lake core Mid-2 using equations 4 and 7. The equation number refers to the equation given in the text of this report.

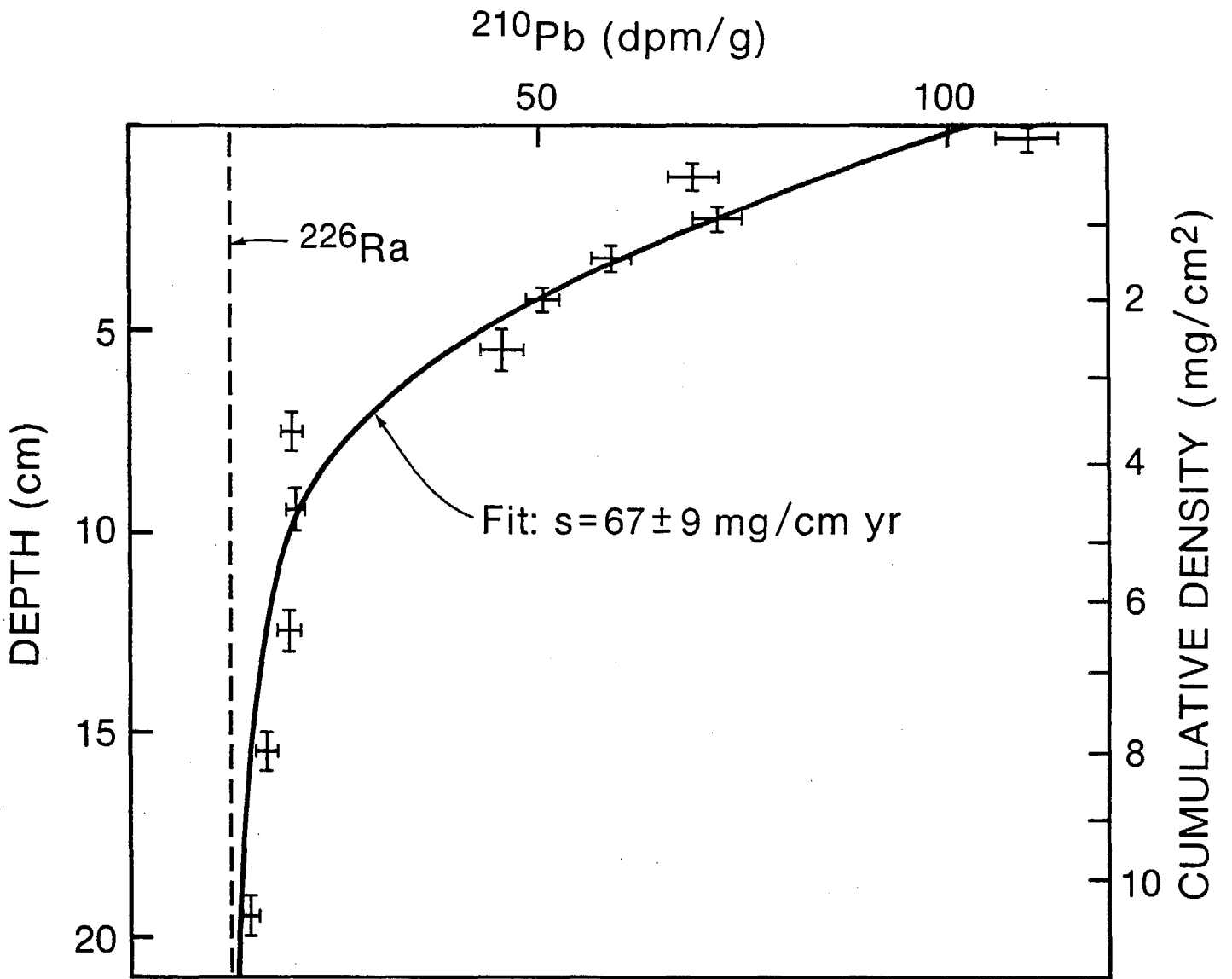
Core Depth Interval (cm)	Lead 210 Date	Estimated Alkalinity $\mu\text{equiv./l/}$			
		Log Alk. (Eq. 4)	Alk. (Eq. 4)	Log Alk. (Eq. 7)	Alk. (Eq. 7)
0.0 - 0.5	1982	1.896	79	1.887	75
0.5 - 1.0	1979	1.840	70	1.858	72
1.0 - 1.5	1976	1.772	59	1.824	67
1.5 - 2.0	1973	1.809	64	1.825	67
2.0 - 2.5	1969	1.479	54	1.778	60
2.5 - 3.0	1965	1.647	44	1.690	49
3.0 - 3.5	1961	1.771	59	1.828	67
3.5 - 4.0	1957	1.751	56	1.725	53
4.0 - 4.5	1953	1.763	60	1.796	63
4.5 - 5.0	1948	1.729	54	1.789	62
5.0 - 5.5	1940	1.754	57	1.810	65
6.0 - 7.0	1932	1.743	55	1.765	58
7.0 - 8.0	1926	1.742	55	1.770	60
4.5 - 5.0	1948	1.729	54	1.789	62
5.0 - 5.5	1940	1.754	57	1.810	65
6.0 - 7.0	1932	1.743	55	1.765	58
7.0 - 8.0	1926	1.742	55	1.770	60
8.0 - 9.0	1920	1.735	54	1.830	68
9.0 - 10	1913	1.569	37	1.648	44
10 - 11	1903	1.719	52	1.770	59
11 - 12	1893	1.642	44	1.685	48
12 - 13	1885	1.662	46	1.720	52
13 - 14	1876	1.614	41	1.619	42
14 - 15	1868	1.710	51	1.773	59
15 - 16	1860	1.675	47	1.723	53
16 - 17	1852	1.762	58	1.727	53
18 - 19	(1832)	1.714	52	1.764	58
19 - 20	(1825)	1.716	58	1.794	62

Table III-5. pH estimates from four core depth intervals in three Emerald Lake cores using the five equations developed in the present and previous study.

Core Depth Interval (cm)	Core No.	Log Index B			Multiple Linear Regression		
		Eq. 1	Eq. 5	Eq. 3	Eq. 2	Eq. 6	Eq. 6A
0.0-0.5	Mid-2	6.4	6.3	7.0	6.8	6.6	6.4
	Left-1	6.7	6.6	6.8	6.8	6.5	6.4
	Right	6.5	6.5	6.8	6.7	6.5	6.4
5.0-6.0	Mid-2	6.6	6.5	6.8	6.7	6.5	6.5
	Left-1	6.5	6.5	6.8	6.7	6.5	6.4
	Right	6.4	6.3	6.8	6.7	6.5	6.4
15 - 16	Mid-2	6.2	6.1	6.7	6.6	6.4	6.4
	Right	6.1	6.0	6.7	6.6	6.4	6.4
16 - 17	Mid-2	6.7	6.6	6.9	6.8	6.4	6.4
	Left-1	6.2	6.2	6.6	6.5	6.4	6.5

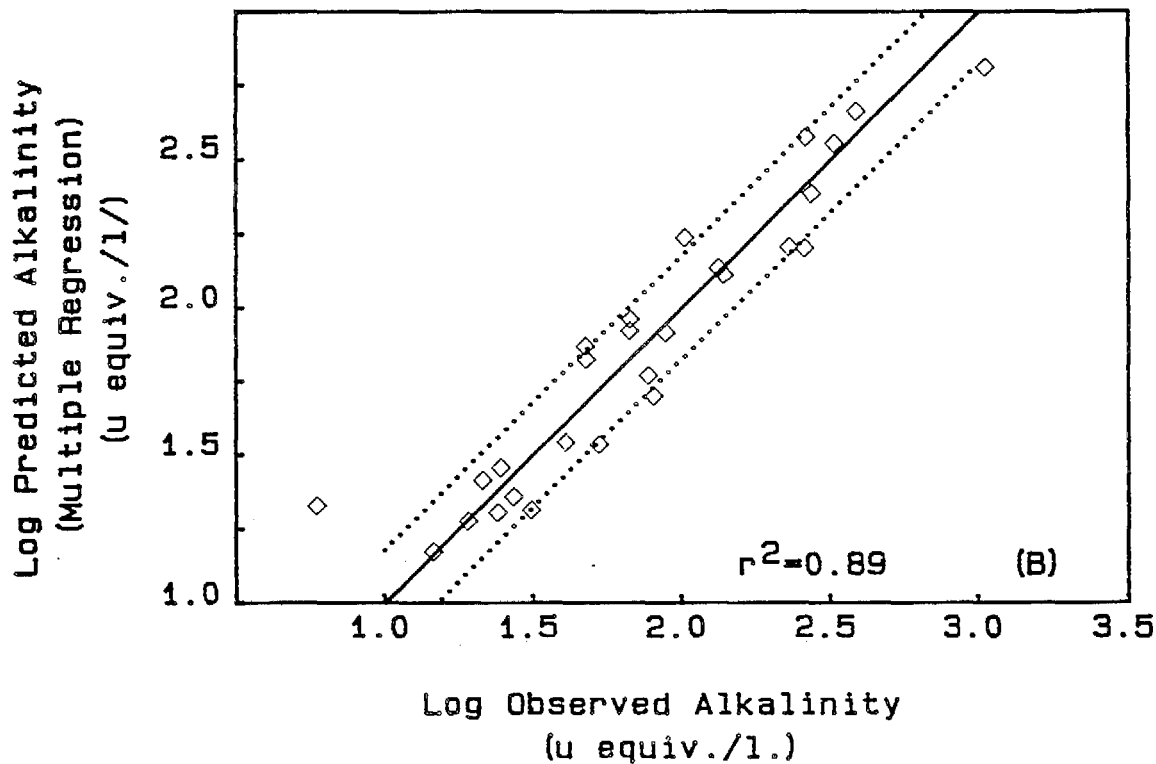
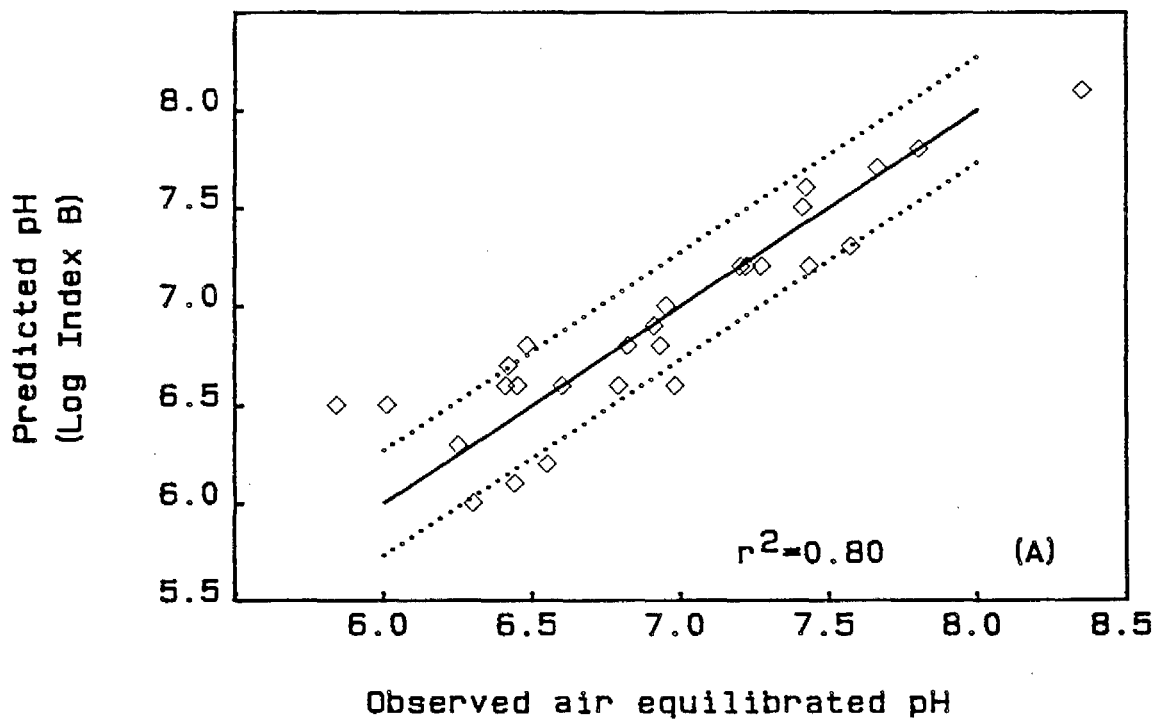
FIGURE III-1
Sediment Dry Weight and Ignition Loss
in Three Emerald Lake Cores





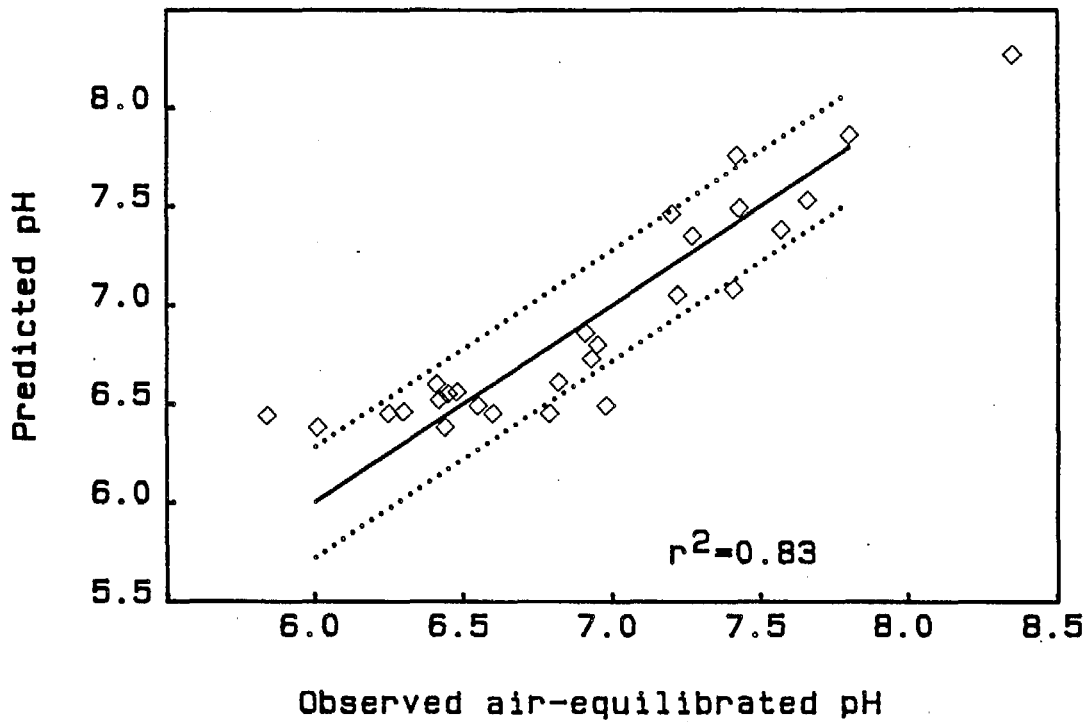
^{210}Pb profile in Emerald Lake core Mid-2

FIG. III-2



Observed and predicted air equilibrated pH and alkalinity (μ equiv./l.) in 27 high elevation Sierra Nevada Lakes. A) Predictions obtained using Log Index B (Equation 5). B) Equation 7 used which employs 4 alkalinity categories.

FIG. III-3



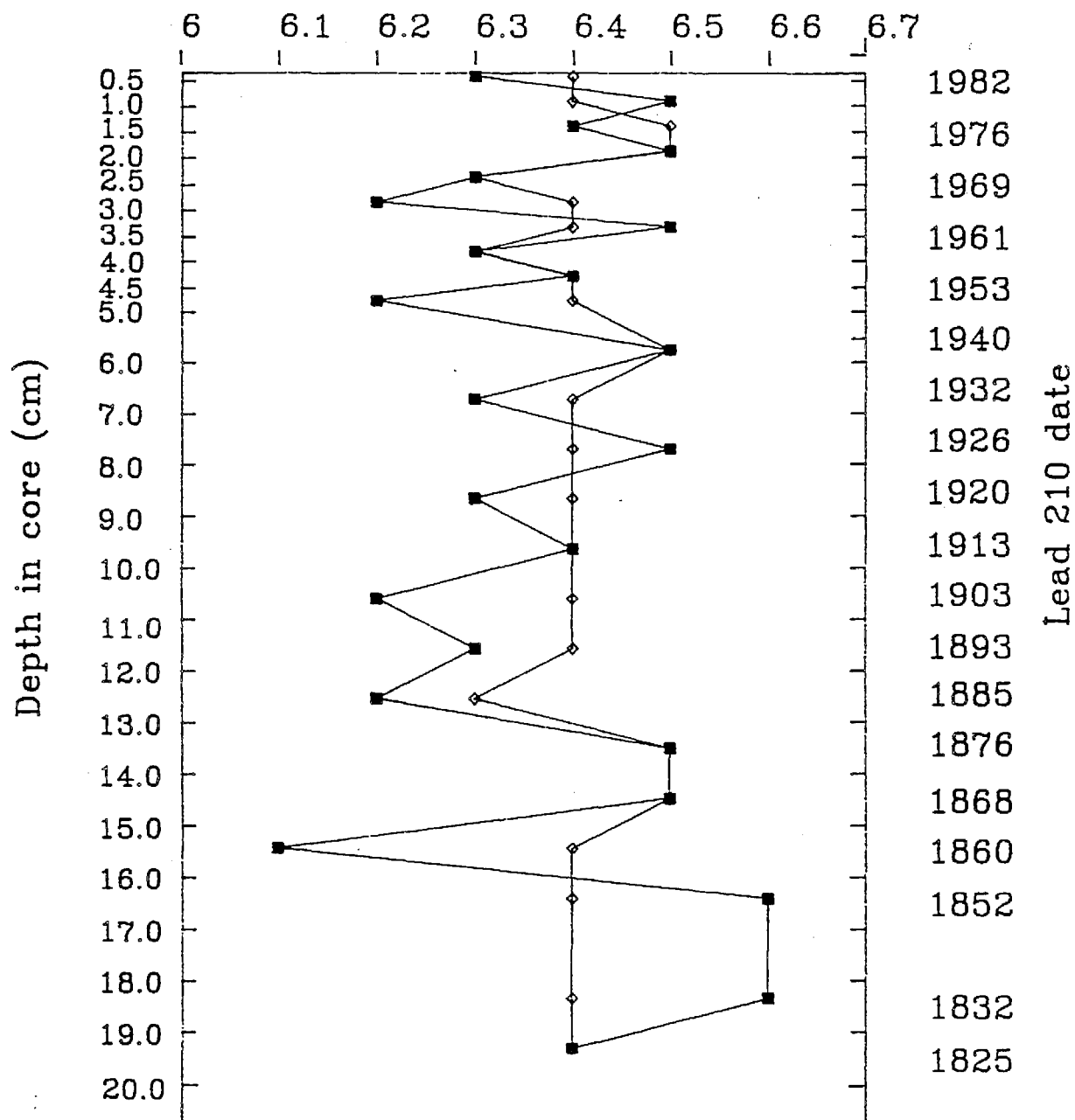
Observed and predicted air equilibrated pH in 27 high elevation Sierra lakes using multiple linear regression equation 6A.

FIG. III-4

ESTIMATED pH

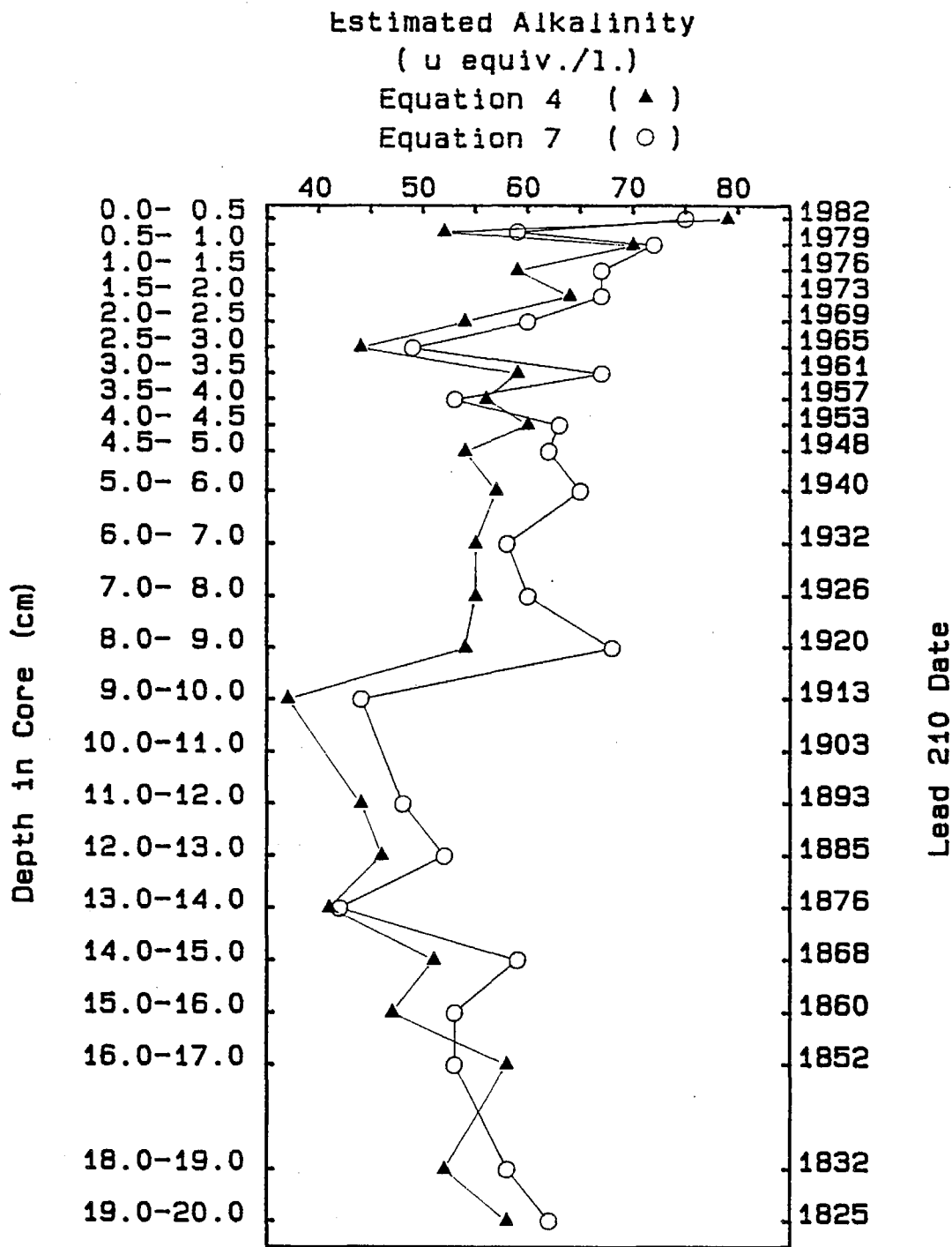
Log Index B (Eq. 5 ■)

Mult. Lin. Reg. (Eq. 6A ◇)



pH reconstructions of Emerald Lake Core Mid-2 using Log Index B [Eq. 5] and Mutiple Linear Regession [Eq. 6A].

FIG. III-5



Alkalinity reconstruction of Emerald
Lake Sediment Core Mid-2 using
equations 4 and 7.

FIG. III-6

APPENDIX III-A

Diatom genera and species (and their taxon number) observed in the present study

Taxon No.	Taxon Name
2002	Achnanthes austriaca Hust. v. austriaca
2003	Achnanthes austriaca v. helvetica Hust.
99360	Achnanthes austriaca v. ventricosa Krasske
2049	Achnanthes bioreti Germain v. bioreti
2042	Achnanthes detha Hohn & Hellerm. v. detha
2022	Achnanthes levanderi Hust. v. levanderi
2024	Achnanthes linearis (W. Smith) Grun. v. linearis
2028	Achnanthes marginulata Grun. v. marginulata
99007	Achnanthes 1 SN
99008	Achnanthes 2 SN
99010	Achnanthes 4 SN
2021	Achnanthes 6 PIRLA
99015	Achnanthes 10 SN
99018	Achnanthes 16 SN
99021	Achnanthes 21 SN
99361	Achnanthes (Navicula) 24 SN
99023	Achnanthes 28 SN
99030	Achnanthes 38 SN
99371	Achnanthes 42 SN
2889	Achnanthes spp
8003	Anomoeoneis serians (Breb. <u>ex</u> Kütz.) Cl. v. serians
8005	Anomoeoneis serians v. brachysira (Breb. <u>ex</u> Kütz.) Hust.
8008	Anomoeoneis 1 PIRLA
12001	Caloneis bacillum (Grun.) Cl. v. bacillum
23004	Cymbella cesatii (Rabh.) Grun. <u>ex</u> A.S. v. cesatii
23007	Cymbella gaeumannii Meist. v. gaeumannii
99362	Cymbella hauckii V.H. v. hauckii
23008	Cymbella hebridica Grun. <u>ex</u> Cl. v. hebridica
99046	Cymbella hebridica 1-NE
99363	Cymbella lata Grun. v. lata
23009	Cymbella lunata W. Sm. v. lunata
23012	Cymbella minuta Hilse <u>ex</u> Rabh. v. minuta
23013	Cymbella minuta f. latens (Krasske) Reim.
23014	Cymbella minuta v. pseudogracilis (Choln.) Reim.
23015	Cymbella minuta v. silesiaca (Bleisch <u>ex</u> Rabh.) Reim.
23016	Cymbella naviculiformis Auers. <u>ex</u> Heib. v. naviculiformis
99392	Cymbella naviculiformis 1 SN
99057	Cymbella 6 SN
99058	Cymbella 7 SN

Taxon No.

Taxon Name

99060	<i>Cymbella</i> 9 SN
99062	<i>Cymbella</i> 11 SN
23889	<i>Cymbella</i> spp
27001	<i>Diatoma anceps</i> (Ehr.) Kirchn. v. <i>anceps</i>
99364	<i>Diatoma hiemale</i> (Lyngb.) Heiberg v. <i>hiemale</i>
27002	<i>Diatoma hiemale</i> v. <i>mesodon</i> (Ehr.) Grun.
99365	<i>Eunotia alpina</i> (Naeg.) Hust. v. <i>alpina</i>
33004	<i>Eunotia bidentula</i> W. Sm. v. <i>bidentula</i>
33008	<i>Eunotia curvata</i> (Kütz.) Langerst. v. <i>curvata</i>
33009	<i>Eunotia curvata</i> v. <i>capitata</i> (Grun.) Woodhead & Tweed
33010	<i>Eunotia curvata</i> v. <i>subarcuata</i> (Naeg.) Woodhead & Tweed
99071	<i>Eunotia curvata</i> 1 SN (<i>indentata</i>)
33011	<i>Eunotia denticulata</i> (Breb.) Rabh. v. <i>denticulata</i>
33015	<i>Eunotia exigua</i> (Breb. <u>ex</u> Kütz.) Rabh. v. <i>exigua</i>
99366	<i>Eunotia faba</i> (Ehr.) Grun. v. <i>faba</i>
33018	<i>Eunotia fallax</i> Cl.-Eul. v. <i>fallax</i>
33140	<i>Eunotia fallax</i> v. <i>gracillima</i> Krasske
33026	<i>Eunotia incisa</i> W. Sm. <u>ex</u> Greg. v. <i>incisa</i>
33081	<i>Eunotia incisa</i> v. 2 PIRLA
33031	<i>Eunotia meisteri</i> Hust. v. <i>meisteri</i>
33033	<i>Eunotia microcephala</i> Krasske <u>ex</u> Hust. v. <i>microcephala</i>
33039	<i>Eunotia pectinalis</i> (O.F. Müller?) Rabh. v. <i>pectinalis</i>
33040	<i>Eunotia pectinalis</i> v. <i>minor</i> (Kütz.) Rabh.
99367	<i>Eunotia polydentula</i> Brun v. <i>polydentula</i>
33046	<i>Eunotia praerupta</i> v. <i>bidens</i> (Ehr.) Grun.
33045	<i>Eunotia praerupta</i> Ehr. v. <i>praerupta</i>
33051	<i>Eunotia rhomboidea</i> Hust. v. <i>rhomboidea</i>
33053	<i>Eunotia septentrionalis</i> Øst. v. <i>septentrionalis</i>
33054	<i>Eunotia serra</i> Hust. v. <i>serra</i>
33059	<i>Eunotia sudetica</i> (Grun.) Cl. v. <i>sudetica</i>
33060	<i>Eunotia tenella</i> (Grun.) A. Cl. Eu. v. <i>tenella</i>
33061	<i>Eunotia trinacria</i> Krasske v. <i>trinacria</i>
33062	<i>Eunotia trinacria</i> v. <i>undulata</i> Hust.
33066	<i>Eunotia vanheurckii</i> v. <i>intermedia</i> (Krasske <u>ex</u> Hust.) Patr.
99074	<i>Eunotia</i> 1 SN
33991	<i>Eunotia</i> 2 PIRLA
99075	<i>Eunotia</i> 2 SN
99076	<i>Eunotia</i> 4 SN
99082	<i>Eunotia</i> 12 SN
99085	<i>Eunotia</i> 15 SN
99368	<i>Eunotia</i> 17 SN
99369	<i>Eunotia</i> 18 SN
99393	<i>Eunotia</i> 19 SN
33090	<i>Eunotia</i> 44 PIRLA
33889	<i>Eunotia</i> spp
34016	<i>Fragilaria construens</i> v. <i>venter</i> (Ehr.) Grun.
34030	<i>Fragilaria vaucheriae</i> (Kütz.) Lange-Bertelot v. <i>vaucheriae</i>
34032	<i>Fragilaria virescens</i> Rolfs v. <i>virescens</i>
35001	<i>Frustulia rhomboides</i> (Ehr.) de T. v. <i>rhomboides</i>
35003	<i>Frustulia rhomboides</i> v. <i>capitata</i> (A. Meyer) Patr.
35004	<i>Frustulia rhomboides</i> v. <i>crassinervia</i> (Breb. <u>ex</u> W. Sm.) Ross

Taxon No.

Taxon Name

35005	<i>Frustulia rhomboides</i> v. <i>saxonica</i> (Rabh.) De T.
99102	<i>Frustulia rhomboides</i> v. 1 SN
35889	<i>Frustulia</i> spp
37010	<i>Gomphonema parvulum</i> (Kütz.) Kütz. v. <i>parvulum</i>
99105	<i>Gomphonema puiggarianum</i> v. <i>aequatorialis</i> (Cl.) Camburn
99107	<i>Gomphonema tackei</i> v. <i>brevistriatum</i> Camburn
99109	<i>Gomphonema</i> 3 SN
99112	<i>Gomphonema</i> 6 SN
99359	<i>Gomphonema</i> 15 SN
99388	<i>Gomphonema</i> 16 SN
37889	<i>Gomphonema</i> spp
40002	<i>Hantzschia amphioxys</i> (Ehr.) Grun. v. <i>amphioxys</i>
44001	<i>Melosira ambigua</i> (Grun.) O. Mull. v. <i>ambigua</i>
44002	<i>Melosira distans</i> (Ehr.) Kütz. v. <i>distans</i>
44045	<i>Melosira distans</i> 6 PIRLA
44010	<i>Melosira italica</i> (Ehr.) Kütz. v. <i>italica</i>
44040	<i>Melosira italica</i> subsp. <i>subarctica</i> f. <i>tenuissima</i> (Grun.) Camburn
44014	<i>Melosira lirata</i> (Ehr.) Kütz. v. <i>lirata</i>
44050	<i>Melosira roseana</i> Rabh. v. <i>roseana</i>
44027	<i>Melosira</i> 1 PIRLA
99126	<i>Melosira</i> 1 SN
99127	<i>Melosira</i> 2 SN
99128	<i>Melosira</i> 3 SN
99372	<i>Melosira</i> 9 SN
44889	<i>Melosira</i> spp
45001	<i>Meridian circulare</i> (Grev.) Ag. v. <i>circulare</i>
45002	<i>Meridian circulare</i> v. <i>constrictum</i> (Ralfs) V.H.
46002	<i>Navicula angusta</i> Grun. <i>angusta</i>
46008	<i>Navicula bremensis</i> Hust. v. <i>bremensis</i>
46026	<i>Navicula hassiaca</i> Krasske v. <i>hassiaca</i>
46095	<i>Navicula heimansii</i> van Dam & Kooijman v. <i>heimansii</i> PIRLA
46032	<i>Navicula laevissima</i> Kütz. v. <i>laevissima</i>
46038	<i>Navicula mediocris</i> Krasske v. <i>mediocris</i>
99138	<i>Navicula mediopunctata</i> Hust. v. <i>mediopunctata</i>
46042	<i>Navicula mutica</i> Kütz. v. <i>mutica</i>
46102	<i>Navicula mutica</i> v. <i>Cohnii</i> (Hilse) Grun.
46103	<i>Navicula mutica</i> f. <i>undulata</i> (Hilse) Cl.
46048	<i>Navicula perpusilla</i> (Kütz.) Grun. v. <i>perpusilla</i>
46050	<i>Navicula pseudoscutiformis</i> Hust. v. <i>pseudoscutiformis</i>
46051	<i>Navicula pupula</i> Kütz. v. <i>pupula</i>
46054	<i>Navicula pupula</i> v. <i>rectangularis</i> (Greg.) Grun
46056	<i>Navicula radiosa</i> Kütz. v. <i>radiosa</i>
46057	<i>Navicula radiosa</i> v. <i>parva</i> Wallace
46058	<i>Navicula radiosa</i> v. <i>tenella</i> (Breb. ex Kütz.) Grun.
46070	<i>Navicula seminulum</i> Grun. v. <i>seminulum</i>
99140	<i>Navicula subtilissima</i> 1 SN
46113	<i>Navicula</i> cf. <i>subtilissima</i> 2 PIRLA
46121	<i>Navicula</i> cf. <i>subtilissima</i> 4 PIRLA
99355	<i>Navicula subtilissima</i> 5 SN

Taxon No.

Taxon Name

99373	<i>Navicula subtilissima</i> 6 SN
46082	<i>Navicula tenuicephala</i> Hust. v. <i>tenuicephala</i>
46084	<i>Navicula tridentula</i> Krasske var. <i>tridentula</i>
99391	<i>Navicula</i> 5 NE
99374	<i>Navicula</i> 8 SN
99145	<i>Navicula</i> 9 SN
99148	<i>Navicula</i> 13 SN
99149	<i>Navicula</i> 14 SN
46133	<i>Navicula</i> 14 PIRLA
99150	<i>Navicula</i> 16 SN
99153	<i>Navicula</i> 22 SN
46123	<i>Navicula</i> 23 PIRLA
99154	<i>Navicula</i> 24 SN
99157	<i>Navicula</i> 27 SN
46098	<i>Navicula</i> 28 PIRLA
99161	<i>Navicula</i> 30 SN
99163	<i>Navicula</i> 32 SN
99176	<i>Navicula</i> 47 SN
99177	<i>Navicula</i> 48 SN
99179	<i>Navicula</i> 50 SN
99375	<i>Navicula</i> 86 SN
99361	<i>Navicula</i> 87 SN
99389	<i>Navicula</i> 88 SN
46889	<i>Navicula</i> spp
47001	<i>Neidium affine</i> (Ehr.) Pfitz. v. <i>affine</i>
47002	<i>Neidium affine</i> v. <i>amphirhynchus</i> (Ehr.) Cl.
47003	<i>Neidium affine</i> v. <i>ceylonicum</i> (Skv.) Reim.
47007	<i>Neidium bisulcatum</i> (Lagerst.) Cl. v. <i>bisulcatum</i>
47008	<i>Neidium bisulcatum</i> v. <i>baicalense</i> (Skv. & Meyer) Reim.
99376	<i>Neidium bisulcatum</i> v. <i>subundulatum</i> (Grun.) Reim.
99377	<i>Neidium hankensis</i> Skv. v. <i>hankensis</i>
99395	<i>Neidium hercynicum</i> f. <i>subrostratum</i> Wallace
47014	<i>Neidium iridis</i> (Ehr.) Cl. v. <i>iridis</i>
47016	<i>Neidium iridis</i> v. <i>amphigomphus</i> (Ehr.) Temp. & Perag.
47015	<i>Neidium iridis</i> v. <i>ampliatum</i> (Ehr.) Cl.
99218	<i>Neidium</i> 1 SN
47025	<i>Neidium</i> 2 PIRLA
99220	<i>Neidium</i> 3 SN
99224	<i>Neidium</i> 7 SN
47889	<i>Neidium</i> spp
99226	<i>Nitzschia acuta</i> Hantzsch v. <i>acuta</i>
48008	<i>Nitzschia dissipata</i> (Kütz.) Grun. v. <i>dissipata</i>
99228	<i>Nitzschia dissipata</i> f. <i>undulata</i> Sov.
99230	<i>Nitzschia frustulum</i> 2 SN
99231	<i>Nitzschia frustulum</i> 3 SN
48035	<i>Nitzschia</i> 1 PIRLA
99240	<i>Nitzschia</i> 5 SN
99241	<i>Nitzschia</i> 6 SN
99244	<i>Nitzschia</i> 9 SN

Taxon No.

Taxon Name

99250	Nitzschia 15 SN
99394	Nitzschia 20 SN
99267	Nitzschia 36 SN
48889	Nitzschia spp
52001	Pinnularia abaujensis (Pant.) Ross v. abaujensis
52002	Pinnularia abaujensis v. linearis (Hust.) Patr.
52078	Pinnularia abaujensis 2 PIRLA
52011	Pinnularia biceps Greg. v. biceps
52074	Pinnularia biceps v. 1 PIRLA
52013	Pinnularia borealis Ehr. v. borealis
52083	Pinnularia borealis v. rectangularis Carlson
52016	Pinnularia braunii v. amphicephala (A. Mayer) Hust.
52086	Pinnularia cf. braunii v. amphicephala f. subconica Venkataraman PIRLA
52025	Pinnularia divergens W. Sm. v. divergens
52027	Pinnularia divergentissima (Grun.) Cl. v. divergentissima
52038	Pinnularia maior (Kütz.) Rabh. v. maior
52041	Pinnularia maior v. transversa (A.S.) Cl.
52080	Pinnularia cf. pseudomicrostauron Gandhi v. pseudomicrostauron PIRLA
52069	Pinnularia termitina (Ehr.) Patr. v. termitina
99276	Pinnularia 1 SN
99277	Pinnularia 2 SN
99279	Pinnularia 7 SN
99280	Pinnularia 8 SN
99281	Pinnularia 9 SN
99282	Pinnularia 10 SN
99283	Pinnularia 11 PIRLA
99286	Pinnularia 15 SN
99289	Pinnularia 18 SN
99290	Pinnularia 19 SN
99300	Pinnularia 29 SN
99379	Pinnularia 42 SN
99380	Pinnularia 44 SN
99381	Pinnularia 45 SN
99382	Pinnularia 50 SN
99383	Pinnularia 51 SN
52889	Pinnularia spp
62002	Stauroneis anceps Ehr. v. anceps
62003	Stauroneis anceps f. gracilis Rabh.
62024	Stauroneis anceps 1 PIRLA
62022	Stauroneis anceps 2 PIRLA
62016	Stauroneis phoenicenteron f. gracilis
99313	Stauroneis 1 SN
99314	Stauroneis 2 SN
63002	Stenopterobia intermedia (Lewis) V.H. v. intermedia
65011	Surirella delicatissima Lewis v. delicatissima
65033	Surirella delicatissima f. tenuissima Mang.
65014	Surirella linearis W. Sm. v. linearis

Taxon No.

Taxon Name

99323	Surirella 2 SN
99357	Surirella 4 SN
99384	Surirella 5 SN
99385	Surirella 6 SN
65889	Surirella spp
66889	Synedra spp
67006	Tabellaria flocculosa (Roth) Kütz., strain IV sensu Koppen
89889	Unidentified pennate diatoms

APPENDIX III-B

Diatom species occurrences by taxon number and their assigned pH preference categories (ACP = Acidophilic, IND = Indifferent, CN = Circumneutral, ALP = Alkaliphilic, ALB = Alkalibiontic). Occurences are broken down as follows: a) observed in the ARB Lake Survey; b) in Emerald Lake short cores; c, d, and e) on hard (H) or soft (S) substrate in Emerald Lake, inlet streams, and the outlet stream, respectively. A plus sign (+) signifies non-living taxa, while an asterisk (*) denotes living taxa.

Taxon No.	pH Category	Lake Survey	EML Core	Lake		Inlet		Outlet	
				H	S	H	S	H	S
2002	ACP	+	+	+	+		+	*	*
2003	ACP	+	+	*	*	*	*	*	*
99360			+						
2049	ACP	+	+	+	+				*
2042	ACP	+	+	*	+		+	+	+
2022	ACP	+	+	*	*	*	*	*	*
2024		+	+						
2028	ACP	+	+	*	*	*	*	*	*
99007	ACP	+	+						
99008		+						+	
99010		+			+				
2021				+					
99015	ACP	+	+	*	*				+
99018		+					+		
99021	ALB	+	+		+		+		
99361			+						
99023								+	
99030			+		+				+
99371			+	*		*	*	+	
2889		+	+	*	*	*	*	*	*
8003	ACP	+	+						
8005	ACP	+	+	*	*	*	*	*	*
8008					+				
12001	IND	+					*		
23004	ACP	+	+					*	*
23007	ACP	+	+	+	+	+	*		*
99362			+						
23008	ACB	+	+	+	+			*	*
99046			+	+	+			*	
99363			+						
23009	ACP	+	+	*	*		*	*	*
23012	IND	+	+	*		+			
23013		+	+						
23014		+	+						
23015	IND	+	+	*	+			*	
23016	CN	+	+		+		+		
99392		+	+			+			

Taxon No.	pH Category	Lake Survey	EML Core	Lake		Inlet		Outlet	
				H	S	H	S	H	S
99057				*	+	+	+	*	*
99058			+						
99060	ACP	+	+	+	+			*	*
99062			+		+				
23889				+	*	+	*	*	*
27001		+	+	+	+	*	+	*	+
99364			+						
27002		+	+	*	*	*	*	+	+
99365	ACP		+	*					
33004	ACP		+						
33008	ACP	+	+	+	+	*		*	*
33009	ACP		+						
33010	ACP		+	*	+				+
99071	ACP	+	+				*		
33011	ACP	+	+		+	+	+	+	*
33015	ACP	+	+	+		*	*	*	*
99366	ACP		+						
33018	ACP	+	+						
33140	ACP	+	+				+		
33026	ACP	+	+	+	+			+	+
33081	ACP							*	
33031	ACP		+		+	+	*	*	*
33033	ACP		+						
33039	ACP	+	+				+		
33040	ACP	+	+				*	+	*
99367	ACP		+						
33046	ACP				+				
33045	ACP	+	+	+	+	+			
33051	ACP	+	+					+	
33053	ACP		+			+	+		+
33054	ACP	+	+		+				
33059	ACP	+	+						
33060	ACP	+	+	*	+	*	*	*	*
33061	ACP	+	+		+	+	+		+
33062	ACP		+						
33066	ACP	+				*	*	*	*
99074	ACP	+	+						
33991	ACP	+		*				*	
99075	ACP	+	+	*	*	*	*	*	*
99076	ACP								*
99082	ACP	+	+	*		*	*		*
99085	ACP		+		*	*	*	*	*
99368	ACP		+						
99369	ACP		+	+			+		
99393	ACP						+		*
33090	ACP		+						
33889	ACP	+	+		*	*	*	*	+
34016	IND	+	+						
34030	IND	+	+	*	+	*	*	*	*

Taxon No.	pH Category	Lake Survey	EML Core	Lake		Inlet		Outlet	
				H	S	H	S	H	S
34032	ALP								+
35001	ACP	+	+	+	*	+	+	+	+
35003		+	+						+
35004			+	+	+		*	+	+
35005	ACP	+	+		+	*	*	*	*
99102	ACP	+	+	+	+		+		+
35889								*	
37010		+	+						
99105	ACP	+	+	*	*		*	+	
99107	ACP		+		+	+			
99109		+	+	*	*	*	*	*	*
99112			+						
99359			+	*	+		+	*	
99388				*	+				
37889				+					
40002		+	+	+			+		
44001	ALP	+	+						
44002		+	+						
44045			+						
44010	ALP	+	+						
44040	ALP	+	+			+			
44014	CN	+	+	+	+	*			
44050			+	+	+	+	+	+	+
44027		+	+	*	*	*	*	*	*
99126	ACP	+			*			*	*
99127		+	+						
99128	CN	+	+	*	*	*	*	*	*
99372			+						
44889		+							
45001	ACP	+	+	+	*	*	*	+	+
45002			+		+				
46002			+		+	+		+	+
46008		+	+						
46026			+		+				
46095	ACP	+	+	*	*	*	+	*	*
46032	IND	+	+						
46038	ACP	+	+	+	*	*	*	+	*
99138	ACP	+	+						
46042		+	+		+	+	+		+
46102							+	+	+
46103			+						+
46048			+						
46050	CN	+	+						
46051	ALP	+	+						
46054		+	+						
46056	CN	+	+					*	
46057		+	+	*	*	*		*	*
46058							+		

Taxon No.	pH Category	Lake Survey	EML Core	Lake		Inlet		Outlet	
				H	S	H	S	H	S
46070			+						
99140	ACP		+						
46113	ACP	+	+				+	+	+
46121	ACP	+	+		+		+		
99355		+	+		+				
99373			+						
46082	ACP	+	+	*	*	*	*	*	*
46084			+	*	+				
99391					+				
99374			+						
99145	ACP	+	+						
99148	ACP	+	+	*	+	*	*	*	*
99149	ACP	+	+						
46133	ACP	+	+	+		+		+	
99150	ACP	+	+	*	+	+			
99153		+	+		+	+	*		
46123	ACP	+	+		*	+	*		
99154		+			+				
99157	ALP	+					*		
46098			+		+				
99161		+	+						
99163	ACP	+	+						
99176	ACP	+	+		+	*	*	+	
99177			+				+		
99179	ACP	+						+	
99375			+						
99361			+						
99389							+		
46889			+	+		*	+		*
47001	ACP	+	+	+	*	+	*	+	*
47002	CN	+					+		
47003			+						
47007	ACP	+	+	+	*	*	*	+	*
47008		+	+						
99376			+						
99377			+						
99395			+						
47014		+	+	+	*				
47016		+	+		+				
47015			+		+				
99218					+		*		
47025	ACP	+	+	+	*	*	*	+	*
99220		+					+		
99224					+				+
47889			+	+	+	+	+		
99226			+		+				
48008			+		+				
99228	ACP	+	+	*	+				
99230	IND	+	+						

Taxon No.	pH Category	Lake Survey	EML Core	Lake		Inlet		Outlet	
				H	S	H	S	H	S
99231	IND	+	+	*	*	*	*	*	*
48035	ALP	+	+						
99240	IND	+	+	*	*	*	*	*	*
99241	IND	+	+	*	+	*			*
99244	ACP	+	+	+	*	*	*	+	*
99250		+				+		*	
99394									+
99267	ALP	+						+	
48889			+	+	+	*	+		
52001		+	+		*				
52002	ACP	+		+					
52078	ACP		+						
52011		+	+	+	*	*		*	+
52074		+	+	*	*	+	*	*	*
52013		+	+		+				+
52083			+	+	+		*	+	+
52016			+		+				
52086	ACP	+	+	+	*		+		*
52025		+	+		+	+	*		
52027	ACP	+	+	*	+	*	*	+	
52038	ACP	+	+						
52041			+						
52080	ACP	+	+				*		
52069		+	+			+	+	+	+
99276	ACP	+	+		+				
99277	ACP	+	+	*	*	+	+		
99279			+						
99280		+							
99281	ACP	+	+		+	+	*		*
99282		+	+						
99283	ACP	+			+				
99286			+	+	+	+	*	+	*
99289			+		+				
99290			*	*	+		+	*	*
99300						+			
99379			+						
99380			+						
99381			+				+		*
99382			+						
99383			+						
52889			+	+	*	*	*	+	+
62002		+	+	+	*				
62003	ALP	+	+						
62024	ACP	+	+						
62022	ACP	+	+		*			+	
62016					+				
99313			+						
99314			+	+	+		+	+	*

Taxon No.	pH Category	Lake Survey	EML Core	Lake		Inlet		Outlet	
				H	S	H	S	H	S
63002	ACP	+	+	*	+		+	*	*
65011	ACB	+	+	*	*		+	*	*
65033	ACP	+	+		*				*
65014	ACP	+	+	*	*				
99323			+						
99357			+						
99384			+		+				
99385					+				
65889			+		+	+		*	+
66889			+						
67006	IND	+	+	*	*	*	*	*	*
89889			+	+	*	*	*	*	*

Chapter IV.1

PHYTOPLANKTON

Introduction

Phytoplankton community responses to pH change have included shifts in composition and abundance (Yan and Stokes, 1978; Kwiatkowski and Roff, 1976). These responses have been observed both in the field (Hendry, 1980) and in the lab (Tonnessen, 1983). Earlier studies have focused on European, Canadian, and northeastern U.S. lakes. Little is known about the potential effects of acid deposition on Sierran lakes. Tonnessen (1983) conducted microcosm studies using phytoplankton assemblages from the Sierra and noted changes in phytoplankton composition, with an increase in filamentous forms, dinoflagellates and cryptomonads and a decrease in chrysophytes and cyanobacteria under increased acidification.

During this study, we tried to identify the existence of sensitive biological species or diagnostic changes (such as shifts in size spectra) that would indicate ecological changes resulting from increasing acidification. Seasonal variability was measured in order to separate these changes from biological responses resulting from acidic pulses.

Materials and Methods

A. Seasonal variability

Sample collection - A phytoplankton survey was conducted at Emerald Lake for a two year period (17 August 1984-17 July 1986). Samples were collected from the deepest part of the lake at biweekly intervals during ice-free seasons and at monthly intervals during winter. Sample collection procedures were modified during the course of the study as follows: In summer of 1984, samples were collected by lowering a one-gallon jug to the lake bottom at a constant rate, returning it to the surface, mixing its contents well, and pouring 250 ml aliquots into clean polyethylene bottles. A plastic Kemmerer bottle was used to collect water from four discrete depths (1, 4, 7, and 9.5 meters) during the ice-covered season. These aliquots were combined in a clean bucket, mixed and subsampled. An integrating water sampler was used during the ice-free months of 1985 and 1986. This sampling device consisted of a 10-meter flexible, plastic tube that was weighted at one end (Lund,

1949). The weighted end was lowered through the water, coring the water column. The surface end was then pinched, the lowered end raised, and its contents flushed into a clean one liter container. Two 250 ml aliquots were then poured into polyethylene bottles and preserved. Samples collected to determine the comparability of these different sampling techniques indicated no significant difference.

Sample preservation - Acidic Lugol's solution (Vollenweider, 1969) was used to preserve most phytoplankton samples. Lugol's solution stains cells a brownish-yellow color, thus increasing visibility, and decreases settling time via incorporation of the iodine. Cells preserved with Lugol's do not exhibit the flagellar loss accompanied by other preservation techniques. Disadvantages include sample oxidization with time, silica dissolution after prolonged storage, and internal structure obscuration with overstaining. A second preservative, formaldehyde, was used on rare occasions. Frequent flagellar loss was the principle disadvantage of this method; additional problems included bleaching of cell contents and distortion of naked cell forms. Vibrations could encourage aggregate formation within a sample regardless of preservative used, so samples were agitated as infrequently as possible during storage.

Lugol's was added until the sample was a pale brown, generally requiring 1 to 3 ml. Samples were shaken and stored in the dark until microscopic analysis could take place. Samples were examined periodically, and additional preservative was added if necessary.

Enumeration and Identification - Samples were counted using Utermohl's inverted microscope method (Hasle, 1978). Samples were given a thorough, gentle shaking to dislodge cells that had attached to the sides of the storage bottle and to randomize distribution. Ten-milliliter samples were poured into closed settling chambers and allowed to settle for a minimum of two days. No significant differences were noted between settling times greater than twenty-four hours. For standardization, most samples were allowed to settle 48 hours. Extremely sparse samples, such as those collected during ice-covered periods, were settled in 50 ml chambers and settling time was increased to five days. Randomization within the chamber was assumed to have been accomplished by mixing of the sample before removal of the aliquot and by careful, undisturbed settling.

Samples were examined using brightfield illumination at low power to confirm that no obvious clumping had occurred. Randomly selected cross-diameter transects were then examined under oil immersion magnification (1250x on the Leitz or 1000x on the Nikon microscopes) until a minimum of 500 cells had been counted. The counting chamber was rotated between traverses to avoid field overlap. In some instances, fields were counted instead of transects.

Colonial and filamentous forms were counted as units (Lewis, 1978) and the number of cells per colony or filament was also noted. Cells which were more than half out of a field were not counted. Cells recognizable as dead before preservation were noted but not included in the counts.

Limitations set by the nature of the phytoplankton and preservation method prevented even a modest taxonomic study of the phytoplankton. The majority of the cells were less than five microns in diameter and could not be identified even to the class level without observation of pigment, storage products, or ultrastructural features (Guillard, 1978). Identifications, when made, were based on Skuja (1946), Smith (1950), Contant and Duthie (1978), Bourelly (1957), and Findlay and Kling (1979). In addition, a classification for Emerald Lake phytoplankton was developed based on cell size and shape. Distinct morphotypes were identified and assigned a code number. Photographs were taken of each morphotype using a Canon 35mm camera mounted using an OM-mount photomicro adaptor and Kodak Technical Pan film for documentation.

Analysis - Abundance data were expressed as cell counts (cells/ml), biomass (mg/l), and cells per size class. Counts from each sample were first converted from cells/transect to cells/ml. Cell counts were then converted to biomass estimates and size fractions.

Cell volume was calculated for each morphotype by choosing an equivalent geometric shape (one that most closely simulated the shape of the morphotype), and computing volume based on a few key dimensions. Cell volume is expressed in $\mu\text{m}^3/\text{ml}$. Key dimensions of twenty-five randomly selected cells were measured for each morphotype except for rare forms. Skeletal material (e.g. spines) was not included in volume estimates. The volume of each measured cell was calculated, and the mean morphotype volume was then determined. Total phytoplankton volume for a sample was then calculated as:

$$V_{\text{total}} = V_1N_1 + V_2N_2 + \dots + V_iN_i$$

where V_i = mean cell volume and N_i = number of individuals of species i . Total volume was then transformed to a live weight estimate by assuming a density of unity. Mean morphotype volume was assumed to remain constant throughout the study period.

Phytoplankton abundance data was transformed into size spectra using Dussart's (1965) classification system as modified by Munawar and Munawar (1981). The average measure of the longest dimension (also known as the greatest axial linear dimension, or GALD) was used to assign each morphotype to a size category.

Size classification	GALD (microns)
Ultrannoplankton	<5
Nannoplankton	5-19.9
Microplankton	20-64
Netplankton	>64

Additional data used in analysis of phytoplankton include temperature, pH, chlorophyll a , and zooplankton abundances. Methods used to obtain these data are described in other chapters of this report.

B. Bag experiment #3

A randomized block experiment was run during the summer of 1985 to separate potential effects of increased acidity from increased nutrient loading. The experiment initially consisted of six treatments, with four replicates per treatment. Treatments are summarized below. Treatment 2 (HCl addition) was subdivided into two treatments of two replicates after noting that two discrete pH levels had been attained. The physical design of this experiment is discussed in Chapter II.4. Bag 14 (treatment 6, acid + P04) exhibited anomolous results for the duration of the experiment. Data analysis for treatment 6 was done in two phases: including bag 14 and excluding bag 14 and generating a dummy bag such that the ANOVA residuals due to the dummy bag equalled zero.

Emerald Lake, Bag experiment #3, 1985
Experimental manipulations

Treatment	Bag				Manipulation
1	1	11	17	21	KNO ₃ + NaSO ₄
2.1		12	15		HCl (low)
2.2		3	20		HCl (high)
3	4	10	13	23	PO ₄
4	2	7	16	22	H ₂ SO ₄ + HNO ₃
5	5	9	18	19	Control
6	6	8	14	24	H ₂ SO ₄ + HNO ₃ + PO ₄

Samples were collected over a five week period using a four meter integrating sampler. Replicate samples were not taken within bags. All other aspects of sample collection and preservation paralleled biweekly sampling procedures. Three hundred cells were counted per sample. Identification procedures were the same as those developed for biweekly samples.

Data were tabulated by morphotype and experimental unit (bag), for each treatment and sampling time. Cell counts were then expressed as cells/ml, mg/l, and size spectra. Mean, variance, and standard error were calculated. The mean-variance relationships were examined before any additional statistical procedures were run, to determine which transformations, if any, were needed to meet the assumptions of a normal population. These assumptions include equalized variances, minimal skewness, and additivity. Once these assumptions were met, errors were equal and uncorrelated with the magnitude of mean and variance components.

Transformations were determined by plotting log(mean) vs. log(variance) and fitting a line using the least-squares regression, such that

$$s^2 = am^b$$

where m is arithmetic mean and s^2 is the variance of a group of replicate samples, and a and b are constants (Taylor, 1961). It has been suggested

that b is a species specific characteristic (Downing, 1986). The original data (X) is then transformed to (X') such that

$$X' = X(1-b/2)$$

(Taylor, 1961; Prepas, 1984). Thus, we were able to develop exact power transformations calculated from site-specific s^2 and m .

Before ANOVAs were run on morphotype data, cell counts were converted to relative abundances, such that p_1 through p_6 corresponded to the 6 most common morphotypes (each of which contributed 5% or more to the total abundance), and p_7 was the proportion remaining, corresponding to the sum of all other morphotypes, i.e. relative abundance of morphotype i = (total cells of morphotype i /total live cells) and $p_7 = (1 - p_1 - p_2 - \dots - p_6)$. The data were then transformed based on s^2 - x relationships, and a repeated measures ANOVA performed (Aitchison and Shen, 1980). Size class information was also expressed as relative abundance before ANOVAs were performed.

A split-plot ANOVA was run to examine effects of treatment across all dates for each measured parameter. When treatment effects were indicated Duncan's multiple range test was used to examine significant differences between treatments. Differences among treatments were examined using appropriate t tests. A nested ANOVA was performed to test for effects of subsampling.

Results

Seasonal variability - Phytoplankton densities ranged from 150 cells/ml (January 1986) to 9100 cells/ml (April 1986) (Fig.IV-1). Lowest densities generally occurred during periods of ice-cover. Cell concentrations reached peaks in autumn and spring.

Total cell abundance shifted throughout the study period, accompanied by a corresponding shift in community composition. Dominance (as determined by total cell counts) shifted from Chlorophytes (autumn 1984) to small flagellates and Dinobryon spp. (winter 1984) to coccoid Chlorophytes (spring 1985) to small flagellates and rod-shaped Chlorophytes (summer 1985) to flagellates (autumn 1985) to small coccoid Chlorophytes and Cyanophytes (winter and spring 1986).

The smaller size classes dominated the total cell counts. Ultrannoplankton contributed more than 50% of the total cells on all but four sample dates (Fig. IV-2). The second most abundant size class was the nanoplankton. Microplankton never contributed more than 10% of the total cell count, and the netplankton proportion was never more than 0.5%.

The dominant morphotypes (those contributing more than 5% of the total cells/ml on more than 50% of the sample dates) were o02, r01, and r03. Several other morphotypes were dominant for shorter periods. Key characteristics of the dominant phytoplankton morphotypes are summarized below.

Morphotype	Shape	Size (microns) (length, width)	Comments
a01	cocccoid	1.0	biflagellate
a02	cocccoid	1.5	uniflagellate
a28	cocccoid	1.5	biflagellate
a29	cocccoid	2.2	biflagellate
a53	cocccoid	2.0	uniflagellate
b06	ellipsoid	2.6,1.9	biflagellate
b12	ellipsoid	5.3,3.55	biflagellate
b22	ellipsoid	8.8,2.2	uniflagellate
b23	frustrum	13.4,2.2	biflagellate
b40	flattened frustrum	10.3,4.8	uniflagellate
d31	cylinder	41.8,7.9	colonial diatom
o02	ellipsoid	4.0,1.5	chlorophyte
r01	cocccoid	<2.0	LRGT
r03	ellipsoid	5.7,5.4	cyst
r20	cocccoid	6.2	chlorophyte
s13	cocccoid	2.0	cyanophyte

The timing of the morphotype maxima are as follows:

Time	Dominant morphotypes
autumn mixing	1984: a29, b12, b22, m2 1985: b6, b23, r1
snowmelt	1985: o2, r3, r20, s13 1986: o2, r1
summer	1984, 1985: a1, a2, a29, a53, o2

Biomass values ranged from 0.01 to 0.63 mg/l, with maxima occurring shortly after autumn turnover and minima occurring during periods of ice-cover (Fig. IV-3). Ultrannoplankton contributed the major biomass proportion on only two dates, as dominance shifted to nanoplankton. Netplankton values remained low, although they contributed 10.8% of the total biomass on one date (Fig. IV-3). Morphotypes b40, d31, r03, and r20 contributed at least 5% each to the total biomass on at least 50% of the sampling dates.

Community dominance as determined by biomass differs from that determined by cell counts. The importance of Dinophyceae and Cryptophyceae (in particular Peridinium and Cryptomonas) and Chrysophytes (in particular Dinobryon and the diatoms) is understated by total cell counts. These two groups dominate biomass for brief periods during winter and mid-summer.

Station to station variability was least on 26 September 1985 (Station A: 1200 cells/ml, Station B: 1400 cells/ml) and greatest on 16 October 1985 (Stations A: 1400 cells/ml, Station B: 4200 cells/ml).

Bag experiment #3, 1985 - There was no significant difference among bags when the experiment was begun. Phytoplankton concentrations ranged from ca. 6000 to 9000 cells/ml, and composition was dominated by morphotypes a28, a53, o02, r01, and r03 (see Fig. IV-4).

After nine days, all treatments (with the exception of PO₄+acid) declined in number to about 2500 cells/ml. Cell concentrations for the PO₄+acid treatment remained near 6000 cells/ml. The morphotype composition shifted in all cases (Fig. IV-4). Dominant morphotypes were as follows:

treatment	dominant morphotype	comments
PO ₄ +acid	a53	
control	r03	no a28, few a53
HNO ₃ +H ₂ SO ₄	b23	
PO ₄	o02,r03	
HCl:high	other	
HCl:low	other	
NO ₃ +SO ₄	o02,r03	no a28, few a53

There was no significant difference between the control and NO₃+SO₄ treatments.

After 23 days, there was a highly significant difference in abundance between treatments adding phosphate and treatments that added no phosphate (Fig. IV-4). Abundances were slightly less than 2000 cells/ml for all non-phosphate treatments. The treatment consisting of phosphate addition alone had a cell concentration of 19,000 cells/ml. The response to acid and phosphate together was a bloom of over 27,000 cells/ml. Morphotype composition shifted between treatments as follows:

treatment	dominant morphotype
PO ₄ +acid	a53
control	r01
H ₂ SO ₄ +HNO ₃	other
PO ₄	r01
HCl:high	r01,other
HCl:low	o02,r01
NO ₃ +SO ₄	other

There was no significant difference in total numbers between the non-phosphate treatments. However, there were significant shifts in dominant morphotype.

Discussion

Variation in cell size is a major feature in describing a plankton community, and spatial and temporal variations of cell size are common (Semina, 1972; Sheldon et al., 1972). Average size is a function of intraspecific variation of cell size and of the number of species present of a given average size. Cell size can be a determinant or prime descriptor of processes such as ingestion (Kalff, 1972), respiration (Nival and Nival, 1976), production (Banse, 1976), and reproduction (Banse and Mosher, 1980), nutrient competition (Eppley et al., 1969), resource availability (Gliciwz, 1980), and predator-prey relationships (Kerr, 1974).

The size distribution of Emerald Lake phytoplankton is typical of a subalpine lake. Keefer and Pennak (1977) studied a lake in Colorado where ultranannoplankton cells dominated the cell counts. Pavoni (1963) has shown that the proportion of nannoplankton tends to be higher in oligotrophic lakes. Nannoplankton contributed more than 50% of the total cells for most of the year in three subalpine lakes studied by Kristiansen (1971). Nannoplankton dominated biomass of these lakes for much shorter periods.

The timing of the biomass peaks is somewhat variable (see below). Maxima tend to occur shortly after ice-out, with minima occurring during mid-summer. However, this is subject to flushing rates, nutrient availability, and a variety of other factors.

Subalpine phytoplankton biomass maxima/minima

Reference	Lake	Biomass maxima	Biomass minima
Hermann 1978	Long	prior to ice-out	July
Kalff 1972	Hertel	Aug-Sept	Mar-Apr
Keefer 1977	Long	ice cover(May)	June
Kristiansen 1971	Tystrup	May	September
Tilzer 1972	Finstertaler	summer	late winter
Tilzer 1972	Esrom	May	September
Tilzer 1972	Bavelse	June	September

Shifts in plankton composition during periods of acidification have been noted by several researchers, including Schindler et al. (1985), Kwiatkowski and Roff (1976), and Johnson et al. (1970). Our results indicate that Emerald Lake responds in a similar manner.

Changes in other phytoplankton parameters are variable. Raddum et al. (1980) surveyed several lakes and observed that species numbers were generally lower in lakes of increased acidity. Yan (1979) also observed decreased number of taxa in lakes undergoing acidification. However, experimental acidification of Lake 223 by Schindler et al. (1985) resulted in little change in either species diversity or species number. Phytoplankton response in Emerald Lake was not clearcut; morphotype numbers (which should parallel changes in species numbers) decreased with acidification unless accompanied by nutrient addition.

There are no strong correlations between acidification and shifts in phytoplankton biomass. Hendry et al. (1976) reviewed data from several lakes and concluded that biomass decreased with lake acidification. Grahn et al. (1974) observed increased oligotrophication with increasing acidification, but noted that shifts in biomass might not occur until a threshold pH was passed (pH 4.4-5.4). The response of Lake 223 phytoplankton (Schindler et al., 1985) contradicts these results, where biomass increased slightly. In Yan et al.'s study (1979), phosphorus was a better predictor of biomass than pH.

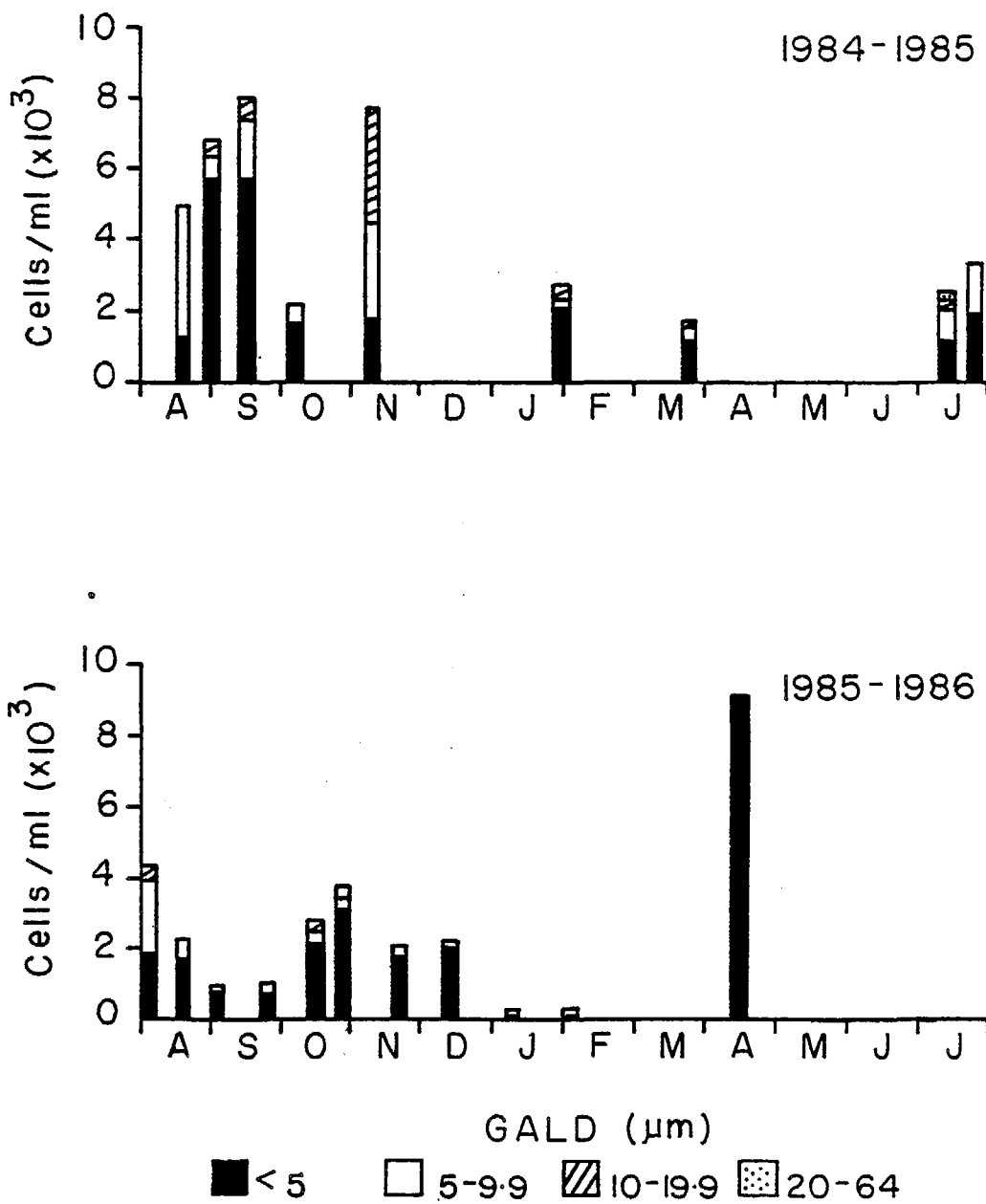


Figure IV-1. Emerald Lake phytoplankton abundances from August 1984 to April 1986 by size class.

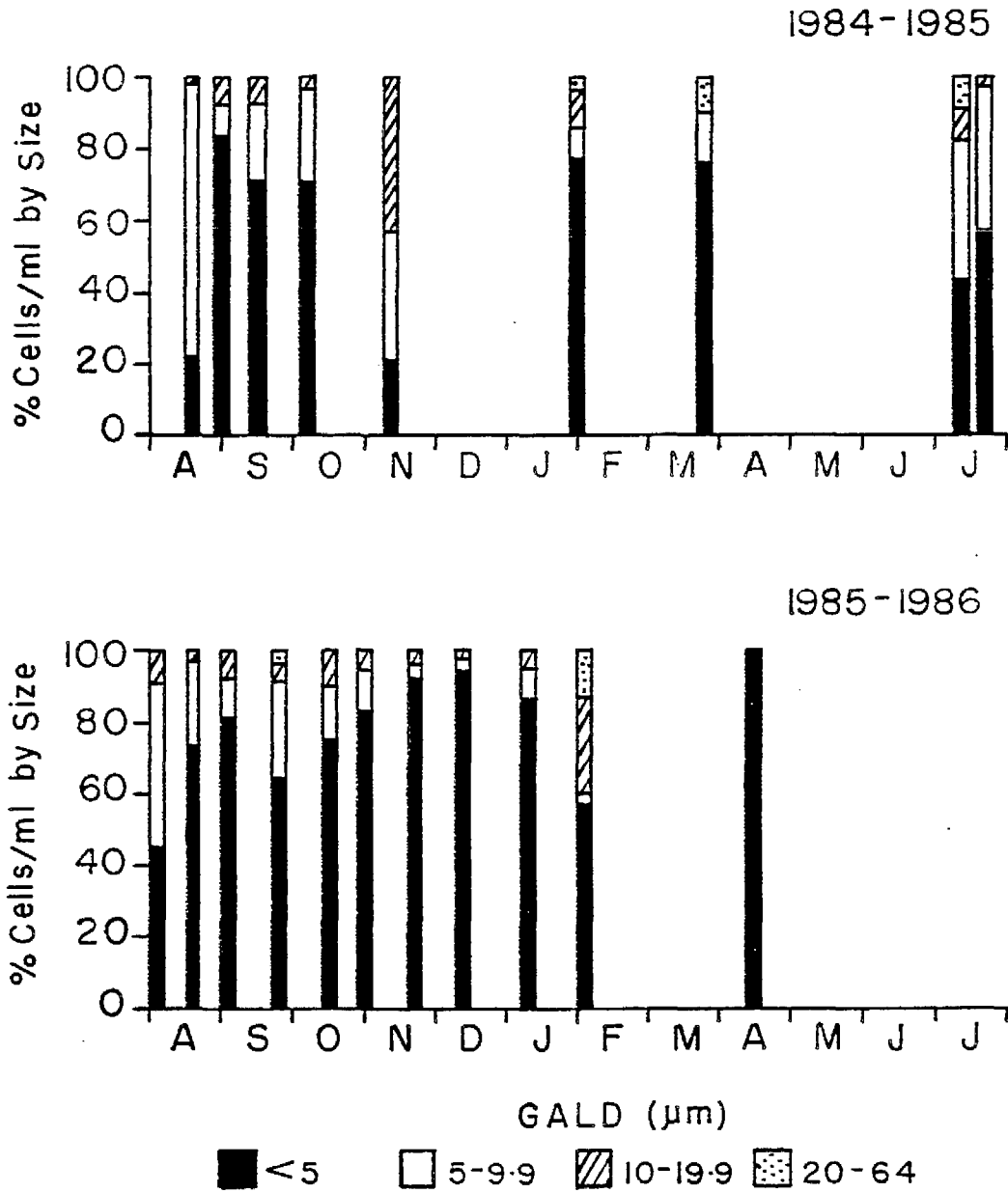


Figure IV-2. Relative abundances of Emerald Lake phytoplankton size classes.

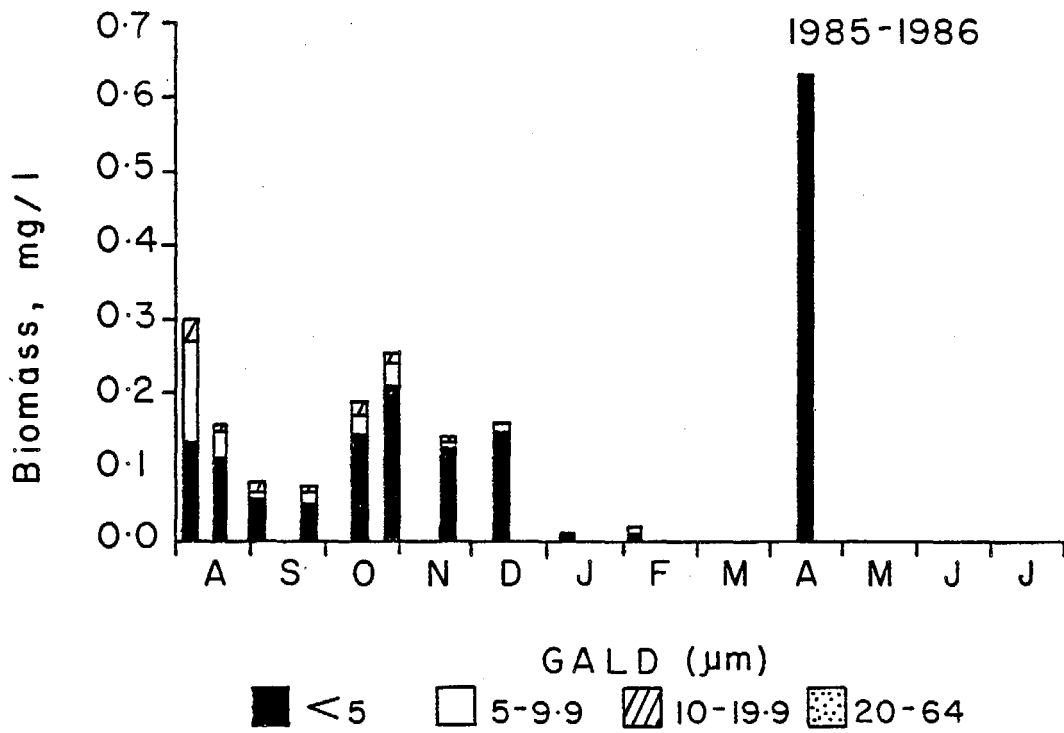
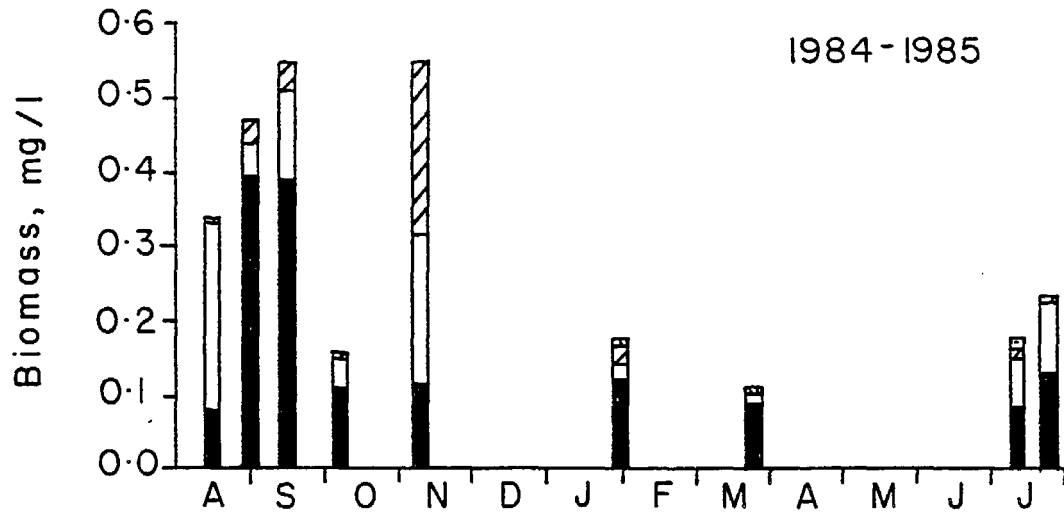


Figure IV-3. Emerald Lake phytoplankton biomass from August 1984 to April 1986 by size class.

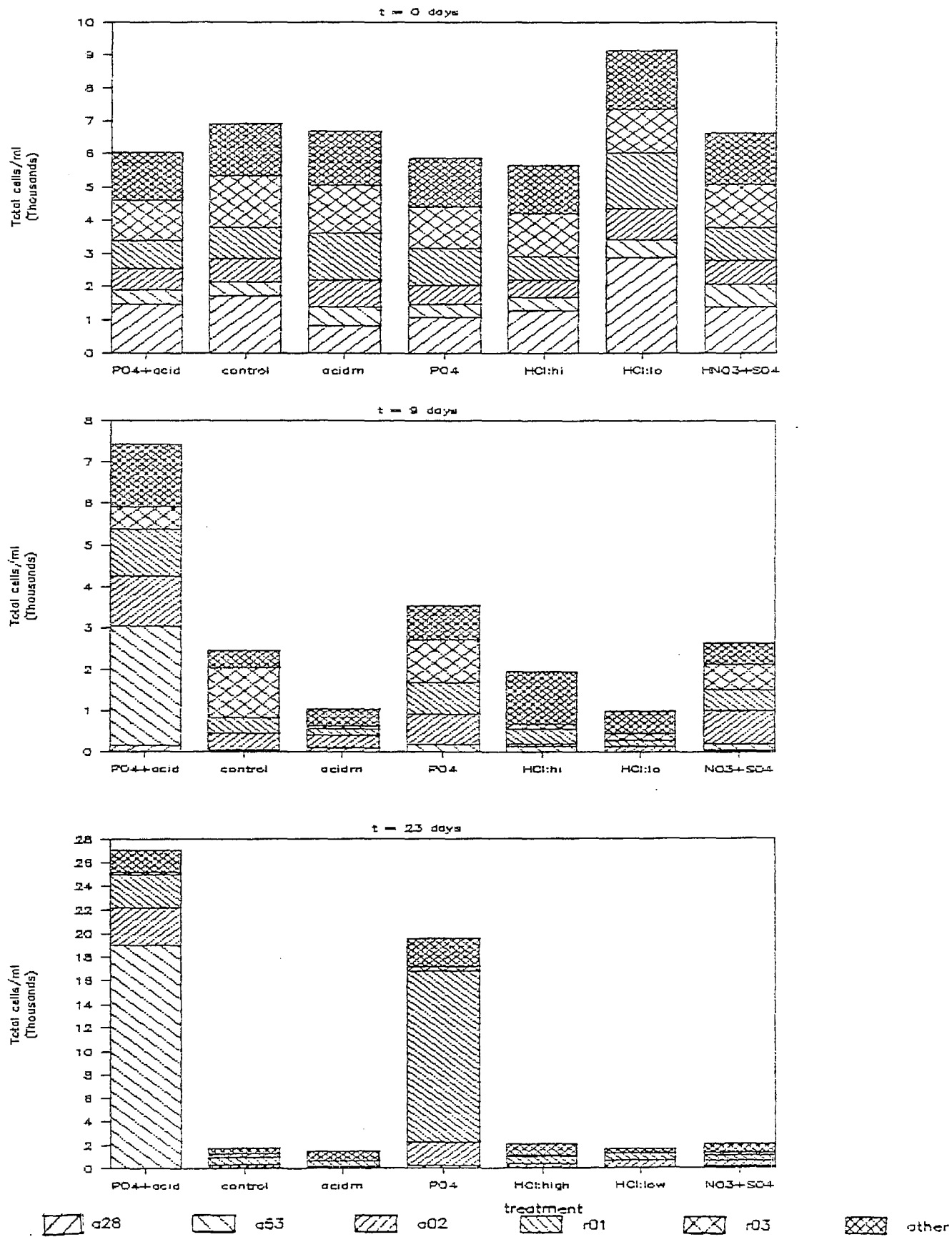


Figure IV-4. Abundances of dominant phytoplankton morphotypes in bags assigned to different treatments (day 0, 9, and 23) in Emerald Lake.

Chapter IV.2

BENTHIC DIATOMS IN EMERALD LAKE AND ASSOCIATED STREAMS

Introduction

Diatoms are especially good indicators of perturbation such as acidic deposition because they are diverse, generally abundant, have a short generation time, and are readily preserved in the sediments. Many species have optimum occurrences at particular pHs or pH ranges (Hustedt, 1939). Artificial acidification experiments indicate that changing algal composition, a decrease in diversity, increase in biomass, and a shift toward acid-tolerant species with loss of alkaline species are among the responses to decreasing pH (Hendrey 1976, Hall et al. 1980 and Muller 1980). Long term algal community monitoring would provide a base from which perturbations could be identified and measured.

Benthic diatom assemblages consist of both living and non-living algae. Diatoms grow, die, and are accumulated on the surfaces upon which they were living or are dispersed and deposited in other aquatic habitats. It is necessary to distinguish between the living and non-living diatoms so that the confounding influence of valves representing past assemblages or other locations in the watershed is averted and those species reflecting extant conditions are identified.

The primary purpose of this study was to determine the benthic diatom species composition by sampling Emerald Lake and associated streams on a bi-monthly basis. Two communities, epilithic (ceramic tiles) and epipsammic and epipellic (sediments) were considered to be the primary contributors to the Emerald Lake sediments. Macroalgal and moss epiphytic communities were not sampled.

In addition to providing useful baseline data, the composition of the diatom flora observed growing on tiles and in sediments in Emerald lake and its inflowing streams can be used to test the accuracy of the pH predictive equations developed in this (Chapter III) and a previous ARB study (Holmes 1986).

Methods

Sampling sites and collection methods

Two substrate types were sampled in Emerald Lake and associated streams for benthic diatoms during the 1985 summer season: stream and lake

sediments, (i.e., soft substrates), and ceramic tiles (i.e., hard substrates). A variety of grain sizes representing a gradient from silt to very coarse sand-sized particles occur among the sediment sampling sites. On each sampling date, four soft substrate samples from each of three locations, (lake, inlets, and outlet), were collected. The needle-end of a 60cc disposable syringe tube was cut off and the tube (2.7 cm inner dia.) served as a coring device. A metal plate was used to seal the mouth of the tube after it was inserted into the sediments. Sediment volumes ranging from 4 to 23 mls were collected, transferred (sediment and overlying water) to individual sample jars and fixed with 1-2 mls of 8% reagent grade gluteraldehyde. Sediment volumes varied with sediment type. Depth to bedrock at thin sediment sites and tangled root systems at other sites determined to some extent the volume collected. Within stream locations, care was taken to choose sampling sites representing a variety of grain sizes, flow regimes, water depths, and light conditions in order that variability within the location be represented. Lake samples were collected from several depths by SCUBA.

Hard substrates, consisting of 6.76 cm² ceramic tiles, were placed in groups of three at four sites in each of the study locations (lake, inlets, and outlet). Prior to placement, the unglazed side of each tile was sanded on a lap wheel using 400 mesh grit to eliminate grout grooves and ensure that the surfaces to be colonized were comparable. The tiles were then attached in groups with velcro to 12 large, approximately flat-surfaced granite rocks collected from the watershed. As with soft substrates, sites for placement were chosen to represent the variety of habitats in each of the three locations. On each collection date, the epilithic diatom population was sampled by removing one tile from each site. Tiles were placed on end into individual 7 dram vials containing ambient water then fixed with 1-2 mls of 8% reagent grade gluteraldehyde. The vial diameter was comparable to the tile dimensions; the inserted tile thus maintained a fixed position for transport with minimum disturbance of the colonized surface.

For all samples, locations and qualitative descriptions of sites were recorded. All collecting dates and sample numbers are summarized in the table below:

	Inlets		Lake		Outlet	
	Soft	Hard	Soft	Hard	Soft	Hard
7/1/85	4	3			4	4
7/11/85			4			
9/8/85			4	4		
9/20/85	4	4			4	6
10/25/85				4		

Site locations are marked on the Emerald Lake map presented in Fig. I-3. Stations 1, 4, 5 and 6 are soft, and stations 2, 3, 7 and 8 are hard.

Sample processing and counting

Each soft substrate sample was settled and the fixative was removed with successive rinses of deionized water. Coarse samples were fractionated before rinsing by repeated swirling and decanting. A measured aliquot of suspended sample was mounted directly on a coverslip using a hot plate to evaporate the deionized water followed by Cumar R-9 mountant (Holmes, Wilson, and Amspoker, 1981). Standard microscope slides were then lowered onto the coverslips. The slides were turned over and heated to drive off the solvents and harden the mountant.

Tile samples were briefly air dried (15 min.), wetted with several drops of reagent grade acetone, and covered with 8 cm² pieces of 0.075 mm (3 mil) acetate film. The acetate film became temporarily viscous, filling interstices in the tile matrix and embedding the surficial material. After one hour, the acetate was peeled off of the tile and dissolved in acetone to release the diatoms. The acetone was removed by successively rinsing with deionized water (three times). Slides were made as described for soft substrate samples above.

Diatom valve counts were made at 1000X using a Zeiss compound microscope with a 100X neofluar oil immersion objective (n.a. 1.30) and Kohler illumination. Random transects 100 microns wide were scanned on each slide. All whole valves encountered were identified to species until at least 500 valves were counted for each sample, except in cases where densities were extremely low. A minimum of two transects were used. The number of traverses for each sample was recorded, and the total area scanned calculated. Broken valves were counted as one valve if more than one half of the valve was present or the central area was intact and identifiable to species. Where fragments were small but recognizable, two fragments with like distal morphology were counted as one valve. Frustules were considered

to have been live at the time of collection if protoplasm was visible within the cells. For small and/or delicate species, phase contrast was used to enhance recognition of frustular contents. Moribund taxa could not be separated from healthy individuals so were considered live as well. One frustule was counted as two valves. Species information and a live or dead determination was recorded for each specimen. Many species were documented by photomicrography. Those taxa for which references could not be located or do not exist were assigned numbers as described by Holmes (1986).

Precautions were taken to ensure that species identifications were as accurate and consistent as possible. As taxa were encountered, a card file was compiled with species names, photomicrographs, and brief descriptions of the Emerald Lake and stream diatoms. This file was constantly compared to the Sierra Nevada species file being established concurrently by R. W. Holmes and M. C. Whiting. Published taxonomic references were used and cooperation with PIRLA (Paleolimnological Investigation of Recent Lake Acidification) taxonomists was maintained.

In addition, species/area curves were plotted for the first several slides to determine the number of valves necessary to adequately represent rare species. The cumulative number of valves counted was plotted against the number of species encountered. A slope of zero occurred between 350 and 500 valves. Thus, at least 500 valves were counted in subsequent samples.

Live community densities, relative species abundances, live to dead ratios, Lorenz values, and pH predictions were calculated for each sample from the species counts as follows:

$$A) \text{ Soft substrate live diatom density: } \frac{\text{valves/ml}}{\text{NL} \times \text{CA} \times \text{VV} \times \text{SV}} \\ \text{TC} \times \text{AT} \times \text{SS1} \times \text{SS2} \times 5.67$$

$$B) \text{ Hard substrate live diatom density: } \frac{\text{valves/cm}^2}{\text{NL} \times \text{CA} \times \text{VV}} \\ \text{NT} \times \text{AT} \times \text{TA} \times \text{SS2}$$

Where: NL = total number live (valves)
 CA = area of coverslip (mm²)
 VV = vial volume (mls)
 SV = total sediment volume (mls)
 NT = number of transects counted
 AT = area of one transect (mm²)
 TA = tile area (cm²)

SS1 = subsample 1 (mls)
SS2 = subsample 2 (mls)
5.67 = volume equivalent for 1 cm depth (mls)

C) Species relative abundance: % of total represented by species n1 =
$$\frac{\text{total live (species n1)} \times 100}{\text{total live}}$$

D) Live to dead ratio:
$$\frac{\text{total live density}}{\text{total dead density}}$$

E) Lorenz values:

For each sample, species were ranked in descending order by their relative abundances. Lorenz curves were graphed by plotting the cumulative number of individuals on the abscissa against the cumulative number of species on the ordinate (Tailee, 1979). The Lorenz curve is the polygonal path joining the data points. The area under the curve describes the distribution of individuals among species (evenness). An iterative area calculation was performed for each sample. All species occurring with a relative abundance >1% were used in the calculation. Areas were multiplied by 2 to establish an index ranging from 0 to 1 (1 = perfect evenness).

F) pH predictions:

Diatom species were assigned pH classifications as determined by the ARB Lake Survey species distribution (Holmes, 1986) and the literature (for thirteen species abundant in Emerald Lake but not well represented in the lake survey). For each sample or combination of samples, relative abundances were summed over pH categories (acb = acidobiont, acp = acidophil, ind = indifferent, alp = alkaliphil, and alb = alkalibiont).

Regression equations, developed by R. W. Holmes (Chapter III) were applied to both the living species and the total species (living plus dead) in the following combinations:

- 1) each sample individually
- 2) samples summed over location (inlets, lake, outlet)
- 3) samples summed over substrate type (hard or soft) by location

Regression equations were as follows:

(1) $\text{pH} = 7.12 - 0.39 \log (\text{index B})$
 $r^2 = 0.81$ (Equation 5 (Chapter III))

$$(2) \text{ pH} = 6.41 - 0.031 (\% \text{ acb}) + 0.0014(\% \text{ acp}) + 0.010(\% \text{ ind}) + \\ 0.021(\% \text{ alp}) + 0.13(\% \text{ alb}) \\ r^2 = 0.83 \quad (\text{Equation 6A (Chapter III)})$$

Results

Fifty six of 101 taxa observed (Appendices III-A and B) in the inlet streams were alive (54% on both substrate types, 34% on soft only, and 12% on hard only), and 60 of 123 species in Emerald Lake were found alive (37% on both soft and hard, 28% on soft only and 35% on hard only). Sixty two of 98 taxa found in the outlet stream were living (55% occurring on both tiles and in sediments, 31% in sediments only, and 14% on tiles only).

Figure IV-5 shows the average number of live species per sample for each location by substrate and month. Vertical lines represent ranges. The number of live diatom taxa increased between July and September in the soft substrate of the inlet streams while the number of species living on tiles decreased. Both soft and hard substrate species increased in the outlet stream over the same period of time. Live species in lake sediments decreased between July and September/October.

Table IV-1 lists living diatom taxa observed on tiles and in sediments in Emerald Lake and associated streams. Appendix III-B provides a complete list (living as well as dead) of species (taxonomic codes) by location. A key to the numerical taxonomic codes is provided in Appendix III-A.

Relative species abundances (live assemblages) are summarized in pie diagrams (Fig. IV-6) by substrate, location and month. Twelve species occur in all locations and on both substrate types: Achnanthes austriaca v. helvetica, A. levanderi, A. marginulata, A. serians v. brachysira, Eunotia 2 SN, Gomphonema 3 SN, Melosira 1 PIRLA, M. 3 SN, Navicula tenuicephala, Nitzschia frustulum v. 3 SN, N. 5 SN, Tabellaria flocculosa strain IV.

Of these, three species were never found in high concentrations. Nitzschia 5 SN does not reach a relative abundance >1.5%. Navicula tenuicephala peaks at 1.9% in September lake sediments, and Nitzschia frustulum v. 3 SN is most abundant in the outlet stream (ca. 2% on both substrate types, July and September).

Three of the remaining ubiquitous species are abundant on tiles or in sediments for particular sample dates but are generally present in low numbers. Melosira 3 SN is fairly abundant in lake sediments throughout the

season (5.0 - 7.4%). Anomoeoneis serians v. brachysira represents 9.5% of the September tile assemblage in Emerald Lake, increasing to 13.7% in October. 34% of the individuals from inlet tiles in September were Gomphonema 3 SN, while lake tiles had 11.2% during the same period, increasing to 17.3% in October.

The genus Achnanthes is an important component of the diatom community on nearly all sampling dates, representing 23 - 67% of all specimens, except in lake sediments (1.6 - 4.9%). Achnanthes austriaca v. helvetica, A. levanderi, and A. marginulata were found on both substrates and all sampling dates in varying numbers (refer to figs. IV-6a - IV-6l). Achnanthes 42 SN dominated inlet tiles in September (34.5%) and increased from 2.9% to 11.1% through the season on lake tiles.

Eunotia 2 SN, a ubiquitous taxon, was very abundant on outlet tiles in July (15%) and in outlet sediments in September (7%), but was rare in all other samples. Eunotia is a common stream genus, especially in July where the sum of Eunotia individuals in the inlet streams was 31.1% in sediments and 29.6% on tiles. The majority of these individuals were represented by Eunotia tenella which was the most abundant tile acidobiont in July (up to 22.1% in any one sample) and decreased in September to a maximum of 3.2%. Eunotia tenella was also abundant in July sediments (up to 56.4% of the diatom flora), and decreased in September to a maximum of 8.5%. Eunotia species are rare in Emerald Lake, with only 7 out of 18 species present and all <<1.5% abundance.

Tabellaria flocculosa strain IV, while present in sediment from all locations, is exceptionally well developed on tiles. On lake tiles, it increases from a low of 5.3% in September to dominate at 22.5% in October and increases from 8.8% on outlet tiles in July to 42.8% in September. T. flocculosa strain IV is fairly abundant in outlet sediments, 5.1% in September, but is not common in inlet or lake sediments. There is some taxonomic difficulty with this species which will be resolved in the next few months.

Melosira 1 PIRLA is the most common taxon, ranking among the 11 most abundant species for both substrate types, on all sampling dates, and at all locations (with one exception: none were found on outlet tiles in July). M. 1 PIRLA was the predominant species in the inlet and lake sediments for the entire 1985 season, representing from 26.3 - 52.8% of the assemblage

(refer to figs. IV-6b, -6d, -6f, -6h). July sediment samples from the outlet show 6.6% M. 1 PIRLA, increasing to 15.3% (the dominant) in September. Outlet tiles showed an increase from 0% in July to 10.2% in September. Relative abundances on inlet and lake tiles decreased over the same period. M. 1 PIRLA is also the most common taxon at every interval in the Emerald Lake core (mid-2), relative abundance ranges from 13.8 to 37.5%. M. 1 PIRLA has not been found in the literature and is believed to be a new species. The following living species were unique to the inlet streams: Caloneis bacillum, Eunotia curvata v. 1 SN, Frustulia rhomboides v. crassinervia, Melosira lirata, Navicula 22 SN, Neidium 1 SN, Pinnularia divergens, P. cf pseudomicrostauron.

All of these except Caloneis bacillum and Neidium 1 SN were found in the lake core analysed by R. W. Holmes. Valves of all but C. bacillum, E. curvata v. 1 SN, and P. cf. pseudomicrostauron were found in Emerald Lake.

Species occurring alive in the lake only: Achnanthes detha*, A. 10 SN, Cymbella minuta*, Eunotia curvata subarcuata, Frustulia rhomboides*, Gomphonema 16 SN, Navicula tridentula, N. 16 SN*, Nitzschia dissipata f. undulata, Pinnularia abaujensis.

All but G. 16 SN were found in the lake core. Valves of the four species with asterisks (*) were found in the inlet streams as well.

The following species only occur alive in the outlet stream: Achnanthes austriaca, A. bioreti, Cymbella cesatii, C. hebridica, C. hebridica v. 1 NE, Eunotia denticulata, E. incisa v. 2 PIRLA, E. 4 SN, E. 19 SN, Navicula radiosa, Nitzschia 15 SN, Pinnularia 45 SN, Stauroneis 2 SN.

Of these, only valves of E. incisa v. 2 PIRLA, E. 4 SN and E. 19 SN were never found in the lake samples or the core.

Twenty eight species occur alive only in soft substrates (see Appendix III-B). Of these, only Navicula 22 SN and Pinnularia cf. braunii v. amphicephala f. subconica occur in more than one sample or greater than 3.5% relative abundance.

Sixteen species were found alive only on tiles (Appendix III-B). Gomphonema 16 SN was present on 6 out of 8 lake tiles. Relative abundance ranged from 0.5 to 4.8%. Diatoma anceps occurred on all the July tiles with relative abundances from 0.8 to 24.4%. All other species were rare.

Ten species found in the the uppermost interval (0.5 cm) of one or more of the Emerald Lake cores also occurred alive in streams (inlets or inlets and outlet), but were not found alive in the lake. A lake bloom may not have been detected with bimonthly sampling. These species and their pH preference classifications are: Cymbella 9 SN* (acp), C. gaeumanii* (acp), Diatoma anceps*, Eunotia curvata* (acp), E. exigua* (acb), E. pectinalis v. minor* (acp), Frustulia rhomboides v. crassinervia (acp), F. rhomboides v. saxonica* (acp), Melosira lirata (cn), Pinnularia 15 SN*.

Asterisks (*) indicate presence (alive) in the inlet and outlet streams. Of the ten species, Diatoma anceps, Melosira lirata (circumneutral) and Pinnularia 15 SN were not included in pH predictive calculations (they are unclassified or circumneutral) and thus would not effect pH inferences. All but Cymbella gaeumanii and Cymbella 9 SN were recorded as single valve occurrences in core counts and were rare (with the exception of Frustulia rhomboides v. saxonica) in my inlet samples. Cymbella 9 SN was found in the upper interval of all three replicate lake cores but was more abundant in cores left-1 and right than in the mid-2 core. Cymbella 9 SN was common and occasionally abundant (6.3%) in live inlet assemblages from both substrate types and was abundant in total inlet assemblages but was rare in total lake assemblages. Cores left-1 and right were taken from locations closer to the inflows than was core mid-2, suggesting that locations nearer the inflows may tend to concentrate inflow flora. In contrast, Cymbella gaeumanii was most abundant in total lake assemblages and was rare (although found alive) in the inlet streams. Cymbella gaeumanii was more evenly represented in the three lake cores, suggesting that inlet taxa may be fairly well mixed in the Emerald Lake sediments. Neither Cymbella 9 SN nor Cymbella gaeumanii were abundant enough to skew pH inferences.

Lorenz values (Tailee, 1979), describing the distribution of individuals among different species, were calculated for each sample. Values are scaled between 0 (for a single species occurrence), and 1.0 (for a perfectly even species distribution). The range of Lorenz values for the outlet samples was 0.15 - 0.56 (n=18). Soft substrate samples maintained nearly the same average value throughout the sampling season (avg. 0.49 and 0.48) while tiles became more uneven from July (0.50) to September (0.33). Inlet sample values ranged from 0.19 - 0.51 (n=15). Sediment assemblages were more uneven in July (avg. 0.39) than they were in September (avg. 0.47), and tiles species

became more uneven over the same period (avg. 0.45 - 0.29). Lake samples varied from 0.22 - 0.61 (n=16). Soft substrate samples maintained nearly the same degree of evenness (avg. 0.43 and 0.44), while tile assemblages became slightly more uneven from September to October (avg. 0.38 - 0.34).

Lorenz curves for four samples representing the range of Lorenz values for the season over all substrates and locations are shown in Figures IV-7a - IV-7d.

These diatom abundance data have also been employed to estimate the pH of the inlet streams and Emerald Lake using the pH predictive equations developed by R. W. Holmes (see Methods section and Chapter III in the present report).

Lake pH inferences:

Measured lake pH (air equilibrated), varied from 5.9 to 6.5 during the combined incubation and sampling period (6/85 - 11/85), with a mean pH of 6.3. The predicted mean pHs for Emerald Lake using both the living and the total sediment diatom assemblages fall within this range (Table IV-2). Lake tile assemblages yield somewhat higher mean pH estimates than lake sediments, exceeding the measured pH values by 0.1 pH unit. The predicted mean pHs for sediments and tiles together are 6.5, except for the log index B live assemblage prediction, which exceeds measured values by 0.1 pH unit.

Tile assemblages predict more variable pH values, with a higher mean pH, than do sediment assemblages. This is due primarily to much higher proportions of indifferent taxa on tiles:

	range	mean
live,tiles	2.5-51.4%	17.3%
total,tiles	2.2-28.1%	13.6%
live,sed.	0.0-02.2%	1.3%
total,sed.	2.1-04.9%	3.4%

and higher proportions of acidobionts in the sediments:

	range	mean
live,tiles	0.0-1.1%	0.5%
total,tiles	0.0-2.7%	1.0%
live,sed.	0.0-6.0%	2.0%
total,sed.	1.3-8.6%	4.3%

The percentages of acidophilous individuals were higher in sediment assemblages as well.

Tabellaria flocculosa strain IV, an indifferent taxon, comprises 0.0-47.6% of each lake tile sample (live assemblages), almost all of the indifferent class contribution. Best development is at or below 5 meters depth (1.7-47.6%). Other taxa contributing to the lake tile indifferent class are (in order of relative abundance) Fragilaria vaucheriae, Nitzschia 6 SN, Cymbella minuta v. silesiaca, and C. minuta.

Seasonal and depth effects are apparent from lake tile assemblages. T. flocculosa IV is much more abundant (at comparable depths ≥ 5 m) in October than it is a month earlier. In general, acidophilic taxa Achnanthes levanderi and A. 10 SN (both at 5 m and shallower) and Gomphonema puigiarianum v. aqueatorialis are much more abundant in September. Accordingly, pH inferences are slightly lower for September than October (0.2 pH unit for MLR, 0.3 for log index B). Seasonality is much more apparent on tiles than in sediments, where only the minor species exhibit a seasonal shift (refer to Figs. IV-6e, -6f, -6g, -6h).

Mean pH predictions for live assemblages and total assemblages are similar for lake tiles (both MLR and log index B).

In general, acidophils are more abundant in shallow lake water (5 m. or less). Achnanthes levanderi, A. 10 SN, and Anomoeoneis seriens v. brachysira on tiles, and many taxa which occur at low relative abundances in the lake sediments.

Inlet Stream inferences:

Measured pH (air equilibrated) for the inlet streams varied from 6.1 to 6.5, with an average pH of 6.3. The predicted mean pHs using the living and total sediment assemblages are within the measured range except for the MLR prediction for live sediment assemblages, which is 0.1 of a pH unit below the lower limit of the measured range (see Table IV-3). The mean tile predictions fall within the measured range, but the predicted pHs for individual samples are more variable than measured values. The predicted values for sediment and tile assemblages together are similar to measured values.

The wide range of inlet tile predictions (using both live and total assemblages) reflects a seasonal shift from high proportions of acidophils

(primarily Achnanthes marginulata, A. austriaca v. helvetica, Eunotia 12 SN and E. 15 SN) and acidobionts (almost exclusively E. tenella) and low proportions of indifferent taxa in July to low proportions of acidophilous and acidobiontic taxa and abundant indifferents (Fragilaria vaucheriae) in September. July samples predict lower pHs than do September samples:

	range index B	range MLR
July live,inlets	5.9-6.3	5.8-6.3
Sept live,inlets	6.5-6.9	6.4-6.7
July total,inlets	6.0-6.3	6.0-6.4
Sept total,inlets	6.4-6.8	6.3-6.6

This is the trend in measured pH values as well, although the prediction equations exaggerate the variation. Inferred pH ranges are narrower for inlet tile total assemblages because the effect of seasonality is mitigated by the accumulation of taxa throughout the sampling period.

Inlet sediments have the highest proportion of acidobiontic taxa (22.06-58.2% for live assemblages, almost entirely E. tenella). The sediments reflect the same seasonal shift from high acidobionts and low indifferents in July to low acidobionts and high indifferents (F. vaucheriae again) in September. The percentage of acidophils in the inlet sediments remains fairly constant throughout the season. The total assemblage for the inlet sediments is quite similar to the living assemblage in this regard.

Inlet tiles consistently predict a lower pH than do lake tiles by one to three tenths of a pH unit because they have a higher proportion of acidobiontic taxa:

	range	mean
live,inlet	0.0-22.8%	7.5%
total,inlet	0.4-17.6%	7.7%
live,lake	0.0-0.9%	0.5%
total,lake	0.0-2.7%	1.0%

and fewer indifferent taxa:

	range	mean
live,inlet	0.5-39.3%	9.6%
total,inlet	0.4-31.2%	10.3%
live,lake	2.5-51.6%	17.3%
total,lake	2.2-28.1%	13.6%

Discussion

According to Hustedt's (1939) definition, acidophilic species should exhibit their widest distribution at pH less than 7.0. The average air-equilibrated pH during the study period was 6.3. As expected, then, all benthic habitats surveyed in Emerald Lake and associated streams support a predominantly acidophilic diatom flora. A total of 56 acidophilic taxa, 5 acidobiontic, 8 indifferent, 1 alkaliphilous, 0 alkalibiontic, 3 circumneutral, and 22 unclassified taxa were collected and identified.

Stream sediments have the richest flora (average number of species), followed by tiles from all locations and lake sediments. Acidophilic taxa account for 22-23 species on tiles and 28-35 species in sediments and represent from 28.5-53.5% of the diatom flora on all substrates in all locations. Total acidobiont abundances are low in all habitats (0.5-7.5% for tiles, and 2.0-16.2% for sediments, mean values). No living alkaliphilous or alkalibiontic taxa were found during the sampling period with the exception of Navicula 27 SN which occurred at 1% relative abundance in one inlet sediment sample. Indifferent taxa are most abundant (36.7% mean) on outlet tiles and lake tiles (17.3%), and are uncommon in lake sediments. Tabellaria flocculosa IV was the most significant contributor to lake indifferents.

A decrease in pH may result in an increase in the number or abundance of acidobiontic species. However, an acidic Ontario lake (pH < 4.6) studied by Dixit and Evans (1986) had a similar floristic composition: primarily acidophilic taxa with five acidobiontic taxa which were never very abundant.

The sediment and tile assemblages are very heterogeneous. The habitats studied were sampled with insufficient frequency to clearly separate spatial from temporal variability, but some observations are notable. Seasonal interpretations are based on samples collected from the same sites. Patterns emerge for a few individual taxa and pH preference groups. They are discussed below in the context of Emerald Lake and inlet stream pH inferences.

The pH predictive equations make use of the relative proportions of the various pH preference groups occurring in diatom assemblages. Acidobionts are very heavily weighted in both the log index B and MLR equations. Acidophilic and acidobiontic taxa shift inferences toward low pHs, while indifferent taxa shift the pH predictions towards neutrality.

Lake sediment samples predicted mean pH values that differed from the measured mean pH (air-equilibrated) by no more than 0.2 pH units. Tile assemblages consistently predicted higher mean pH values (0.3 pH unit higher than the mean) due to the abundance of Tabellaria flocculosa IV on tiles (an indifferent) and higher frequencies of acidophils and acidobionts in sediment samples. The seasonal and depth distribution of Tabellaria flocculosa IV and the acidophilic preference groups on lake tiles affected the range of values predicted.

Mean pH predictions for live assemblages and total assemblages were similar for lake tiles. This may be because valves are retained on the tiles upon which the diatoms were living over the sampling period and are only minimally diluted by mixing and the sedimentation of inwashed valves. Sediments are more likely to incorporate taxa from many habitats (hard and soft substrates, from other lake locations and inlet streams). Unlike tiles, soft substrate samples incorporate several years of sediment accumulation (based on the sediment depth collected and the calculated sedimentation rate), and therefore represent diatom assemblages spanning more than one season.

Total assemblage sediment pH predictions might be expected to fall somewhere between inferences from live sediment and tile assemblages because the lake sediments incorporate remains from all habitats. However, since soft substrates represent the majority of the benthic surface area in Emerald Lake, hard substrates would contribute less material to the sediments. This is reflected in the low percentage of indifferent taxa in the total sediment assemblages and the lower pHs inferred by total sediment assemblages. Lake total sediment assemblage inferences would be less variable except for the occurrence of two Achnanthes 21 SN valves (an alkalibiontic taxon) in one sample. This sample represents the upper limit of the range of pHs predicted by both equations. If these two valves are excluded, the ranges are commensurate with the live assemblage ranges (6.2 - 6.4 in both cases). This would bring the mean values down to 6.3 - 6.4 for both equations, the measured lake mean.

Inlet stream predictions based on combined tile and sediment assemblages (live and total) vary by 0.1 pH unit from the measured (air-equilibrated) mean inlet pH. Inlet predictions tend to be lower than lake predictions because of the high abundance of Eunotia tenella (an acidobiont) in inlet

sediments and the generally lower occurrence of indifferent taxa (almost no Tabellaria flocculosa IV and very few Fragilaria vaucheriae) for both substrate types. The same shift from higher acidophilic and acidobiontic abundances with a low proportion of indifferents early in the season to the opposite conditions the next month is evident in the inlet streams.

The total assemblages for the inlet sediments are quite similar to the living assemblages. This is probably because the inlet does not incorporate valves over time to the extent that the lake sediments do. Valves are likely to be exported continually, especially during spates. Thus valves encountered in inlets are probably fairly recent.

For the inlet streams, the inferred pHs using the total sediment assemblages fall between the predictions for the live sediment and tile assemblages, tending toward the higher pHs predicted by the live tile assemblages. Unlike the lake, the majority of the inlet stream surface area is represented by hard substrate. Taxa from hard substrates would therefore contribute considerably to the inlet sediment assemblages and have a more significant effect on inlet pH predictions.

The lake sediment pH predictions (means, both living and total assemblages) compare favorably with the uppermost core interval inference calculated by Holmes (Chapter III). Multiple linear regression predicts the same pH in all cases (6.4) and log index B varies by no more than 0.2 pH units (core: 6.3, live sediment assemblages: 6.2, and total sediment assemblages: 6.5).

TABLE IV-1 List of living diatom species collected from Emerald Lake and associated streams between July and October 1985 and their pH preference categories. Asterisks (*) indicate presence on hard (H) or soft (S) substrate by location.

Taxon No.	pH Cat.	Taxon Name	Lake		Inlet		Outlet		
			H	S	H	S	H	S	
2002	ACP	<i>Achnanthes austriaca</i> Hust. v. <i>austriaca</i>						*	*
2003	ACP	<i>Achnanthes austriaca</i> v. <i>helvetica</i> Hust.	*	*	*	*	*	*	
2049	ACP	<i>Achnanthes bioreti</i> Germain v. <i>bioreti</i>						*	
2042	ACP	<i>Achnanthes detha</i> Hohn & Hellerm. v. <i>detha</i>	*						
2022	ACP	<i>Achnanthes levanderi</i> Hust. v. <i>levanderi</i>	*	*	*	*	*	*	
2028	ACP	<i>Achnanthes marginulata</i> Grun. v. <i>marginulata</i>	*	*	*	*	*	*	
99015	ACP	<i>Achnanthes</i> 10 SN	*	*					
99371		<i>Achnanthes</i> 42 SN	*		*	*			
2889		<i>Achnanthes</i> spp	*	*	*	*	*	*	
8005	ACP	<i>Anomoeoneis serians</i> v. <i>brachysira</i> (Breb. <u>ex</u> Kutz.) Hust.	*	*	*	*	*	*	
12001	IND	<i>Caloneis bacillum</i> (Grun.) Cl. v. <i>bacillum</i>				*			
23004	ACP	<i>Cymbella cesatii</i> (Rabh.) Grun. <u>ex</u> A.S. v. <i>cesatii</i>						*	*
99060	ACP	<i>Cymbella falaisensis</i> (Grun.) Kramer & Lange-Bertalot v. <i>falaisensis</i>			*	*	*	*	
23007	ACP	<i>Cymbella gaeumannii</i> Meist. v. <i>gaeumannii</i>				*		*	
23008	ACP	<i>Cymbella hebridica</i> Grun. <u>ex</u> Cl. v. <i>hebridica</i>						*	*
99046		<i>Cymbella hebridica</i> 1-NE						*	
23009	ACP	<i>Cymbella lunata</i> W. Sm. v. <i>lunata</i>	*	*		*	*	*	
23012	IND	<i>Cymbella minuta</i> Hilse <u>ex</u> Rabh. v. <i>minuta</i>	*						
23015	IND	<i>Cymbella minuta</i> v. <i>silesiaca</i> (Bleisch <u>ex</u> Rabh.) Reim.	*					*	
99057		<i>Cymbella</i> 6 SN	*					*	*
23889		<i>Cymbella</i> spp		*		*	*	*	
27001		<i>Diatoma anceps</i> (Ehr.) Kirchn. v. <i>anceps</i>				*		*	
27002		<i>Diatoma hiemale</i> v. <i>mesodon</i> (Ehr.) Grun.	*	*	*	*			
99365	ACP	<i>Eunotia alpina</i> (Naeg.) Hust. v. <i>alpina</i>	*						
33008	ACP	<i>Eunotia curvata</i> (Kutz.) Langerst. v. <i>curvata</i>				*		*	*
33010	ACP	<i>Eunotia curvata</i> v. <i>subarcuata</i> (Naeg.) Woodhead & Tweed	*						
99071	ACP	<i>Eunotia curvata</i> 1 SN (indentata)					*		
33011	ACP	<i>Eunotia denticulata</i> (Breb.) Rabh. v. <i>denticulata</i>							*
33015	ACP	<i>Eunotia exigua</i> (Breb. <u>ex</u> Kutz.) Rabh. v. <i>exigua</i>				*	*	*	*
33081	ACP	<i>Eunotia incisa</i> v. 2 PIRLA							*
33031	ACP	<i>Eunotia meisteri</i> Hust. v. <i>meisteri</i>					*	*	*
33040	ACP	<i>Eunotia pectinalis</i> v. <i>minor</i> (Kutz.) Rabh.					*		*
33060	ACP	<i>Eunotia tenella</i> (Grun.) A. Cl. Eu. v. <i>tenella</i>	*		*	*	*	*	*
33066	ACP	<i>Eunotia vanheurckii</i> v. <i>intermedia</i> (Krasske <u>ex</u> Hust.) Patr.				*	*	*	*
33991	ACP	<i>Eunotia</i> 2 PIRLA	*					*	
99075	ACP	<i>Eunotia</i> 2 SN	*	*	*	*	*	*	*
99076	ACP	<i>Eunotia</i> 4 SN							*
99082	ACP	<i>Eunotia</i> 12 SN	*		*	*		*	
99085	ACP	<i>Eunotia</i> 15 SN		*	*	*	*	*	*
99393	ACP	<i>Eunotia</i> 19 SN							*
33889	ACP	<i>Eunotia</i> spp		*	*	*	*		

Taxon No.	pH Cat.	Taxon Name	Lake		Inlet		Outlet	
			H	S	H	S	H	S
34030	IND	<i>Fragilaria vaucheriae</i> (Kutz.) Lange-Bertelot v. <i>vaucheriae</i>	*		*	*	*	*
35001	ACP	<i>Frustulia rhomboides</i> (Ehr.) de T. v. <i>rhomboides</i>		*				
35004		<i>Frustulia rhomboides</i> v. <i>crassinervia</i> (Breb. ex W. Sm.) Ross					*	
35005	ACP	<i>Frustulia rhomboides</i> v. <i>saxonica</i> (Rabh.) De T.			*	*	*	*
35889		<i>Frustulia</i> spp						*
99105	ACP	<i>Gomphonema puiggarianum</i> v. <i>aequatorialis</i> (Cl.) Camburn	*	*		*		
99109		<i>Gomphonema</i> 3 SN	*	*	*	*	*	*
99359		<i>Gomphonema</i> 15 SN	*					*
99388		<i>Gomphonema</i> 16 SN	*					
44014	CN	<i>Melosira lirata</i> (Ehr.) Kutz. v. <i>lirata</i>			*			
44027		<i>Melosira</i> 1 PIRLA	*	*	*	*	*	*
99126	ACP	<i>Melosira</i> 1 SN		*				*
99128	CN	<i>Melosira</i> 3 SN	*	*	*	*	*	*
45001	ACP	<i>Meridian circulare</i> (Grev.) Ag. v. <i>circulare</i>		*	*	*		
46095	ACP	<i>Navicula heimansii</i> van Dam & Kooijman v. <i>heimansii</i> PIRLA	*	*	*		*	*
46038	ACP	<i>Navicula mediocris</i> Krasske v. <i>mediocris</i>		*	*	*		*
46056	CN	<i>Navicula radiosa</i> Kutz. v. <i>radiosa</i>						*
46057		<i>Navicula radiosa</i> v. <i>parva</i> Wallace	*	*	*		*	*
46082	ACP	<i>Navicula tenuicephala</i> Hust. v. <i>tenuicephala</i>	*	*	*	*	*	*
46084		<i>Navicula tridentula</i> Krasske var. <i>tridentula</i>	*					
99148	ACP	<i>Navicula</i> 13 SN	*		*	*	*	*
99150	ACP	<i>Navicula</i> 16 SN	*					
99153		<i>Navicula</i> 22 SN				*		
46123	ACP	<i>Navicula</i> 23 PIRLA		*		*		
99157	ALP	<i>Navicula</i> 27 SN				*		
99176	ACP	<i>Navicula</i> 47 SN			*	*		
46889		<i>Navicula</i> spp			*			*
47001	ACP	<i>Neidium affine</i> (Ehr.) Pfitz. v. <i>affine</i>		*		*		*
47007	ACP	<i>Neidium bisulcatum</i> (Lagerst.) Cl. v. <i>bisulcatum</i>		*	*	*		*
47014		<i>Neidium iridis</i> (Ehr.) Cl. v. <i>iridis</i>	*					
99218		<i>Neidium</i> 1 SN				*		
47025	ACP	<i>Neidium</i> 2 PIRLA		*	*	*		*
99228	ACP	<i>Nitzschia dissipata</i> f. <i>undulata</i> Sov.	*					
99231	IND	<i>Nitzschia frustulum</i> 3 SN	*	*	*	*	*	*
99240	IND	<i>Nitzschia</i> 5 SN	*	*	*	*	*	*
99241	IND	<i>Nitzschia</i> 6 SN	*		*			*
99244	ACP	<i>Nitzschia</i> 9 SN		*	*	*		*
99250		<i>Nitzschia</i> 15 SN						*
48889		<i>Nitzschia</i> spp			*			
52001		<i>Pinnularia abaujensis</i> (Pant.) Ross v. <i>abaujensis</i>		*				
52011		<i>Pinnularia biceps</i> Greg. v. <i>biceps</i>		*	*		*	
52074		<i>Pinnularia biceps</i> v. 1 PIRLA	*	*		*	*	*
52083		<i>Pinnularia borealis</i> v. <i>rectangularis</i> Carlson				*		
52086	ACP	<i>Pinnularia</i> cf. <i>braunii</i> v. <i>amphicephala</i> f. <i>subconica</i> Venkataraman PIRLA		*				*
52025		<i>Pinnularia divergens</i> W. Sm. v. <i>divergens</i>				*		
52027	ACP	<i>Pinnularia divergentissima</i> (Grun.) Cl. v. <i>divergentissima</i>	*		*	*		
52080	ACP	<i>Pinnularia</i> cf. <i>pseudomicrostauron</i> Gandhi v. <i>pseudomicrostauron</i> PIRLA				*		*
99277	ACP	<i>Pinnularia</i> 2 SN	*	*				

Taxon No.	pH Cat.	Taxon Name	Lake		Inlet		Outlet	
			H	S	H	S	H	S
99281	ACP	Pinnularia 9 SN					*	*
99286		Pinnularia 15 SN					*	*
99290		Pinnularia 19 SN	*				*	*
99381		Pinnularia 45 SN						*
52889		Pinnularia spp		*	*	*		
62002		Stauroneis anceps Ehr. v. anceps		*				
62022	ACP	Stauroneis anceps 2 PIRLA		*				
99314		Stauroneis 2 SN						*
63002	ACP	Stenopterobia intermedia (Lewis) V.H. v. intermedia	*				*	*
65011	ACP	Surirella delicatissima Lewis v. delicatissima	*	*			*	*
65033	ACP	Surirella delicatissima f. tenuissima Mang.		*				*
65014	ACP	Surirella linearis W. Sm. v. linearis	*	*				
65889		Surirella spp						*
67006	IND	Tabellaria flocculosa (Roth) Kutz., strain IV sensu Koppen	*	*	*	*	*	*
89889		Unidentified pennate diatoms		*	*	*	*	*

Table IV-2. Summary of Emerald Lake pH inferences using MIR and log Index B predictive equations for live and total (living and dead) assemblages by substrate type.

<u>Live Assemblage</u>		<u>MLR</u>	<u>log Index B</u>
	<u>Lake Sed.</u>		
	Range	6.2 - 6.5	6.3 - 6.4
	Mean (n=8)	6.4	6.2
	Lake Tiles		
	Range	6.5 - 6.9	6.2 - 7.0
	Mean (n=8)	6.6	6.6
	Sed. + Tiles		
	Mean (n=16)	6.5	6.6
<u>Total Assemblage</u>		<u>MLR</u>	<u>log Index B</u>
	<u>Lake Sed.</u>		
	Range	6.2 - 6.5	6.2 - 6.8
	Mean (n=8)	6.4	6.5
	Lake Tiles		
	Range	6.5 - 6.7	6.2 - 6.8
	Mean (n=8)	6.6	6.6
	Sed. + Tiles		
	Mean (n=16)	6.5	6.5

Table IV-3. Summary of inlet stream pH inferences using MIR and log Index B for live and total assemblages by substrate type.

		<u>MLR</u>	<u>log Index B</u>	
Live <u>Assemblage</u>	<u>Inlet Sed.</u>			
	Range	4.7 - 6.6	5.9 - 6.7	
	Mean (n=8)	6.0	6.3	
	<u>Inlet Tiles</u>			
	Range	5.8 - 6.7	5.9 - 6.9	
	Mean (n=7)	6.3	6.5	
	<u>Sed. + Tiles</u>			
	Mean (n=15)	6.2	6.4	
			<u>MLR</u>	<u>log Index B</u>
	Total <u>Assemblage</u>	<u>Inlet Sed.</u>		
Range		5.3 - 6.4	6.2 - 6.6	
Mean (n=8)		6.2	6.5	
<u>Inlet Tiles</u>				
Range		6.0 - 6.6	6.0 - 6.8	
Mean (n=7)		6.3	6.5	
<u>Sed. + Tiles</u>				
Mean (n=15)		6.2	6.4	

Fig. IV-5. The average number of species (richness) per sample by substrate type, location and month. Vertical lines represent the range of values encountered.

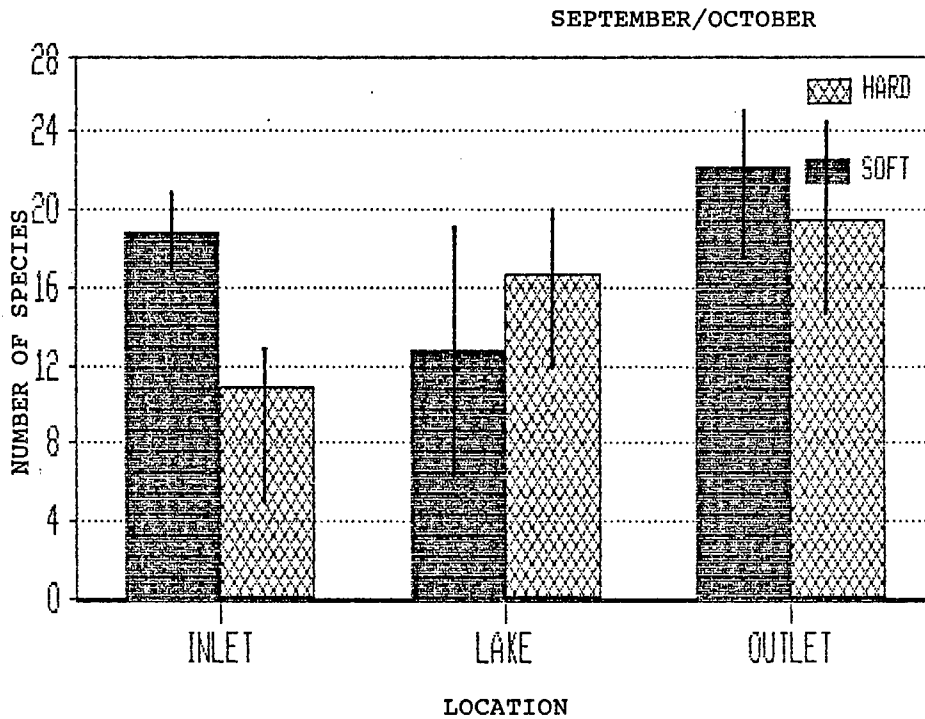
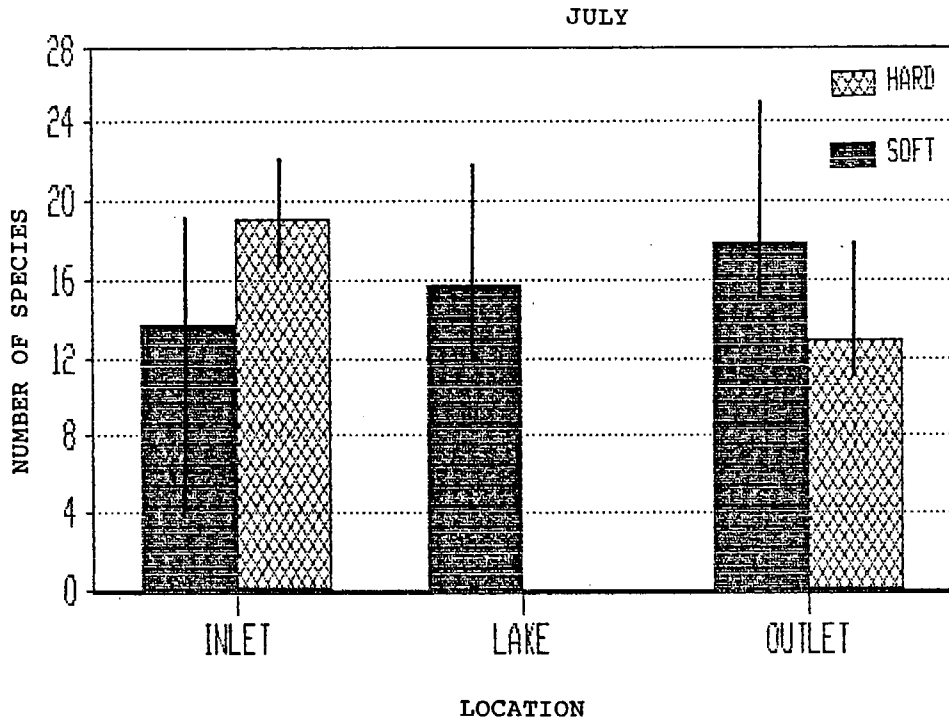


Fig. IV-6a

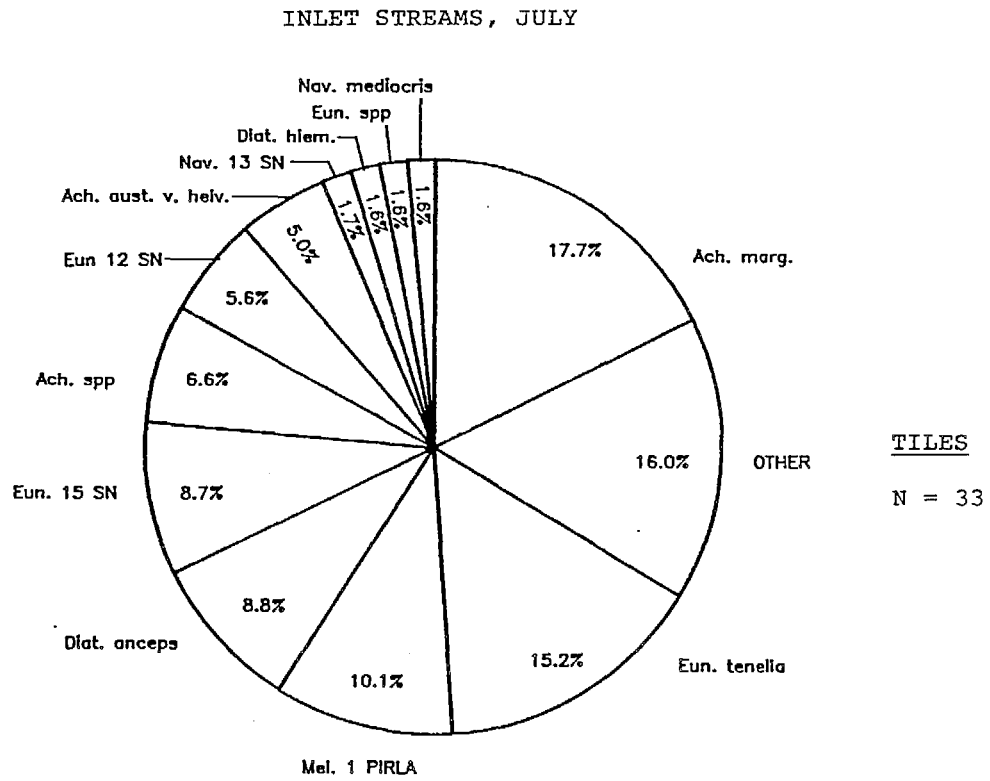
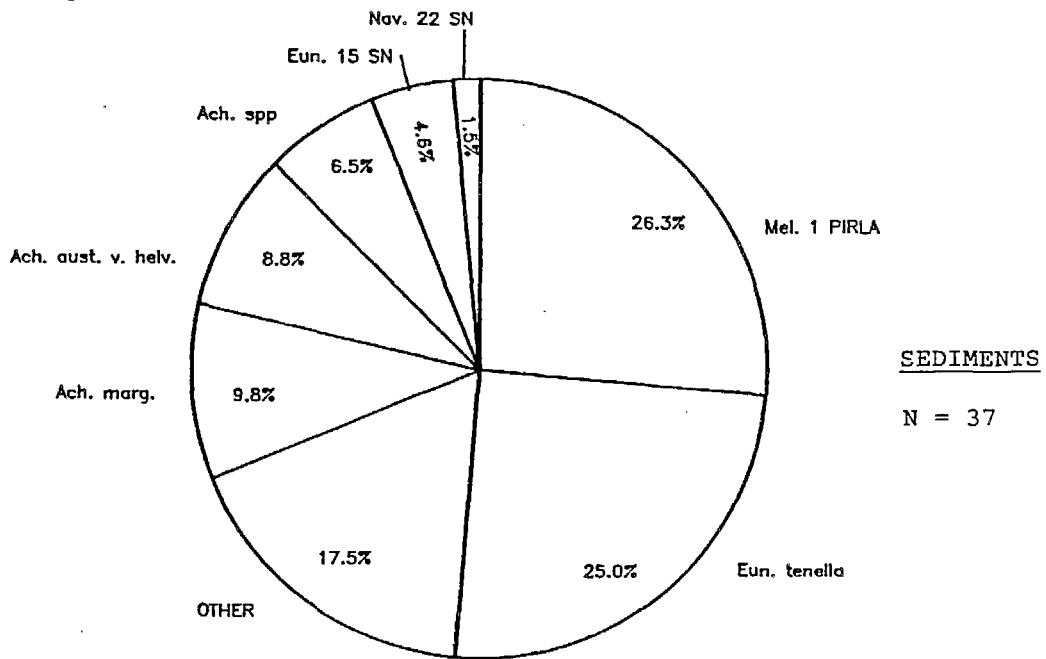


Fig. IV-6b



Figures IV-6a to 6l Relative abundances averaged over four to six samples by substrate type and location for July, September, and October (lake only) sampling dates. All species with an average relative abundance greater than or equal to 1.5% are represented. Addendum: All entries reading Tab. floc. III should read Tab. floc. IV.

Fig. 6c

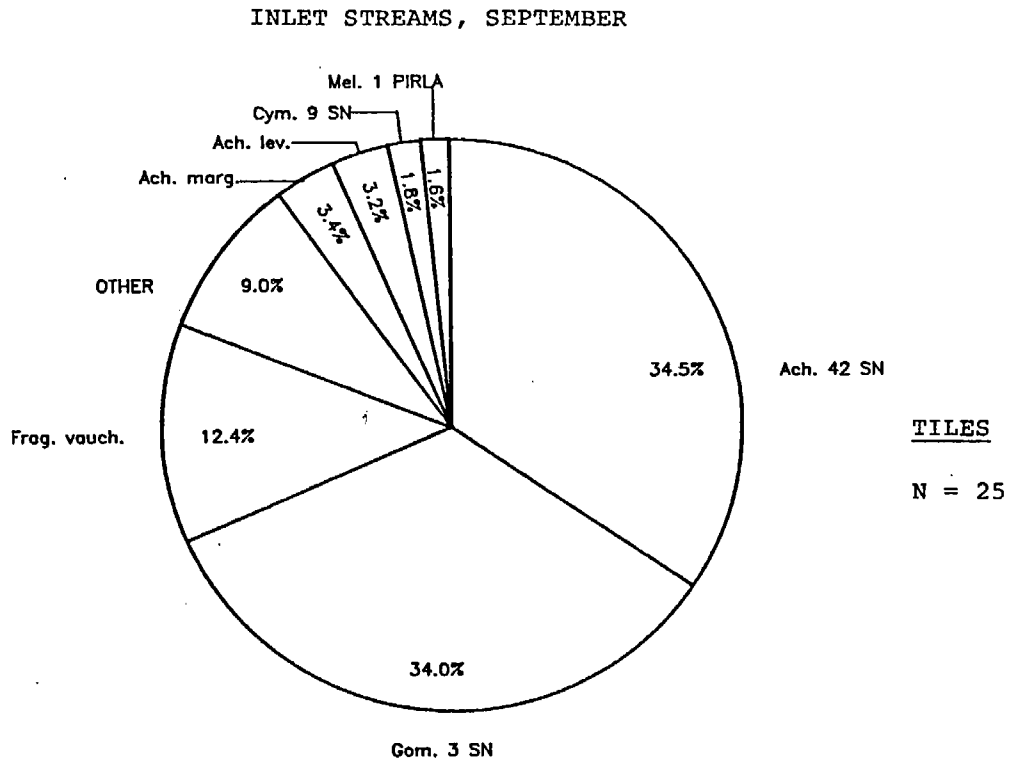


Fig. 6d

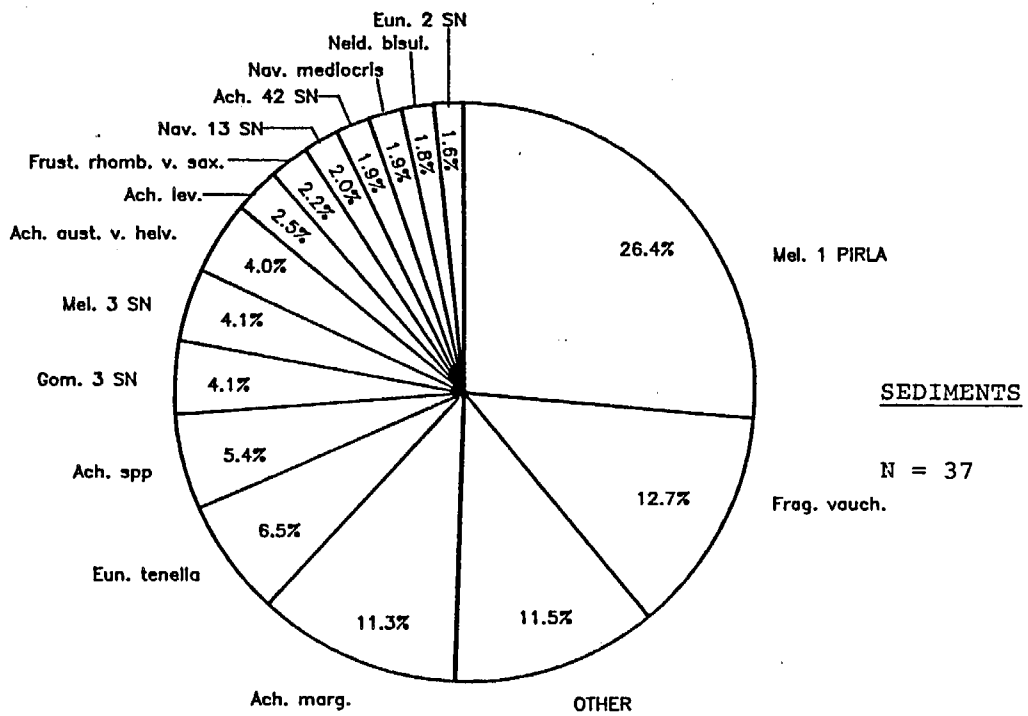


Fig. 6e

LAKE, OCTOBER

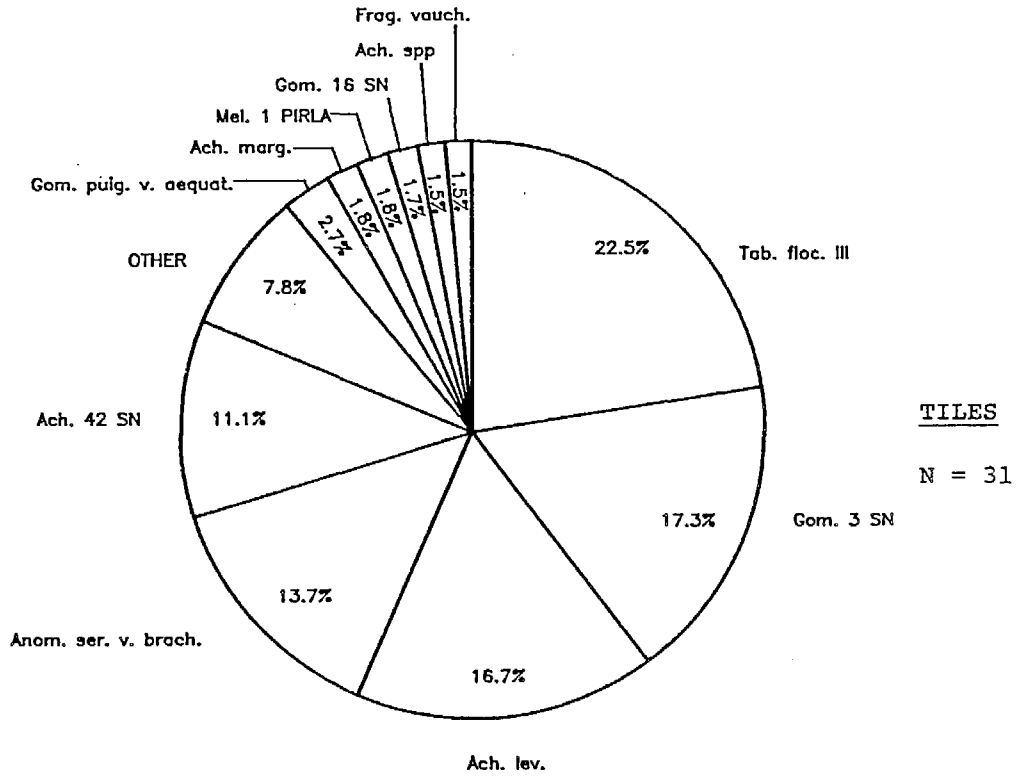


Fig. 6f

LAKE, JULY

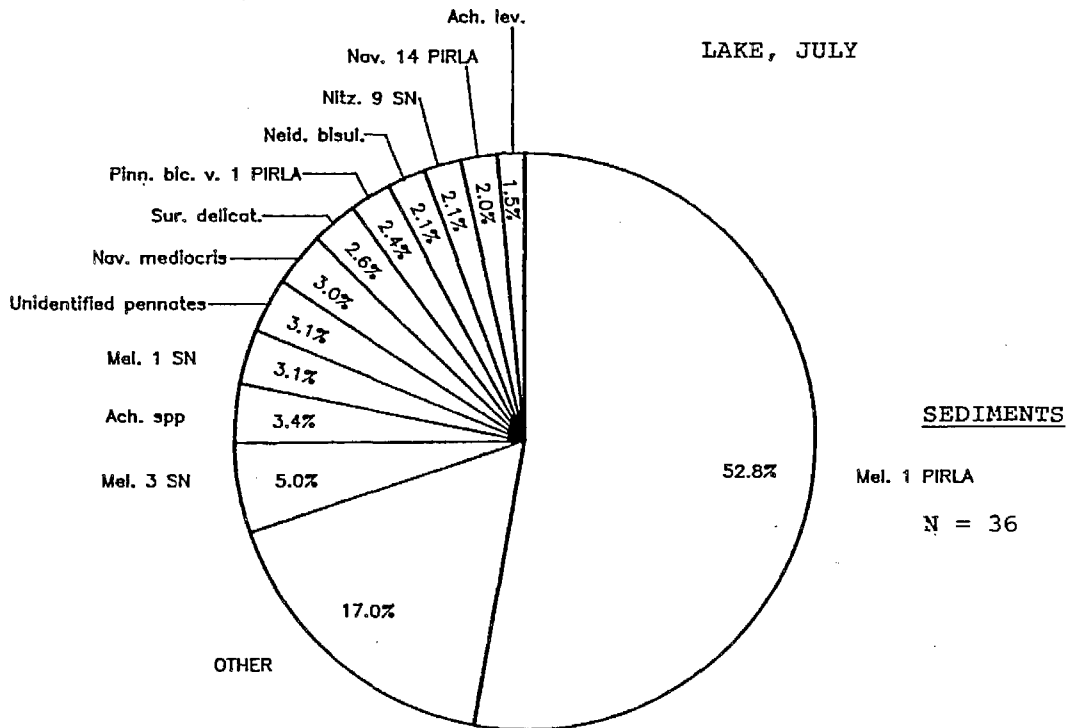


Fig. 6g

LAKE, SEPTEMBER

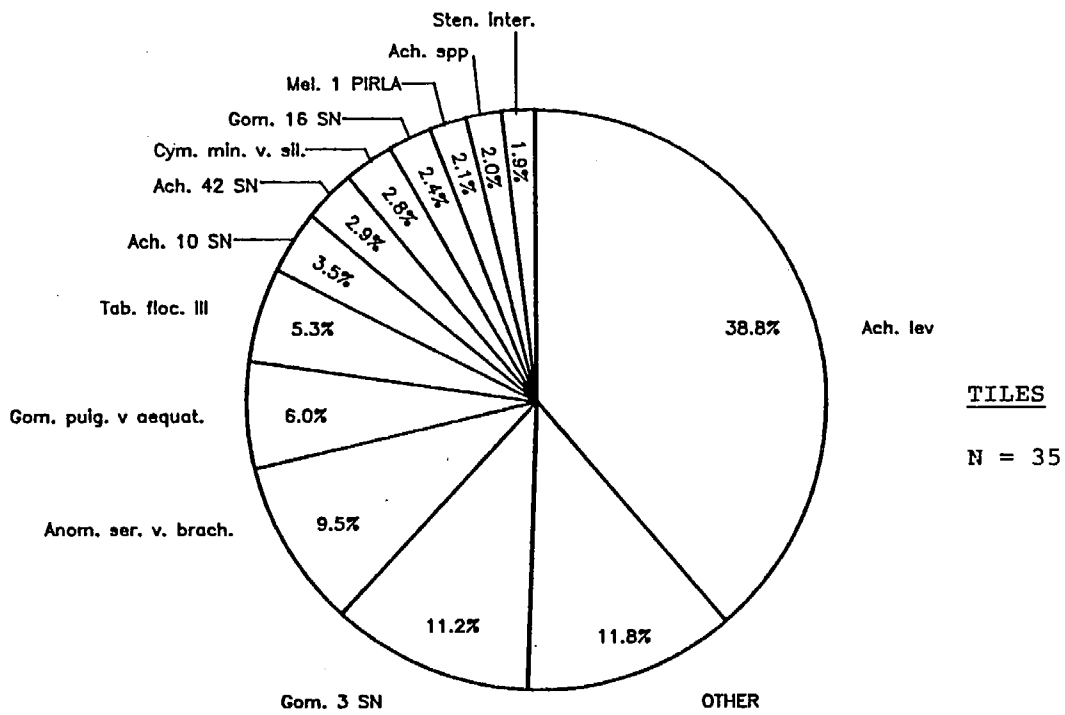


Fig. 6h

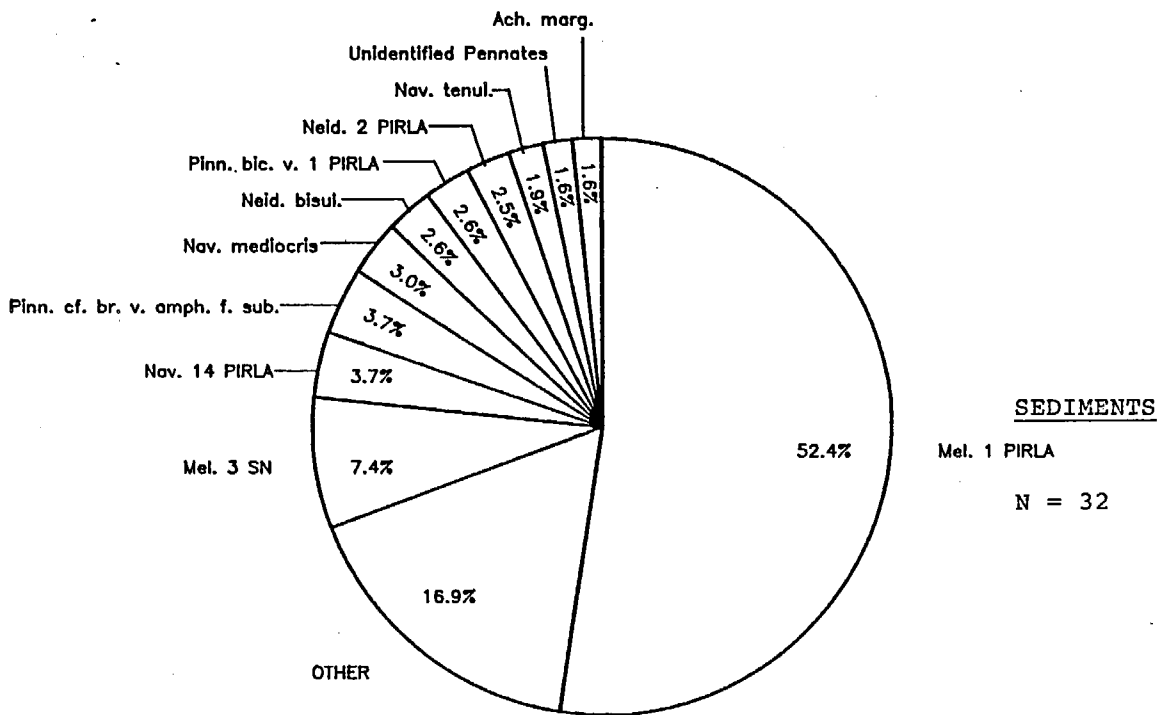


Fig. 6i

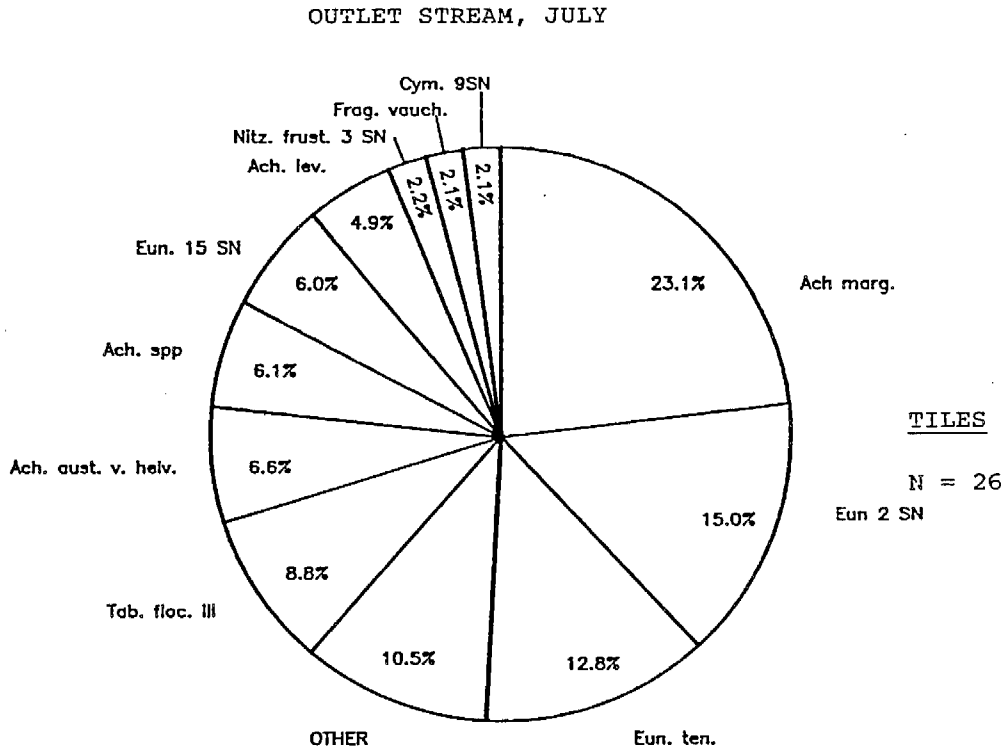


Fig. 6j

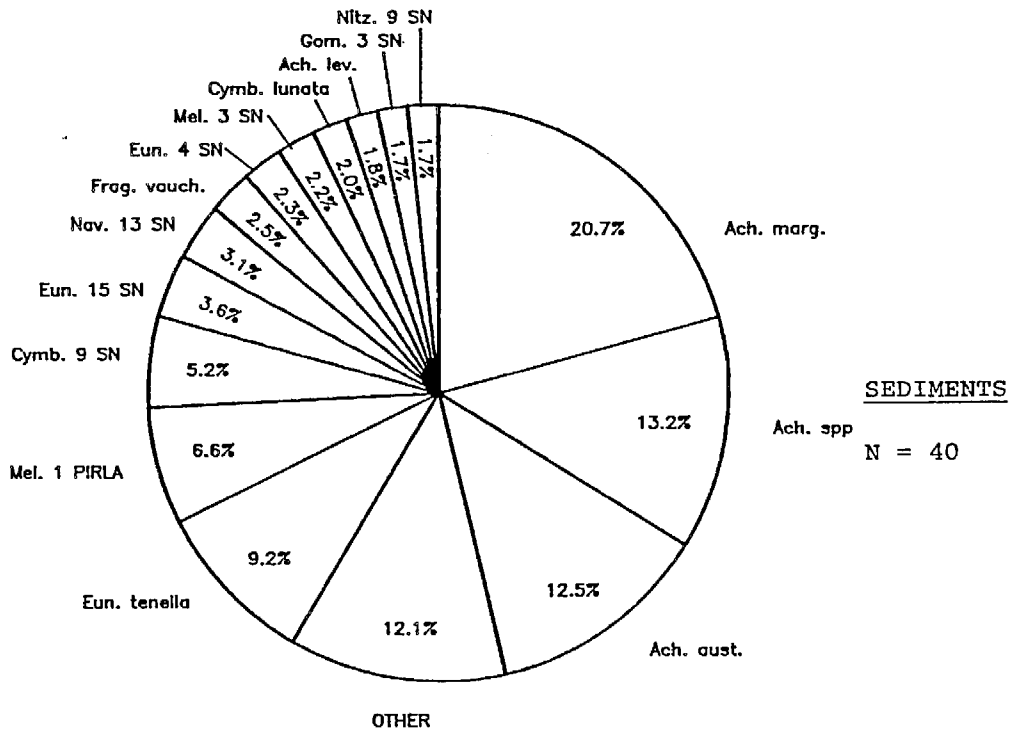


Fig. 6k

OUTLET STREAM, SEPTEMBER

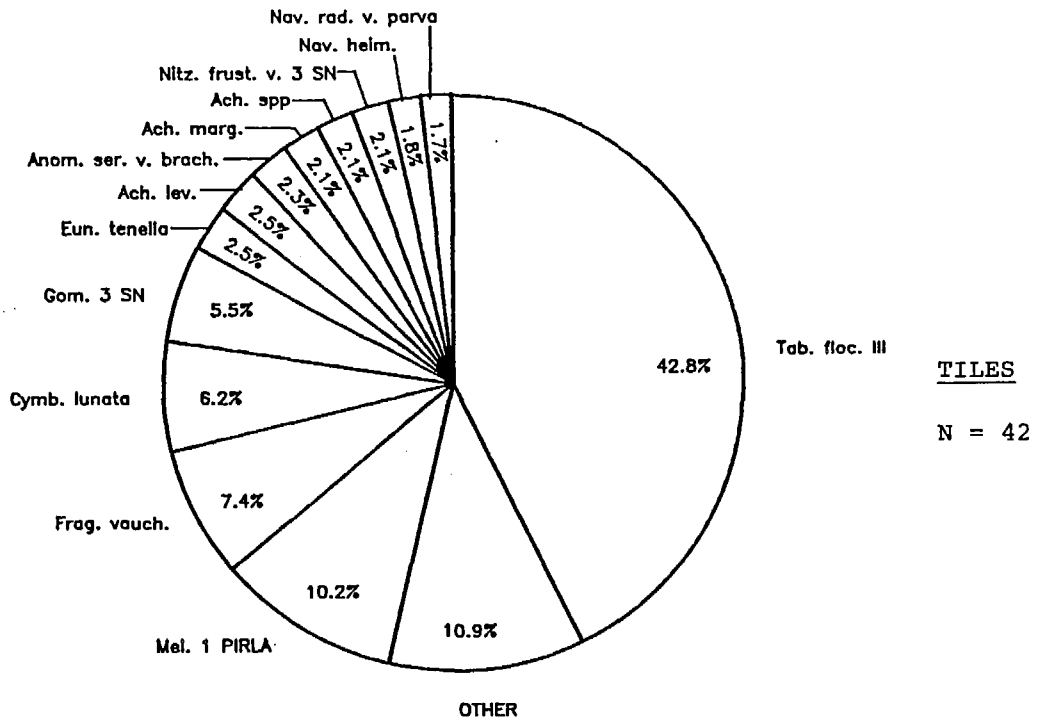


Fig. 6l

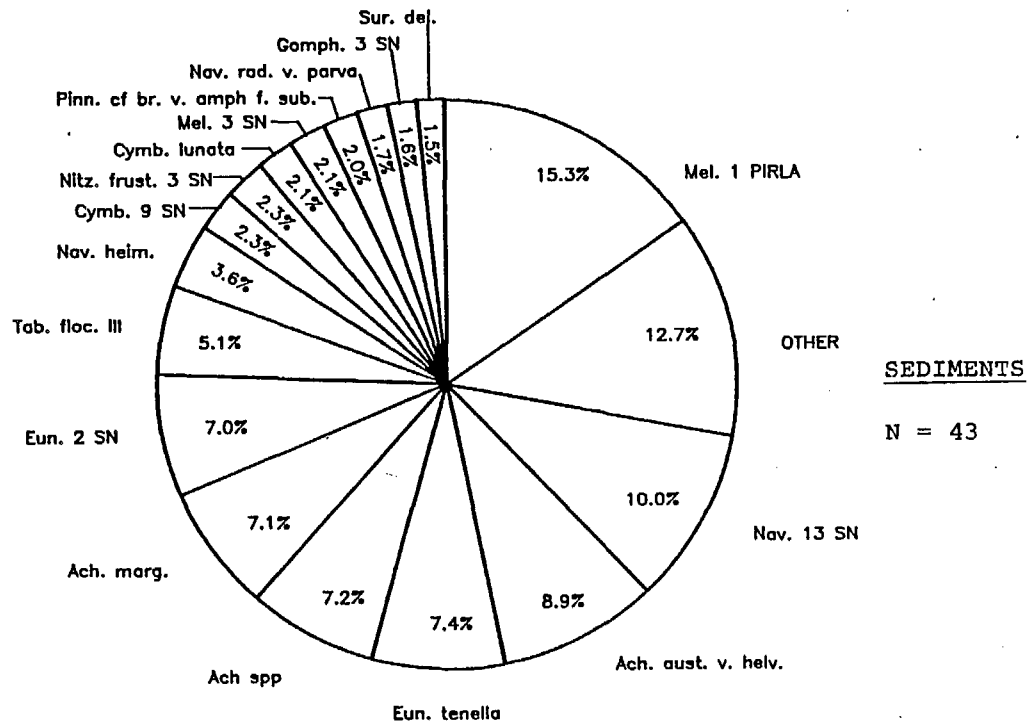
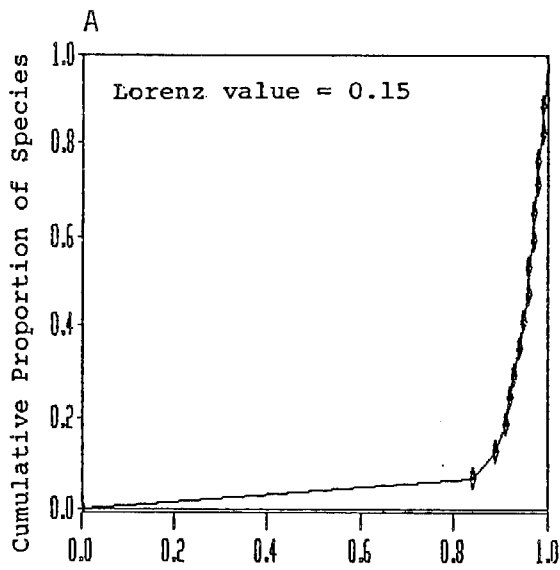
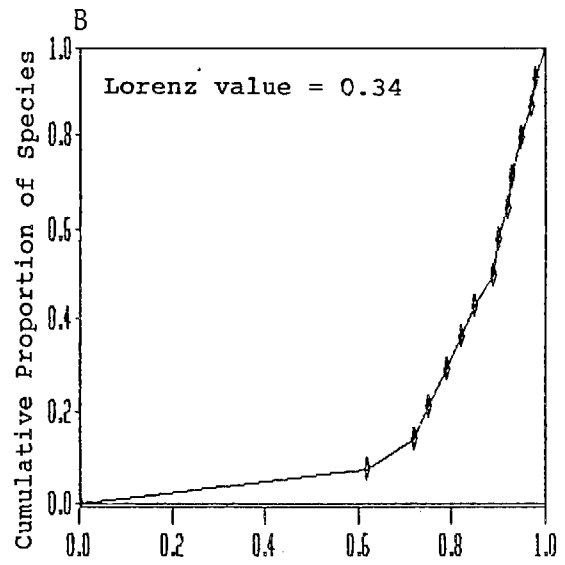


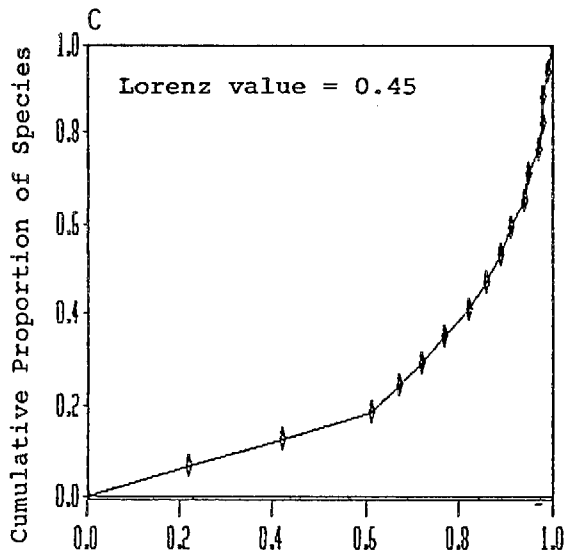
Figure IV-7. Lorenz curves plotted for four samples which demonstrate the range of Lorenz values which occurred over the sampling period.



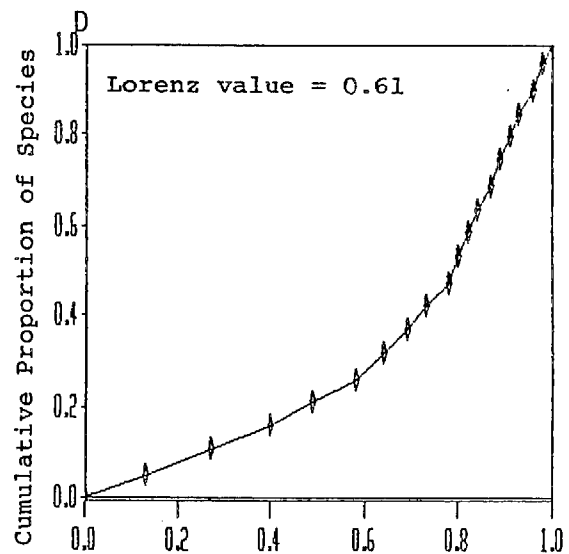
Cumulative Proportion of Individuals



Cumulative Proportion of Individuals



Cumulative Proportion of Individuals



Cumulative Proportion of Individuals